

https://dspace.org/

Estimation of the propensity of remnant underground coal pillars to spontaneously combust during opencast mining at a colliery in the Witbank coalfield

Gemmell, Graham Barry

2017

https://hdl.handle.net/10539/25542

Gemmell, Graham Barry (2017) Estimation of the propensity of remnant underground coal pillars to spontaneously combust during opencast mining at a colliery in the Witbank coalfield, University of the Witwatersrand, <https://hdl.handle.net/10539/25542>

Downloaded from a DSpace repository. https://dspace.org/



ESTIMATION OF THE PROPENSITY OF REMNANT UNDERGROUND COAL PILLARS TO SPONTANEOUSLY COMBUST DURING OPENCAST MINING AT A COLLIERY IN THE WITBANK COALFIELD

A research report submitted to the Faculty of Engineering,
University of the Witwatersrand,
in fulfilment of the requirements for the degree of Master of Science in Engineering
Johannesburg 2016

Graham Barry Gemmell

ABSTRACT

Spontaneous combustion of coal may occur when coal is mined, stored or transported and is influenced by a combination of intrinsic and /or extrinsic factors. While it is unusual for intact seams to burn in the highwall, the most common occurrence is when surface mines extract seams previously partially mined by underground bord and pillar operations.

The aim of the study is to provide a predictive model (matrix) of the spontaneous combustion potential of remnant pillars at Colliery X. A number of different thermal, chemical and petrographic tests (coal factors) will be undertaken to determine their individual and collective impacts on the sponcom predictive model. The primary geology at the mine is conformable with that of the Witbank Coalfield. Battacharyya (1982) described 3 main factors in the spontaneous combustion of coal, mining factor, coal factor and geological factor which have an aggregate effect.

Some of the main historical and present theories of sponcom are the pyrite theory, the bacterial theory, the oxidation theory and the humidity theory. It is important to note that no single factor is responsible for spontaneous combustion. The oxidation of coal occurs constantly. The temperature of the coal is a function of the rate of heat generation versus the rate of heat loss. Fires can start at outcrops and move through interconnected workings with heat transfer by conduction (into the overburden) or convection (between panels).The overburden can also insulate the burning coal seam. Geological factors such as depth of overburden, the degree of fracturing, and the nature of the overlying strata vary between coalfields.

A coal seam fire or mine fire is the underground smouldering of a coal deposit, often in a coal mine. Such fires have economic, social and ecological impacts In order to extinguish a fire, one of three elements, fuel, oxygen, or energy, must be removed. The components of the fire triangle can be further subdivided into conventional mine control techniques and more or less unconventional or unproven mine fire control techniques. The thermal techniques discussed include the crossing point temperature, thermogravimetric analyses and oxygen absorption. Macerals, the microscopically identifiable organic constituents of coal, are one of the three basic parameters that define coal. The other two parameters are the coal rank and the mineral matter Vitrinite is the principal maceral group of the No.5 seam and inertinite dominates the No.2 and No.4 seams.

The results obtained from the 22 drill-core samples and 2 ROM samples were matched to the existing borehole dataset (2296 boreholes) based on similarity of heat value (figure 3.11). A total of 24 test results (thermal, chemical and petrographic) from borehole A and borehole B were thus assigned to the borehole database which has approximately 1500 samples for each seam. By linking the laboratory datasets (borehole A and B) and the existing borehole database used for resource modelling, the sponcom variables could be modelled in a similar way to the coal resources.

The overall risk matrix was calculated on a full seam basis by combining 15 variable scores, each variable having a score of 0, 1 or 2 (low-mod-high probability). The overall results from this research produced clear and unambiguous contour plans of different factors effecting sponcom of coal using single variable and combined variable datasets. In conclusion, it appears that the acceptability of a method for determining spontaneous heating characteristics of coal mainly depends upon how closely it predicts the spontaneous heating behaviour in the field conditions

ACKNOWLEDGEMENTS

The following people are thanked for their support and encouragement during the Research Programme

Mr W. Schluter (Colliery Technical Manager)

Mr V. Makoanyane (Colliery Lab supervisor Colliery)

Prof N. Wagner (University of Johannesburg)

Prof R. Falcon (University of the Witwatersrand)

Mr P. Dekker (Manager external laboratory)

DEDICATION

To my son Michael: ““Success is not final, failure is not fatal: it is the courage to continue that counts.” Winston S. Churchill

To all the “older students: “Anyone who stops learning is old, whether at twenty or eighty. Anyone who keeps learning stays young.” H. Ford

CONFIDENTIALITY

The name and exact location of the Colliery may not be disclosed in this report.

The study area is referred to as Colliery X.

DISCLAIMER

Although some of the information used to compile this Thesis was provided by South32 SA Coal Holdings Proprietary Limited or its affiliates, the statements, views and opinions expressed herein reflect the views and opinions of the author and do not reflect the official policy, opinions or position, in any manner, of South32 SA Coal Holdings Proprietary Limited or any of its subsidiaries, affiliates, or associated group companies.

DECLARATION

I declare that this research report is my own unaided work. It is being submitted for the Degree of Master of Science in the University of the Witwatersrand, Johannesburg. It has not been submitted before for any degree or examination in any other University

Signed G.B.Gennell

This day of 28 August 2017

TABLE OF CONTENTS

LIST OF FIGURES x

LIST OF TABLES xii

APPENDIX LIST xiii

List of Acronyms xvii

1 BACKGROUND 1

1.1 Occurrence of Spontaneous combustion 1

1.2 Basic concepts of self-oxidation 3

1.2.1 Intrinsic factors 3

1.2.2 Extrinsic factors 3

1.3 Aim of the study 4

1.4 Geology 6

1.4.1 Formation of Coal 6

1.4.2 Local Geology 8

1.4.3 Structure 11

1.5 Coal qualities 12

1.6 Pillar resources 13

1.6.1 Historical mining methods 13

1.7 Resource Estimation 14

1.8 Reserve Estimation 15

1.8.1 Planning methodology 15

1.9 Modifying factors 16

2 Literature Review 17

2.1 Main factors in defining self-oxidation of coal 17

2.2 Spontaneous combustion theories 18

2.2.1 The pyrite theory 19

2.2.2 The bacterial theory 19

2.2.3 The oxidation theory 20

2.2.4 The Humidity Theory 21

2.3 Coal Particle Size 22

2.4 Mining factors that affect sponcom 22

2.5 Geological Factors related to sponcom 26

2.6 Oxidation Theory 27
2.7 Control measures 30
2.8 Thermal analysis methods of coal 32
2.8.1 Crossing point temperature (CPT) 32
2.8.2 Thermogravimetric analysis (TGA) 34
2.8.2.1 Types of TGA Curves 35
2.8.3 The Rate equation 38
2.9 Oxygen absorption tests (Smith and Glasser method) 38
2.9.1 Moisture 40
2.9.2 Particle size 41
2.10 Petrology 41
2.10.1 Inorganic Matter in coal 42
2.10.2 Rank 43
2.10.3 Macerals 45
2.10.3.1 Vitrinite 45
2.10.3.2 Liptinite 46
2.10.3.3 Inertinite 46
2.10.3.4 Aromaticity 47
2.11 Case studies 48
2.11.1 China 49
2.11.2 India 49
2.11.3 South Africa 51
2.11.4 United States 52
3 METHODOLOGY 54
3.1 Background to investigative area 54
3.1.2 Analyses and tests conducted 54
3.2 Sample extraction and preparation 55
3.3 Methods used for thermal analysis 56
3.3.1 Crossing point temperature (CPT) 56
3.3.2 Thermo-gravimetric analysis (TGA) 58
3.3.2.1 Intrinsic Reactivity 58
3.3.2.2 Spontaneous combustion testing 59
3.3.2.3 Absorption of oxygen 59
3.3.3 Oxygen adsorption test (Smith-Glasser) 60

1.3.3.1 Mine method 60
1.3.3.2 Smith and Glasser method 61
3.4 Chemical analysis 62
3.4.1 Moisture (Standard Method: ASTM D3173, ISO 11722, and AS1038.3) 63
3.4.2 Ash (Standard Method: ASTM D3174, ISO 1171, and AS1038.3) 64
3.4.3 Ash element analysis 65
3.4.4 Sulphur 65
3.4.4.1 Total Sulphur 65
3.4.4.2 Sulphide Sulphur 65
3.4.4.3 Sulphate Sulphur 65
3.4.5 Calorific Value 66
3.4.6 Volatile matter 66
3.4.7 Fixed carbon 67
3.4.8 Ultimate analysis 67
3.5 Petrographic analysis 68
3.5.1 Vitrinite reflectance 68
3.5.2 Condition/weathering analysis 68
3.5.3 Maceral analysis 68
3.6 Computer modelling 69
3.6.1 Correlations 71
4 Results 71
4.1 Crossing point temperature 71
4.2 Thermogravimetric analysis (TGA) 75
4.2.1 TG spi (spontaneous combustion index) 75
4.2.2 TGA curves 77
4.2.3 Tstart (T1) and Tpeak (T2) 82
4.2.4 Weight Gain 84
4.3 Oxygen Absorption Test (Smith and Glasser) 89
4.4 Chemical Analysis 94
4.5 Petrographic Analysis 100
4.5.1 Abnormal condition analysis 100
4.5.1.1 Micrographs 101
4.5.2 Maceral composition 103
4.5.3 Vitrinite reflectance 104

4.6 Geology 112
4.6.1 Mudstone roof and floor 112
4.6.2 In-seam partings 114
5 DISCUSSION 115
5.1 Cross-Correlations 115
5.1.1 CPT (crossing point temperature) correlations 116
5.1.2 TGA (thermogravimetric) correlations 118
5.1.3 Oxygen absorption correlations 120
5.1.4 Chemical analysis correlations 122
5.1.5 Petrographic correlations 124
5.1.6 Geological correlations 126
5.2 Combined Risk Matrix 130
6 Conclusion 134
6.1 General Conclusions 134
6.2 Predictive methods to estimate the potential of coal to spontaneous combustion 134
6.2.1 Thermal properties 134
6.2.2 Chemical properties 135
6.2.3 Petrographic properties 135
6.2.4 Mining and Geological factors 135

LIST OF FIGURES

Figure 1.1: Distribution of major global coal fire events (after Avila, 2012) 2
Figure 1.3 - Different ranks of coal and their chemical ranges (daf basis) (Avila 2012) 7
Figure 1.4: Locality plan of the main Coalfields in South Africa 9
Figure 1.5: Local stratigraphic column of the study area 10
Figure 1.14: Dyke and fault plan Colliery X 12
Figure 1.18: Generalised mining stratigraphic column (not to scale) 15
Figure 1.19: Burn zone around a mine addit due to sponcom 17
Figure 2.1: Wasted-coal fire in an abandoned mine showing emission of smoke and fumes through cracks and fractures and intake of fresh air through openings and overburden. (Adapted from Kim and Chaiken 1993) 25
Figure 2.2: Fire triangle showing the three essential elements for any fire: fuel, oxygen, ignition source (adapted from Kim and Chaiken 1993) 28
Figure 2.3: Zonation of outer layer of coal pillars (after Banerjeee,1985) 30
Figure 2.4: Identical CPT for two different coals (after Nandy,1972) 33
Figure 2.5: TG curve and corresponding DTG curve (after Viamakis) 35
Figure 2.6: Main types of thermo-gravimetric (TG) curves(after Brown,1972) 36
Figure 2.7: Weight variation of coal with progress of oxidation (after Oreshko,1961) 37
Figure 2.8: Modified Schopf diagram illustrating the variation in rates between individual macerals and maceral groups 45
Figure 2.9: Mollecular structure of vitrinites showing the principal structural states at three levels of rank (after Hirsch 1954). 48
Figure 2.11: Incidents of underground fires caused by spontaneous combustion on an area basis for the period 1970 to 1985 (Morris and Badenhorst, 1987) 52
Figure 2.10: Major causes of 254 colliery fires reported from 1970 to 1990 52
Figure 3.1: Simplified modelling methodology 54
Figure 3.2: Core tray with coal samples and density log for determining sample intervals 55
Figure 3.3: Crushing of drill-cores to 20mm top size 56
Figure 3.4: Crossing point temperature instrument with control unit and furnace 57
Figure 3.5: Furnace with aluminium reaction vessel 58
Figure 3.6: TGA analyser used at Wits University 60
Figure 3.7: Oxygen adsorption test apparatus at mine laboratory 61
Figure 3.8: Static isothermal apparatus used by Smith and Glasser (2004) 62
Figure 3.9: Drying oven for sample preparation at 105 °C 64
Figure 3.10: CV Calorimeter for determination of heat value (MJ/kg) 66
Figure 3.11: Volatile furnace (950 °C) 67
Figure 4.1: Sample CPT compared to safe limit of 200 °C (SGS method) and risk limit of 140 °C (Banerjee) 72
Figure 4.2: Combined histogram of the modelled No.5, No.4U and No.2 seam CPT 74
Figure 4.4: No.4U crossing point temperature 74
Figure 4.3: No.5 seam CPT 74
Figure 4.5: No.2 seam crossing point temperature 75
Figure 4.6: TG plot calculated from the derivative of weight gain and heating rate for sample Z013. .76
Figure 4.9: Oxygen absorption for sample Z01 at 3 °C ramp 78
Figure 4.10: TG spc values Avila method 81
Figure 4.11: TG spi at different heating rates 81
Figure 4.13: T peak (T2) for the No. 4U seam 82
Figure 4.12: T peak (T2) for the No. 5 seam 82
Figure 4.14: T peak (T2) for the No.2 seam 83

Figure 4.16: T peak (T2) for combined seam sample dataset -3C ramp 84
Figure 4.15: T start (T1) for combined seam sample dataset -3C ramp 84
Figure 4.17: TGA profile of low and high reactive coals (Avila, 2012) 85
Figure 4.18: TGA profile of high reactive coals from sample dataset –sample Z01 85
Figure 4.20: S4U weight gain (%) 86
Figure 4.19: S5 weight gain (%) 86
Figure 4.21: S2 weight gain (%) 86
Figure 4.23: % weight gain for combined seams sample dataset (3C ramp) 87
Figure 4.22: % derivative of weight gain for combined seams sample dataset (3C ramp) 87
Figure 4.24: Correlation between %WT gain and net adsorption temperature range at 3C with poor correlation coefficient (Z01-Z24) 89
Figure 4.25: Relationship between CV and volume of oil displaced (oxygen adsorbed) 90
Figure 4.26: Oxygen absorption rate of the sample set from Boreholes 1 and 2 90
Figure 4.27: Effect of particle size on oxygen absorption rate (McGeer, 2015) 91
Figure 4.29: Volume oil displaced (oxygen reactivity) in S4U seam coal 93
Figure 4.28: Volume oil displaced (oxygen reactivity) in S5 seam coal 93
Figure 4.30: Volume oil displaced (oxygen reactivity) in S4U seam coal 93
Figure 4.31: Volume of oil displaced in Smith-Glasser test for the sample dataset 94
Figure 4.33: RD-AS correlation plot for combined seams 95
Figure 4.32: CV-AS correlation plot for combined seams 95
Figure 4.34: Ash analysis of the sample set 96
Figure 4.35: Forms of Sulphur of the sample set 96
Figure 4.36: Ultimate analysis of the sample set 97
Figure 4.37: Fuel ratio and IM 97
Figure 4.38: Zeiss Axiolmager reflectance light petrographic microscope 100
Figure 4.40: Sample Z01 showing cracked and fissure particle 101
Figure 4.39: Sample Z01 showing cracked inertinite and vitrinite 101
Figure 4.42: Sample Z01 showing pyrite and cracked vitrinite 102
Figure 4.41: Sample Z01 showing enhanced vitrinite reflectance and fissured inertinite 102
Figure 4.43: Sample Z06 showing pyrite infilling cracks 102
Figure 4.44: Maceral composition of the sample set 103
Figure 4.45: Maceral content from three nearby collieries within the Witbank Coalfield 104
Figure 4.46: Vitrinite reflectance of sample set 105
Figure 4.47: S5 abnormal condition analysis (%) 109
Figure 4.48: S4U abnormal condition analysis (%) 109
Figure 4.49: S2 abnormal condition analysis (%) 109
Figure 4.51: S4U total reactives (%) 110
Figure 4.50: S5 Total reactives (%) 110
Figure 4.52: S2 total reactives (%) 110
Figure 4.53: S5 seam VR 111
Figure 4.54: S4U seam VR 111
Figure 4.55: S2 seam VR 111
Figure 4.57: S4U seam roof mudstone 113
Figure 4.56: S5 seam roof mudstone 113
Figure 4.58: S2 seam roof mudstone thickness 113
Figure 4.60: S2 mudstone parting thickness 114
Figure 4.59: S4U mudstone parting thickness 114
Figure 5.2: Correlation between CV and CPT for the sample dataset 116
Figure 5.1: Correlation between CV and CPT for the model dataset 116
Figure 5.4: Correlation between TR (total reactives) and CPT for the sample dataset 117
Figure 5.3: Correlation between OS and CPT for the sample dataset 117
Figure 5.5: Correlation between VM (volatile matter) and CPT for the sample database 117

Figure 5.7: Sample dataset correlation of WT (weight gain %) and T1 (start temperature) 118
Figure 5.6: Sample dataset correlation of VR (vitrinite reflectance) and T2 (peak temperature) 118
Figure 5.8: Sample dataset correlation WT and temperature differential 119
Figure 5.9: WT increase and TG spi correlation 120
Figure 5.11: Correlation between CPT and oxygen absorption GLI 121
Figure 5.10: Correlation between AS and oxygen absorption GLI 121
Figure 5.13: Correlation between derivative of TR and oxygen absorption (GLI) 121
Figure 5.12: Correlation between (DER) and oxygen absorption (GLI) 121
Figure 5.15: Correlation between WT and H 123
Figure 5.14: Correlation between CPT and H 123
Figure 5.16: Correlation between CPT and O 123
Figure 5.18: Correlation between Fe2O3 and TR 125
Figure 5.17: Correlation between CV and TR 125
Figure 5.20: Correlation between T2 and VR 125
Figure 5.19: Correlation between CPT and TR 125
Figure 5.21: Correlation between CPT and AB 126
Figure 5.23: Correlation between CPT and seam depth 127
Figure 5.22: Correlation between CPT and seam thickness 127
Figure 5.24: Histogram of matrix scores per sponcom factor and seam in the mined out pillar area 131
Figure 5.26: No.S4U seam combined factor sponcom risk matrix 132
Figure 5.25: No.S5 seam combined factor sponcom risk matrix 132
Figure 5.28: All seams sponcom risk matrix 132
Figure 5.27: No. S2 seam combined factor sponcom risk matrix 132

LIST OF TABLES

Table 1.2: Coal classification by rank and vitrinite reflectance 8
Table 1.3: Resource quality ranges at Colliery X 13
Table 1.5: General pillar dimensions 14
Table 2.1: Intrinsic factors related to self-heating of coal 18
Table 2.2: Extrinsic factors related to self-heating of coal 18
Table 2.3: Parameters affecting the oxygen adsorption of coal; after Wade (1988) 20
Table 2.5: Spontaneous fire risk factors as proposed by Banerjee (1982) 24
Table 2.6: Summary of the main sponcom control measures 31
Table 2.10: Processes accompanied by weight change 34
Table 2.11: Coal classification based on weight change(Avila,2014) 38
Table 2.12: Classification of macerals into subgroups and groups, based on international committee for coal and organic petrology (ICCP, 1998, 2001) 42
Table 3.1: Methods used at SGS laboratory to determine chemical parameters of the coal samples. 63
Table 3.2 - Vitrinite reflectance parameters measured in coal samples 68
Table 3.3: Maceral groups and reactive inertinite groups identified in the samples 69
Table 3.4: Risk matrix used for modelling of sponcom risk factors 70
Table 4.1: Crossing point temperature of samples at different ramping rates 73
Table 4.2: Results of TGA analysis done at Wits University 77
Table 4.3: Calculated TG spc values (Avila method) at different heating rates 80
Table 4.4: Weight gain and temperature range of seams modelled 87
Table 4.5: Weight gain and temperature range (T2-T1).Samples matching Avila criteria for sponcom risk marked with in red text 88
Table 4.6: Results of Smith-Glasser oxygen absorption 92

Table 4.7: Proximate and Ultimate analysis of sample set (Air dry basis) 99
Table 4.8: Abnormal particle analysis 106
Table 4.9: Summary of major coal characteristics 107
Table 4.10: Rock lithology qualities..... 112
Table 5.1: Variables used in modelling and correlations 115
Table 5.2: Cross correlation of all sample database variables - blue shade >80% correlation , green shade >70% correlation and yellow shade >50% correlation 128
Table 5.3: Cross correlation of all modelling database variables - blue shade >80% correlation , green shade >70% correlation and yellow shade >50% correlation 129
Table 5.4: Variables used in risk matrix model 130
Table 5.5: Risk matrix values for the total mine area on a seam basis 130
Table 5.6: Risk matrix values for the pillar area on a seam basis..... 130

APPENDIX LIST

Appendix 1: No S4U seam mined height of pillars - excludes top coal..... 148
Appendix 2: No S2 seam mined height of pillars - excludes bottom coal 148
Appendix 3: No.S4U seam floor elevation 149
Appendix 4: No.S2 seam floor elevation..... 149
Appendix 5: Crossing point temperatures for samples Z01-Z13..... 149
Appendix 6: Crossing point temperatures for samples Z13-Z22..... 149
Appendix 7: Crossing point temperatures for samples ROM1 and ROM2 150
Appendix 8: Crossing point temperature histogram for No.S5 seam..... 150
Appendix 9: Crossing point temperature histogram for No.S4U seam 150
Appendix 10: Crossing point temperature histogram for No.S2 seam..... 151
Appendix 12: Derivative of weight gain No.S4Useam (TGA)..... 151
Appendix 11: Derivative of weight gain No.S2 seam (TGA) 151
Appendix 14: Histogram of weight gain (%) No.S4U seam (TGA)..... 152
Appendix 13: Histogram of weight gain (%) No.S2seam (TGA) 152
Appendix 16: Histogram of T1 of No.S5 seam (TGA)..... 152
Appendix 15: Histogram WT (%) No.S5 seam (TGA)..... 152
Appendix 18: Histogram of T1 of No.S2 seam..... 153
Appendix 17: Histogram of T1 of No.S4U seam (TGA) 153
Appendix 20: Histogram of peak temperature of No.S5 seam (TGA)..... 153
Appendix 19: Histogram of peak temperature of No.S5 seam (TGA)..... 153
Appendix 22: Oxygen absorption for sample Z01 at 3 degree C ramp (TGA 154
Appendix 21: Histogram of peak temperature of No.S2 seam (TGA 154
Appendix 24: Oxygen absorption for sample Z01 at 7 degree C ramp (TGA)..... 154
Appendix 23: Oxygen absorption for sample Z01 at 5 degree C ramp (TGA)..... 154
Appendix 26: Oxygen absorption for sample Z01 at 20 degree C ramp (TGA)..... 155
Appendix 25: Oxygen absorption for sample Z01 at 10 degree C ramp (TGA)..... 155
Appendix 27: Oxygen absorption mix for sample Z01 (TGA)..... 155
Appendix 28: Ignition test mix for sample Z01(TGA) 155
Appendix 29: Oxygen absorption for sample Z02 at 3 degree C ramp (TGA)..... 156
Appendix 30: Oxygen absorption for sample Z02 at 5 degree C ramp (TGA)..... 156
Appendix 32: Oxygen absorption for sample Z02 at 10 degree C ramp (TGA)..... 156
Appendix 31: Oxygen absorption for sample Z02 at 7 degree C ramp (TGA)..... 156
Appendix 34: Oxygen absorption mix for sample Z02 (TGA)..... 157
Appendix 33: Oxygen absorption for sample Z02 at 20 degree C ramp (TGA)..... 157
Appendix 36: Oxygen absorption for sample Z03 at 3 degree C ramp (TGA)..... 157

Appendix 35: Ignition test mix for sample Z02(TGA) 157
Appendix 38: Oxygen absorption for sample Z03 at 7 degree C ramp (TGA) 158
Appendix 37: Oxygen absorption for sample Z03 at 5 degree C ramp (TGA) 158
Appendix 40 Oxygen absorption for sample Z03 at 20 degree C ramp (TGA) 158
Appendix 39: Oxygen absorption for sample Z03 at 10 degree C ramp (TGA) 158
Appendix 42: Oxygen absorption for sample Z04 at 3 degree C ramp (TGA) 159
Appendix 41: Ignition test mix for sample Z03 (TGA) 159
Appendix 44: Oxygen absorption for sample Z04 at 7 degree C ramp (TGA) 159
Appendix 43: Oxygen absorption for sample Z04 at 5 degree C ramp (TGA) 159
Appendix 45: Oxygen absorption for sample Z04 at 10 degree C ramp (TGA) 160
Appendix 46: Oxygen absorption for sample Z04 at 20 degree C ramp (TGA) 160
Appendix 47: Ignition test mix for sample Z04 (TGA) 160
Appendix 48: Oxygen absorption for sample Z05 at 3 degree C ramp (TGA) 160
Appendix 50: Oxygen absorption for sample Z05 at 7 degree C ramp (TGA) 161
Appendix 49: Oxygen absorption for sample Z05 at 5 degree C ramp (TGA) 161
Appendix 52: Oxygen absorption for sample Z05 at 20 degree C ramp (TGA) 161
Appendix 51: Oxygen absorption for sample Z05 at 10 degree C ramp (TGA) 161
Appendix 53: Ignition test mix for sample Z05 (TGA) 162
Appendix 54: Oxygen absorption mix for sample Z05 (TGA) 162
Appendix 56: Oxygen absorption for sample Z06 at 5 degree C ramp (TGA) 162
Appendix 55: Oxygen absorption for sample Z06 at 3 degree C ramp (TGA) 162
Appendix 58: Oxygen absorption for sample Z06 at 10 degree C ramp (TGA) 163
Appendix 57: Oxygen absorption for sample Z06 at 7degree C ramp (TGA) 163
Appendix 60: Ignition test mix for sample Z06 (TGA) 163
Appendix 59: Oxygen absorption for sample Z06 at 20 degree C ramp (TGA) 163
Appendix 62: Oxygen absorption for sample Z07 at 3 degree C ramp (TGA) 164
Appendix 61: Oxygen absorption mix for sample Z06 (TGA) 164
Appendix 64: Oxygen absorption for sample Z07 at 5 degree C ramp (TGA) 164
Appendix 63: Oxygen absorption for sample Z07 at 7 degree C ramp (TGA) 164
Appendix 66: Oxygen absorption for sample Z07 at 20 degree C ramp (TGA) 165
Appendix 65: Oxygen absorption for sample Z07 at 10 degree C ramp (TGA) 165
Appendix 68: Oxygen absorption mix for sample Z07 (TGA) 165
Appendix 67: Ignition test mix for sample Z07 (TGA) 165
Appendix 70: Oxygen absorption for sample Z08 at 5 degree C ramp (TGA) 166
Appendix 69: Oxygen absorption for sample Z08 at 3 degree C ramp (TGA) 166
Appendix 72: Oxygen absorption for sample Z08 at 10 degree C ramp (TGA) 166
Appendix 71: Oxygen absorption for sample Z08 at 7 degree C ramp (TGA) 166
Appendix 74: Ignition test mix for sample Z08 (TGA) 167
Appendix 73: Oxygen absorption for sample Z08 at 20 degree C ramp (TGA) 167
Appendix 76: Oxygen absorption for sample Z09 at 3 degree C ramp (TGA) 167
Appendix 75: Oxygen absorption mix for sample Z08 (TGA) 167
Appendix 77: Oxygen absorption for sample Z09 at 5 degree C ramp (TGA) 168
Appendix 78: Oxygen absorption for sample Z09 at 7 degree C ramp (TGA) 168
Appendix 79: Oxygen absorption for sample Z09 at 10 degree C ramp (TGA) 168
Appendix 80: Oxygen absorption for sample Z09 at 20 degree C ramp (TGA) 168
Appendix 82: Oxygen absorption mix for sample Z09 (TGA) 169
Appendix 81: Ignition test mix for sample Z09 (TGA) 169
Appendix 84: Oxygen absorption for sample Z10 at 5 degree C ramp (TGA) 169
Appendix 83: Oxygen absorption for sample Z10 at 3 degree C ramp (TGA) 169
Appendix 85: Oxygen absorption for sample Z10 at 7 degree C ramp (TGA) 170
Appendix 86: Oxygen absorption for sample Z10 at 10 degree C ramp (TGA) 170
Appendix 88: Ignition test mix for sample Z10 (TGA) 170

Appendix 87: Oxygen absorption for sample Z10 at 20 degree C ramp (TGA) 170
Appendix 90: Oxygen absorption for sample Z11 at 5 degree C ramp (TGA) 171
Appendix 89: Oxygen absorption for sample Z11 at 3 degree C ramp (TGA) 171
Appendix 92: Oxygen absorption for sample Z11 at 10 degree C ramp (TGA) 171
Appendix 91: Oxygen absorption for sample Z11 at 7 degree C ramp (TGA) 171
Appendix 94: Ignition test mix for sample Z11 (TGA) 172
Appendix 93: Oxygen absorption for sample Z11 at 20 degree C ramp (TGA) 172
Appendix 96: Oxygen absorption for sample Z12 at 5 degree C ramp (TGA) 172
Appendix 95: Oxygen absorption for sample Z12 at 3 degree C ramp (TGA) 172
Appendix 98: Oxygen absorption for sample Z12 at 10 degree C ramp (TGA) 173
Appendix 97: Oxygen absorption for sample Z12 at 7 degree C ramp (TGA) 173
Appendix 100: Ignition test mix for sample Z12 (TGA) 173
Appendix 99: Oxygen absorption for sample Z12 at 20 degree C ramp (TGA) 173
Appendix 102: Oxygen absorption for sample Z13 at 3 degree C ramp (TGA) 174
Appendix 101: Oxygen absorption mix for sample Z12 (TGA) 174
Appendix 104: Oxygen absorption for sample Z13 at 7 degree C ramp (TGA) 174
Appendix 103: Oxygen absorption for sample Z13 at 5 degree C ramp (TGA) 174
Appendix 106: Oxygen absorption for sample Z13 at 20 degree C ramp (TGA) 175
Appendix 105: Oxygen absorption for sample Z13 at 10 degree C ramp (TGA) 175
Appendix 108: Oxygen absorption for sample Z14 at 3 degree C ramp (TGA) 175
Appendix 107: Ignition test mix for sample Z13 (TGA) 175
Appendix 110: Oxygen absorption for sample Z14 at 7 degree C ramp (TGA) 176
Appendix 109: Oxygen absorption for sample Z14 at 5 degree C ramp (TGA) 176
Appendix 112: Oxygen absorption for sample Z14 at 20 degree C ramp (TGA) 176
Appendix 111: Oxygen absorption for sample Z14 at 10 degree C ramp (TGA) 176
Appendix 114: Oxygen absorption for sample Z15 at 3 degree C ramp (TGA) 177
Appendix 113: Ignition test mix for sample Z14 (TGA) 177
Appendix 116: Oxygen absorption for sample Z15 at 7 degree C ramp (TGA) 177
Appendix 115: Oxygen absorption for sample Z15 at 5 degree C ramp (TGA) 177
Appendix 118: Oxygen absorption for sample Z15 at 20 degree C ramp (TGA) 178
Appendix 117: Oxygen absorption for sample Z15 at 10 degree C ramp (TGA) 178
Appendix 120: Oxygen absorption for sample Z16 at 3 degree C ramp (TGA) 178
Appendix 119: Ignition test mix for sample Z15 (TGA) 178
Appendix 122: Oxygen absorption for sample Z16 at 7 degree C ramp (TGA) 179
Appendix 121: Oxygen absorption for sample Z16 at 5 degree C ramp (TGA) 179
Appendix 124: Oxygen absorption for sample Z16 at 20 degree C ramp (TGA) 179
Appendix 123: Oxygen absorption for sample Z16 at 10 degree C ramp (TGA) 179
Appendix 125: Ignition test mix for sample Z16 (TGA) 180
Appendix 126: Oxygen absorption for sample Z17 at 3 degree C ramp (TGA) 180
Appendix 128: Oxygen absorption for sample Z17 at 7 degree C ramp (TGA) 180
Appendix 127: Oxygen absorption for sample Z17 at 5 degree C ramp (TGA) 180
Appendix 130: Oxygen absorption for sample Z17 at 20 degree C ramp (TGA) 181
Appendix 129: Oxygen absorption for sample Z17 at 10 degree C ramp (TGA) 181
Appendix 132: Oxygen absorption for sample Z18 at 3 degree C ramp (TGA) 181
Appendix 131: Ignition test mix for sample Z17 (TGA) 181
Appendix 134: Oxygen absorption for sample Z18 at 7 degree C ramp (TGA) 182
Appendix 133: Oxygen absorption for sample Z18 at 5 degree C ramp (TGA) 182
Appendix 136: Oxygen absorption for sample Z18 at 20 degree C ramp (TGA) 182
Appendix 135: Oxygen absorption for sample Z18 at 10 degree C ramp (TGA) 182
Appendix 138: Oxygen absorption for sample Z19 at 3 degree C ramp (TGA) 183
Appendix 137: Ignition test mix for sample Z18 (TGA) 183
Appendix 140: Oxygen absorption for sample Z19 at 7 degree C ramp (TGA) 183

Appendix 139: Oxygen absorption for sample Z19 at 5 degree C ramp (TGA) 183
Appendix 142: Oxygen absorption for sample Z19 at 20 degree C ramp (TGA) 184
Appendix 141: Oxygen absorption for sample Z19 at 10 degree C ramp (TGA) 184
Appendix 144: Oxygen absorption for sample Z20 at 3 degree C ramp (TGA) 184
Appendix 143: Ignition test mix for sample Z19 (TGA) 184
Appendix 146: Oxygen absorption for sample Z20 at 7 degree C ramp (TGA) 185
Appendix 145: Oxygen absorption for sample Z20 at 5 degree C ramp (TGA) 185
Appendix 148: Oxygen absorption for sample Z20 at 10 degree C ramp (TGA) 185
Appendix 147: Oxygen absorption for sample Z20 at 10 degree C ramp (TGA) 185
Appendix 150: Oxygen absorption for sample Z21 at 3 degree C ramp (TGA) 186
Appendix 149: Ignition test mix for sample Z20 (TGA) 186
Appendix 152: Oxygen absorption for sample Z21 at 7 degree C ramp (TGA) 186
Appendix 151: Oxygen absorption for sample Z21 at 5 degree C ramp (TGA) 186
Appendix 154: Oxygen absorption for sample Z21 at 20 degree C ramp (TGA) 187
Appendix 153: Oxygen absorption for sample Z21 at 10 degree C ramp (TGA) 187
Appendix 156: Oxygen absorption for sample Z22 at 3 degree C ramp (TGA) 187
Appendix 155: Ignition test mix for sample Z21 (TGA) 187
Appendix 158: Oxygen absorption for sample Z22 at 7 degree C ramp (TGA) 188
Appendix 157: Oxygen absorption for sample Z22 at 5 degree C ramp (TGA) 188
Appendix 160: Oxygen absorption for sample Z22 at 20 degree C ramp (TGA) 188
Appendix 159: Oxygen absorption for sample Z22 at 10 degree C ramp (TGA) 188
Appendix 162: Oxygen absorption for sample ROM1 at 3 degree C ramp (TGA) 189
Appendix 161: Ignition test mix for sample Z22 (TGA) 189
Appendix 164: Oxygen absorption for sample ROM1 at 7 degree C ramp (TGA) 189
Appendix 163: Oxygen absorption for sample ROM1 at 5 degree C ramp (TGA) 189
Appendix 166: Oxygen absorption for sample ROM1 at 20 degree C ramp (TGA) 190
Appendix 165: Oxygen absorption for sample ROM1 at 10 degree C ramp (TGA) 190
Appendix 168: Oxygen absorption for sample ROM2 at 3 degree C ramp (TGA) 190
Appendix 167: Ignition test mix for sample ROM1 (TGA) 190
Appendix 170: Oxygen absorption for sample ROM2 at 7 degree C ramp (TGA) 191
Appendix 169: Oxygen absorption for sample ROM2 at 5 degree C ramp (TGA) 191
Appendix 172: Oxygen absorption for sample ROM2 at 20 degree C ramp (TGA) 191
Appendix 171: Oxygen absorption for sample ROM2 at 10 degree C ramp (TGA) 191
Appendix 174: Correlation between derivative of weight gain and % weight gain (TGA) 192
Appendix 173: Ignition test mix for sample ROM2 (TGA) 192
Appendix 176: Histogram of oxygen absorption test for No.5 seam (Smith-Glasser) 192
Appendix 175: Correlation between % oxygen (ultimate) and % weight gain (TGA) 192
Appendix 177: Histogram of oxygen absorption test for No.4U seam (Smith-Glasser) 193
Appendix 178: Histogram of oxygen absorption test for No.2 seam (Smith-Glasser) 193
Appendix 179: Correlation between of oxygen absorption and crossing point temperature for combined seams 193
Appendix 180: Chemical analysis of samples Z1-Z22, ROM1-2 from SGS laboratories 194
Appendix 181: Abnormal condition analysis performed at Wits University (Z1-Z22) 197
Appendix 183: Micrograph showing fresh particle and fusinite 199
Appendix 182: Micrograph showing highly cracked inertinite 199
Appendix 185: Micrograph showing fresh inertinite 199
Appendix 184: Micrograph showing highly cracked inertinit 199
Appendix 187: Micrograph showing framboidal pyrite 200
Appendix 186: Micrograph showing fresh vitrinite and pyrite nodules 200
Appendix 188: Coal maceral analysis 201
Appendix 189: Vitrinite random reflectance 203
Appendix 190: Abbreviations and terms 205

Appendix 191: Major coal characteristics 206
Appendix 193: No. S4U seam mudstone floor thickness 208
Appendix 192: No.S5 seam mudstone floor thickness 208
Appendix 194: No.S2U seam mudstone floor thickness 209
Appendix 195 :Frequency analysis for risk matrix grids 209
Appendix 198: sponcom image 210
Appendix 199: sponcom image 210
Appendix 200: sponcom image 210
Appendix 201: sponcom image 210
Appendix 202: Difference between sample database correlations and modelling dataset correlations 211

LIST OF ACRONYMS

Acronym	Description
AB	Abnormal condition analysis
ALG	Alginite
AS	Ash
C	total carbon
Colliery X	study area
CPT	crossing point temperature
CV	calorific value
DER	derivative weight gain
F/SEC	Fusinite/secretinite
FC	fixed carbon
GLI	oxygen absorption (Smith-Glasser)
H	Hydrogen
I INT	Inert inertodetrinite
IM	inherent moisture
ISF	Inert semifusinite
MIC	Micrinite
MST	Mudstone seam thickness
N	Nitrogen
O	Oxygen
OS	organic sulphur
PS	pyritic sulphur
PV	Pseudovitrinite
R INT	Reactive inertodetrinite
RD	relative density
RIT	relative ignition temperature
Rmax %	Maximum reflectance of vitrinite (calculated)
Rr %	Random reflectance of vitrinite, oil immersion (determined)
RSF	Reactive semifusinite
S/R/C	Sporinite/resinite/cutinite
S2	No. 2 coal seam
S4	No. 4 coal seam
S5	No. 5 coal seam
SPONCOM	spontaneous combustion
SS	sulphate sulphur

T1	start temperature
T2	peak temperature
TGA	thermogravimetric analysis
TOT I	Total inertinite
TOT L	Total liptinite (formerly referred to as exinite)
TR	total reactives
TS	total sulphur
TV	Total vitrinite
VIT	Vitrinite
VM	volatile matter
WT	weight gain

1 BACKGROUND

The estimation of the propensity of remnant underground coal pillars to spontaneously combust during opencast mining is highly variable and a challenge to predict. The most common occurrence of spontaneous combustion (sponcom) is when surface mines extract seams previously partially mined by underground bord and pillar methods.

Furthermore, the fact that different types of coals have different spontaneous heating characteristics makes it necessary for the coal to be classified according to its susceptibility to spontaneously combust in order to decide on safety measures in its handling. The classification is based on two principles (Banerjee, 1981).

- examination of coal constituents; involving petrological examination;
- studies on coal-oxygen interaction; involving the determination of oxygen-avidity and thermal behaviour during oxidation

With the growth of knowledge and the accumulation of large amounts of test data it is now being realized that the problem of indexing the susceptibility to spontaneous combustion remains elusive (Banerjee, 1981; Chandra et al., 1987) because of certain inherent deficiencies. Some of these are:

- The inability to simulate seam conditions in the laboratory for the sample to be tested.
- Any one or even a group of tests cannot accurately determine the degree of sponcom susceptibility nor integrate all the factors responsible for sponcom (Banerjee, 1981 and Chandra et al., 1987).
- Within narrow ranges of low rank coal (volatile matter more than 35%, oxygen 7-12% and moisture 4-6%) the values of CPT do not change much. (Nandy et al., 1972).
- Empirical tests are unable to ascertain which one factor, or which combination of factors, is responsible for causing spontaneous combustion. A single factor by itself (for example, a rain storm) can in one instance trigger the reaction. At a different time and place, the same factor, even in combination with others, might fail to cause spontaneous combustion.

1.1 Occurrence of Spontaneous combustion

Spontaneous combustion of coal occurs wherever coal is mined, stored or transported. The causes of the phenomenon are multifactorial and sometimes difficult to predict. Exact figures on the location and frequency of mine fires attributed to self-heating are not readily available, although historical data regarding the world's major coalfields does give a reasonable idea of the scale of the problem.

Different terms have been used by researchers to refer to the phenomenon of spontaneous combustion. These include: spontaneous combustion, self-heating, incipient heating, spontaneous heating, spontaneous ignition and autogenous heating (Wade, 1988).

Self-oxidation and spontaneous combustion of coals is a problem of global concern (Figure 1.1). There are social, economic and environmental costs associated with this phenomenon and major incidents can, in extreme cases, lead to human casualties. More often however, damage is made to commercial facilities, the calorific value of the fuel is reduced and substantial release of noxious gases, particulate matter and CO_2 may contribute to local and international pollution levels (Avila, 2012).

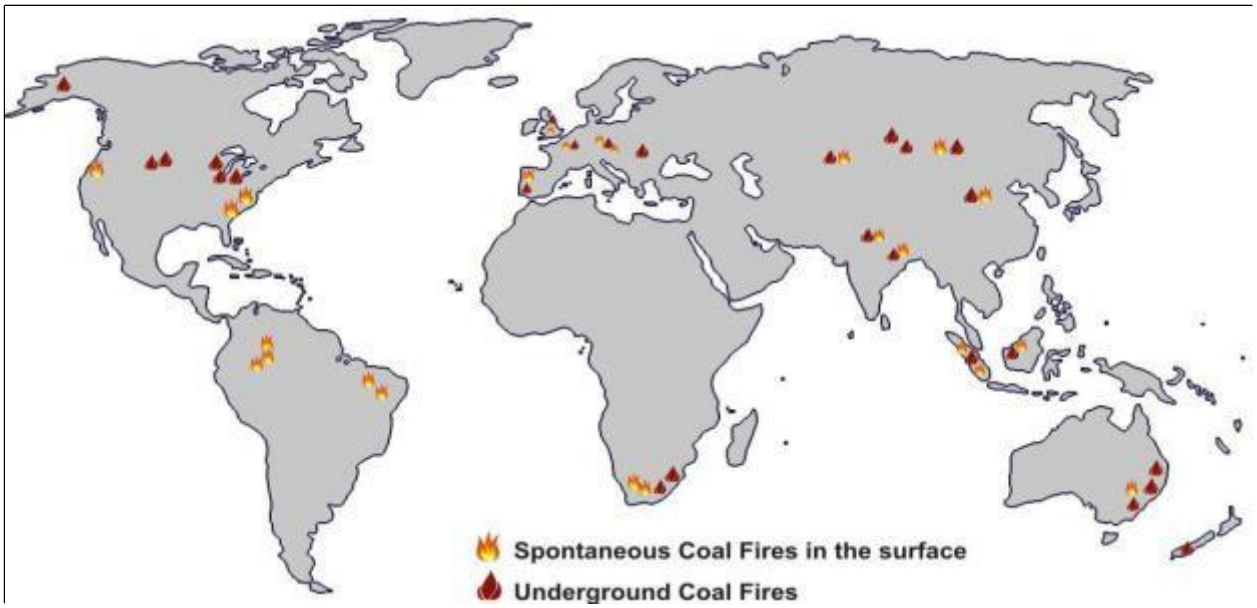


Figure 1.1: Distribution of major global coal fire events (after Avila, 2012)

Stracher and Taylor (2004) listed major coal fires from around the world, namely: Xinjiang coal field in Northern China; Rujigou coalfield in Ningxia, China; Pennsylvanian coal fires in the United States; and the Jharia Coalfield (JCF) in Bihar , India. Wherever coal is strip or deep mined, the potential for fire exists. Coal fires associated with the abandoned workings or workings of coal mines are reported from mining areas around the world.

Although there have been many cases of spontaneous combustion in underground coal mines in South Africa, in surface dumps, in shallow workings in the vicinity of Witbank and even in ships carrying export coal from South Africa, the biggest problem currently is in surface mining. While it is unusual for intact seams to burn in the highwall, the most common occurrence is when surface mines extract seams previously partially mined by underground bord and pillar operations. Once exposed to air the pillars that had been left from the previous mining operations start to burn within days and require special prevention and control techniques.

Current literature indicates that spontaneous combustion is now rare in underground coal mines in South Africa. The Witbank and Sasolburg coalfields experience spontaneous combustion mostly in surface mines that were previously mined by bord and pillar methods (Coaltech, 2011).

In China, the world‘s biggest coal producer with an annual output around 2.5 billion tons, coal fires are a dangerous problem. It has been calculated that some 10-20 million tons of coal are lost to sponcom annually, and that the same amount again is rendered inaccessible to mining. Up to 10 coal fires per year in the Ruhr area of Germany are induced by spontaneous heating. In the JCF Coalfield in India, about 1864 million tonnes of coal is inaccessible from about 65 fires spread over an area of 17.32 sq. km. This constitutes a staggering 12% of the total coal reserves. Many coalfields in the USA are subject to spontaneous heating. The Federal Office of opencast Mining (OSM) asserts a database (AMLIS), which in 1999 named 150 fire zones. In Pennsylvania, 45 fires zones are known, the most famed being the fire in the Centralia mine in the hard coal region of Columbia County (Singh, 2013).

1.2 Basic concepts of self-oxidation

Self-heating in coal has been extensively studied. The tendency to self-heating decreases with increasing rank of the coal. Lignite coals are more reactive than bituminous coals, which, in turn, are more reactive than anthracite coals. Freshly mined coal consumes oxygen more rapidly than weathered coal, and freshly mined coal self-heats to a greater extent than weathered coal. The presence of water vapor may also be important, as the rate of heat generation accompanying the absorption of water in dry coal from saturated air can be an order of magnitude or more than the same amount of dry air (Bowes, 1984).
In general, the following, often interrelated, properties of coal are said to affect spontaneous combustion of coal (Kaymakci and Didari, 2002).

1.2.1 Intrinsic factors

- Moisture content and volatile matter
- Particle size and available surface area
- Mineral matter type and pyrite content in particular
- Coal rank, and
- Petrographic composition (coal type)

1.2.2 Extrinsic factors

- Climatic conditions (temperature, relative humidity, barometric pressure and oxygen concentration)
- Stockpile compaction, as related to height and method of stockpiling
- Dump consolidation, influenced by height, method of formation and equipment used
- The presence of timber or other organic waste material in abandoned areas or dumps

- Excavation stability and maintenance (for open-cut highwall faces)
- Strata conditions, method of working and ventilation (for shallow underground workings).

In underground mines that use a bord and pillar mining system, a relatively large portion (30-60%) of the coal is left in place. The roof coals, floor coals and carbonaceous shales are also left in the mine. The tonnage of combustible material remaining in the mine may exceed that extracted during mining (Dalverney and Chaiken, 1991).Surface expressions of underground coal fires observable in the field include baked rocks, areas of dead vegetation, land subsidence, and gas vents and fissures with encrusted mineral (Gupta and Prakash, 1998).Fractured and faulted thick coal seams with pyrite and organic shale partings are particularly susceptible to spontaneous combustion (Falcon, 1986).

The minimum temperature in which a coal will self-heat is about 35 degrees Celsius (°C) for lignite,subbituminous,and high volatile bituminous coal ,135 °C for bituminous coal and 140 °C for anthracite coal (Smith and Larazza,1987). Smouldering fires of coal can burn in shallow or deep fronts and each has different dynamics. A shallow front burns near the free surface and is open to the atmosphere, thus having large supplies of oxygen available but exposed to convective heat losses. A deep subsurface fire burns many meters below the ground and thus has a limited supply of oxygen but is insulated from heat losses to the atmosphere (Hadden and Rein, 2010).

The fundamental difference between smouldering and flaming combustion is that, in the former, the oxidation reaction and the heat released occur in the solid surface of the fuel. In flaming combustion, these occur in the gas phase surrounding the fuel. Low temperature smouldering is characteristically an incomplete oxidation reaction and thus emits a mixture of unburned fuel and toxic gases. Carbon monoxide (CO) is an important factor in smouldering fires (Purser, 2002).

1.3 Aim of the study

The aim of the study is to provide a predictive model (matrix) of the spontaneous combustion potential of remnant pillars at Colliery X. A number of different thermal, chemical and petrographic tests (coal factors) will be undertaken to determine their individual and collective impacts on the sponcom predictive model.

It is known that mining factors contribute significantly to self-heating; however these factors will be ignored in the predictive model. Coal factors and Geological factors will therefore be used in creating the sponcom matrix. Most of the previous research indicates that an absolute scale to determine sponcom risk has not yet been established and would remain improbable given the multifactorial nature of this phenomenon. Due to chemical differences in the No.5 seam, No.4U seam and No.2

seam, each of the economic zones will be modelled individually and later a composite matrix created for the combined seams. The North-South extent of the mined out pillars is approximately 12km.

The individual and collective results of the sponcom tests for each seam will be modelled in a geological computer programme (Minex 6.05) and presented as contour plans for each parameter. The composited individual factors will then be combined to produce a sponcom risk matrix based on multiple factors. The influence of geological structures and igneous intrusions is known to influence sponcom but due to their linear nature or geometry are difficult to model in the same way as the laboratory and borehole data.

Several indices such as the Oplinski and FCC (Banerjee,1985) have been used historically and include mining parameters such as ventilation method and intensity,ventilation pressure differential and mining method etc.As the mining factors are not as yet detrmined the predictive model is based on equal weighting of geological and coal factors.

For the purpose of this excersize an equal weighting is given to each of the factors used in modelling.No accepted standard exists for the weighting of sponcom risk factors and several empirical matrixes have been used in different countries to predict liability of coal to self heating.

The risk factors to be modelled at Colliery X to create a sponcom risk matrix are assigned an arbitary weighting of :

- 0 (low risk),
- 1(moderate risk) or
- 2(high risk)

The following factors (table 1.1) will be incorperated into the sponcom model to develop a risk matrix for each coal seam.

Table 1.1:Factors used in developing a sponcom risk matrix at Coliery X.

Geological Factors	Coal Factors		
	Chemical	Thermal	Petrographic
seam thickness	ash	crossing point temperature	*vitrinite reflectance
overburden depth	volatile matter	oxygen absorption	abnormal condition analysis
mudstone roof/floor thickness	inherent moisture	thermogravimetric analyses	total reactives
parting thickness	total sulphur		

* calculated with mineral matter

Once mining commences it may be possible to create a model that does not use an arbitrary weighting of the individual factors. Rather a model that is weighted more toward the most influential sponcom factors could be generated A total of 15 variables will be used to generate contour plans of individual and cumulative risk factors.The different sponcom categories will be added up to produce a final risk matrix.Predictive models have been built by different authors using different criteria,but ultimately the aim is to give some indication of the potential risk of spontaneous combustion.By cretaing a visual spatial distribution of sponcom risk factors for each seam ,the pillar areas more likely to produce coal losses by insitu burning when mined are highlighted.

1.4 Geology

1.4.1 Formation of Coal

Coal swamps were formed at a site in which carbonaceous sediments could accumulate by erosion and retreat of shallow seas. The consistent gradual rise in sea level or continuous slow land subsidence was required for between 1000 and 100000 years to form a 10m peat deposit which would convert to a 1.5m coal seam (Ashley, 1928). The rate of sediment deposition within or immediately above the peat would affect the concentration of syngenetic minerals, while sandstones deposited above a coal seam could increase the concentration of epigenetic minerals (McCulloch et al., 1975).

Peat formation is considered the biochemical stage of coal formation, during which plant residues are partially decomposed. The geochemical stage of coalification is a continuous and irreversible process that produces a rock from the organic sediment. In the long term, coalification produces progressively higher rank coals from lignite through subbituminous, high-volatile bituminous, medium volatile bituminous, low volatile bituminous to anthracite (ASTM,2005). Heat and pressure are the primary agents of coal metamorphism, rather than time (Figure 1.3). Temperature and pressure increase with depth, high temperature is also related to folding and faulting and to the presence of igneous intrusions. The first step in coalification is the removal of water due to the weight of overlying sediments. An increase in the carbon concentration and a decrease in the hydrogen and oxygen concentrations are noted in higher rank coals (Hessley and Riley, 1986).



Figure 1.3 - Different ranks of coal and their chemical ranges (daf basis) (Avila 2012).

Coal comes in four main levels of rank or maturity: lignite or brown coal, bituminous coal or black coal, anthracite and graphite. Each rank of coal has a certain set of physical parameters which are mostly controlled by moisture, volatile content (in terms of aliphatic or aromatic hydrocarbons) and carbon content (Wikipedia).

Coal macromolecules are formed from altered biopolymers in plants (Hatcher and Clifford, 1997). Dehydroxylation, ether cleavage, and demethylation are proposed mechanisms by which brown coal and lignite are produced from lignin. The removal of alkyl side chains and condensation reactions are assumed to account for increasing aromatic character. Coalification to the bituminous rank involves the reduction in oxygen content through pyrolitic condensation to form polycyclic aromatic ring structures with the loss of side chain carbons. During geochemical coalification, there is an increase in carbon content, and a decrease in concentration of oxygen and hydrogen. Humic structures become more aromatic, and alkyl chains are split off to form CO_2 and CH_4 (Teichmuller and Teichmuller, 1967). Anomalous variations in rank unrelated to depth of burial or igneous activity have been attributed to the transient geothermal gradients due to the migration of hydrothermal fluids (Hower and Gayer, 2002).

Vitrinite reflectance is the percentage of light reflected from the surface of polished vitrinite. It is a standard measurement used to classify organic rocks into degrees of maturity, and standard values are associated with various ranks of coal (Table 1.2). According to Cooper (1996), the time-

temperature index (TTI), based on both laboratory studies and observations of reflectance and temperature in drill holes, assumes the vitrinite reflectance doubles for every 10 degrees Celsius increase in temperature. In another laboratory experiment (Dalla Tore et al., 1997) the change in vitrinite reflectance was determined over a pressure range of 0.5-20.0kbar at temperatures between 300 and 350 ^{o}C.The results indicate that applied pressure suppressed increase in vitrinite reflectance.

On the basis of proximate analysis, coal is composed of inherent moisture, ash (mineral matter), volatile matter, and fixed carbon (by difference). Coal-mineral matter includes a variety of minor or trace elements and can vary considerably within and between different seams. Ultimate analysis of coal is the determination of the carbon, hydrogen, sulphur, nitrogen and oxygen. On a microscopic scale, three macerals, the organic equivalents of minerals (ASTM, 2005) are identified, namely: vitrinite, liptinite and inertinite. Vitrinite is the predominant maceral in coal and has a relatively high concentration of oxygen and a moderate amount of hydrogen and volatile matter. Liptinite is rich in hydrogen and is primarily aliphatic. Inertinite is aromatic and has low volatile matter content (Petrakis and Grandy, 1980).

Table 1.2: Coal classification by rank and vitrinite reflectance

Coal Rank		% Ro			
Class	Group	Range *	Random ^	Maximum ^	Minimum #
Anthracite	Meta-anthracite				
	Anthracite		6.55	7	2.5
	Semi-anthracite		2.65	2.83	1.92
Bituminous	Low volatile		1.85	1.97	1.51
	Medium volatile	1.00-1.40	1.49	1.58	1.12
	High volatile	0.3-1.00			0.5
Subbituminous		<0.40-0.6	0.6	0.63	0.42
Lignite			0.4	0.42	

*Pearson Coal Petrography
^White 2002
Smith et al. (1994)

1.4.2 Local Geology

The primary geology at the mine is conformable with that of the Witbank Coalfield. Coal deposition was largely controlled by glacial pre-Karoo topography. The undulating floor dips gently (<2 degrees) towards the south and strongly influenced sedimentation patterns and the extent of various coal seams. The lower coal measures abut against basement highs comprising of Dwyka tillite and the pre-Karoo Bushveld Igneous Complex felsites. The formation of the thick coal deposits took place in the deeper parts of the basin, while the coal seams thinned rapidly or petered out against the palaeo high areas. Figure 1.4 depicts the main coalfields in South Africa and Figure 1.5 shows a generalized stratigraphic column of the study area.

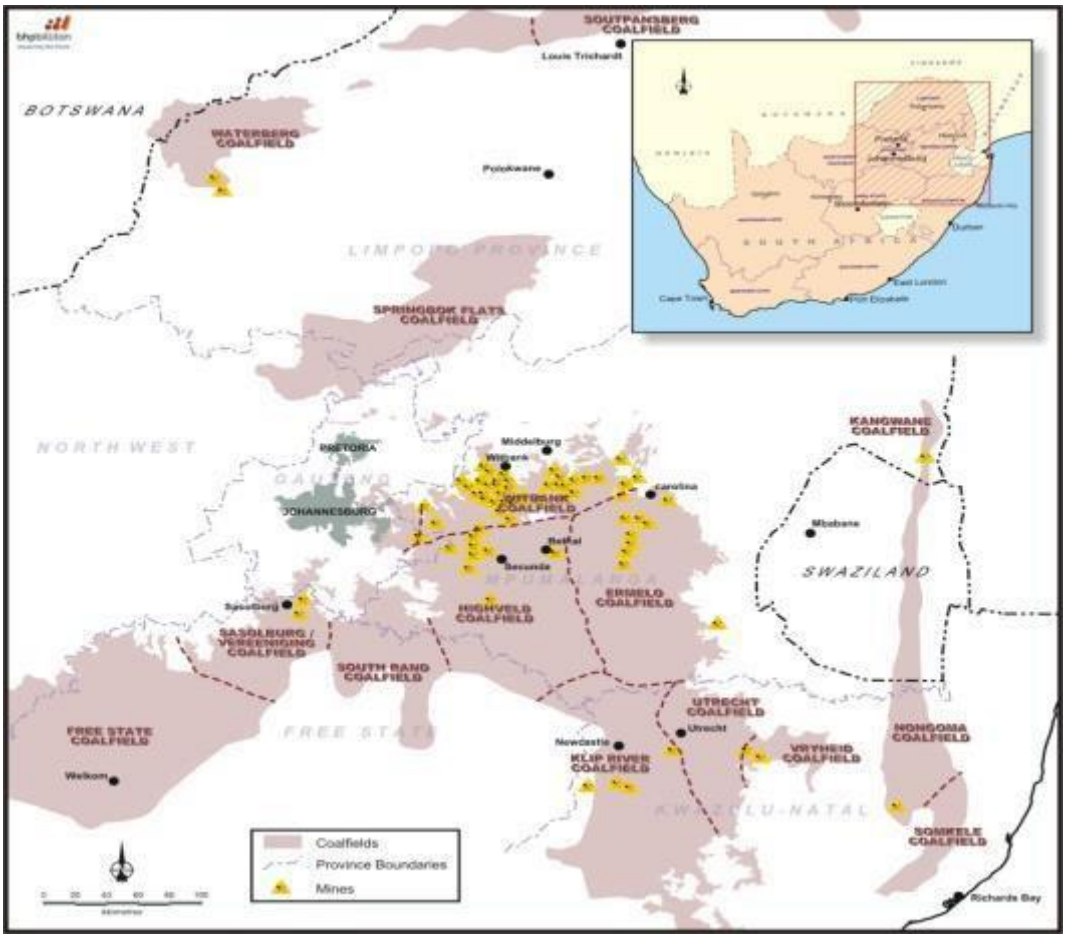


Figure 1.4: Locality plan of the main Coalfields in South Africa

Five distinct coal seams, or major splits of these seams, of interest to this study are in stratigraphical order from top to bottom, No.5 seam, No.4U seam, No.4L seam, No.3 Seam, No. 2 seam and No.1 seam. Of primary economic interest are the No. 5, No.4U and No.2 seams. The No 2 seam is thinner to the north of the lease area whereas the No 4 upper seam has a more consistent thickness. Seam thickness (>5m) and parting thickness (>2m) are included in the risk matrix as geological factors affecting sponcom liability.

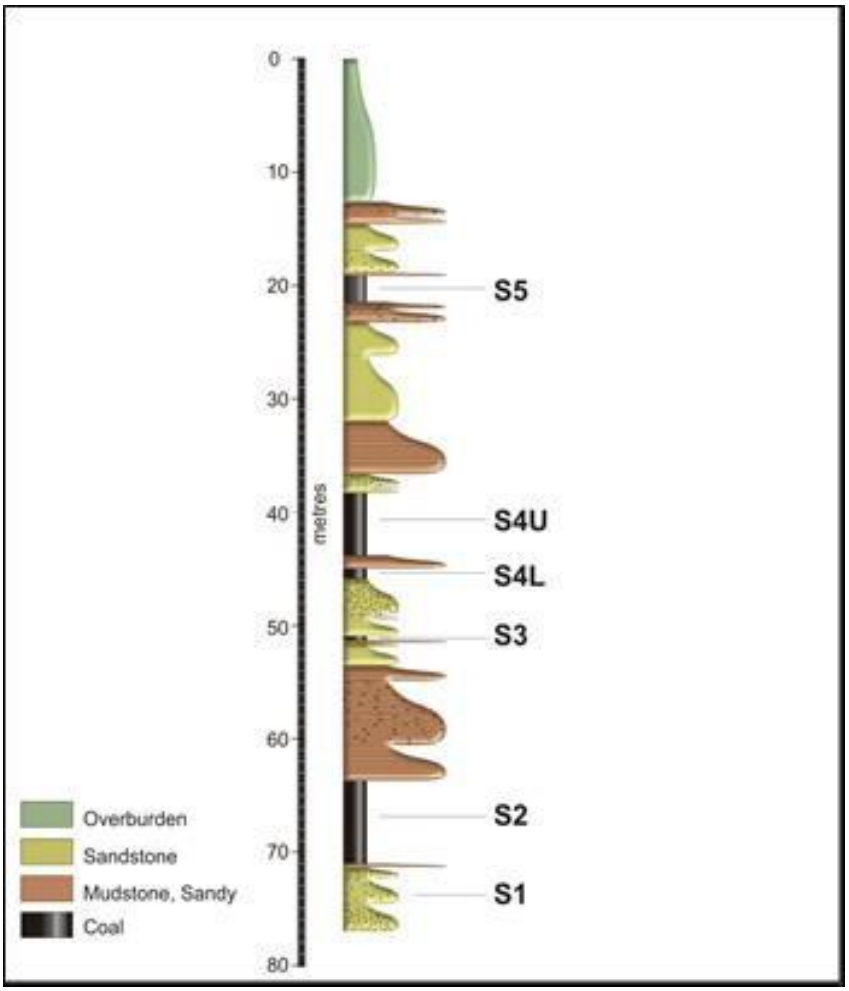


Figure 1.5: Local stratigraphic column of the study area

The No 2 seam is up to 9m thick and thins against the basement palaeohigh structures. The current mining height for bord and pillar sections ranges between 3.8-4.5m which leaves 1-4m of coal in the floor over most of the area (appendix 1 -3).The No 4U seam is up to 8m thick and is less affected by basement high structures. The seam thickness and qualities are less variable than the No.2 seam. Select mining of the 4P (primary) cut has resulted in 1-3m of coal being left in the roof horizon (appendix 2-4).The No.5 seam is well developed over most of the mined out pillar areas with a thickness of 1-2 m. The seam is mostly unmined and coal qualities are of export grade.

Parting thicknesses include all bands with >50% ash. The individual bands are added together to model a total parting thickness. Individual sandstone and mudstone bands are also modelled but are not continuous in all the areas. These are used in mine planning to select the best mining plies for the seam. Parting thicknesses include all bands with >50% ash. The S4U tends to have more argillaceous material in the partings compared to the No.2 seam partings which are more siliceous.

The No 5 seam is consistently developed across the property and where absent is mainly due to weathering and to a lesser extent the palaeo ridges. This good quality bright-banded coal seam with an average thickness of 1.95m is not dedicated to the Power station.

The depth of cover to the seams generally increases in the southern portions of the mine property. The depth to the roof of the No.5, No.4U and No.2 seams is approximately 87m, 100m and 130m respectively along the southern edge of the property. The parting thickness between the two top seams is fairly constant while the thickness between the No.4U and No.2 seams increases from approximately 10m in the north to 20m in the south (unreferenced-unpublished). Shallow seams are more prone to sponcom as they may be connected to the surface via structure and depth of seam is included in the risk matrix if less than 40m deep. Multiple seams operations are also more liable to sponcom than single seam operations.

The No 2 seam overburden thickness ranges between 40-140m and generally increases to the southern lease boundary. The No.4U seam overburden thickness ranges between 20-120m and generally increases to the southern lease boundary. The No.5 seam overburden thickness ranges between 20-80m and generally increases to the southern lease boundary. The depth of cover has a similar trend for all the mineable seams with the central and northern portions having the lowest potential strip ratios. The No. 5 seam is too deep to mine alone by opencast methods and would have to be mined with the No.2 and No.4U seams to achieve an optimal cumulative strip ratio.

1.4.3 Structure

Generally, the coal bearing strata in the region are flat lying and little structural disturbance to the coal seams is noted. However, a major graben structure transects the north-central mine boundary striking northeast southwest and effectively divides the property into distinct Northern and Southern areas. This feature consists of a block, down faulted by up to 20m and is on average 120m in width. The coal to the south of this feature is accessed by two development sections.

A number of identified dolerite dykes transect the property and have led to coal deterioration in its immediate proximity through the loss of volatiles (heat oxidation, cinder zones). The dykes are generally less than 2m in thickness, near vertical and cause fracturing and deeper than normal weathering along their contacts. From the underground mine workings, the position of the dykes that have been encountered during mining have been mapped and projected into future mining areas. These narrow dykes cannot be reliably located with surface-based exploration practices without great expense. Potentially, additional unmapped dykes may be encountered in the future and will have some impact on mining. Dykes are associated with devolatilization and reconcentration of these volatiles several meters away from the intrusion possibly increasing

sponcom risk. Associated fracturing adjacent dykes will also allow more air flow and exposure of the seams to oxygen.

In terms of faulting, the mine property has a number of nested north-south striking normal dip-slip faults that have limited displacement (<2m) in the area north of the graben. The majority of these faults have been intersected by the underground workings of the No. 4U and No.2 seams in this area, and are well identified. To the south-east of the mine, a large fault (displacement 2-4m) transects the coal seams on a north-south orientation. This has influenced the layout of underground workings and has been taken into consideration in the planning of future underground panels.

There are two sets of northwest-southeast orientated faults that were identified in drilling and lie across potential future mining areas. Note the exaggeration of the vertical scale. A structural plan showing the main geological features interpreted from underground mapping are shown in figure 1.14.Geological structure provides access of air and moisture to the coal seams and thus increases sponcom liability.

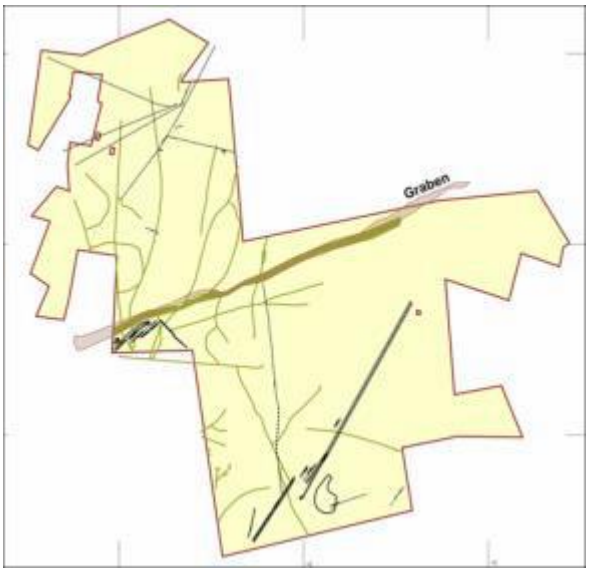


Figure 1.14: Dyke and fault plan Colliery X

1.5 Coal qualities

The No.2 seam and No.4 seam at Colliery X are mined for a nearby power-station. The No.5 seam has historically been sold as a local metallurgical coal and export thermal coal, and would require testing to verify its suitability to use in the power-station. The heat values of the main economic seams (S5, S4U and S2) are shown in Table 1.3.The heat value of the No.2 seam declines significantly to the south of the lease area. The heat value of the No.4U seam shows less variability than the No.2 seam but is generally of lower quality. Coal qualities have a significant effect on self-heating

propensity with ash(AS%),inherent moisture(IM%),volatile matter (VM%) and total sulphur (TS%) included in the risk matrix. The select mining horizons do show quality variation that may favour sponcom origin in some of these zones (Seam 2B has low ash and seam 4P has relatively high volatile matter). The effect of washing the coal at 1.8WD (destoning) will reduce the yields of the No.2 seam and No.4 seam by 25% and 35% respectively.

Table 1.3: Resource quality ranges at Colliery X

Pillar Resources at Colliery X-approximate ranges				
Seam	Thickness m	CV MJ/kg	VM %	TS %
S5	1.5-2.5	22-26	25-30	<1.7
S4U	1.8-8.0	18-22	19-22	<1.3
S2	1.8-9.0	18-24	19-24	<1

The 2B and 4P horizons have the highest volatile matter and these coal layers may be first to show signs of sponcom (figure 1.8). The No.5 seam has the highest VM, IM and TS of all the seams and is the most likely seam to develop sponcom.

1.6 Pillar resources

1.6.1 Historical mining methods

The study area has been mined since the mid 1980's to supply thermal coal from the No 2 seam and No 4U seam to a nearby power station. Mining methods have been exclusively by continuous miner using the bord and pillar method. The No 5 seam above the pillars has not been mined but will be included in future opencast or underground mining operations.

The preferred mining horizon for the No.4U seam has been the 4 primary (4P) cut which is taken against the floor of the seam and leaves a top coal (4T) in the roof of the seam. The preferred mining horizon for the No.2 seam has been the 2 first (2F) cut which is taken against the roof of the seam and leaves a floor coal (2B) in the bottom of the seam. Figure 1.18 shows the generalised mining column.

Due to mining height limitations on the continuous miners, the 4P and 2F cuts range between 3.8m-4.5m in height. In limited panels (<5%) top or bottom coaling has been done and the panels were

pre-designed for this purpose. Top and Bottom coal bands are known to increase sponcom liability by increasing the coal surface area exposed to the atmosphere.

The pillars from the No 2 seam and No 4U seam are superimposed according to the rock engineering department design criteria. The pillar width to parting width ratio determines whether seams should be superimposed or not. If the parting width is less than 75% of the pillar width then the No.2 and No.4 seam pillars are superimposed. The general pillar dimensions for each seam are displayed in Table 1.5. Distinct quality horizons within the No.2 and No.4 seams may mean that sponcom may originate in more reactive coal bands rather than across the full seam width.

Table 1.5: General pillar dimensions

Seam	Pillar centres (m)	Pillar width (m)	Bord width (m)	Safety Factor SF	Volumetric extraction (%)
S4U	19.5x17.8	12.7x11.2	6.6-6.8	1.6-2.0	35.7
S2	21.8x20.72	15.2x13.9	6.6-6.9	1.6-2.1	33.8

The generalised stratigraphic/mining sequence below shows the historical mining cuts and relative depths of the economic seams. The No.4 lower seam and No.3 seam are not considered economic horizons in the colliery study area and are excluded from resources.

1.7 Resource Estimation

The mineral resources were modelled and evaluated using the Horizon module of GEMCOM MINEX Software version 6.2, at a grid node spacing (mesh size) of 50m by 50m, using the General Gridding (Growth or ECS) algorithm. This algorithm is used in the GeoVia (previously GEMCOM) software for Coal deposit modelling and is used by many major and smaller mining houses across industry. ECS is used as the standard for generating value positional grids on the South Africa operating collieries and projects.

The current borehole database of some 2200 diamond cored boreholes was used in the modelling. The assumption of a 4.5m mining height was applied for both mined out seams to estimate resources.

The global volumetric extraction was calculated using the formulae

*% extraction = ROM (run of mine)*100/GTIS (gross tons in situ)*

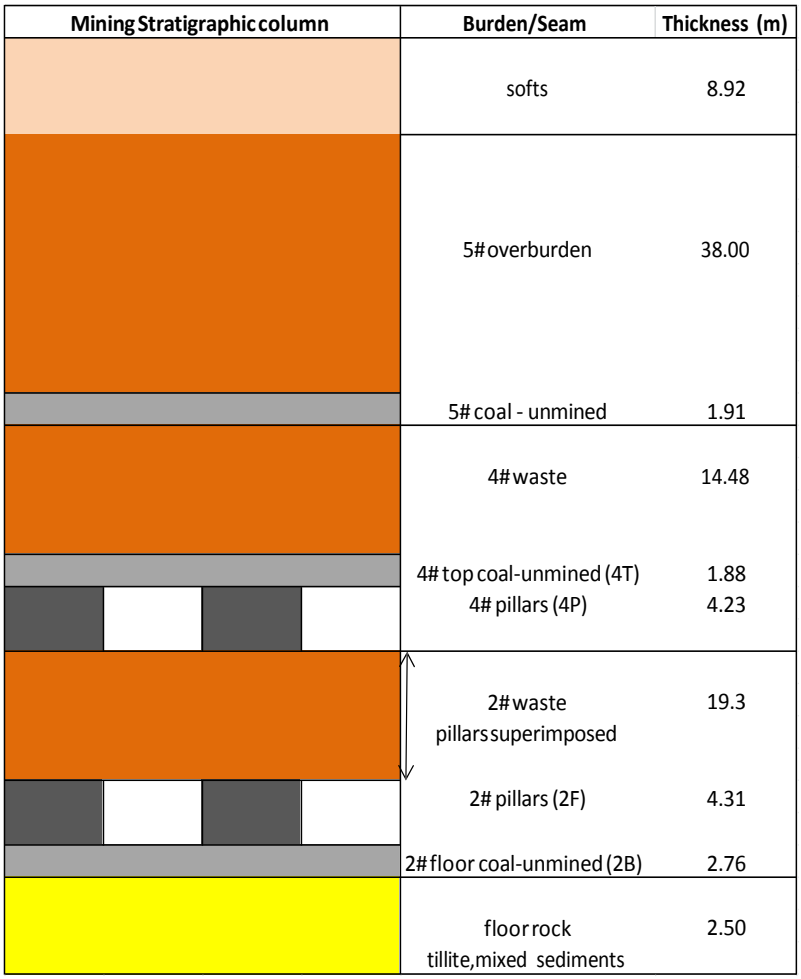


Figure 1.18: Generalised mining stratigraphic column (not to scale)

This value includes all coal left behind i.e. geological losses, mining losses, barrier pillars and in panel pillars and is tabled with the resources. Run of mine (ROM) figures are supplied by the survey department and a fairly reliable estimate of the remaining tons is then calculated to estimate the percentage extraction. The average volumetric extraction in the mined out areas is approximately 38 % for the No.4 seam and 32% for the No.2 seam.

1.8 Reserve Estimation

1.8.1 Planning methodology

Reserves are estimated by the planning department and include modifying factors such as mining losses, geological losses and dilution etc. At this stage no reserve estimate is available for the pillars but it is assumed that environmental restrictions will not allow the conversion of all resources into reserves. The process of establishing a robust and executable mine plan is carried out using several

software packages. It is not uncommon for scheduling activities to flow iteratively between steps until the optimal mine plan is developed.

The extent of the mined out pillar areas is approximately 10-11 km in a North-South direction and 4-5 km in an East-West direction. Mined out areas are compartmentalised and will reduce the potential risk of fires migrating at a later stage. Compartmentalizing also limits exposure to fresh air although smouldering combustion can be maintained with very low oxygen content (2-4%). The central and North-East areas show lower strip ratios and may be considered starting points for future pillar mining.

The cumulative strip ratio for the above seams takes into account the coal mined out in the No.2 seam and No.4 seam. The No.5 seam would automatically be part of any future opencast operation. Strip ratios are most favourable in the central and northern areas.

1.9 Modifying factors

Geological losses in the area are minimal (<2%) and the coal is therefore mostly mineable from a practical point of view. A geological loss percent has been used to discount the reserves for unknown and unpredictable geological conditions between vertical points of observation which may not necessarily be modeled, such as possible dolerite dykes, increase in basement elevation which may truncate the resource from below, and a highly variable weathering profile. Geological loss will also account for changes in thickness and quality between points of observation, and the geological loss factor accounts for a component of block or regional prediction or estimation error, as well as inaccuracies in apparent density measurements.

External waste (contamination) is expected to range between 0.2-0.4m depending on the type of lithology in the roof/floor material as well as control during mining operations. If a de-stoning plant is used yields would range between 70-90%.Mining losses of 10-15% could be expected.



Figure 1.19: Burn zone around a mine addit due to sponcom

2 LITERATURE REVIEW

The literature review is sourced from online publications and books. Few texts directly address the issue of sponcom when mining remnant underground pillars by opencast methods. However, oxidation theory and testing methods are applicable to coal in most environments and the relevance to mining of remnant pillars is still valid. What follows is an outline of sponcom factors, sponcom theories, sponcom control measures and case studies.

2.1 Main factors in defining self-oxidation of coal

Battacharyya (1982) described 3 main factors in the spontaneous combustion of coal and these factors have an aggregate effect

- Coal factor
- Geological factor
- Mining factor

.Each factor can be further reduced to a sum of subfacors which are classed as either intrinsic or extrinsic. The mining factor is extrinsic and controllable while the other two factors are intrinsic and uncontrollable (Eroglu et al., 1991). The intrinsic and extrinsic factors are summarized in Table 2.1-2.2 (Wade et al., 1986).

Table 2.1: Intrinsic factors related to self-heating of coal

Intrinsic factors affecting self-heating	
coal factors	geological factors
low rank	thick seams
high reactive macerals	highly faulted
high sulphur	poor caving characteristics
high porosity	high virgin coal temperature
easily friable	outburst prone
high alkaline content	carbonaveous strata or roof

Table 2.2: Extrinsic factors related to self-heating of coal

Extrinsic factors affecting self-heating
mining factors
accumulation of broken coal
stress distribution causing fracture
low production rates
limited ventilation through worked out areas
heat from machines
relative humidity differential between air and coal

The total risk of an occurrence of spontaneous combustion is defined as being the product of these factors (Bhattacharyya, 1982).

Total risk = coal factor *geological factor * mining factor

2.2 Spontaneous combustion theories

Some of the main historical and present theories of sponcom are discussed below (Eroglu, 1992):

- The pyrite theory
- The bacterial theory
- The oxidation theory
- The humidity theory

Gouws (1992) concludes that the self-heating of coal is primarily due to the oxidation of the coal, with the heat of wetting of a sample being a major contributory factor. The risk of an incident of spontaneous combustion occurring is a function of factors relating to the mine environment, geological and mining factors, and to the properties inherent in the coal itself, coal factor.

The rank of a coal is also a factor in the incidence of coal fires. Generally, lower rank coals tend to be more susceptible to spontaneous combustion. Although lignites and subbituminous coals are more prone to spontaneous combustion, spontaneous combustion in higher rank coals can be supposed from the number of fires in which no other cause is suggested.

2.2.1 The pyrite theory

The pyrite theory has been questioned for many decades and can be traced as far back as,1848.This is when De La Beche and Playfair (quoted by Coward,1957) deducted that iron pyrites in combination with a second form of heating acted together to produce what is termed spontaneous combustion. Various authors have supported the role of pyrite in combustion of coal (Li and Parr (1926), Graham and Jones (1924), whereas others have argued against pyrite being a sponcom factor (Percy (1875), Haedicke (1880), Brakeley (1916), Porter and Ovitz (1912), Erdmann (1922). In 1870, Richter argued that the high pyrite content in coal would heat too slowly to induce spontaneous combustion. He suggested that in spontaneous combustion of coal there was no correlation with the pyrite content.

The pyrite theory can be shown by the chemical reaction in the equation:
$2FeS_2 + 7O_2 + 2H_2O = 2H_2SO_4 + 2\ FeSO_4$

In 1915 Winmill reasoned that if the rate of oxidation of pyrite was equal to that of coal then pyrite could be a factor in sponcom (the reaction generates heat at a rate of 4.3 calories per cubic centimeter of oxygen absorbed). Li and Parr (1926) concluded that under suitable conditions the pyrites in coal would oxidize rapidly and might be a dominating factor in certain cases for the self-heating of coal. Marcasite and pyrite oxidize at about the same rate, but the former breaks down more easily producing fine particles, thus facilitating its oxidation.

In conclusion, pyrite cannot be the major causative factor of spontaneous combustion unless:

- It is present in large quantities
- It is in a finely divided state

Eroglu (1992) believes there are other causative factors with pyrite being a secondary factor in sponcom. Gouws (1992) also notes that fracturing of coal creates an increased surface area and a greater volume of reaction products compared to the initial volume of pyrite.

2.2.2 The bacterial theory

.In 1908 Potter isolated a pure culture of diplococcus from a soil extract cultivated on sterilized charcoal. He inoculated coal and charcoal with this strain and found an approximate heat increase of 1.19 degrees Celsius in both samples after a week period. Galle (1910) found Bacillus subtilis,

Bacillus nacreceus, Bacillus mesentericus and Bacillus pseudosubtilis to increase coal temperatures by 0.28 to 1.9 degrees Celsius. He suggested the importance of bacteria in sponcom especially at low temperatures but though other major factors were responsible for the observed heat increase

In 2014 Graham worked with two coals and found absorption of oxygen and bacterial activity to be independent. This was true for sterilized and inoculated coals.

Fuchs (1927) observed bacterial activity on different types of coal which resulted in gas evolution and temperature increase within a narrow range. When temperatures get too hot bacteria die off and have no further effect. The pyrite theory and bacterial theory are considered secondary to the oxidation theory in respect to sponcom origin.

2.2.3 The oxidation theory

Richters (1868) notes an initial weight increase when a dry coal sample was heated (180-200 °C) I air and after approximately 20 hours the sample began to lose weight instead.He suggested condensation of oxygen was the first stage in oxidation of coal caused. Fayol (1879) found the reaction of oxygen and organic coal mollecules produced heat which was dependent on the physical conditions present at any given time.

Several past researchers mentioned the heat liberated at low temperature oxidation The amount of oxygen consumed and associated weight changes vary in coals with different heat values. Values of 2.1cal/ml (Winmill,1914),3.1-4.4cal/ml (Scott,1914),3.3 cal/ml(Lamplough and Hill,1912) are some of the past experimental numbers quoted. In 1988, Wade pointed out the intrinsic and extrinsic factors affecting the oxygen adsorption of coal (Table 2.3).

Table 2.3: Parameters affecting the oxygen adsorption of coal; after Wade (1988)

Effect on oxidation rate as parameter increases	parameter
particle size	decreases
temperature	increases
wetness	increases
previous heating	increases
oxygen partial pressure	increases
volatile content	increases
rank	decreases
carbon content	decreases
oxygen content	increases
inherent moisture	increases

The mechanism of coal oxidation includes four stages:

- Coal + oxygen = physical adsorption of oxygen on coal surface
- Saturated coal + oxygen = chemisorption to coal-oxygen + heat
- Coal-oxygen complex + oxygen = carbon dioxide +CO+ water+ aromatics + heat
- Aromatics + coal + heat = ignition

2.2.4 The Humidity Theory

Davis and Byrne (1926) indicated that dry coal absorbed oxygen and it was better to store coal moist as there was less pore space for oxygen absorption. This is contrary to the observation of Winmill (1915).Rosin (1928) also observed that stockpiles experienced sponcom after warm rainy weather. Berkowitz and Schein (1950) postulated that ignition was more likely if small-medium stockpiles were partially dried and rapidly wetted by weather change. Normal heats of oxidation did not produce large temperature ranges in stockpiles.

The heat of wetting and initial moisture content of coal show an inverse relationship and act as a trigger for sponcom.The heat of wetting must significantly influence the oxidation velocity of coals dried out slightly by weather factors. Petschuk and Majewskaya (1954) noticed sponcom was notably increased by the draining of previously waterlogged underground workings

Stott (1956) showed that heat of oxidation was insufficient to remove water from coal and therefore evaporation of moisture prior to oxidation of coal would increase heating temperatures.*Bhattacharyya, Hodges and Hinsley (1969) note that sorptionof water increased oxidation and heating and vice-versa.* Berkowitz (1979) observed that ignition occurred at the dry/wet interface of coal, with the amount of wet surface area being an important factor (moisture capacity).

In general, lower rank coals are more hydrophilic in nature. Wetting, or gaining or adsorption of water, is an exothermic process and the heat liberated may in itself be enough to cause spontaneous combustion (Kim, 1977).Kim also claims that the heat of wetting is greater than the heat of oxidation for a given coal at temperatures below 100 °C.

Coal moisture is usually in equilibrium with atmospheric moisture with no net heat transfer resulting from adsorption or desorption. When non-equilibrium conditions prevail adsorption/desorption processes have a pronounced effect (Berkowitz, 1957).Desorption of water by flow of dry air over moist coal decreases coal temperature. Heat of wetting on the other hand increases coal temperature by 2261J kg/ H_2O.

2.3 Coal Particle Size

The surface area available for oxidation increases with the reduction of particle size. As the rate of oxygen absorption increases with the fineness of coal, early researchers believed that spontaneous combustion was a surface phenomenon (Gouws,1992).

Winmill (1915) found the rate of oxygen absorption was attributable to outer surface area and internal surface area of the coal. Winmill also coal mass determined the volume of oxygen absorbed if time was sufficient. Scott found oxygen absorption proportional to surface area when the particle size was greater than 20 mesh but this proportionality decreased for smaller coal particles. Berkowitz(1979) found lower rank coals to have more pore space.

Kaji et al. (1983) found that pore structure had significant effect on oxidation rate. They concluded that the oxidation rates were directly proportional to volume of pore of radius greater than 12 Å. However, it was found that pores which have opening greater than 100 Å radius were only responsible for reaction and that gaseous O_2 may not penetrate to smaller pores.

Schmal et al.(1984) found porosity influenced gas velocity and thermal conductivity and thereby influences sponcom. Porosity also had a greater effect in the absence of moisture. Arisoy and Akgun (1994) found oxidation to be reduced as coal particle size increased although increased temperature can offset this relationship.

Above the critical particle size oxidation rate is proportional to the cube root of the external surface area and at smaller particle sizes a reduced oxygen reactivity is seen (Küçük et al., 2003, Kaji et al., 1985; Ren et al., 1999.At the critical diameter oxygen penetrates the particles without mass-transfer resistance.

The critical diameter depends upon factors such as the reaction conditions and the porosity of the coal. It varies significantly between coals. It has been reported that the surface area of lower-rank coals, and consequently their reactivity, is independent of particle size (Nugroho et al., 2000). It has also been suggested that the surface area of a particle is reduced by low-temperature oxidation (Kaji et al., 1985). The effect is particularly noticeable in low-rank coals, where a reduction of up to 30% has been measured following oxidation at 35 °C.

2.4 Mining factors that affect sponcom

It is important to note that no single factor is responsible for spontaneous combustion. Laboratory experiments could identify high risk coals, allowing the total risk factor to be decreased by altering the mining factor. Knowledge of this risk index will enable mining engineers to design with greater emphasis on safety. Methane may form an envelope around coal preventing air access and create an anaerobic environment and explain why coals with a low C.P.T do not combust in their natural

environment. Anomalous results between field observation and laboratory experiments may be due to mining practice etc. where a strong mining factor causes a moderate geological factor coal to self-heat (such as unmined coal in a goaf with low ventilation).

The Oplinski and FCC sponcom risk indices has several anomalies that may be related to the arbitrary nature assigned to the risk factor. These risk indices are viewed as being too simplistic. Banerjee and his group (1988) later modified these models using similar limitations and having 4 types of rating: low, moderate, high and very high (Table 2.5).

Table 2.5: Spontaneous fire risk factors as proposed by Banerjee (1982)

risk priority	mining parameter	set elements	probability of spontaneous fire risk
1	category of coal	a.highly susceptible to	
		spontaneous heating	high
		b.poorly susceptible	low
2	friability of coal	a.highly friable	high
		b.poor friability	low
3	method of working	a.bord and pillar	high
		b.longwall type	low
4	state of stowing	a.extraction with caving	high
		b.complete stowing	low
5	seam thickness	a.>5m	high
		b.<4m	low
6	state of extraction	a.partial extraction	high
		b.complete extraction	low
7	nature of extraction	a.more than 1 lift	high
		b.1 lift	low
8	geological disturbance	a.present	high
		b.absent	low
9	rock bumps	a.present	high
		b.absent	low
10	dykes	a.present	high
		b.absent	low
11	overburden	a.>300m	high
		b.<300m	low
12	parting	a.shale/fractured strata	high
		b.rockt and consolidated	low
13	state of consolidation of	a.fractured and crushed	high
	barrier/gate road/pillar	b. well consolidated	low
14	scope of accumulation	a.fine accumulation sustain	high
	of fines,due to roof fall e	b.fines avoided	low
15	method of ventillation	a. advancing type	high
		b. retreating type	low
16	quantity of ventillation	a.high pressure diff	high
		b.low pressure diff	low
17	humidity	a.wet	high
		b.dry	low
18	source of hot spots	a.present	high
	hot springs,adjoining fires	b.absent	low
19	gas emission rate	a.low	high
		b.high	low
20	size of panel	a.large	high
	length of face	b.high	low
21	rate of face advance	a.slow	high
		b.fast	low
22	chances for blockage	a.present	high
	stopping of face advance	b.absent	low

Fires can start at outcrops and move through interconnected workings with heat transfer by conduction (into the overburden) or convection (between panels).The overburden can also insulate the burning coal seam.

As the overburden becomes warmer or as the coal pillars fail, the overburden subsides, creating a system of cracks and fractures through which smoke and fumes leave the mine and fresh air enters the mine (Figure 2.1).Under these conditions most abandoned mine fires exhibit smouldering combustion, involving relatively small amounts of coal at any given time, with little visible flame. They can continue to burn in an atmosphere with only 2% oxygen. Such fires can burn for extended periods of time (10-80 years) and are difficult to extinguish (Dalvermy et al., 1991).

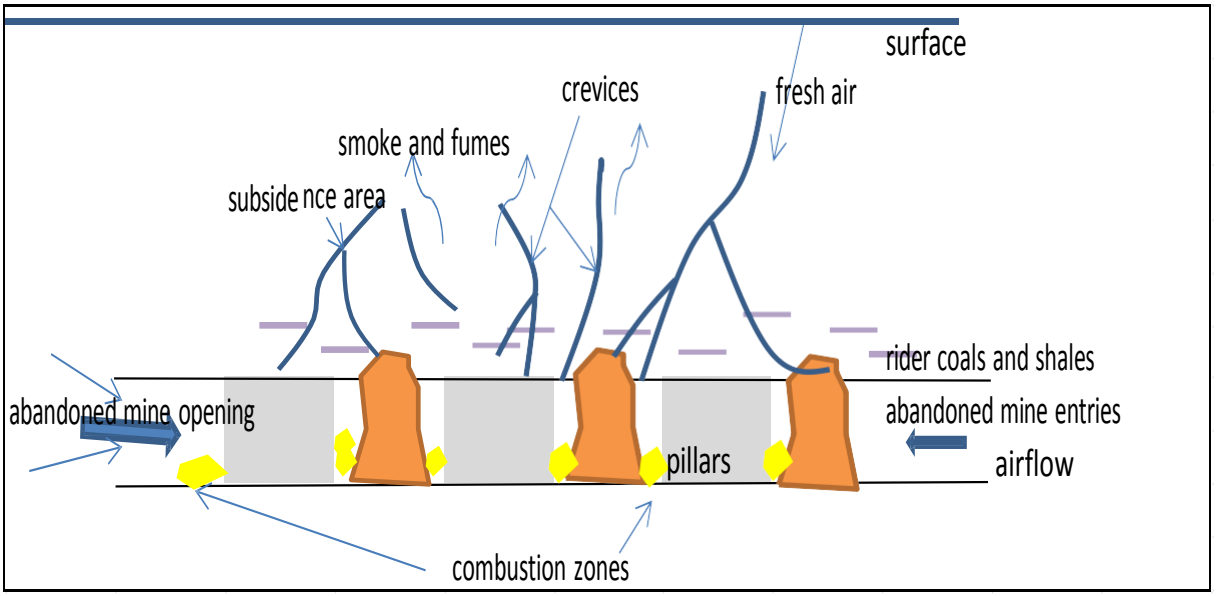


Figure 2.1: Wasted-coal fire in an abandoned mine showing emission of smoke and fumes through cracks and fractures and intake of fresh air through openings and overburden. (Adapted from Kim and Chaiken 1993)

Boundary pillars, interburden and degree of fracturing determines the amount of heat transfer between coal zones and how a fire may propagate away from source (White 1973).

Low temperature smouldering yields greater amounts of toxic gases and particulates than flaming combustion and favours CO_2 to CO ratios around 1 (as opposed to ratios around 10 in flaming combustion) (Purser, D.A., 2002).The extent of mined out workings, unmined zones, carbonaceous lithologies etc. increase the amount of available fuel for sponcom (Kim and Chaiken, 1993)

Because the rubbleized coal has a larger surface area than solid coal, it is more combustible. Main entries may be high oxygen areas along which a fire may propagate. The number of openings in the outcrop, the number of ventilation shafts, the competence of overlying strata, and the prevalence of subsidence induced fractures are other factors that contribute to the prolonged propagation of

abandoned mine fires. The condition of the mine determines the amount and surface area of fuel; the availability of oxygen determines the direction, and rate of propagation of fire. The rate of heat generation versus the rate of heat loss, the heat generating reactions and the insulation provided by adjacent strata control the amount of energy within the system (Kim and Chaiken., 1993).

Flame spread mechanisms have predictable pathways along which the coal fire spreads ,however when combustion zones are discontinuous the movement of hot gases may be a factor in propagation (Chaiken et al., 1979,Kim and Dalverny, 1994).The fire induces circulating air currents, which carry fumes and heat into nonadjacent areas approaching 100 °C, the coal is conditioned by drying, leading to accelerated oxidation reactions. If the heat is not dissipated, the temperature of the coal continues to rise until spontaneous ignition occurs.

The water table serves as a barrier to sponcom by limiting the amount of oxygen for absorption and by absorbing energy released by the fire. Natural barriers prevent uncontrolled and rapid propagation of fires (Kim and Chaiken, 1993). Boundary pillars are considered natural barriers to fire propagation because solid coal seams do not burn readily.

2.5 Geological Factors related to sponcom

Geological factors such as depth of overburden, the degree of fracturing, and the nature of the overlying strata vary between coalfields. Shallow mines are more permeable and the strata is more fractured. Shallow coal seams are frequently above the water table. Oxygen concentration is also increased near outcrops and fires propagate toward the source of oxygen. Smouldering can occur at less than 3% oxygen (Leicht, 1940; Justin and Kim, 1987).

Barometric changes cause the mine to breathe and ultimately bring in fresh air that supports very slow spread of fires over long periods of time. The dip or pitch of anthracite mine can influence the propagation of fire as does the interburden thickness (heat conduction)

Geological barriers affect fuel availability as well as heat generation and retention. A rock mass surrounding a burning coal seam has low heat conductivity and insulates the seam, thereby promoting combustion. Roof and floor coal, as well as carbonaceous lithologies adjacent the seams can assist in spreading a fire. Conduction is an extremely slow cooling process. For example, the combustion of 1 ton of medium-volatile bituminous coal releases 7565 thermochemical calories. If this energy is simply adsorbed by the roof rock, it would raise the temperature of 75 tons of rock to 500 °C.

If all combustion ceases, it would take 10-20 years for this amount of heat to dissipate by conduction through the overburden. Long-term cooling rates, measured in mines have been found to be as low

as 0.1 °C per year (Hansen et al., 1990). Natural barriers to subsurface fire propagation include faults where vertical displacement disrupts the continuity of the coal bed (Kim and Chaiken, 1993).

Coal seams in warm climates experience increased oxidation rates. Intrusive bodies also increase sponcom risk (Stach et al., 1982).

Humidity normally facilitates oxidation, but it is retarded by dry and per-humid conditions. High rates of gas emission from coal seams, although posing high fire risks from extraneous sources, inhibit oxidation and self-heating (Banerjee, 1981). External factors, such as tectonic disturbance, pressure of overburden, igneous intrusion, blasting and working conditions in coal mines, etc., directly aid in reducing the size of the coal particles through crushing and shattering, thereby creating secondary porosity and increasing the internal surface area and facilitating the access of oxygen and the absorption of moisture.

Sanyal (1984) notes a strong relation between fire incidents and igneous intrusions in the Ranigani coalfield. Fire susceptibility is not uniform in the seams. Secondary porosity was brought about by intrusions, earth movement, overburden stress and growth of post diagenetic pyrite and calcite. This resulted in:

- a reduction in the size of the coal particles and the creation of a considerable internal surface area;
- a lowering of the thermal conductivity.

This resulted in increased airflow, moisture absorption, heat accumulation and oxidation. (Chandra and Prasad, 1990 don't believe the pyrite content (.2-2.4%) influences sponcom propensity in this coalfield. Large day/night temperature ranges result in accelerated oxidation and wetting of seams.

The combustion reactivities of vitrinite and liptinite are strongly influenced by rank and petrography. Pressure and stress result in a change in orientation of maceral optical properties. It may be difficult to optically separate the effects of stress from temperature increase which also modifies optical properties.

2.6 Oxidation Theory

As with any fire, coal fires require three elements: fuel, oxygen and ignition source (Figure 2.2).In coal combustion, the fuel is the carbon in the coal. If combustion is consistent the exothermic reaction of carbon and oxygen to form CO_2, is written as:

$$C + O_2 \longrightarrow CO_2 + HEAT$$

The amount of heat liberated is 93.7-kcal/mol.

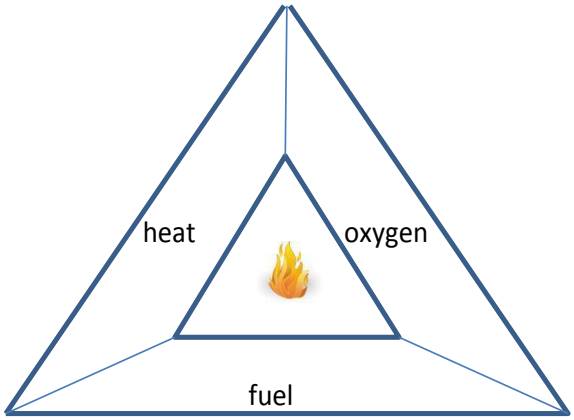


Figure 2.2: Fire triangle showing the three essential elements for any fire: fuel, oxygen, ignition source (adapted from Kim and Chaiken 1993)

Coal contains between 60% to 90% carbon on a mineral matter free basis. The remaining constituents are hydrogen, oxygen, nitrogen, and sulphur. The stoichiometric combustion of coal can be written as (Chaiken, 1977).

$$CH_{1.18}NO_{0.15}O_{0.35}S_{O.005} + 1.12O_2 + 4.15N_2 \longrightarrow CO_2 + 0.58H_2O + 0.005SO_2 + 4.157N_2 + HEAT$$

This reaction produces 138.4 kcal/mol. Combustion reactions are exothermic and depending on the rank of the coal, combustion produces from 5 to 10 kcal/ g of coal or between 6 and 16000Btu/lb.

The oxidation of coal occurs constantly. The temperature of the coal is a function of the rate of heat generation versus the rate of heat loss. Since the rate of heat generation is an exponential function of temperature and the rate of heat loss is a linear function of temperature, as the temperature increases, the reaction rate increases faster than the heat loss.

Ignition is a function of the amount of energy released by a reaction and the rate at which it is released, as well as the rate at which energy is transferred from the reacting mass to the surroundings. The reaction rate is a function of the concentration of reactants, carbon and oxygen, the surface area, particle size, temperature, and activation energy (Kanury, 1975).

Sponcom is accompanied by conduction and convection of heat to adjacent coal areas. (Banerjee, 1985). The oxidation of pyrite and the absorption of water on the coal surface also are exothermic reactions that increase the probability of spontaneous combustion. Oxidation is a slow process such

as the weathering of coal, whereas combustion is a rapid process giving off heat and light. Surface to volume ratios of equal sized particles may differ and effect coal reactivity irrespective of the chemical activity (Burdukov et al., 2014).

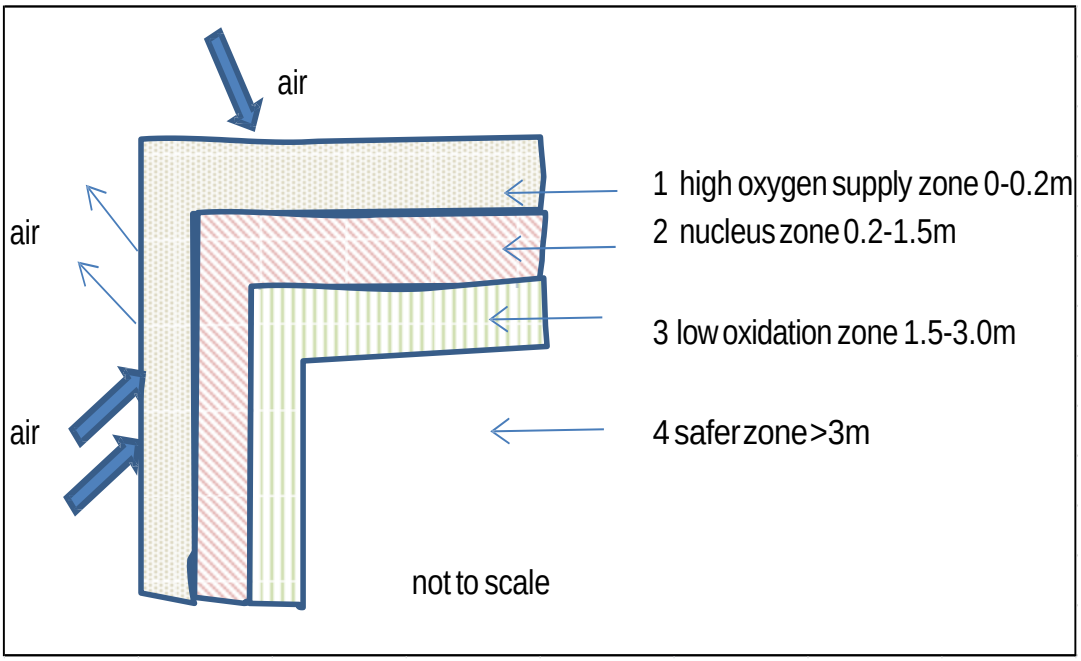
The balance between heat generation and heat loss determines the probability of sponcom The character of the coal will have some effect as shown by (Lawn et al., 1981), but in the main, the all-important terms are the heat of reaction (*Q)*, the reactivity (*A)*, and the activation energy (*E*a) (Nugroho et al., 2000).

Based on studies by (Liottta et al., 1983) and others:

- Release of moisture from coal facilitates spontaneous heating opening up the active centres in the coal matrix.
- Aerial oxidation of coal at temperatures, a little above the ambient level occur mainly on the aliphatic part of the coal structure.
- In the initial stage methylene groups produce peroxides/hydroperoxides initiating the process of oxidation through chain reaction forming free radicals.
- At 50 °C or so alkyl structure may get oxidized to aldehydes (particularly for low rank coals)
- Oxidation of methylinic groups to ketones or phenolic structures to quinone occurs in a wide range of temperature between 50-150 ^{0}C
- High oxygen content of coal particularly the phenolic hydroxyl groups promote reactivity to oxygen. On the contrary carbonyl groups have a deactivating effect.

Cracks and fractures are created in the outer layer of coal benches during mining and these become conduits for air movement. Three subzones can be identified as shown in figure 2.3 (Banerjee, 1985)

- High oxygen intake zone
- Inner nucleus zone
- Low oxidation zone



Zone	Oxygen/air supply	Heat build up
1	high,natural draft	high accumulation and dissipation
2	higher, increased rate	higher most vulnerable zone
3	poorer ,O2 depleted air	lower,heating by conduction mainly
4	almost nil	no heat build up,temperature rise by conduction only
	Temperature 40-90 ^{0}C	

Figure 2.3: Zonation of outer layer of coal pillars (after Banerjeee,1985)

2.7 Control measures

In order to extinguish a fire, one of three elements, fuel, oxygen, or energy, must be removed. Fuel is removed when it is consumed or when it is physically separated from the burning mass. Oxygen removal depends on either the introduction of an inert atmosphere or the isolation of the fire zone from sources of fresh air. Heat removal can be accomplished by moving a heat-absorbing agent (usually an inert gas or water) through the mine. To prevent re-ignition of the fire, all coal and heated rock must be cooled below the re-ignition temperature. Even very small isolated areas where the coal is oxidizing at a high rate can serve as re-ignition points if the control measure fails and oxygen becomes available. It is generally assumed that if the temperature is below 100 °C, the chance of re-ignition is small (Kim and Chaiken, 1993).

The components of the fire triangle can be further subdivided into conventional mine control techniques and more or less unconventional or unproven mine fire control techniques. The former includes conventional construction procedures such as total excavation (of the burning seam), isolation trenches, and mine void filling. The latter may include less conventional or novel techniques

including chemical treatment (including nitrogen entrainment in foam), in situ coal gasification, and burn-out control (Michalski et al., 1997).

Each coal fire will have its own unique characteristics and there seems to be no approved general methodology for investigating and controlling all types of coal fires. However, a number of techniques are recognized. These involve depriving the fire of oxygen, building barriers to isolate the burn front, saturating the coal with water and grout slurry mixes. These techniques require significant financial resources which unfortunately are not always available in many countries (USBM, 1971). Remote sensing is the acquisition of information about an object or phenomenon without making physical contact with the object and thus in contrast to on site observation.

Remote sensing is a sub-field of geography. In modern usage, the term generally refers to the use of aerial sensor technologies to detect and classify objects on Earth (both on the surface, and in the atmosphere and oceans) by means of propagated signals (e.g. electromagnetic radiation). It may be split into active remote sensing (when a signal is first emitted from aircraft or satellites) or passive (e.g. sunlight) when information is merely recorded Remote sensing (Wikipedia).

Some of the commonly used sponcom control measures and methods are summarized in Table 2.6 and useful references are provided on these extensive topics for further reading.

Table 2.6: Summary of the main sponcom control measures

Control Measure	Method	Useful references
Ventilation	Gas monitoring	Gouws,1987;Graham 1914;Coward,1957;Purshall,1965;Criddle,1961
Inert substances	Nitrogen	Harris,1981
	Inundation	
	Flushing	Stracher et al,2011
	Grouting	Colliazi,2004;Terry,1987;Bell,1996;Michalski and Gray ,2001
	Surface sealing	USBM,1993
	Inert gases	Adamus, 2002
	Flooding	Bullock and Bell, 1997
	Controlled explosions	Bell and Donnelly, 2006
	Cladding	Discover 1999
Remote sensing	Magnetics	Gielisch, 2007
	Airborne Thermal Infrared Imaging	Ellyett, 1974; Rathmore, 1993; Vice, 2007
	Colour Infrared imaging	Shallenberger ,1993;Bakker et al., (1978)
	Reflection aureole mapping	Gupta and Prakash, 1998
	Fire depth estimation	Saraf et al, 1995
	Heat conduction models	Cassels, 1998

The effectiveness and cost of some of these control measures for bituminous and anthracite coalfields in the U.S.A. indicates excavation and surface sealing to be most effective methods (40-80%). The use of flushing or trench digging is less effective (25-40%) (USBM, 1978).

2.8 Thermal analysis methods of coal

A number of physical and chemical affects can be produced by temperature changes and characterize the material being analyzed. These changes indicate the temperature at which the material ceases to be stable under normal conditions (Weisstein, undated).The thermal techniques discussed include the crossing point temperature, thermogravimetric analyses and oxygen absorption.

2.8.1 Crossing point temperature (CPT)

The ignition temperature and the initial temperature are related to rank and at the same rank may vary due to composition of coal, degree of oxidation, seam thickness and particle size. CPT is the most widely used thermal test for sponcom susceptibility. Coal with a CPT value of 120-140 ° C indicates high susceptibility, 140-160 ° C moderate susceptibility and more than 160 ° C poor susceptibility (Banerjee, 1981).

The CPT is defined when the coal temperature exceeds the surrounding temperature (Banerjee et al (1972)CPT values are increased with increasing rank, although moisture content, sulphur and experimental conditions have an important effect on CPT values. The best experimental conditions are still disputed and results can be inconsistent.

The CPT is affected by coal characteristics and also by test conditions and the test facility. CPTs must be determined under the same, or nearly the same conditions, when contrasting them to evaluate the spontaneous combustion of coal. Some experimental results demonstrate that air humidity is an important factor in determining whether a heating will progress rapidly or not (Rena et al, 1999).

Higher rank coals have fewer active groups (Xie, 2002). Higher ranks of coal are less reactive and correspondingly less heat is released by the reaction as well (Pietrzak and Wachowska,2003). This results in smaller temperature increases and higher CPT for higher rank coals. Moisture and mineral components also affect spontaneous combustion. The CPT is a reflection of all these factors. The fact that CPT rises with increasing coal rank is only an approximate relationship.

High moisture content causes a delay phenomenon during the self-heating of the coal (Singh, 2012). Banerjee et al., (1972) found that the CPT is usually inaccurate for those coals with high moisture

content and suggested the evaluation of such coals by both CPT and temperature increase rate. Barve and Mahadevan (1994) determined a binary quadratic equation for CPT that related it to moisture and ash contents. Above 4-6% moisture content (arb) the CPT values show rather a rising trend. There are instances where the release of moisture in high moisture coals has been instrumental in shifting the CPT to high values as shown in (Figure 2.4) (Nandy et al., 1972).

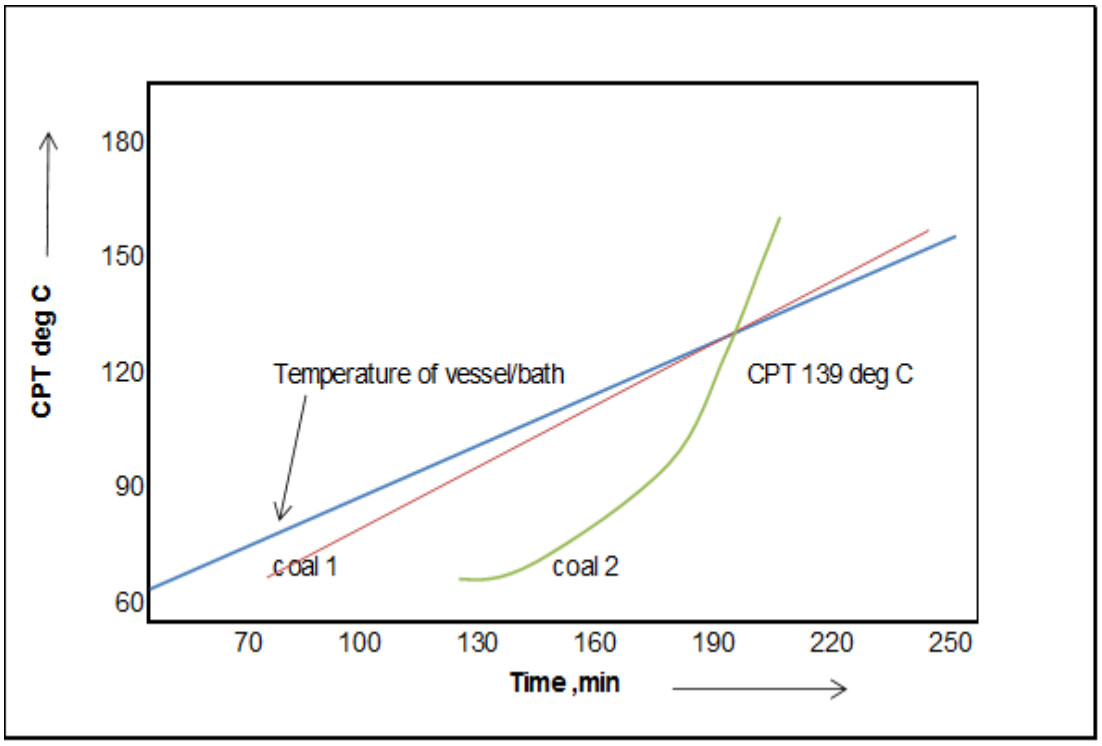


Figure 2.4: Identical CPT for two different coals (after Nandy,1972)

From figure 2.4 it is noted that the sample with the greater heat evolution rate (slope) will be more likely to self-heat that a sample with the same CPT but which has a gentle heating slope (Nandy et al., 1967).Some CPT experiments (column reaction vessel) indicate that CPT decreases with decreasing particle size and air humidity but increase with reduced moisture content in coal (Barve and Mahadevan, 1994). Kadioglu and Varamaz (2003) suggested that CPT rose with an increase in moisture content and the particle size of the coal.

Nandy et al. (1967), suggested that the CPT dropped with an increase in volatile matter, oxygen content, and moisture content. From the correlation analysis it is found that the susceptibility to spontaneous combustion of coal increases with increase of moisture, volatile matter and fixed carbon whereas it decreases with increase of ash.

Heating rates for CPT of 1˚C/min. have better correlation with proximate analysis parameters than experimenting with a ramp of 2˚C/min (Singh et al., 2007). Nandy et al. (1972) also noted the variation in CPT values with volatile matter, oxygen percentage and the moisture content of coal They found that CPT normally decreases with increase in each of these constituents of coal but beyond 35% V.M., 9% Oxygen or 4-6% moisture content-there is not much change in the CPT values.

2.8.2 Thermogravimetric analysis (TGA)

TGA is a technique which measures change in weight as a function of controlled temperature change. In most TGA studies, mass loss is read directly in units of weight percent of the original sample quantity (Table 2.10). The results from thermo-gravimetric analysis may be presented by (1) mass versus temperature (or time) curves, referred to as Thermo-gravimetric curve, or (2) rate of mass loss versus temperature curve, referred to as Derivative Thermo-gravimetric (DTG).. If a species is thermally stable within a certain temperature range then no change in mass is noted (Vaimakis, undated)

TGA can be used to reflect the physical and chemical structure of coals and determine the parameters obtained from proximate analysis. TGA is also capable of revealing activation energy the coal needs during the oxidation process and provides an independent method to determine the self-heating potential of coal.

Table 2.10: Processes accompanied by weight change

Process	Weight gain	Weight loss
Adsorption	X	
Absorption	X	
Desorption		X
Drying		X
Dehydration		X
Desolvation		X
Vaporization		X
Decomposition		X
solid-solid reactions		X
solid-gas reactions	X	X
Oxidation	X	

The output signal may be differentiated electronically to give a derivative thermo-gravimetric (DTG) curve and represent the rate of mass change.

$$\text{DTG signal} = dm/dt \quad (1)$$

When the TGA curve is stable the DTGA curve is fitted in zero line. The peak maximum temperature is corresponded with the inflection point of the TGA curve (Figure 2.5)

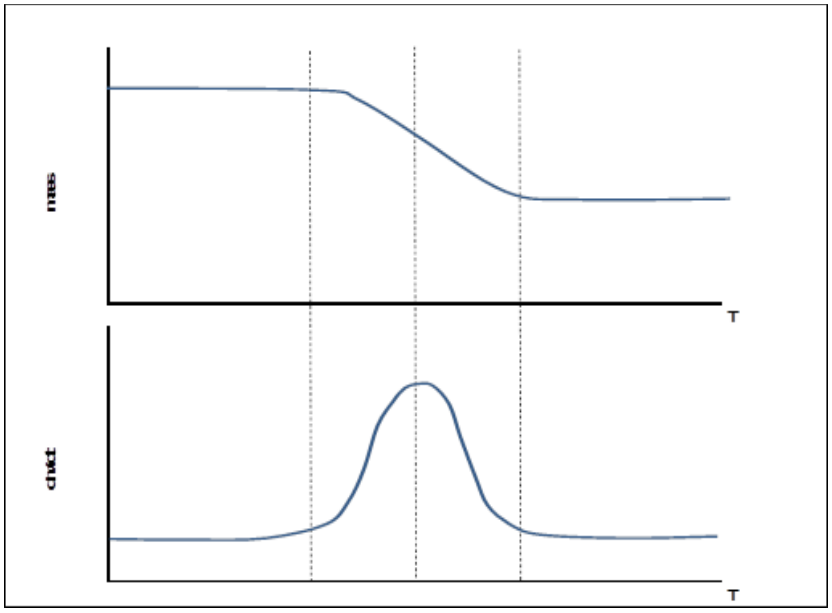


Figure 2.5: TG curve and corresponding DTG curve (after Viamakis)

2.8.2.1 Types of TGA Curves

Actual TG curves obtained from experimentation (Brown et al., 1980) may be classified into various types as illustrated in Figure 2.6. Possible interpretations are as follows:

- Type (1) curve. The weight sample is stable over the temperature range considered. No information is obtained, however, on whether solid phase transitions, such as melting, polymerization or other reactions involving no volatile products have occurred.
- Type (2) curve. The rapid initial mass loss observed, is characteristic of desorption or drying. The buoyancy phenomenon is observed.
- Type (3) curve represents decomposition of the sample in a single stage. The curve may be used to determine the stoichiometry of the reaction, and to investigate the kinetics of reaction.

- Type (4) curve indicates multi-stage decomposition with relatively stable intermediates. The curve may be used to determine the stoichiometry and to investigate the kinetics of reaction, for all stages.
- Type (5) *curve* also represents multi-stage decomposition, but in this example stable intermediates are not formed and little information for the stages can be obtained. At lower heating rates, type (5) curves may tend to resemble type (4) one, while at high heating rates both type (4) and type (5) curves may resemble type (3) curves and hence the detail information for stages is lost.
- Type (6) curve. The weight sample is increased as a result of reaction of the sample with the surrounding atmosphere. A typical example would be the oxidation of a metal sample.
- Type (7) curve. This is a characteristic TG curve representing an oxidation reaction which decomposes again at higher temperatures

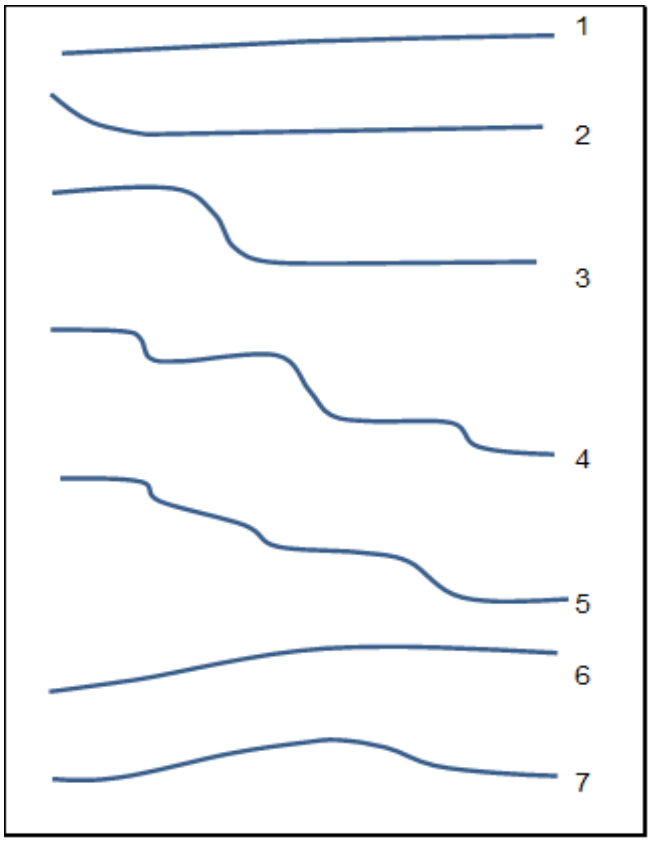


Figure 2.6: Main types of thermo-gravimetric (TG) curves(after Brown,1972)

Oreshko (1961) recognized four stages of coal oxidation (Figure 2.7), between 0-300 °C temperatures. During the first stage up to 70 °C, an increase in weight by chemisorption of oxygen was observed. From 70 to 150 °C there was a decrease in weight due to the breakdown of the peroxy-complex. Between 150-230 °C the increased weight is linked to the formation of a more stable

oxy-complex. Above this temperature incineration of the coal occurs. Due to the overlapping of various stages, allowance was made for the consecutive character of the reaction. The activation energies at the various oxidation stages were 3.4kcal/mol,6kcal/mol,16kcal/mol and 23kcal/mol respectively.

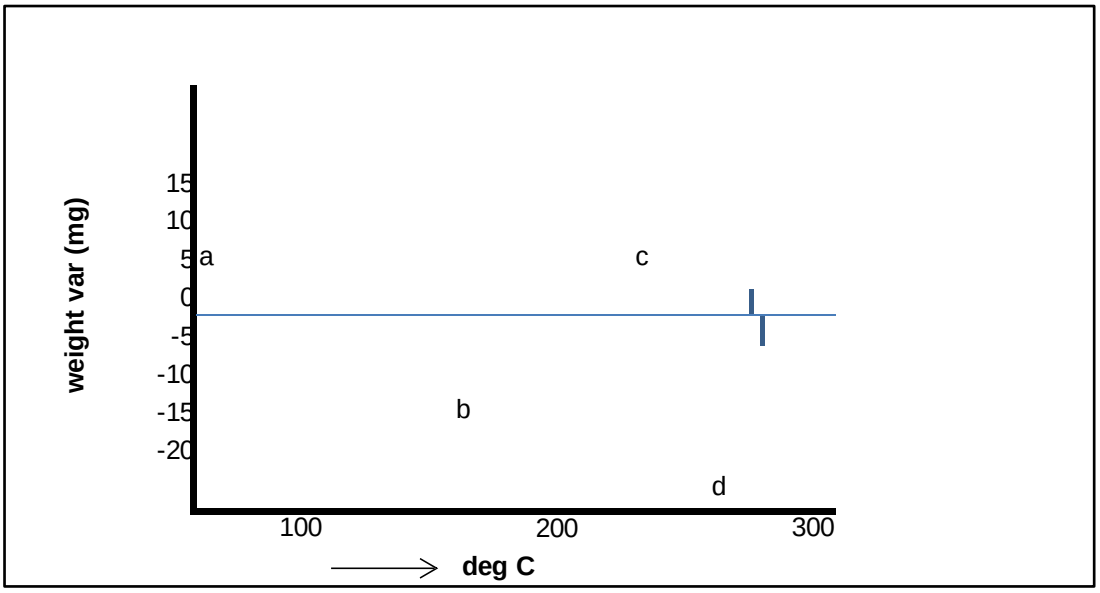


Figure 2.7: Weight variation of coal with progress of oxidation (after Oreshko,1961)

Avila (2014) states that the oxygen absorption test is closely linked to “spontaneous combustion” while the TGspi method is closely linked to the ignition phenomenon and subsequent high temperature combustion, noticed when comparing the CPT to TGspi values. The nature of both reactions is totally different, and the key to obtain a reliable prediction of the self-heating phenomenon is to differentiate between them. Coals with zero weight increase appear to continue to react faster with air at higher temperatures, whereas coals with high mass increase seem to be more reactive at higher temperatures than coals with smaller weight gains. Unreactive coals at low temperatures can be very reactive during combustion and be high-risk coals if they have low ignition temperatures (table 2.11) (Avila et al., 2014).

Table 2.11: Coal classification based on weight change(Avila,2014)

Oxygen adsorption	Tgspi index
weight increase not seen	high reactive (Tgspi> 0.05)
slight weight increase (0.1-1.0%)	reactive (Tgspi=0.05-0.03)
medium weight increase (1-2%)	low reactive(Tgspi=0.03-0.02)
important weight increase (>2%)	non-reactive (Tgspi<0.02)

2.8.3 The Rate equation

The rate of coal devolatization and coal char oxidation depends on the temperature and the amount of coal. In most dynamic studies that use TGA, the first-order chemical reaction assumption is most frequently used. Therefore, the fundamental rate equation may simply be expressed as follows:

$$dx/dt = A \exp (-E_a/RT)(1-x)$$

where A is the pre-exponential factor, Ea is the activation energy, R is the gas constant, T is the temperature, t is the time, and x is the calculated weight loss fraction (Wang et al., 2011).

The variability of reaction rate explains why some coals are more susceptible to spontaneous combustion than others. Reaction rate is closely linked to the variability seen in the proximate, ultimate and petrographic analyses. Whatever transform of the reaction rate is taken, the volatile matter content (VM) of the material is the most significant regressor, followed by the inherent moisture content (IM). The inherent moisture may be related to the surface area of a coal, in which case the volatile matter may reflect the reactive constituent of a coal.

2.9 Oxygen absorption tests (Smith and Glasser method)

Oxidation rate is highly variable when determining sponcom potential. The static isothermal method has been used by several researchers to directly measure the extent of reaction of coal with oxygen (Sevenster, 1961).

Certain properties, such as the heat capacity, the heat of reaction with oxygen and the activation energy for this reaction, are found to vary to a relatively minor degree for coals of varying rank and

geological origin. However, rates of reaction with oxygen are found to vary by orders of magnitude for different coals. The reaction kinetics is consistent with a diffusion-limited shrinking-core model. 'Adiabatic' experiments are notoriously difficult to perform, though they should yield the most direct information on the low-temperature oxidation of coal, including such parameters as heats of adsorption and reaction, and activation energies. The measured heats of reaction of different coals vary by a significant amount, but are within the same order of magnitude. However, the measurement of oxidation reaction rates immediately established this parameter as being of prime importance with regards to its variance between coal types.

Many researchers have shown that oxygen concentration has a strong influence on rate, but unfortunately the design of the semi-adiabatic apparatus does not allow this to be easily controlled. A change in absolute temperature of only a few percent has a larger effect than a change in oxygen concentration of several hundred percent (Smith and Glaser, 2002).The rate of reaction does not correlate with the content of pyrite or other forms of sulphur. It is therefore unlikely that there is competition for oxygen from the ash component. Both Itay (1983) and Hill (1986) tested shrinking-core particle models, based on results of microscopic examination of 'fresh' and oxidised coal ('oxidation rims').

Itay (1983) assumed first order reaction kinetics, despite experimental evidence for a fractional order of reaction, with the reaction rate being equal to the rate of diffusion through the coal ash layer. It may therefore be that the distribution of micropores and macropores differs for different coal types, and that high temperature rises during reaction will affect some coals more than others.

This hypothesis is supported by the research of Krishnaswamy et al. (1996), who differentiated between internal and external mass transfer resistances, with the reactivity of some coals being independent of particle size, and others showing a dependence on particle size. It is apparent, however, that there is a practical limit to the development of the semi-adiabatic apparatus. If the heat losses are too large, then they mask the effect of the heat 'generated' by the reaction. However, if these losses are too small, then the temperature rises may be too large, invalidating the assumptions underlying the equations.

The heat capacities, heats of reaction with oxygen and activation energies show relatively little variation for coals ranging from lignite to anthracite. In contrast, their rates of reaction vary considerably. The kinetics are found to be consistent with a shrinking-core, diffusion-limited model at temperatures of 50–80 degrees Celsius (Behera, 2009).The main components of the apparatus used comprise a glass reaction bottle, a turntable, a balance and a computer.

2.9.1 Moisture

The relationship between increased inherent moisture and an increased tendency for coal to self-heat is now well established (USDE, 1994).Some authors have suggested that water has a catalytic effect on oxidation rate, but Nordon et al. (1979) found that the activation energy for the oxidation of coal and char was independent of moisture content. Itay (1989) identified two gaseous reaction products (CO and CO2) both of which reduce oxidation rate. Polat and Harris (1989) also reported on reaction product inhibition, due to the water of reaction.

The adsorption and desorption of water vapour from coal takes place in parallel with oxygen adsorption, and may be an important heating effect in the case of a dry coal and a humid environment. The rate of adsorption or desorption of moisture is not as easily measured as the rate of adsorption of oxygen, however, since the moisture content of saturated air at 23 degrees Celsius is only 3.8%. Because of this low concentration, the sorption rates are very low.

The chemisorption of oxygen evolves an order of magnitude more heat than the physical adsorption of water. Temperature rises in a coal bed would tend to cause desorption of water vapour, an endothermic effect. It is therefore likely that adsorption of water is more important in catalysing the oxidation reaction, as suggested by Marinov, (1977), Saranchuk (1978) and Itay (1993). The amount of water is thought to exceed the concentration required by most catalysts. It might be more accurate to describe water as a ‘promoter’ (possibly for bacterial oxidation) rather than a catalyst.

Although ‘heat generation’ by adsorption of water vapour may be neglected at ambient temperatures, it is nevertheless important to consider sorption of water as a risk factor in spontaneous heating. Adsorption of water vapour does not in itself compete with the low-temperature oxidation in terms of ‘heat generation’, but appears to speed up the oxidation rate, and possibly plays a catalytic role. Statistical modelling indicates that the two most important intrinsic coal properties affecting the reaction rate are the volatile matter content and, to a lesser extent, the inherent moisture content. The statistical model has a similar form to the theoretical model.

A marked increase in oxygen content (by a factor of about three), found in oxidatively altered coals, results in a hydrophilic surface character, whereas unaltered coals have a hydrophobic surface character. Moisture promotes oxidation of oxidatively altered coals with an increase in heat up to the critical content of moisture. Moisture hinders the oxidation process in unaltered coals, being hydrophobic in character. Summing up, the reason for the increased oxyreactivity of oxidatively altered bituminous coals can be perceived in: (a) the active, promoting role of moisture in the oxidation mechanism,(b) the increased reactivity of the free radicals generated in the oxidation process, (c) the chemical (not diffusion) controlling regime for their oxidation (Taraba and Pavelek ,2014).

2.9.2 Particle size

At different particle sizes reactivity is a weak function of particle size at ambient temperatures. The oxygen concentration was the most influential parameter measured in one isothermal study. The reactivity of moisture-equilibrated coal samples is greater than the reactivity of as-received samples, possibly as a result of 'outgassing' or cleaning of the coal surfaces. A paper by Androutsopoulos and Linardos (1986) notes an increase in the surface area of lignite samples on drying under vacuum, which will also have an outgassing effect.

Coal reactivity is insensitive to small variations in particle size or carbon monoxide concentration at 23 degrees Celsius. Oxygen concentration and ambient humidity play more important roles, but none of these extrinsic factors account for the order-of-magnitude variations in reactivities for coals of different origins. It is inferred that, as the ambient temperature decreases, micropore diffusional resistance becomes rate-controlling in the oxidation of coal, thus reducing the effect of particle size

Coal appears to oxidize from the surface inwards, with the oxidation causing sufficient strain to cause cracking, thus allowing fresh oxygen to penetrate deeper into the solid. However, the rapid loss of reactivity with degree of oxidation suggests that the new sites are more difficult to get than the original ones (Smith and Glasser, 2002).

2.10 Petrology

The term 'maceral' in reference to coal is analogous to the use of the term 'mineral' in reference to igneous or metamorphic rocks. Macerals are considered to be dehydrogenated plant fragments. Maceral maturity can be estimated by vitrinite reflectance. This gives information on the carbon, hydrogen and nitrogen composition of the coal, and determines the type of coal: lignite, brown coal, bituminous coal, anthracite or graphite. Macerals, the microscopically identifiable organic constituents of coal, are one of the three basic parameters that define coal. The other two parameters are the coal rank and the mineral matter. The ICCP 2001 classification of coal is tabled below (Table 2.12).

The inertinite-rich Witbank coal samples have aromaticity consistent with the petrographic composition thereof, suggesting relatively high aromatic hydrocarbon contents which fail to oxidize at temperatures commonly suggested for spontaneous combustion initiation. The No.2 and No.4 coal seams of the Witbank coalfield possibly have lower propensity to self-heat than the No.5 seam (vitrinite rich and low aromaticity)(Vassil et al.,2010). The No.5 seam of the Witbank Coalfield is dominated by aliphatic hydrocarbons and has increased propensity to spontaneous combustion. Vitrinite is the principal maceral group of the No 5 seam and Inertinite dominates the No.2 and No.4 seams.

Gouws (1992) suggests there is no relationship between vitrinite content and spontaneous combustion propensity. He notes significant relationship between the calorimeter index and rank related qualities (reflectance of vitrinite, moisture content, oxygen content and carbon contents). The propensity of coal to self-heat is strongly dependent on the oxygen/carbon ratio and the dry ash-free oxygen content of the coal

Table 2.12: Classification of macerals into subgroups and groups, based on international committee for coal and organic petrology (ICCP, 1998, 2001)

Maceral group	Maceral subgroup	Maceral (ICCP,1998,2001)
Vitrinite	Telovitrinite	Telinite
		Collotelinite
	Detrovitrinite	Vitrodetrinite
		Collodetrinite
	Gelovitrinite	Gelinite
		Corpogelinite
Liptinite		Sporinite
		Cutinite
		Resinite
		Exsudatinite
		Chlorophyllinite
		Suberinite
		Alginite (var.lamalginite
		telaginite)
		Bituminite
		Liptodetrinite
Inertinite	Telo-inertinite	Fusinite
		Semifusinite
		Funginite
		Secretinite
		Inertodetrinite
	Detro-inertinite	Micrinite
		Macrinite
	Gelo-inertinite	

2.10.1 Inorganic Matter in coal

The most abundant minerals in coal are clays and carbonates, sulphides, silicates and oxides. Texturally, minerals may occur in layers, as filling of cleats and fractures in coal, as fillings of cell lumens in macerals, or intimately associated with macerals or other minerals.

Minerals such as siderite or pyrite can also replace cell walls or be finely dispersed within the coal matrix. Frequently the Parr formulae is used to calculate mineral matter content from the ash yield (Stracher et al., 2011).Heat produced by pyrite oxidation and from the decay of radioactive minerals in intrusive bodies are additional sources. Heat from pyrite oxidation becomes significant only when the pyrite occurs in a finely divided state and its content is more than 5% (Stach et al., 1982).

Heat produced by radioactive minerals tends to maintain higher insitu temperatures than outside in the open atmosphere. (Parr and Kressman, 1910; Kim, 1977).The ash content of the coals may, at low temperatures, enhance the reactivity of coal char by the catalytic activity of mineral matter components such as calcium. At high temperatures however, the rate of combustion is diffusion controlled and under these conditions, ash could create a physical barrier through which oxygen has to penetrate or circumnavigate in order to reach unburnt carbon. This problem increases during burnout as the proportion of ash increases.

The ash content of inertinite is generally higher than for the other macerals constituents and explains why the unburnt carbon in fly ash is related to the inertinite content. It is known that pure coal is more easily oxidized than that with a high amount of inorganic matter (minerals), as coal has lower thermal conductivity (Parr and Kressman, 1910).

2.10.2 Rank

Rank is the measure of degree of organic metamorphism of a coal, ranging from low-rank peat to high-rank meta-anthracite. Rank can be determined through a number of chemical and physical parameters. In general, no single parameter can be used throughout the entire rank range. For example, equilibrium moisture is one of the most appropriate parameters at low ranks, but gives way to heating value and volatile matter at intermediate ranks and hydrogen at the highest ranks. Vitrinite reflectance is a good parameter for many ranks, although it is of questionable value at the lowest ranks (Stracher, 2011).

Chandra et al. (1993) concluded that "spontaneous combustion is a function of oxygen in coal"; and is highest in low rank coals. They also observed that an increase in the inertinite content increases the crossing point temperature of some Indian coals. Evidence for identifying specific macerals as possible causes of spontaneous combustion is still far from convincing.

An increase in rank (associated with decreased porosity, internal surface area, volatile matter and moisture contents) retards the transport of oxygen to the reactive sites. A low rank coal is therefore more prone to self-heating. The rank influences the amount and nature of the volatiles produced. The parent coal petrography influences the reactivity of the residual char (Bailey et al., 1990). Vitrinite

content, temperature, time of devolatilization and the coal rank are important parameters in the release of volatiles and in the development of char type (Rojas-Gonzales, 2013).

Ratnasthein (1985) identified volatile gases as the major cause of spontaneous fire in the lignite seams of Thailand. High contents of "reactive resins/hydrocarbon" (particularly green and yellow fluorescing resinite and perhydrous vitrinite) were presumed to be responsible for spontaneous combustion in Late Permian coal seams of the Raniganj coalfield, India (Saxena et al., 1990). Investigating the same set of samples, Chandra and Prasad (1990) noted that the increase in vitrinite and inertinite contents upwards in the sequence decreases the crossing point temperature of the Raniganj coal seams. The disconformity in these conclusions is surprising.

Coals are comprised of a number of macerals which fall into three groups: vitrinite (dominant in most coals); liptinite; and inertinite (Figure 2.8). The level of reactivity of these three groups generally differs in any individual coal, but also varies with the rank of the coal. Macerals of the inertinite group react vigorously in the early part of their history, the liptinites slowly at first and more rapidly later, with vitrinites altering more steadily throughout the rank series. The properties of the macerals become more similar to one another as rank rises.

The changes of maceral properties are a function of the exposure of the macerals to a number of influences in the natural environment which include rise and derivative of temperature change, duration of exposure to elevated temperatures, oxidative influences, overburden pressure and stress. Thermal conductivities of host sediments vary in a coal formation vary and are an important additional factor. The rise of temperature has been regarded as dominant in causing coal reactions (Hampattsoumiana et al., 1998).

All the macerals, with the exception of the highest rank inertinites, react similarly with rising temperature, displaying increasing reflectance and anisotropy (shown by rising bi-reflectance), at least up to a temperature of 1000 degrees Celsius. At higher temperatures further progress of the optical parameters of carbonized vitrinites is less regular (Murchison, 1990).Goodarzi (1984) attributes the irregularity of optical trends mainly to surface phenomena (coatings of isotropic pyrolytic carbon and surface defects due to shrinkage of mosaic texture).

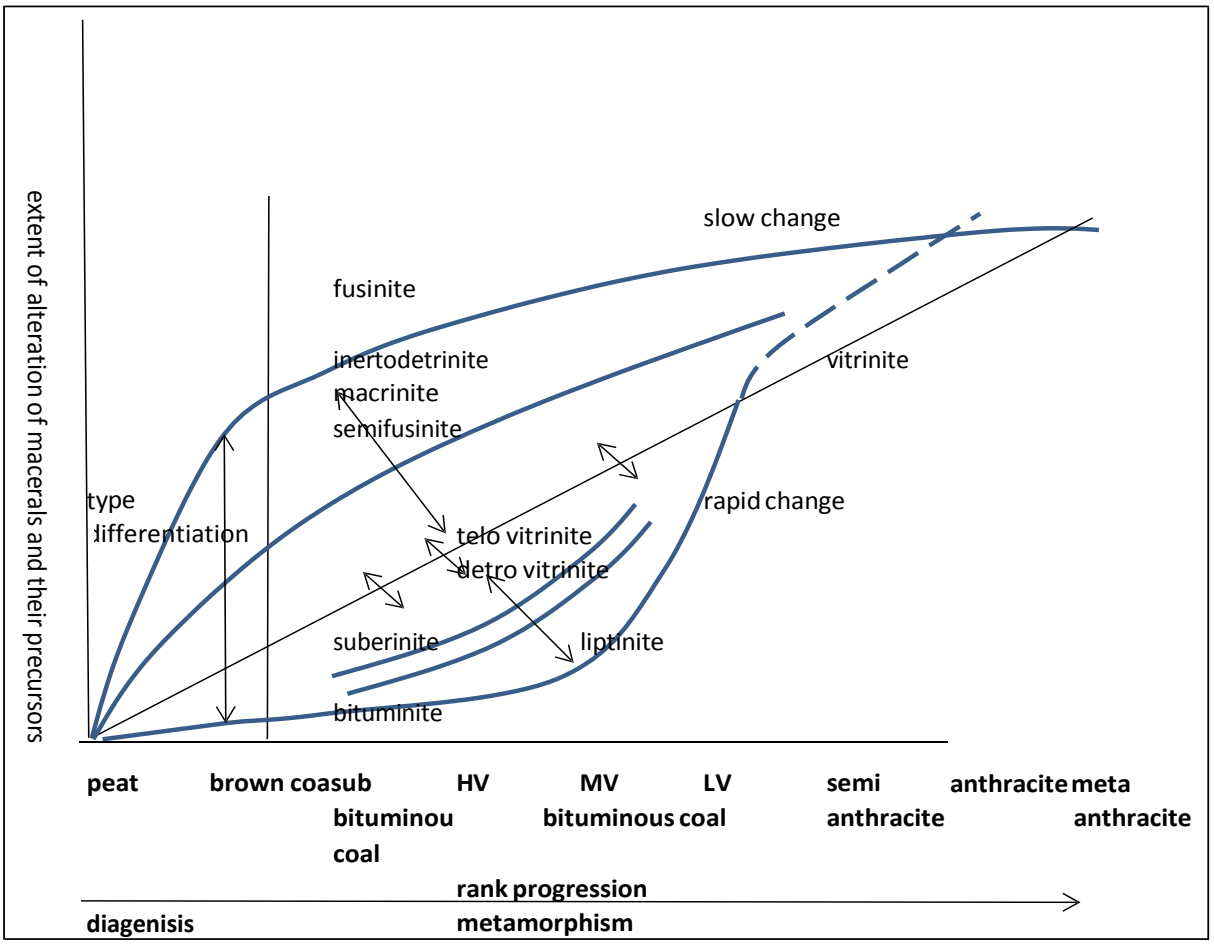


Figure 2.8: Modified Schopf diagram illustrating the variation in rates between individual macerals and maceral groups.

The almost linear change in the properties of vitrinite macerals throughout the rank series is important in their use for rank measurements (Cook, 1980).

2.10.3 Macerals

Macerals in coal are distinguished microscopically by colour, shape, morphology, and degree of preservation of cell structure, reflectance level, and the intensity of fluorescence. These differences between macerals result from different parent material, different depositional environment, or preservation. Macerals are classified into three groups: vitrinite/huminite, inertinite, and liptinite.

2.10.3.1 Vitrinite

The vitrinite group represents woody plant material (e.g., stems, trunks, roots, and branches),derived from lignin and cellulose of plant tissues. Marevich and Travin (1953) found that the dull and semi-dull bands in coal are the most stable and least sorptive, whereas tectonically mylonitized vitrain and

vitrain-fusain in direct contact with each other are particularly susceptible to spontaneous combustion. Ferrari (1938) also recognized that the vitrinite macerals are the most susceptible to spontaneous combustion. Vitrinite macerals have more non-aromatic structures and absorb oxygen readily onto these structures using less activation energy per unit area, and thus experience accelerated oxidation in the earlier stages of self-heating. Although most workers have used chemical parameters (e.g. atomic H/C ratio) as the indicator of rank, a number have used vitrinite reflectance (Axelson (1987); Jones *et al.,* 1986).

2.10.3.2 Liptinite

Maceral composition strongly influences reactivity with liptinite being most reactive and inertinite least reactive (Skorupska et al., 1989).However, the significantly higher proportions of inertinite in some Australian coals have been found to be highly reactive (Thomas et al., 1993).

The liptinite group includes components that are chemically more resistant to physical and chemical degradation than other macerals such as pollen, spores, cuticles, waxes, and resins. Liptinite macerals have a very low porosity but are very reactive in terms of oxygen adsorption. However, the highly porous sacci of gymnospermous pollen, when broken and degraded, as normally they are, particularly in Permian (Lower Gondwana) coals, provide a fair amount of porosity which was not previously recognized.

2.10.3.3 Inertinite

The inertinite ,vitrinite and liptinite maceral groups originate from the same material but inertinite has a higher degree of aromatization and condensation (Kok, 2006). Fusain is extremely soft and crumbles readily into a fine, soot-like powder. Fusain is composed mainly of fusinite (carbonized woody plant tissue) and semifusinite from the maceral inertinite (high carbon, highly reflective) group. It closely resembles charcoal in terms of both chemical and physical properties and is believed to have been formed in peat deposits swept by forest fires or by some bacterial action that generated intense heat [Itay, 1983]. Sinnatt et al. suspected that fusain aids spontaneous combustion.

Moxon and Richardson (1985) on the other hand, believe that an increase in the inertinite content of some Australian bituminous coals decreases their propensity to spontaneous combustion. Potentially the higher porosity (both microscopic and sub-microscopic) of inertinite macerals provides a better passage and storage of air in the coal mass relative to vitrinite and thus indirectly helps auto-ignition.

Inertinite macerals have dense aromatic molecular structures with higher activation energy, reducing susceptibility to oxidation in the initial stages of self-heating. However, their higher microscopic and sub-microscopic porosity (in structured inertinites -semifusinite, fusinite and also resino-inertinite and

bands of inertodetrinite) provide more volume for better air passage in the coals than do the vitrinites. This may explain why the inertinite-rich Permian coal seams in the Talcher, Hutar, North Karanpura and Korba fields of India are prone to auto-ignition.

2.10.3.4 Aromaticity

Previous studies on the aromaticity of coals have either limited themselves to the effects of rank or to differences between the macerals and generally conclude that aromaticity and rank increase simultaneously although not necessarily linearly. One of the most commonly measured structural parameters of either coals or kerogens is the number or fraction of aromatic carbon atoms in the structure.

The main findings of all workers, independent of which technique they used to determine aromaticity, is that aromaticity increases with maturation (Davidson, 1986; Axelson, 1985). Coals like many source rocks generally contain a number of different macerals or kerogens. While the vitrinite reflectance of a coal or source rock is dependent on the presence of, and not the amount of vitrinite, the aromaticity may be dependent on the proportions of the different macerals or kerogens present in the rock. In attempting to interpret the effects of both rank and maceral composition on the aromaticity of a coal, it is necessary to separate the effects of both factors.

At a vitrinite reflectance value of about 3.0% the rate at which the aromaticity increases appears to slow down. Heating of anthracitic coals results in only a small increase in the aromaticity yet the vitrinite reflectance values continue to increase to more than 10%.The relationships observed between aromaticity and vitrinite reflectance and between aromaticity and chemical measurements of maturity by previous workers (Davidson, 1986), suggest that while maturity is the main control on the aromaticity of coals, other factors exert a significant influence.

Maceral association has a greater influence on char formation and its reactivity than particle size. (Malumbazo et al., 2013).Low-temperature oxidation of coal is chiefly restricted to nonaromatic molecular structures: the aromatic skeleton remains unaffected in the initial stages (Banerjee, 1981). Such molecular structures are common in the vitrinite and liptinite maceral groups. Also coal macerals possessing a high inherent porosity, for example cellular cavities (telinite, textinite, ulmo-textinite, etc.), a porous groundmass (desmocollinite, vitrodetrinite, porous telocollinite, attrinire and densinite), and cleats or fractures, are particularly vulnerable to oxidation. Different structures of vitrinite at increasing rank are shown in Figure 2.9.

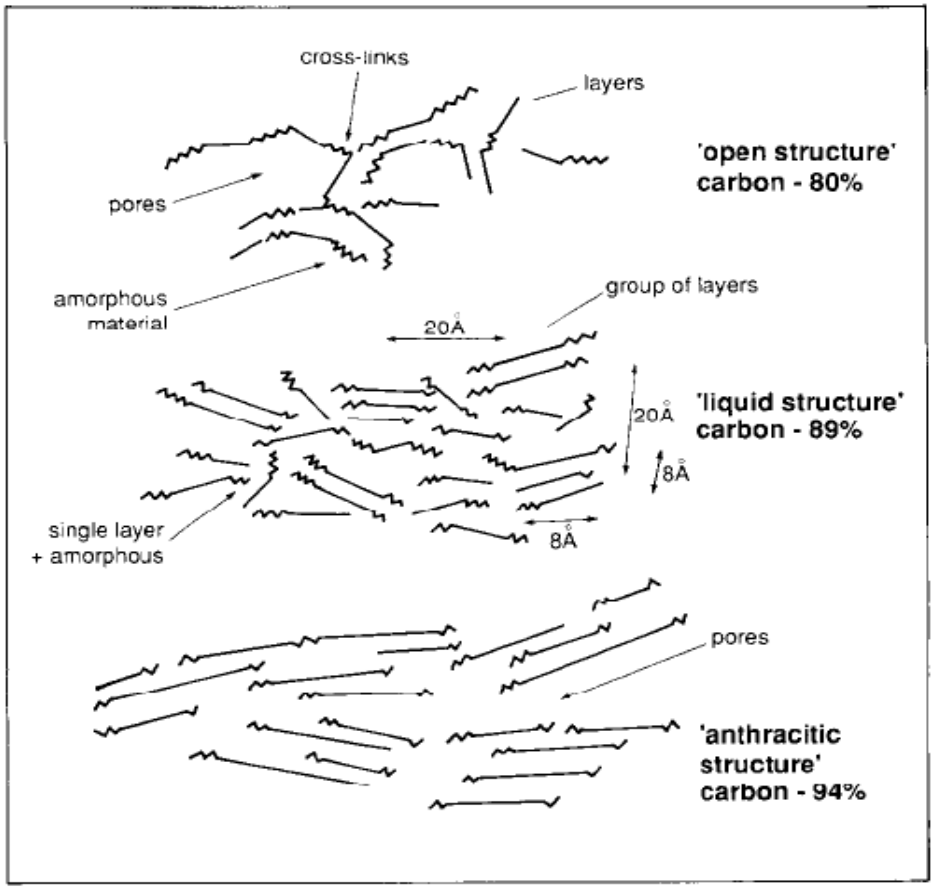


Figure 2.9: Mollecular structure of vitrinites showing the principal structural states at three levels of rank (after Hirsch 1954).

2.11 Case studies

A coal seam fire or mine fire is the underground smouldering of a coal deposit, often in a coal mine. Such fires have economic, social and ecological impacts. They are often started by lightning, grass, or forest fires, and are particularly insidious because they continue to smoulder underground after surface fires have been extinguished, sometimes for many years, before flaring up and restarting forest and brush fires nearby. They propagate in a creeping fashion along mine shafts and cracks in geologic structures (Wikipedia).

Because they burn underground, coal seam fires are extremely difficult and costly to extinguish, and are unlikely to be suppressed by rainfall. There are strong similarities between coal fires and peat fires (Whitehouse and Mulyana, 2004).

Across the world, thousands of underground coal fires are burning at any given moment. The problem is most acute in industrializing, coal-rich nations such as China. Global coal fire emissions are estimated to cause 40 tons of mercury to enter the atmosphere annually, and to represent three percent of the world's annual CO_2 emission (Cray, 2010). Sponcom examples are described below for in India, South Africa, China and the USA.

2.11.1 China

In China, the world's largest coal producer with an annual output around 2.5 billion tons, coal fires are a serious problem. They are concentrated in the provinces of Xinjiang, Inner Mongolia and Ningxia. Beside losses from burned and inaccessible coal, these fires contribute to air pollution and considerably increased levels of greenhouse gas emissions and have thereby become a problem which has gained international attention (Rennie, 2002).

Recent studies by Voigt et al. (2004) claim that 20 million tons of coal is consumed each year in China by uncontrolled fires, while about 200 to 300 million tons of coal in China are inaccessible each year because fires are an obstacle to mining operations.

Investigations in the 1990s led to a threefold classification of Chinese coal fires into: (1) coalfield fires, (2) coal mine fires, and (3) storage/transport fires. Coalfield fires fall within the responsibility of the national government. Coal mine fires and storage-transport fires ought to be controlled by the corporate entity owning the mine or the coal that is being stored/transported (Haiyan, 2005).

The main regions in China affected by coalfield fires are: Xinjiang, Gansu, Qinghai, Ningxia, Shaanxi, Shanxi, Inner Mongolia, Sichuan, Chongqing, and Fujian. A centre of fire activity exists in the desert zone of northern China, where coal fires spread over an area of 5,000 km from east to west, and 150 to 350 km from north to south.

Coal mine fires are coal fires occurring in underground or opencast coal mines; fires in mine dumps and waste heaps also belong to this category. Coal mine fires are distributed over 11 provinces in northern China, affecting 48 collieries. Occurring for the most part in highly combustible, shallow-depth low-ash coal seams of great thickness, coal fires eat up the most valuable (and easy-to-exploit) of coal deposits.

2.11.2 India

In India, as of 2010, 68 fires were burning beneath a 58-square-mile (150 km^2) region of the Jharia coalfield in Dhanbad, Jharkhand. This region has been hit by the unique phenomenon of mine fires which started in 1916 and is rapidly destroying the only source of prime coking coal in the country.

The self-burning Jhingurdah seam of the Singrauli coalfield ccurs in a sub-humid climate and has a brittle and friable texture resulting from structural disturbance. Perhydrous vitrinite and liptinite are common susceptible macerals.. Records of high amounts of siderite concretions (megascopic) from the burning faces of the seam indicates that this mineral may have some definite influence on the heating of the seam.

The Makum coalfield is situated in the per-humid climatic belt of India, as a result it has a very high humidity, low variation in day and night temperatures and a relatively low ambient temperature maintained throughout the year. The seams have been affected by tectonic activity and have a high associated secondary porosity. The Makum seams have very high moisture content and gas emissions. Pyrite (framboidal and granular) in high proportions must cause a significant amount of oxidative heat generation. The coal seams have, by far, the highest amount of susceptible macerals; that is, resinite, porous liptodetrinite (mostly resinite-rich) and perhydrous vitrinite, of all the Indian coals (Chandra et al., 1993).

On the basis of their physical, chemical and petrographic characteristics, the coal seams of the Makuta field should be highly prone to spontaneous combustion. Based on CPT, these coals are highly to moderately susceptible, with CPT values of 139-142°C (Chandra et al., 1993) and 150.5°C (Banerjee, 1981) but still they do not self-ignite. Evidently, the extreme wetness of the seams and high rate of gas emission, especially in the underground mines, act as inhibiting factors and retard auto-ignition.

The high rate of gas emission and the wetness of the insitu coal seams are neutralized by the development of additional secondary porosity and an abrupt reduction in the excessive moisture by evaporation. This results in the coal becoming highly prone to auto-ignition, with a very short incubation period. In the opencast mines, these coal seams are readily and rapidly weathered in the presence of excessive moisture, thus retarding heat accumulation and further oxidation. In fact, the climatic conditions in north-eastern India are highly conducive to the wet weathering of rocks.

The nature of coal oxidation is similar for all types of coal. It is the availability and relative abundance of reactive centres or zones (macerals) that play the decisive role in making one type of coal prone to spontaneous combustion (for example, the Late Permian coal seams of the Raniganj and Singrauli fields), while other types may not be self-burning even in the same coalfield (the Early Permian Turra and Purewa seams in the Singrauli field).

The total amount of heat generated by oxidation in non-prone coal seams tends to be insufficient to induce spontaneous heating, even if the coal possesses most of the properties which lead to auto-ignition. Evidently, all low rank coals are inherently susceptible to spontaneous combustion, and it is

only the external factors which aggravate and induce or retard and inhibit the process in any given condition.

From the preceding critical analysis the following inferences have been deduced (Misra et al., 1994):

- Only the high volatile bituminous (Rom,x 0.50->0.80%) Permian coal seams of the fields situated in the sub-humid climatic belt of India are known to be susceptible to spontaneous combustion..
- The Permian coal and Tertiary coal and lignite seams which are not self-burning but otherwise susceptible and which self-ignite in stockpiles occur in fields in sub-humid, per-humid and semi-arid climatic zones.
- The inherent porosity of a coal or lignite, at any rank stage and under any given condition, does not appear sufficient to have caused spontaneous combustion. It is the additional secondary porosity, accompanied by a reduction in particle size, and its interplay with various climatic factors that have been recognized to be critical for inducing spontaneous combustion in coal/lignite seams and also in coals under storage

2.11.3 South Africa

One of the first local recorded underground heating was mentioned in the records of Griff Colliery for the year 1904 (Morris, 1986). At Northfield Colliery in 1951, the sealing off of an underground fire meant a loss of 2Mt of coking coal, 0.9Mt in pillars and 1.0Mt in-situ (Watson,1977). There is a tendency to report only serious incidents and it is likely that statistics do not reflect the incidents treated successfully at an early stage. DTA tests on waste from Grootegeluk mine showed no liability to spontaneous combustion and could reflect mistakes in stockpile management. Figures 2.10 and 2.11 indicate some of the major causes of fire and coalfields where sponcom has been more frequent in South Africa.

In the late 1930s, a pillar-robbing programme commenced Middelburg Colliery. This has had a marked effect on the environment. Subsidence, tension cracks and crown-hole development began to occur. Air ingress and sponcom followed as pillars strength was reduced by burning.The formation of crownholes and deep tension cracks has increased recharge to the workings (Bell et al., 2001).Transvaal and Delagoa Bay Collieries near Emalahleni (formerly known as Witbank), Mpumalanga has been burning since the mine was abandoned in 1953 (Limpitlaw et al., 2005).

Varga (1967) undertook in situ tests in a sealed roadway after four sampling tubes were installed. The sorption of oxygen from the air was much faster than desorption of carbon monoxide and carbon dioxide produced by the reaction of oxygen with carbon. The lower pressure “underpressure” in the sealed area was seen by Varga to be a potential factor in self-heating

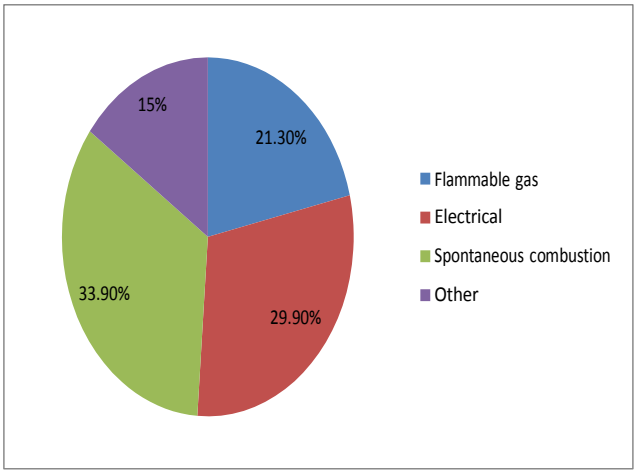


Figure 2.10: Major causes of 254 colliery fires reported from 1970 to 1990

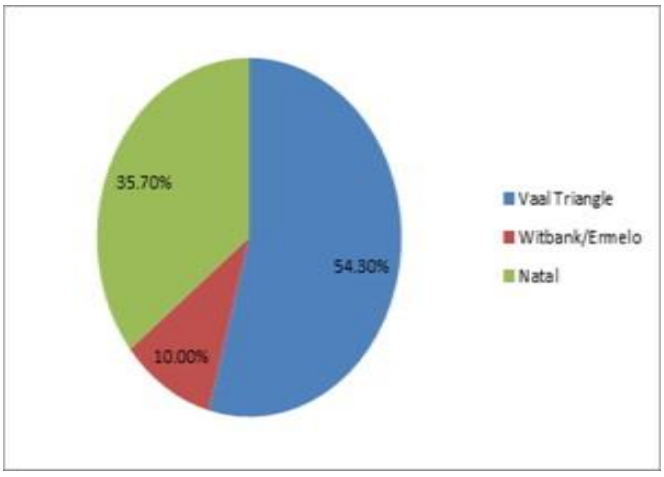


Figure 2.11: Incidents of underground fires caused by spontaneous combustion on an area basis for the period 1970 to 1985 (Morris and Badenhorst, 1987)

Two criteria were used by Chauvin, Lodel and Phillipe (1985) to classify coals according to propensity to self-heat:

- The minimum temperature giving rise to self-heating, and
- The time necessary for the increase in temperature to exceed 40 degrees Celsius.

For each of these criteria a lower value indicated a higher propensity to self-heat. Bunker tests have been used on large samples at the CSIR where coal is aerated at a constant rate until oxidation occurs and the subsequent rise in coal temperature recorded at various levels. Relative humidity and airflow rates can also be modified to represent different storage conditions.

2.11.4 United States

Many coalfields in the USA are subject to spontaneous ignition. The federal Office of Surface Mining (OSM) maintains a database (AMLIS), which in 1999 listed 150 fire zones. In mid-2010, according to OSM, more than 100 fires were burning beneath nine states, most of them in Colorado, Kentucky, Pennsylvania, Utah and West Virginia. But geologists say many fires go unreported, so that the actual number of them is nearer to 200, across 21 states. In Pennsylvania, 45 fire zones are known, the most famous being the fire in the Centralia mine in the hard coal region of Columbia County, which has been burning since 1962 (Cray,2010).

In Colorado, coal fires have arisen as a consequence of fluctuations in the groundwater level, which can increase the temperature of the coal up to 300 °C, enough to cause it to spontaneously ignite.

The Powder River Basin in Wyoming and Montana contains some 800 billion tons of brown coal, and the Lewis and Clark Expedition (1804 to 1806) reported fires there. Fires have been a natural occurrence in this area for about three million years and have shaped the landscape. For example, an area about 4,000 square kilometers in size is covered with coal clinker, some of it in Theodore Roosevelt National Park, where there is a spectacular view of fiery red coal clinker from Scoria Point.

For the last 50 years, the coal fire in Centralia, Pennsylvania has been burning, modifying both the landscape and ecosystem, and has been studied for its impact on soil nutrients and microbiology, vegetation distribution, gas and mineral composition, and on people (Tobin-Janzen et al.,2005 ;Ressler and Markel, 2006).

The locations of the sinkholes coincide with the warmer parts of the landscape. Based on aerial TIR imagery, the sinkholes align to form linear-shaped thermal anomalies with the same orientation and stratigraphic position as the coal splits in the Buck Mountain coal succession. Because the locations of the coal splits match where sinkholes have formed, where the surface heat is the greatest, and where gases from the fire are exhausted, it seems likely that these splits are directly associated with the fire.

It may be that all three anthracite coal splits are burning along fire front 1 in Centralia. This may be possible given the ability of a coal fire to preheat overlying and nearby beds of coal at relatively low temperatures. Anthracite coal may begin to combust under normal surface conditions at nearly 500 °C (Schweinfurth, 2009).Though anthracite coal is less likely to undergo spontaneous combustion due to the low amount of volatile matter, the bedrock in the area is highly fractured from the Appalachian Orogeny (Faill, 1999) and from blasting associated with subsurface mining. Additionally, fractures from mine subsidence may influence the spread of the fire.

Based on the literature review the main potential factors that may contribute to sponcom have been outlined and are further expanded on in the methodology and results sections. Theoretical knowledge is applied to the laboratory results and interpreted in a way that can produce a sponcom risk model.

3 METHODOLOGY

3.1 Background to investigative area

The study area is extensively drilled and has approximately 2296 diamond cored boreholes in the geological database, each with lithological and chemical data. To limit the costs, it was decided to drill 2 specific boreholes-one in the north (borehole A) of the lease area and one in the south (borehole B) of the lease area. The laboratory results obtained from these boreholes were then extrapolated to the existing borehole database (2296 boreholes) using heat value as a common link (Figure 3.1). The newly created sponcom dataset is a highly extrapolated one but robust enough to use in a predictive model. Theoretical relationships between chemical, petrographic and thermal coal properties are long established and the model is expected to mirror some of these relationships in a graphical format using contour plots.

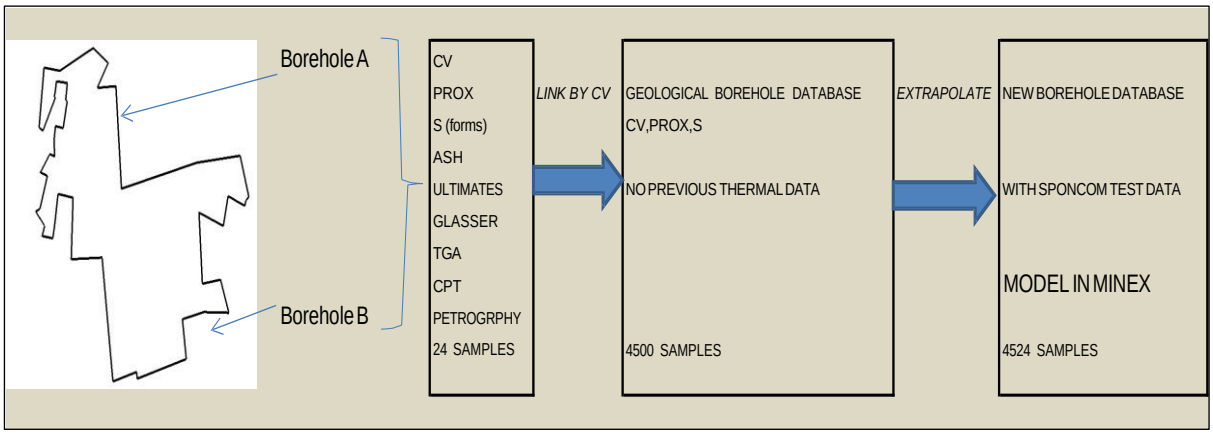


Figure 3.1: Simplified modelling methodology

3.1.2 Analyses and tests conducted

All of the analyses, with the exception of the Smith-Glasser test, were undertaken at external laboratories.

The following tests were performed on each of the sub-samples (Z1-Z22 and ROM1-2).

- Proximate analysis - (SGS laboratory)
- Ultimate analysis - (SGS laboratory)
- Ash analysis - (SGS laboratory)
- Forms of sulphur – (SGS laboratory)
- Crossing point temperature – C.P.T (SGS laboratory)
- Thermogravimetric analysis TGA (Wits University)
- Oxygen absorption (Glasser) – Mine laboratory
- Petrographic analysis – PSA and Wits University

3.2 Sample extraction and preparation

TNW core drilling (71mm diameter) was used to obtain the geological information from borehole A and B. The coal seams from each borehole were sampled using gamma-ray density logs which clearly define different coal/ash bands within a seam (Figure 3.2). A total of 22 coal samples were obtained from the No.5, No.4U and No.2 seams, as well as two ROM (run of mine) samples. These were cling-wrapped and dispatched to SGS laboratory for sample preparation directly after being logged,

The samples were crushed to a 20mm top size and split into 5 sub-samples each (Figure 3.3). A minimum sample mass of 100g was then rotary split after crushing. The sub-samples were vacuum sealed and stored in a fridge at 4 degrees Celsius before delivery to the various laboratories.

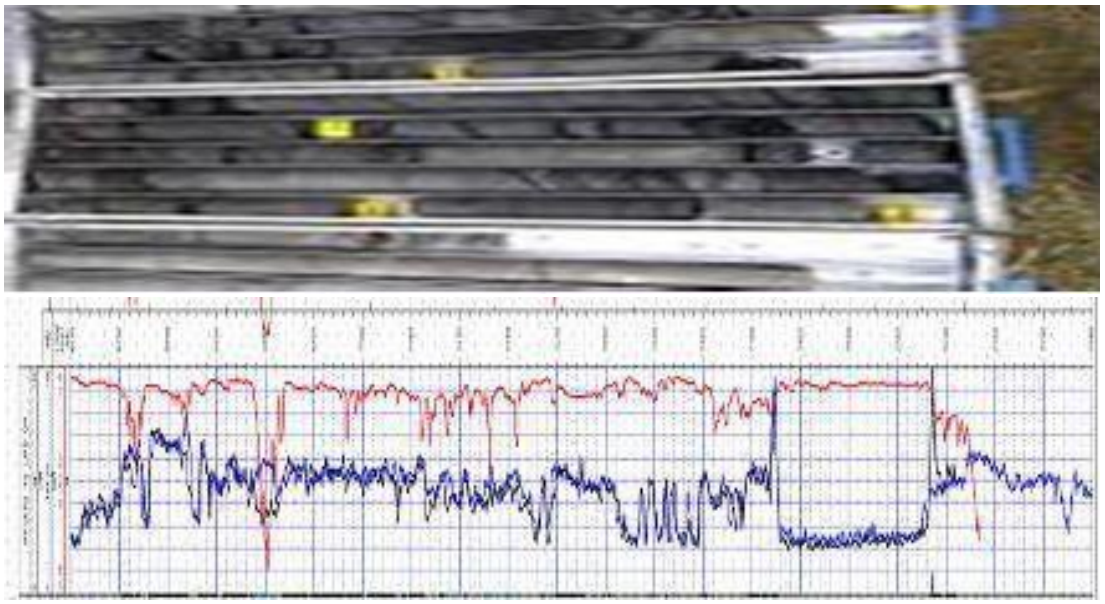


Figure 3.2: Core tray with coal samples and density log for determining sample intervals



Figure 3.3: Crushing of drill-cores to 20mm top size

3.3 Methods used for thermal analysis

Three thermal tests, namely TGA (thermogravimetric), CPT (crossing point temperature) and the Glaser test (oxygen absorption) were used to determine the thermal properties of the coal samples. Although a variety of tests such as DTA (differential thermal analysis) ,WOP (wet oxidation potential) and DSC (differential scanning calorimetry) are commonly used in thermal experimentation, the methods chosen were those available at the facilities and are deemed sufficient for characterizing organic materials.

3.3.1 Crossing point temperature (CPT)

The tests were performed at SGS laboratory and the method is briefly described below. The unit is locally made by Caltech (Figure 3.4-3.5) and consists of the following main components:

- Furnace
- Thermocouples
- Aluminum reaction vessel
- Flow meters
- Drying train

The preparation of samples for this test is very critical. Samples to be tested must be as fresh as possible, before any drying or oxidation can take place. Whenever exposed to prolonged oxidation, reactive solid mineral fuels do not produce the same results as when fresh. The samples were pulverised to -300 micron and stored in a refrigerator before being tested (samples may optionally be

stored under nitrogen). A 5ml sample is placed into the aluminium reaction vessel and any openings are covered with kaowool to insulate.

Two ramping rates of 2 ºC/minute and 1 ºC/minute were used and initially the vessel is nitrogen flushed until a temperature of 70 ºC is reached. Between 70 ºC and 220 ºC or until the CPT is reached the vessel is flushed with oxygen. All samples were tested in duplicate.

When the temperature of the solid mineral fuel within the reaction vessel exceeds the temperature of the furnace, the "crossover" or relative ignition temperature has been reached. The temperature of the solid mineral fuel within the reaction vessel should exceed the furnace temperature by at least 5 ºC to ensure that a definitive result has been obtained before the furnace is turned off.

On a single graph, the temperatures of the furnace and of the solid mineral fuel within the reaction vessel are plotted along the *x* axis and time along the *y* axis (in minutes). The intersection of the two lines is the “relative ignition temperature” (crossover temperature). Alternatively, the controller / computer can determine this crossover temperature electronically.



Figure 3.4: Crossing point temperature instrument with control unit and furnace

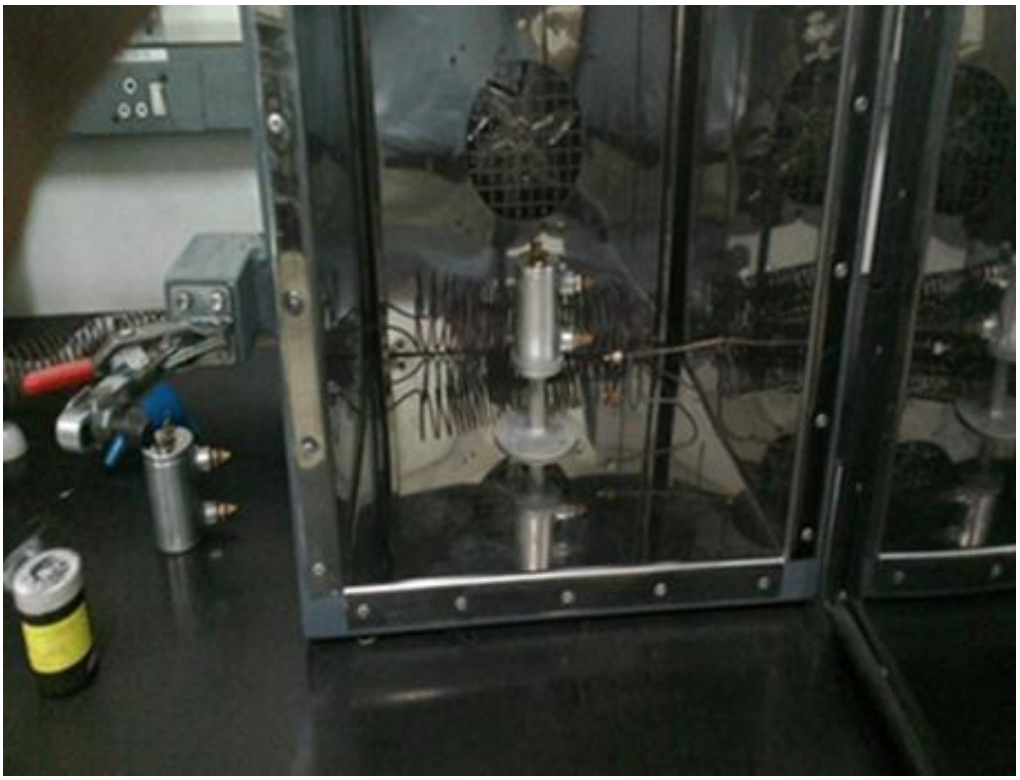


Figure 3.5: Furnace with aluminium reaction vessel

3.3.2 Thermo-gravimetric analysis (TGA)

The method is based on that used by Avila (2012). Thermo-gravimetric analysis (TGA) was carried out using a TA Q500 (TA instruments Co), with a gas flow of 100ml min-1 and a sample size of 4-20mg (Figure 3.6). This instrument has 16 platinum pans located in an auto sampler tray, which is controlled from a remote desktop that is also used to control the heating programs and record the weight of the sample as a function of time. Five main methods can be applied and test for: Proximate analysis, reactivity in air, slow pyrolysis, spontaneous combustion testing, and absorption of oxygen.
The experimental procedure to load the sample pans is described as follows:

- Platinum crucibles are cleaned and tared using the auto sampler tool.
- Approximately 10mg of sample is placed in the platinum crucibles (sample preparation described in section 3.2.3).
- Sample is run using a software controlled program

3.3.2.1 Intrinsic Reactivity

The intrinsic reactivity test identifies the propensity of samples to lose weight whilst being heated at a fixed ramp rate in air (10 ºC min-1). There are key values that can be obtained from this test:

- initial temperature (the stage at which at 1%wt conversion is achieved);
- peak temperature (where combustion or devolatilisation rates reach a maximum); and
- burnout temperature (where 99% of the carbonaceous material has been combusted).

3.3.2.2 Spontaneous combustion testing

This test is used to identify samples which are highly reactive in air at low temperatures. The test consists in a set of different heating ramp rates in air (experiment executed using heating rates of 3, 5, 7, 10, 20, 30, 40 and 50 ºC min-1). There are key values that can be obtained from this test:

- derivatives of weight against time; and
- slope of the derivative plot in the linear segment of the curve, at low temperature.

This information can be plotted to form a profile of heating ramp rate vs slope obtained, which is unique for each sample and possibly relates to the self-heating phenomena.

3.3.2.3 Absorption of oxygen

This test identifies samples which absorb oxygen at low temperature whilst being heated at a slow ramp rate in air (executed twice using heating rates of 3 and 5 ºC min-1 under an air atmosphere). There are key values that can be obtained from this test:

- initial temperature (the stage at which an increase in sample weight starts);
- peak temperature (where increased weight of the sample reach a maximum); and
- % of maximum oxygen absorption (% of weight reached in the peak temperature). This test considers just the net oxygen adsorption.



Figure 3.6: TGA analyser used at Wits University

3.3.3 Oxygen adsorption test (Smith-Glasser)

1.3.3.1 Mine method

The method used at the mine laboratory is a simplified version of that used by Smith and Glaser (2004) (Figure 3.7).The samples were pulverised and screened to a -100 micron size. Fifty grams was weighed out and placed into a conical flask (reactor) with an inlet valve.

The reactor was then placed in a water bath and flushed with pure oxygen for 7 minutes. The reactor was connected to a beaker containing vegetable oil via silicone and U-tubing, and a calibrated pippete. The water bath was then heated to a constant 50 ºC and the rise of oil level in the pipette recorded after 2 hours.

No mass recordings were made and the results are relative for each sample based on the amount of oil suctioned (oxygen adsorbed). Samples were also tested at ambient temperature and normal oxygen concentration (air-flush).



Figure 3.7: Oxygen adsorption test apparatus at mine laboratory

1.3.3.2 Smith and Glasser method

The static isothermal method has been used by several researchers to directly measure the extent of reaction of coal with oxygen. The main components of the apparatus comprise a glass reaction bottle, a turntable, a balance and a computer. A diagram of the reactor is shown in figure 3.8.

The reactor has a lower conical section, in which the coal sample can be placed in a thin layer to avoid mass transfer resistance. The reactor can be flushed with gas via a valve. Dipping the reservoir spout into a beaker of oil seals the reactor. As the coal adsorbs gas, oil is sucked into the pipette. The increase in the mass of the reactor (independent of the beaker of oil) divided by the density of the oil gives a measure of the volume of oxygen adsorbed.

The ideal gas law relates the volume V1 of a reaction bottle to the amount of gas it contains, n_1, by the equation:

$$V_1 = n_1 RT_1 / P_1$$

T_1 and P_1 are measured at the beginning of a run, and n1 and R, are constants. If T_1 and/or P_1 change to T_2 and/or P_1 during the experiment, then V_1 is related to the new volume V_2 by:

$$V_2\text{-}V_1 = n_1RT_1/P_1 - n_1 RT_2/P_2 = m_2\text{-}m_1/p$$

where m_2-m_1 is the measured mass change of the apparatus and r is the density of the oil used. The above can be rearranged to give T_2 and P_2 in terms of the known or measured quantities.

$$T_2/P_2 = T_1/P_1-(m_2-m_1/pn_1R)$$

The reacting case differs in that n1 is no longer constant.

$$V_2-V_1 = n_1RT_1/P_1 - n_2RT_2/P_2 = m_2-m_1/p$$

The previous expression for $T2/P_2$ can then be substituted into the above equation to solve for n2, and hence the oxygen consumed

$$n_2 = (n_1T_1/P_1 - m_2-m_1)/ p R/ (T_1/P_1 - m_2-m_1/pr)$$

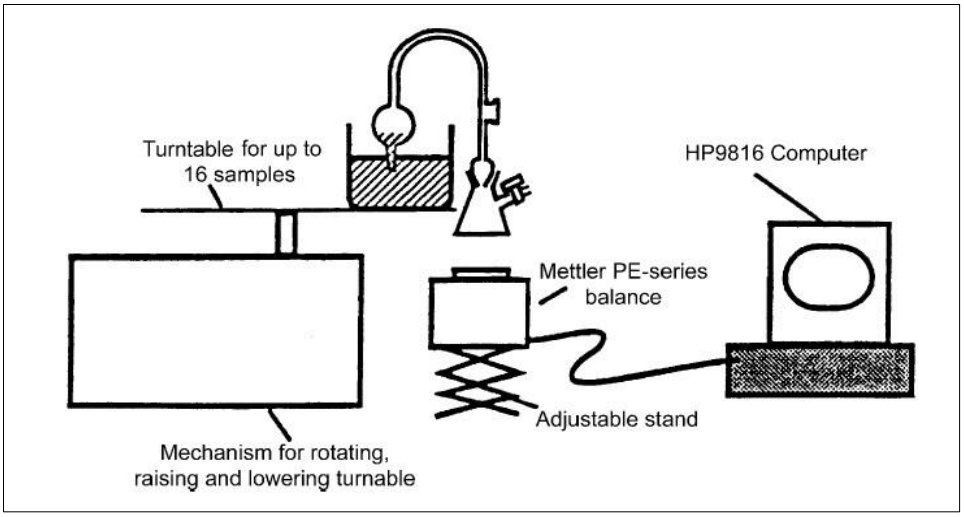


Figure 3.8: Static isothermal apparatus used by Smith and Glasser (2004)

3.4 Chemical analysis

Chemical composition of the coal is defined in terms of its proximate and ultimate (elemental) analyses. The parameters of proximate analysis are moisture, volatile matter, ash, and fixed carbon. Elemental or ultimate analysis encompasses the quantitative determination of carbon, hydrogen, nitrogen, sulphur and oxygen within the coal. Additionally, specific physical and mechanical properties of coal and particular carbonization properties are included.

Both the proximate and the ultimate analysis may be reported on an as received (ar) basis, a dry (d) or moist basis, an ash-free (af) basis, a mineral matter-free (mmf) basis and various combinations of those bases. The basis of the analyses undertaken in this thesis is described in Table 3.1.

Ash and mineral matter are two distinctly different entities. Mineral matter consists of the various minerals contained in the coal. Ash is the inorganic solids' remaining after the coal is completely combusted. The ash is usually lower in mass than the mineral matter because of the weight changes that take place during coal combustion such as the loss of gaseous carbon dioxide from mineral

carbonates, loss of water from silica minerals and loss of sulphur (as gaseous sulphur dioxide) from iron pyrites.

Table 3.1: Methods used at SGS laboratory to determine chemical parameters of the coal samples

	Analysis		Unit	Method / Standard
Analysis on air dry basis	Calorific Value	In Coal	MJ/kg	ISO 1928
	Inherent Moisture	In Coal	%	ISO 5068-2
	Ash	In Coal	%	ISO 1171:1997(E)
	Volatile	In Coal	%	ISO 562
	Fix Carbon	In Coal	%	By Calculation
	Total Sulphur	In Coal	%	ASTM D 4239
Analysis on air dry basis	Carbon	In Coal	%	ASTM D 5373-08
	Hydrogen	In Coal	%	ASTM D 5373-08
	Nitrogen	In Coal	%	ASTM D 5373-08
	Oxygen	In Coal	%	By Calculation
Analysis of the ash	SiO2	In Ash	%	IN HOUSE METHOD by XRF
	Al2O3	In Ash	%	
	Fe2O3	In Ash	%	
	CaO	In Ash	%	
	MgO	In Ash	%	
	Na2O	In Ash	%	
	K2O	In Ash	%	
	P2O5	In Ash	%	
	TiO2	In Ash	%	
	MnO	In Ash	%	
	SO3	In Ash	%	
FORMS OF SULPHUR	Mineral Sulphur	In Coal	%	ISO 157
	Sulphate sulphur	In Coal	%	ISO 157
	Organic Sulphur	In Coal	%	ISO 157
	Pyritic sulphur	In Coal	%	ISO 157

3.4.1 Moisture (Standard Method: ASTM D3173, ISO 11722, and AS1038.3)

Moisture is defined as the water that exists in the coal at the site, time, and under the conditions it is sampled. The amount of moisture in a sample is determined by measuring the loss in mass between an as-mined sample and one that has been heated under controlled conditions to drive off water not contained within the chemical structure of the coal (Figure 3.9).

Moisture is an important property of coal, as all coals are mined wet. Groundwater and other extraneous moisture are known as adventitious moisture and are readily evaporated. Moisture held within the coal itself is known as inherent moisture and is analysed quantitatively. Moisture may occur in four possible forms within coal:

- Surface moisture: water held on the surface of coal particles or macerals
- Hydroscopic moisture: water held by capillary action within the microfractures of the coal

- Decomposition moisture: water held within the coal's decomposed organic compounds
- Mineral moisture: water which comprises part of the crystal structure of hydrous silicates such as clays

Total moisture is analysed by loss of mass between an untreated sample and the sample once analysed. This is achieved by any of the following methods;

1. Heating the coal with toluene
2. Drying in a minimum free-space oven at 150 °C (302 °F) within a nitrogen atmosphere
3. Drying in air at 100 to 105 °C (212 to 221 °F) and relative loss of mass determined

The first two methods are suitable with low-rank coals but method 3 is only suitable for high-rank coals as free air drying low-rank coals may promote oxidation. Inherent moisture is analysed similarly, though it may be done in a vacuum.



Figure 3.9: Drying oven for sample preparation at 105 °C

3.4.2 Ash (Standard Method: ASTM D3174, ISO 1171, and AS1038.3)

The ash was analysed at SGS laboratories using ISO 1171:1997(e).The ash content of coal is the non-combustible residue left after carbon, oxygen, sulphur and water has been driven off during

combustion. The remaining residue or ash is expressed as a percent of the original coal sample weight. The composition of this final ash differs from the inorganic constituents of the coal prior to incineration due to chemical changes during combustion. The total mass of ash produced can differ somewhat from those obtained in power plant furnaces because of dissimilar incineration conditions. Analysis is fairly straight forward, with the coal thoroughly burnt and the ash material expressed as a percentage of the original weight. It can also give an indication about the quality of coal. Ash content may be determined as air dried basis and on oven dried basis. The main difference between the two is that the latter is determined after expelling the moisture content in the sample of coal.

3.4.3 Ash element analysis

The ash elemental analysis was done by XRF (X-ray fluorescence) using an in-house method. The elements analysed for were: SiO2, CaO, Fe_2O_3, Al_2O_3, TiO_2, Mn_3O_4, BaO, SrO, P_2O_5, and SO3. The modern X-ray fluorescence is also a non-destructive technique that is suitable for normal assaying requirements. It typically has an accuracy of 2 to 5 parts per thousand and is well-suited to relatively flat and large surfaces. It is a quick technique taking about three minutes, and the results can be automatically printed out by computer. The process for X-ray fluorescence assay involves melting the material in a furnace and stirring to make a homogenous mix. Following this, a sample is taken from the centre of the molten sample. Samples are typically taken using a vacuum pin tube.

3.4.4 Sulphur

Sulphur content determinations help to evaluate the potential sulphur emissions from coal combustion, or for contract specifications purposes. SGS laboratories use ISO 157 method to determine all forms of sulphur. A leco sulphur analyser was used to determine the forms of sulphur.

3.4.4.1 Total Sulphur

The sample is analysed for total Sulphur using a Leco sulphur analyser. The sample (0.01 to 0.1 g) is heated to approximately 1350 °C in an induction furnace while passing a stream of oxygen through the sample. Sulphur dioxide released from the sample is measured by an IR detection system and the Total Sulphur result is provided.

3.4.4.2 Sulphide Sulphur

A prepared sample is selectively leached in warm sodium carbonate solution to convert the metal sulphate into insoluble carbonates and soluble sulphate. The resulting residue is removed by filtration and the sulphide residue is washed free of carbonate solution and analysed by a Leco sulphur analyser.

3.4.4.3 Sulphate Sulphur

A prepared sample is boiled with a sodium carbonate solution for 30 minutes. Any insoluble materials are removed by filtration and ferric iron is reduced to ferrous iron by the addition of hydroxylamine hydrochloride. The sulphate in the resulting filtrate is then precipitated with barium chloride in a dilute

hydrochloric acid medium. The barium sulphate precipitate is filtered, ignited, weighed and calculated as %S (of total sulphate) in the original sample.

3.4.5 Calorific Value

SGS laboratories used ISO 1928 to determine the calorific value. The calorific value (or heat of combustion) of coal or coke is the heat liberated when the solid fuel undergoes complete combustion in oxygen (Figure 3.10). The fuel sample is burned in a bomb calorimeter and the total heat energy (in MJ/kg) is measured. This is a fundamental test in determining the quality of coal and coke.



Figure 3.10: CV Calorimeter for determination of heat value (MJ/kg)

3.4.6 Volatile matter

SGS laboratories used ISO 562 to determine volatile matter. Volatile matter in coal refers to the components of coal, except for water, which are liberated at high temperature in the absence of oxygen under rigidly controlled conditions. The mass of volatiles liberated is determined through a before and after weight comparison (Figure 3.11). Generally volatile matter is highest in low grades of bituminous coals and lowest in hard coals such as anthracite. Volatile matter is a key component in the classification of coal and represents a real health and safety concern as coals high in volatiles have an increased risk of spontaneous combustion.

Volatiles are usually a mixture of short and long chain hydrocarbons, aromatic hydrocarbons and some sulphur. The volatile matter of coal is determined under rigidly controlled standards. In Australian and British laboratories this involves heating the coal sample to 900 ± 5 °C (1650 ±10 °F) for 7 min.



Figure 3.11: Volatile furnace (950 °C)

3.4.7 Fixed carbon

The fixed carbon content of coal is determined by subtracting the percentages of moisture, volatile matter and ash from the original mass of the coal sample. In practical terms it is the solid combustible residue that remains after a coal has had the volatiles driven off. This differs from the ultimate carbon content of the coal because some carbon is lost in the combustion process as hydrocarbons within the volatile components. Fixed carbon is used as an estimate of the amount of coke that will be yielded from a sample of coal.

3.4.8 Ultimate analysis

Carbon, hydrogen and nitrogen were determined using ASTM D 5373-08 and oxygen calculated by difference. The ultimate analysis produces more comprehensive results than the proximate analysis and is used in the determination of the elemental composition of the coal including moisture, ash, carbon, hydrogen, nitrogen, sulphur, and oxygen (by difference). Each element is determined through

chemical analysis and expressed as a percentage of the total mass of the original coal or coke sample.

3.5 Petrographic analysis

The samples were received, prepared and polished at Petrographics SA. Abnormal condition analysis was conducted by Prof Wagner. The reflectance analysis was conducted at SABS CSIR Campus by Mr Chabalala, and verified by Mrs du Cann of Petrographics SA. The maceral analysis was conducted by Mrs du Cann, and verified by Prof Wagner.

3.5.1 Vitrinite reflectance

Readings were taken in accordance with the ISO Standard 7404 - 5, 1994.

Table 3.2 - Vitrinite reflectance parameters measured in coal samples

Abreviation	Parameter
Rr%	Random reflectance of vitrinite, oil immersion (determined)
	Standard deviation
Rmax%	Maximum reflectance of vitrinite (calculated)

3.5.2 Condition/weathering analysis

The polished blocks were analysed using a semi-automated point counting stage and Petrog software attached to a Zeiss Universal microscope. The abnormal condition analysis is an in-house technique, developed following a PhD study. It is used extensively to quantify weathering, oxidation, and any other unusual features observed in the coal samples. All analyses were conducted at a magnification of x500 under oil immersion. Results are reported on a % volume basis. For the purposes of the current investigation into spontaneous combustion of coal, pyrite was included in the analysis.

3.5.3 Maceral analysis

Maceral analysis was carried out by Petrographics SA (% by volume, mineral matter basis). The group maceral analyses were carried out in accordance with ISO 7404 - 3, 1994. The reactive inertinite macerals were identified according to Steyn & Smith for South African coals (Table 3.3)

Table 3.3: Maceral groups and reactive inertinite groups identified in the samples

Abreviation	Maceral
VIT	Vitrinite
PV	Pseudovitrinite
TV	Total vitrinite
S/R/C	Sporinite/resinite/cutinite
ALG	Alginite
TOT L	Total liptinite (formerly referred to as exinite)
RSF	Reactive semifusinite
ISF	Inert semifusinite
F/SEC	Fusinite/secretinite
MIC	Micrinite
R INT	Reactive inertodetrinite
I INT	Inert inertodetrinite
TOT I	Total inertinite

3.6 Computer modelling

The results obtained from the 22 drill-core samples and 2 ROM samples were matched to the existing borehole dataset (2296 boreholes) based on similarity of heat value. Similar coal types (bright, banded, dull, massive) in each borehole are therefore matched. A total of 24 test results (thermal, chemical and petrographic) from borehole A and borehole B were thus assigned to the borehole database which has approximately 1500 samples for each seam.

Proximate and heat values from the existing borehole database were unchanged. The weighting of risk factors was arbitrarily assigned on 1/3rd percentiles as low-risk (0 points), moderate-risk (1 point) or high-risk (2 points).No recognised method exists for the weighting or selection of sponcom factors in determining a risk matrix.

The risk matrix is empirical and relative. However a reasonable balance of geological, thermal, chemical and petrographic factors has been included to give some indication of seam zones with higher sponcom risk (Table3.4). As stated previously mining factors could not be included in the model at this time, but will be included at once mining commences.

In some of the variables e.g. CPT, the lowest numerical value is assigned the highest risk value (2) and in others e.g. VM, the lowest numerical value corresponds with the lowest risk value (0).This is in accordance with the theory described in section 2.

Table 3.4: Risk matrix used for modelling of sponcom risk factors

Matrix Score	Geological Factor				Coal Factor										
	seam				chemical				thermal				petrographic		
	Parting	Depth	Seam Thick	Roof/floor md	AS	VM	IM	TS	CPT	GLI	T2	WT	AB	TR	VR
	>2m	<40m	>5m	>2m	%	%	%	%	°C	°C	°C	%	%	%	%
min	0	0	0	0	2	0	0	0	2	0	2	0	0	0	2
mid	0	0	0	0	1	1	1	1	1	1	1	1	1	1	1
max	1	1	1	1	0	2	2	2	0	2	0	2	2	2	0

Sponcom analysis does not form part of the usual tests performed on drill-cores and these tests are usually done on stockpile or train samples where sponcom more regularly occurs. To fill this information gap a highly extrapolated model was required that would link existing coal quality information in the GBIS borehole database (2296 boreholes) to the relatively sparse sponcom dataset (2 boreholes with 24 samples).

The 15 parameters in table 6.4 were modelled individually and cumulatively to provide a combined total risk of all the factors used. The geological factors (seam thickness etc.) are not dependant on the sponcom test results. Zones where dykes and/faults occur are known to increase sponcom factors but for practical reasons are not included in the model.

By linking the laboratory datasets (borehole A and B) and the existing borehole database used for resource modelling, the sponcom variables could be modelled in a similar way to the coal resources. Gridded models represent the deposit as a series of layers and are ideal for layered deposits such as coal, bauxite, laterites and phosphate. Minex 6.05 software was used for exercise and is suited for modelling coal seams and tabular ore-bodies. The general purpose gridding method was applied with a 50m mesh size and 2000m scan distance. Approximately 1500 boreholes with No.5 seam, No.4 upper seam and No.2 seam intersections were modelled. Statistical correlations between the variables were also performed in Minex. The gridded contour plans provide an easy visual guide to spatial distribution of the variables.

Typically exploration drilling provides data values Z, at irregularly locations in X and Y space. The process of gridding uses these irregularly spaced data values to create or estimate grid values on a regular spacing. The imaginary grid is usually square but can be rectangular. The size of the grid cells should reflect the data distribution. Typically grid cells should be 20-25% of the data spacing. The growth method (general purpose) is a two stage process. Stage 1 surrounds the data with four grid mesh points. In stage 2 the data is discarded and the grid mesh grows outwards to fill in the remaining grid mesh cells. The growth method is based on a technique used by IBM in the STAMPEDE1 planning software (Geological modelling, Gemcom Minex-white paper, J.Barber, 2012).

3.6.1 Correlations

Correlations are made between all of the tested variables and the meaningful correlations are further explained in the discussion chapter. The correlation diagrams and histograms were generated using Minex 6.05 software.

In statistics, dependence is any statistical relationship between two random variables or two sets of data. Correlation refers to any of a broad class of statistical relationships involving dependence. Formally, dependence refers to any situation in which random variables do not satisfy a mathematical condition of probabilistic independence. Correlation can refer to any departure of two or more random variables from independence, but technically it refers to any of several more specialized types of relationship between mean values.

There are several correlation coefficients, often denoted ρ or r, measuring the degree of correlation. The Pearson correlation coefficient is most commonly used, which is sensitive only to a linear relationship between two variables (which may exist even if one is a nonlinear function of the other). More robust correlation coefficients have been developed that are more sensitive to nonlinear relationships than the Pearson correlation (Wikipedia).

4 RESULTS

Results for each of the tests performed are described in chapter 4 and include histograms, correlation plots and contour plans for each of the seams modelled. Additional data is included in the appendix. As expected the thermal-chemical correlations are not as well defined as certain proximate variable relations, but trends can be observed that support theoretical relationships.

4.1 Crossing point temperature

The crossing point temperatures (CPT) from drill-cores in the study area are tabulated below and are generally above 200 °C or slightly below. Banerjee (1985) uses a 140 °C upper limit for coals with sponcom risk (Figure 4.1).Those samples with a CPT below 200 °C (Z1,Z 2, Z6, Z7, Z8, Z14, Z18) may have a low-moderate risk of self- heating relative to other coals based on the SGS method used. None of the samples tested fall in the high risk category below 140 °C.

Samples with no crossing point temperature (NCPT) were high ash samples that exceed the detection limit of the instrumentation. All of the tested values fall within a fairly narrow range. The average CPT for the 1 °C /min ramp is 206 °C and 229 °C for the 2 °C /min ramp. This agrees with theory that higher heating rates give less time for oxygen interaction which elevates the CPT. The 2 °C ramp tests were only undertaken on the second set of samples (Table 4.1).

Relative ignition temperatures below 140 °C (SGS method) are taken to be indicative of "troublesome" coals, while values above 200 °C are regarded as "safe" coals. The relative ignition temperature is not a physical constant for a given solid mineral fuel because the actual relative ignition temperature is dependent upon the conditions under which the test is performed. As an empirical test, the results are dependent upon strict adherence to test equipment and condition specifications. Therefore, it is critical that all test conditions and equipment specifications be strictly adhered to.

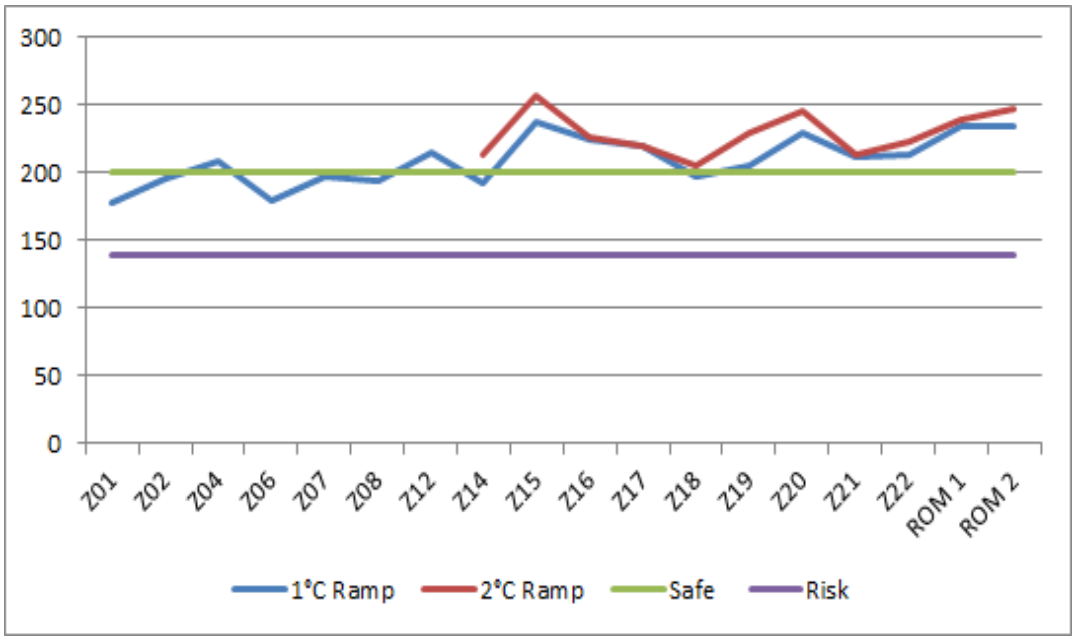


Figure 4.1: Sample CPT compared to safe limit of 200 °C (SGS method) and risk limit of 140 °C (Banerjee)

Individual high CV bands within a coal seam may be more susceptible to sponcom and have a lower CPT than indicated by the full seam CPT. Therefore a seam with 'high' CPT may still have discrete bands that are susceptible to sponcom. The modelling method is thus conservative in approach and considers the average CV/CPT value for the whole seam, rather than individual bands with higher susceptibility that may not be laterally continuous or possible to model in 2 dimensions. The No.5 seam has the highest variance and lowest average CPT followed by the No.2 and No.4U seam (Appendix A8-A13).

Table 4.1: Crossing point temperature of samples at different ramping rates

Sample	Adiabatic Crossing Point Temperature (CPT)		Risk
	1°C Ramp	2°C Ramp	
Z01	178		safe
Z02	195		safe
Z03	NCPT		
Z04	209		safe
Z05	NCPT		
Z06	179		safe
Z07	198		safe
Z08	194		safe
Z09	NCPT		
Z10	NCPT		
Z11	NCPT		
Z12	215		safe
Z13	NCPT		
Z14	192	214	safe
Z15	237	257	safe
Z16	225	227	safe
Z17	220	220	safe
Z18	198	205	safe
Z19	205	230	safe
Z20	230	246	safe
Z21	212	214	safe
Z22	214	223	safe
ROM 1	235	239	safe
ROM 2	234	247	safe

NCPT (CPT above detection limit)

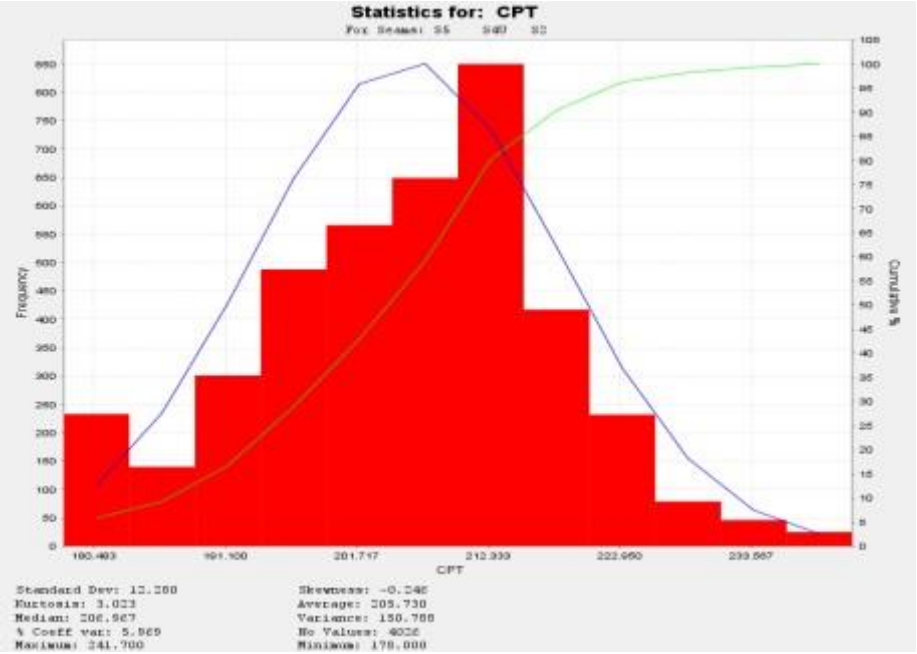


Figure 4.2: Combined histogram of the modelled No.5, No.4U and No.2 seam CPT

The combined seam histogram for the modelled crossing point temperature shows a median value of 206 degrees Celsius. Figures 4.3-4.5 shows the detail contour plots of each of the coal seams

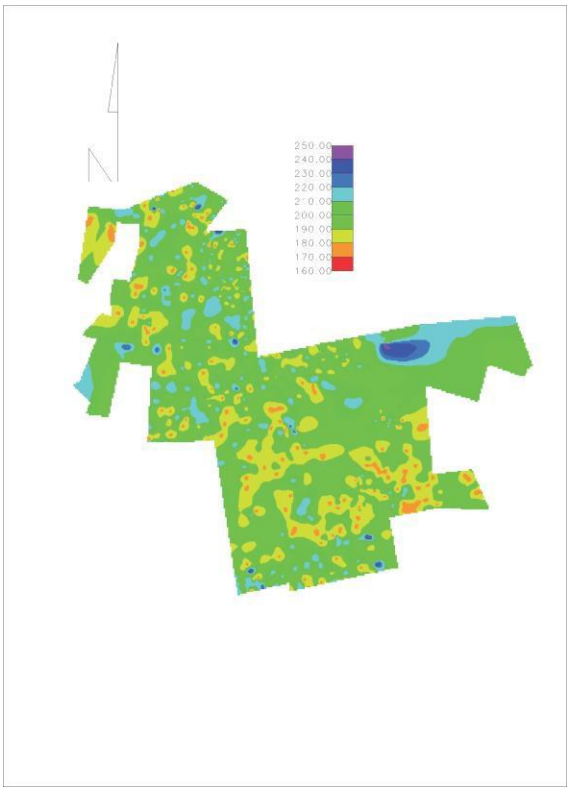


Figure 4.3: No.5 seam CPT

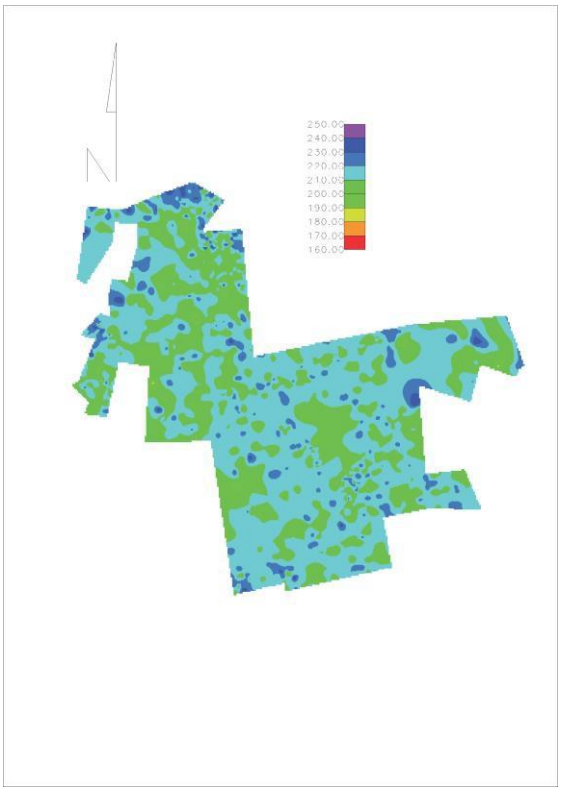


Figure 4.4: No.4U crossing point temperature

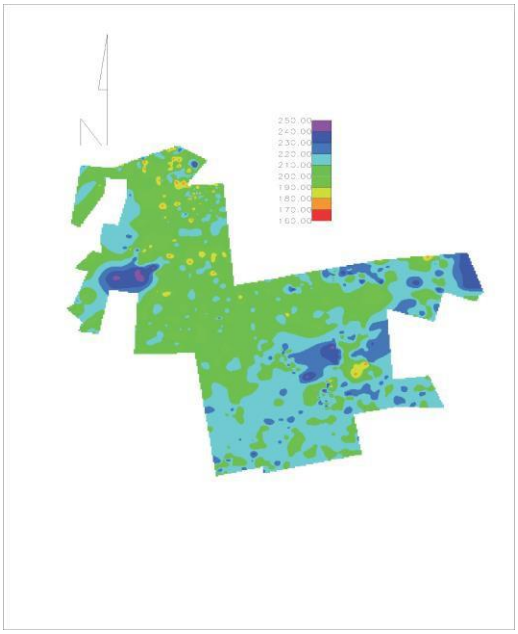


Figure 4.5: No.2 seam crossing point temperature

There is clear zonation between the north mine and south mine CPT in the S2 seam contour plot with lower values north of the graben structure. The No.4U seam shows a fairly homogenous CPT with elevated values relative to the S5 and S2 seams. Very localised spots of 'lower' CPT in the northern areas of the S2 seam may serve as ignition points during mining. The No.5 seam CPT contour plots show distinctly lower values than the other seams with potential 'hotspots' distributed uniformly across the mine area.

4.2 Thermogravimetric analysis (TGA)

The TGA method included an oxygen adsorption test followed by a spontaneous ignition potential test (TGspi).The oxygen adsorption test relates to the chemisorption step with weight increases between 0.0-4.4%.The TGspi test relates more to the combustion process.

4.2.1 TG spi (spontaneous combustion index)

The raw data delivered by the TGA is a sample weight profile (%) in temperature. From this profile, the key values can be obtained directly: a) the initial temperature (the stage at which starts an increase in sample weight); b) peak temperature (where increased weight of the sample reach a maximum); c) the maximum oxygen absorption (% of weight increase reached at the peak temperature) (Avila, 2012). The slope of the derivative curve (linear portion) between 150 and 350 degrees Celsius was obtained from the second TG spi test (Figure 7.12). The results using the formulas below are presented in tables 7.2-7.3 (Avila et al., 2014).

- $TG_{spi(R^2\ calc)}$ = change weight loss rate / change temperature ——(% ^{o} C min $^{-1}$)

The TG spi is calculated for each temperature increment by dividing the derivative of weight gain by incremental temperature change (R2 calculated).A correlation coefficient for each sample at 3,5,7,10,20 degree heating increments is then obtained (R2 graph).The TG spc is then obtained from the formulae below (Figure 4.6).

- TG_{spc} Index = $R^2_{(graph)} - R^2_{(calc)}$

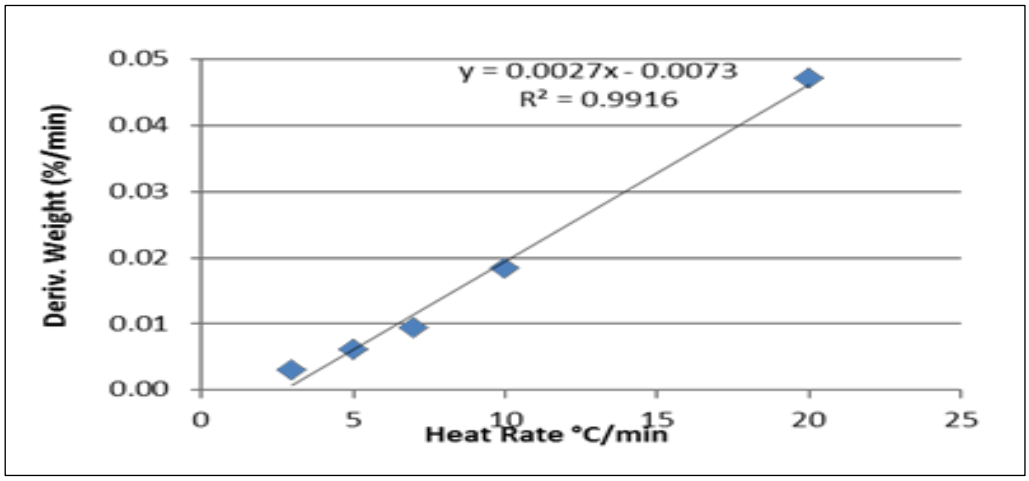


Figure 4.6: TG plot calculated from the derivative of weight gain and heating rate for sample Z013

At each heating rate a unique slope is produced at the initial 'heating segment' of the derivative slope. The relation tends to be linear for most samples.

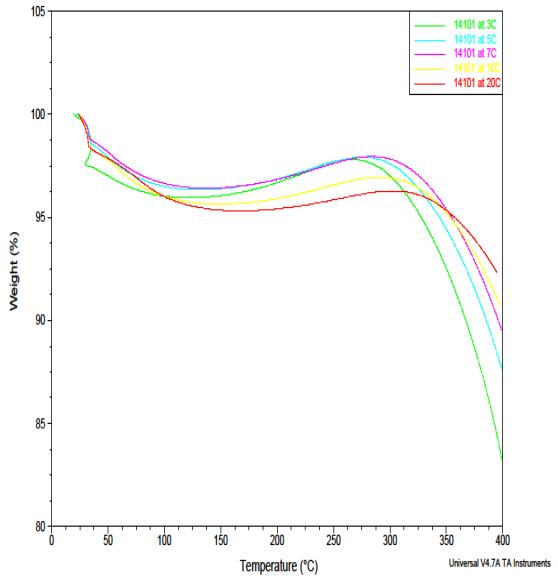
Table 4.2: Results of TGA analysis done at Wits University.

Sample	3C				5C				7C				10C				20C			
	T1`	T2	%WT	DER WT %	T1`	T2	%WT	DER WT %	T1`	T2	%WT	DER WT %	T1`	T2	%WT	DER WT %	T1`	T2	%WT	DER WT %
Z01	132	267	1.85	0.0032	136	276	1.57	0.0052	138	286	1.53	0.0149	158	290	1.29	0.0339	166	300	0.97	0.0938
Z02	128	267	1.34	0.0038	131	284	1.30	0.0112	133	289	1.22	0.0143	147	297	1.09	0.0265	160	309	0.83	0.0449
Z03	172	272	0.32	0.0012	145	291	0.65	0.0038	151	296	0.60	0.0071	158	306	0.58	0.0088	176	321	0.49	0.0405
Z04	124	281	1.49	0.0019	140	290	1.44	0.0036	137	298	1.38	0.0084	145	309	1.34	0.0184	153	322	1.12	0.0472
Z05	128	280	0.89	0.0023	140	290	0.81	0.0069	150	298	0.81	0.0108	148	306	0.74	0.0119	168	319	0.59	0.0653
Z06	134	275	1.69	0.0048	142	294	1.41	0.0091	142	294	1.41	0.0115	144	304	1.39	0.0143	164	316	1.06	0.0938
Z07	159	272	0.83	0.0054	132	286	1.03	0.0072	140	284	0.63	0.0163	149	298	0.89	0.0267	168	312	0.68	0.0628
Z08	126	284	1.59	0.0049	133	294	1.47	0.0127	144	300	1.32	0.0188	138	308	1.23	0.0251	162	324	0.99	0.0696
Z09	112	282	1.21	0.0034	130	293	1.02	0.0127	134	300	0.99	0.0068	150	309	0.90	0.0173	168	323	0.71	0.0477
Z010	134	276	0.95	0.0012	137	289	1.00	0.0054	143	295	0.95	0.0090	149	303	0.87	0.0164	166	316	0.67	0.0417
Z011	166	266	0.23	0.0023	136	284	0.54	0.0044	146	284	0.54	0.0082	144	298	1.19	0.0109	175	316	0.41	0.0418
Z012	125	275	1.50	0.0019	125	283	1.50	0.0073	142	292	1.24	0.0140	151	301	1.23	0.0173	175	310	0.90	0.0863
Z013	132	270	1.12	0.0020	141	280	0.90	0.0066	144	288	0.94	0.0082	156	299	0.88	0.0153	162	312	0.66	0.0590
Z014	129	280	1.42	0.0043	141	289	1.27	0.0099	141	296	1.21	0.0127	154	302	0.99	0.0198	167	320	0.84	0.0670
Z015	117	283	1.60	0.0040	135	291	1.41	0.0091	137	298	1.35	0.0105	137	306	1.31	0.0178	152	321	1.16	0.0342
Z016	126	272	1.90	0.0019	141	280	1.64	0.0053	132	289	1.61	0.0163	134	295	1.57	0.0447	148	312	1.35	0.1133
Z017	127	276	1.84	0.0044	130	285	1.71	0.0074	140	291	1.56	0.0118	139	301	1.51	0.0140	157	312	1.17	0.0699
Z018	118	267	2.55	0.0025	116	281	2.47	0.0059	122	286	2.27	0.0120	134	294	2.12	0.0179	152	306	1.78	0.1739
Z019	130	274	2.17	0.0048	122	281	1.98	0.0083	132	296	1.63	0.0206	134	293	1.65	0.0277	140	286	1.85	0.1108
Z020	117	278	1.84	0.0047	123	290	1.71	0.0054	132	296	1.63	0.0160	131	305	1.57	0.0362	150	320	1.34	0.0771
Z021	124	277	2.43	0.0045	128	288	2.36	0.0067	128	296	2.28	0.0214	134	302	2.09	0.0317	148	317	1.67	0.1507
Z022	134	268	2.03	0.0032	125	279	1.96	0.0059	140	286	1.84	0.0175	143	294	1.64	0.0336	153	305	1.31	0.1048
ROM1	138	278	1.38	0.0060	141	287	1.44	0.0064	135	293	1.33	0.0159	150	301	1.25	0.0256	166	316	0.89	0.0752
ROM2	129	280	1.42	0.0045	141	289	1.27	0.0063	141	296	1.21	0.0147	154	302	0.99	0.0284	167	320	0.84	0.0702

Heating rates of 3^{o}C - 20^{o}C min $^{-1}$ were applied to each sample. Increased heating rates result in decreases oxygen absorption but minimize experimental running time. The adsorption of oxygen produces the mass increase between 100 ^{o}C to 320 ^{o}C. Examples of the experimental curves (Oxygen absorption mix, ignition temperature mix and weight gain) for sample Z01 are shown below and the remaining results of all the test samples are included in appendix A25-A125.

4.2.2 TGA curves

The oxygen absorption per sample, oxygen absorption mix and ignition test mix for samples Z01 to Z24 are included in the appendix A25-A175.Examples of each from sample Z01 can be seen below (Figures 4.7-4.9).



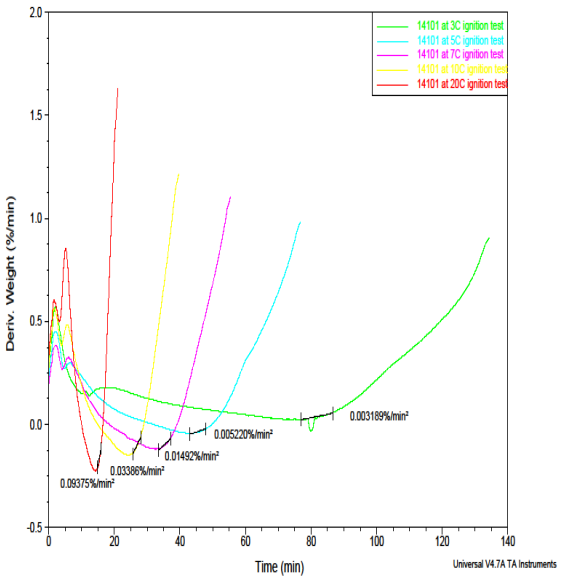


Figure 4.7: Oxygen adsorption mix for sample Z01 **Figure 4.8: Ignition test mix for sample Z01**

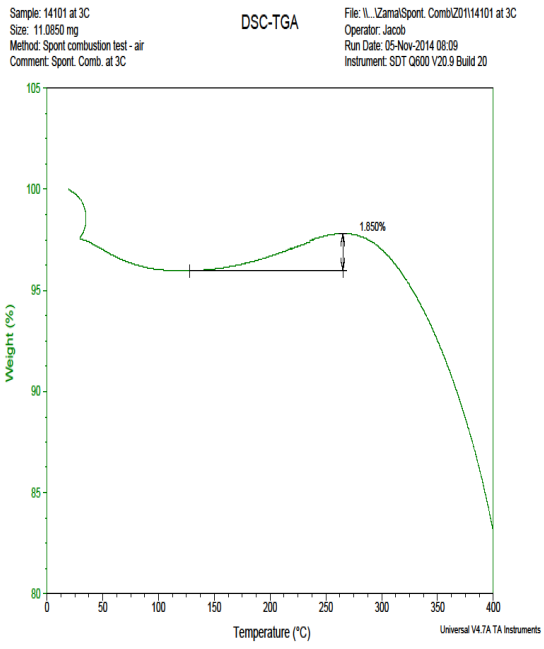


Figure 4.9: Oxygen absorption for sample Z01 at 3 °C ramp

The weight increase at higher heating rates is significantly lower and this trend is seen for all the samples (appendix A26-A175). The TG spi is seen to increase as the heating rate is increases (appendix A26-A175).

Typically, a complete oxidation process can be divided into three stages according to the changing pattern of the T-G curve. In the initial stage, the specimen loses its weight due to the evaporation of the contained moisture and this stage ends at the inflection point T1. Then the specimen could experience a weight gain stage as the low-temperature oxidation occurs before ignition point T2. Point T1 and T2 are two inflection points to define the weight loss and weight gain stages. The third stage is the combustion process of the specimen during which the weight of the specimen decreases rapidly and this stage ends at Tend when all the combustibles in the coal specimen are fully consumed (Wang et al.,2008).

The most useful part of the resulting T-G curve to assess the propensity of a coal's spontaneous combustion is that between the inflection points T1 and T2. Classification into risk categories is relative, based on 1/3rd percentiles (Table 4.3 and Figure 4.10).

Table 4.3: Calculated TG spc values (Avila method) at different heating rates

Sample	TG $_{spc}$ ^{o}C min $^{-1}$					
	3	5	7	10	20	Risk
Z01	0.91	0.91	0.91	0.91	0.90	medium
Z02	0.24	0.24	0.23	0.23	0.23	low
Z03	0.94	0.94	0.94	0.93	0.93	high
Z04	0.89	0.89	0.89	0.89	0.89	medium
Z05	0.87	0.87	0.87	0.87	0.87	medium
Z06	0.79	0.79	0.79	0.79	0.78	low
Z07	0.79	0.78	0.78	0.78	0.78	low
Z08	0.78	0.77	0.77	0.77	0.77	low
Z09	0.79	0.78	0.78	0.78	0.78	low
Z010	0.83	0.83	0.82	0.82	0.82	medium
Z011	0.95	0.95	0.95	0.95	0.95	high
Z012	0.93	0.93	0.93	0.93	0.93	high
Z013	0.95	0.95	0.95	0.95	0.95	high
Z014	0.93	0.92	0.92	0.92	0.92	high
Z015	0.16	0.16	0.16	0.15	0.15	low
Z016	0.87	0.86	0.86	0.86	0.85	medium
Z017	0.83	0.82	0.82	0.82	0.82	medium
Z018	0.92	0.92	0.91	0.91	0.90	medium
Z019	0.95	0.95	0.95	0.94	0.94	high
Z020	0.72	0.72	0.71	0.71	0.71	low
Z021	0.96	0.96	0.96	0.95	0.95	high
Z022	0.95	0.95	0.95	0.94	0.94	high
ROM 1	0.84	0.84	0.84	0.84	0.83	medium
ROM 2	0.86	0.86	0.86	0.85	0.85	medium

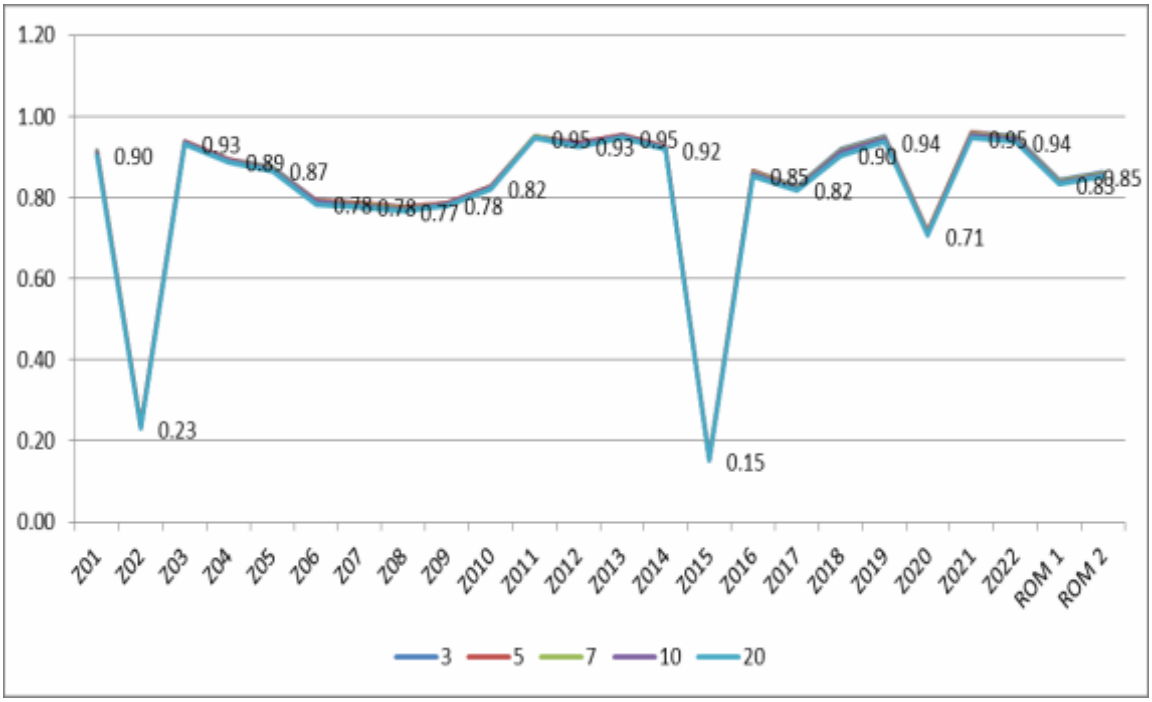


Figure 4.10: TG spc values Avila method

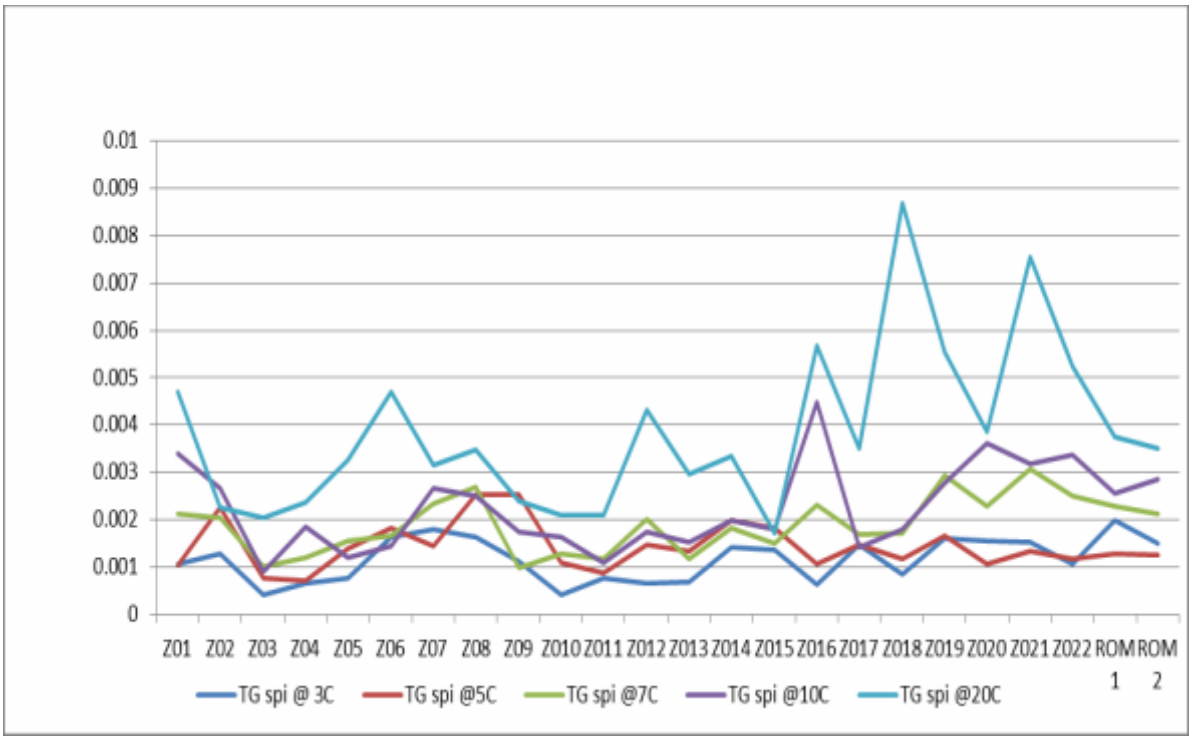


Figure 4.11: TG spi at different heating rates

An increased heating rate increases the TG spi and reduces TG spc (Figure 4.10-4.11) in some samples possibly indicating experimental inconsistency as correlation coefficients at different heating rates should remain similar. Samples Z02 and Z15 have very low correlation at increased heating rates and this is not observed in some of the other high ash samples.

4.2.3 Tstart (T1) and Tpeak (T2)

The T1 and T2 contour plots are shown in figures 4.12 to 4.14. and show little variation with the exception of the S5 seam. The T2 temperatures for all seams generally fall within the same 270-280 degree C range with the No 5 seam showing the most areas of lower T2, followed by the S4U seam. T1 only showed correlation with VR, whereas T2 had some correlation with AS, FC, GLI, H, IM and WT. Poor correlation was found between T1 and T2 as well as T2 and WT. Detailed correlations are discussed in chapter 8. In theory lower T2 equates to a higher sponcom potential. T1 temperatures range from 129-133 degrees C.

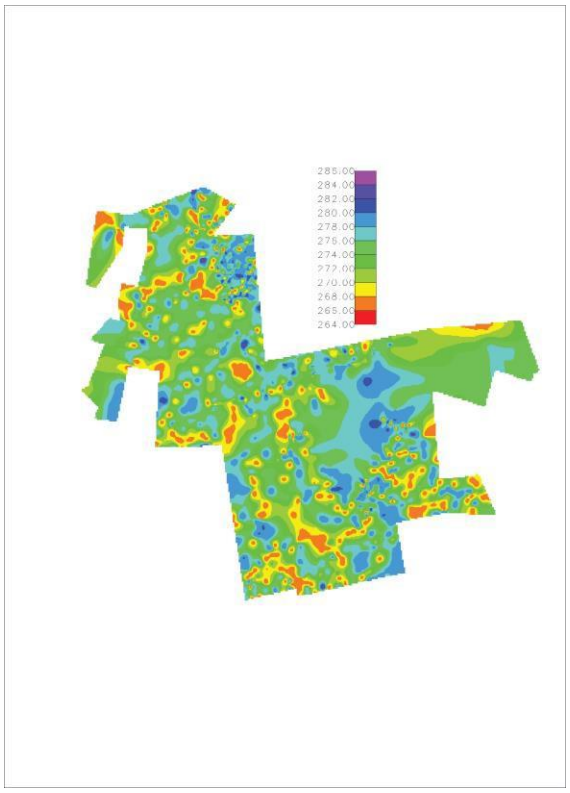


Figure 4.12: T peak (T2) for the No. 5 seam



Figure 4.13: T peak (T2) for the No. 4U seam

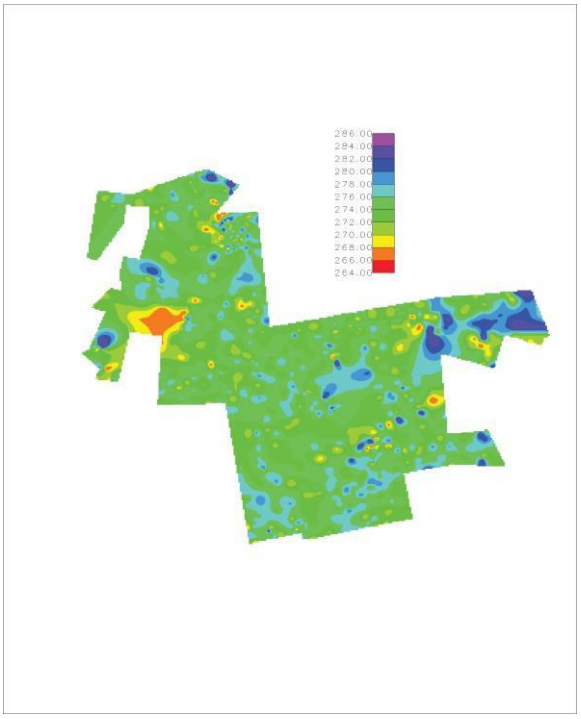


Figure 4.14: T peak (T2) for the No.2 seam

The No.4U seam shows the highest T2 (lowest sponcom) liability with dark green and blue shade fairly common**.**T2 for the No.5 is lower than the No.4 and No.2 seams indicating higher sponcom liability. The lower T2 areas have yellow-brown shading**.** The model dataset histograms are appended for T1 and T2 (Appendix A19-A24).The T1 is lowest for the S5 seam and highest for the S4U seam with a range of 127-133 degrees Celsius for the model dataset. The sample dataset (Figure 4.15-4.16) has very similar T1 and T2 ranges to the model dataset. Variance for T1 is very high.

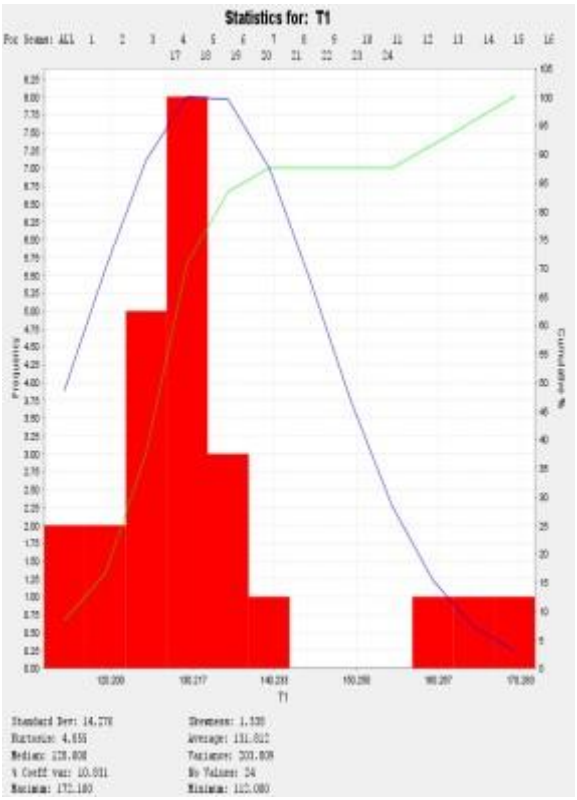


Figure 4.15: T start (T1) for combined seam sample dataset -3C ramp

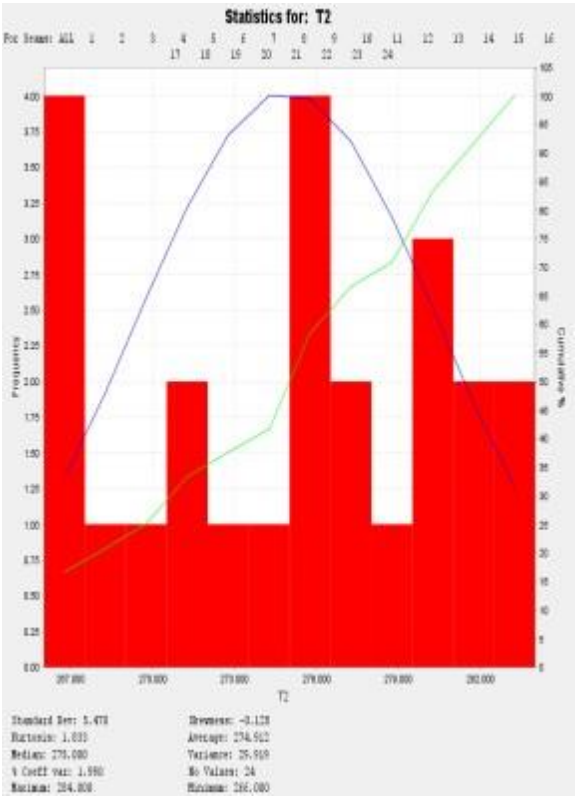


Figure 4.16: T peak (T2) for combined seam sample dataset -3C ramp

4.2.4 Weight Gain

Derivative of weight gain plans are included in the appendix A14-A24.Contour plans of weight gain for each of the seams shows clear zonation especially in the S5 and S4U seams with the S4U having relatively low and homogenous weight gains (Figures 4.19-4.21).Samples not showing a weight gain may indicate moisture desorption or the rapid breakdown of unstable oxy-complexes and are potentially more prone to sponcom. Low reactive coals tend to have sharp weight increase over a wide temperature range and vice-versa (Figures 4.17-4.18).Colliery X samples indicate an opposite relationship to this general theory.

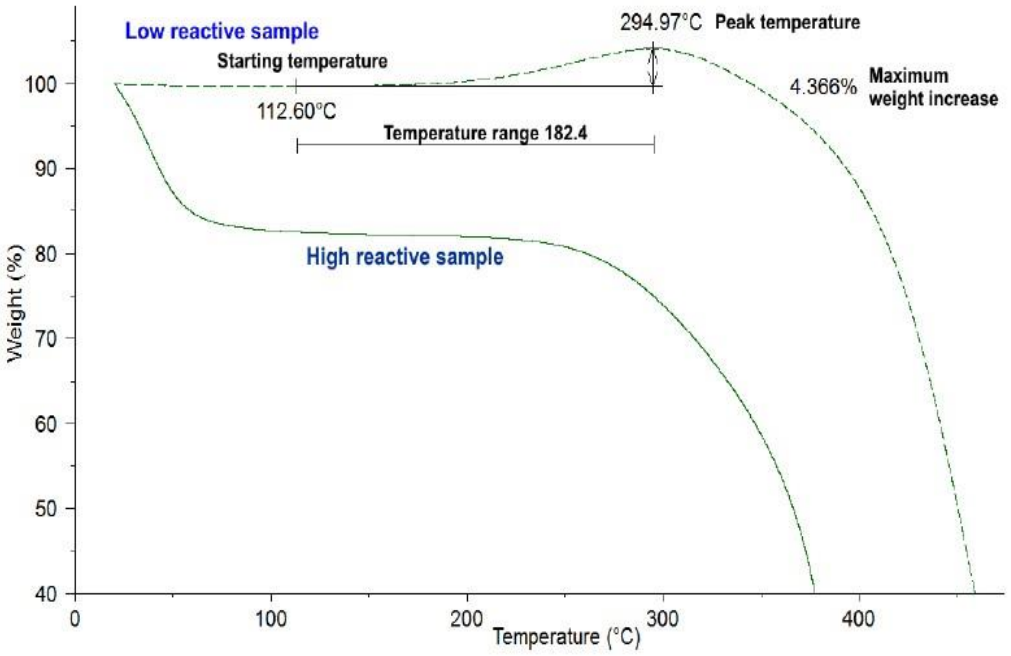


Figure 4.17: TGA profile of low and high reactive coals (Avila, 2012)

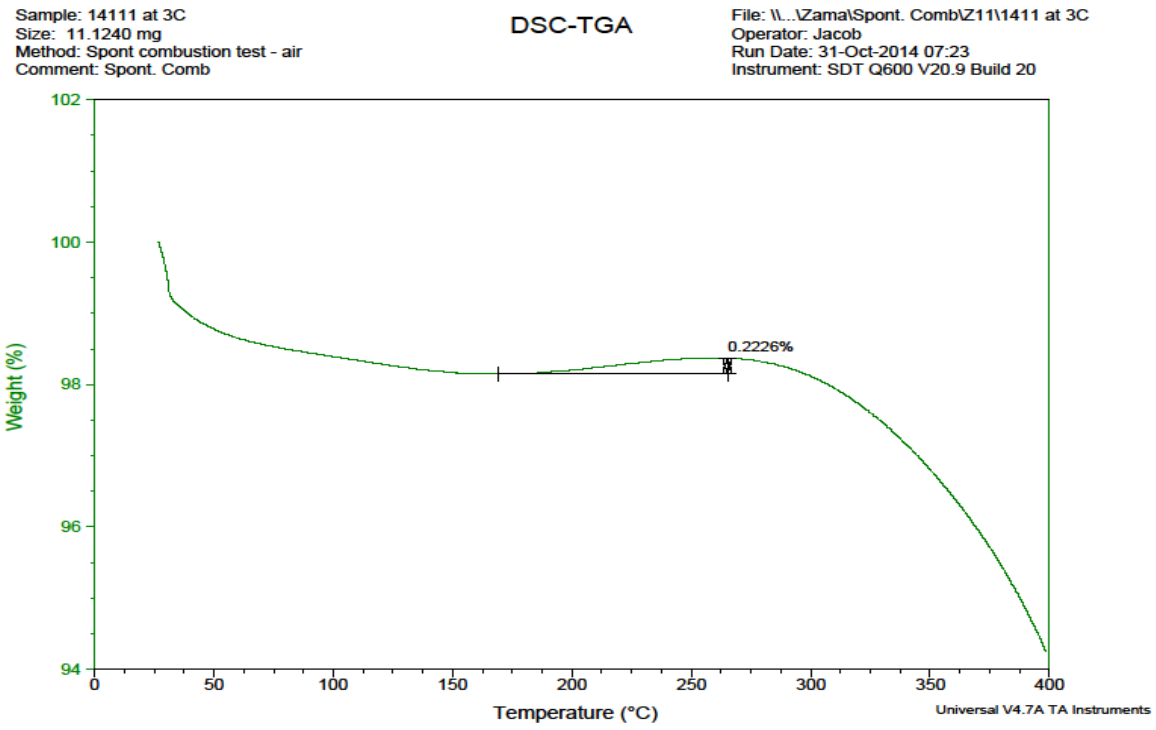


Figure 4.18: TGA profile of high reactive coals from sample dataset –sample Z01

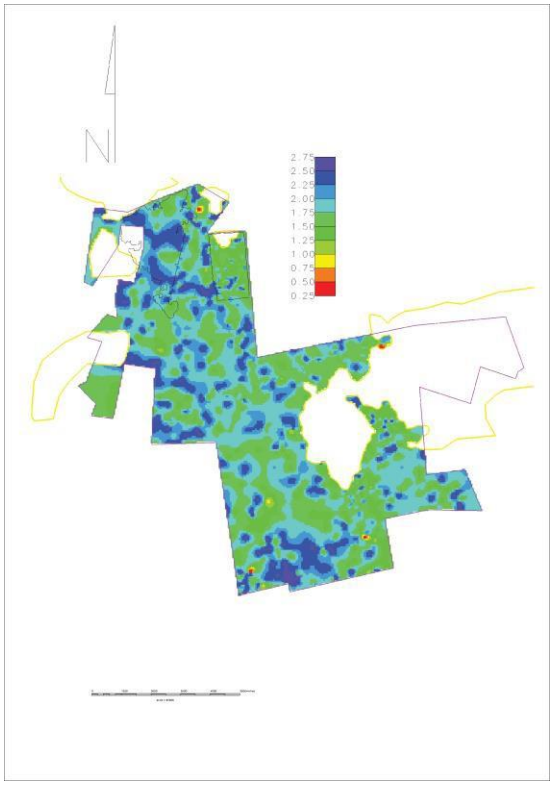


Figure 4.19: S5 weight gain (%)

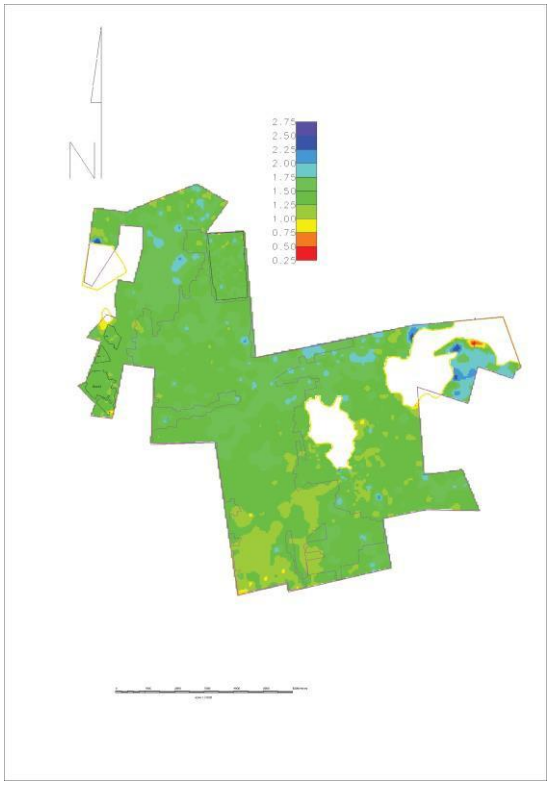


Figure 4.20: S4U weight gain (%)

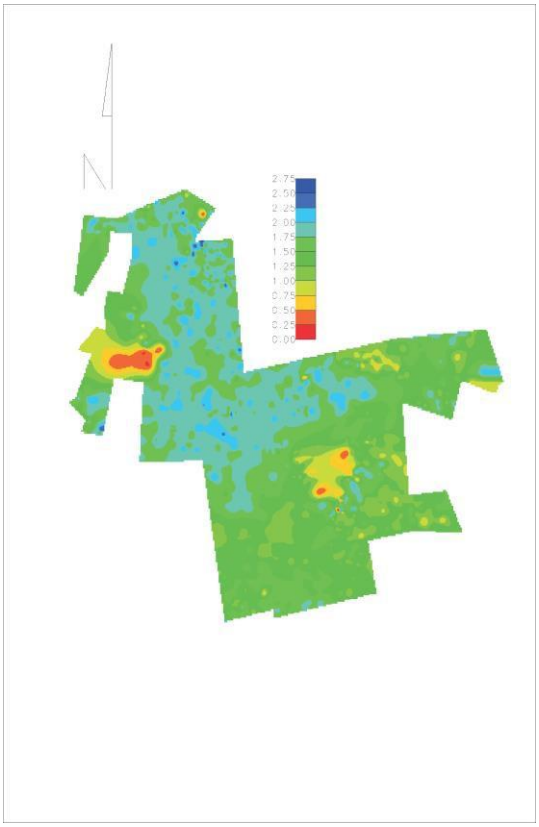


Figure 4.21: S2 weight gain (%)

High % weight gains (WT) are shown in blue shade and would indicate a higher tendency to sponcom. The S4U seam shading is predominantly green with lower weight gains than the S5 seam indicating lower propensity to sponcom. The higher weight gains (blue shade) correlate with high CV areas and possibly higher sponcom probability**.**

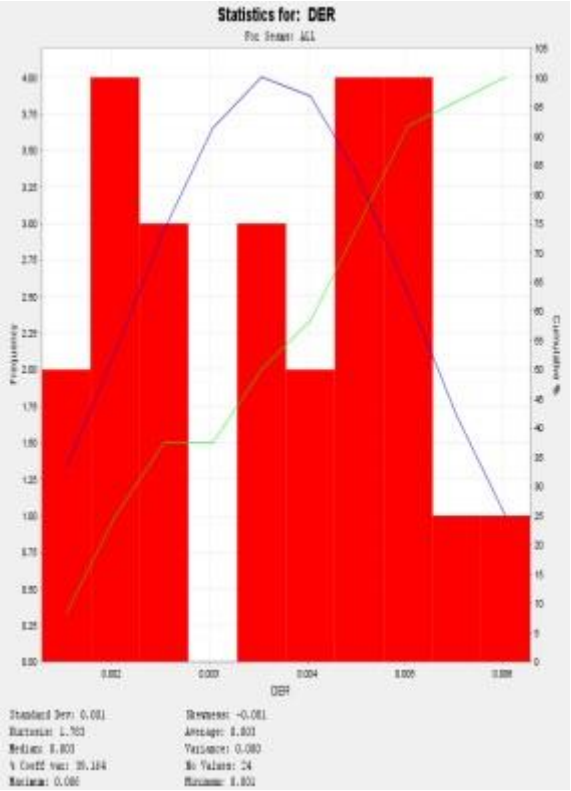


Figure 4.22: % derivative of weight gain for combined seams sample dataset (3C ramp)

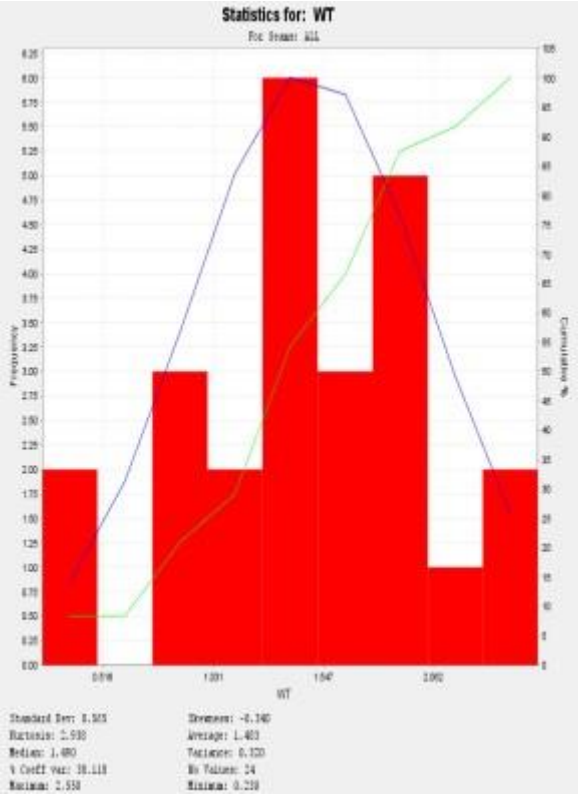


Figure 4.23: % weight gain for combined seams sample dataset (3C ramp)

The S5, S4U and S2 seams from the model dataset showed weight gains and temperature ranges as tabled below (Table 4.4).

Table 4.4: Weight gain and temperature range of seams modelled

Seam	WT % gain	T2	T1	T2-T1
5#	1.822	274.17	127.8	146.37
4u#	1.435	275.04	133.2	141.84
2#	1.622	274.52	131.5	143.02

Avila (2012) categorises coals with a maximum weight increase below 1% and a temperature range under 150 °C as medium reactive; and coals with a maximum weight increase higher than 1% and a temperature range greater than 150°C are classified as unreactive. Coals with no weight gain are most reactive but this is not observed in the sample dataset. Samples Z03, Z10 and Z11 would be most prone to sponcom on this basis. Note that the theory of Wang and Luo (2011) contradicts that of Avila (2012).

Table 4.5: Weight gain and temperature range (T2-T1).Samples matching Avila criteria for sponcom risk marked with in red text

Sample	T ads nett	wt % max
Z01	135	1.85
Z02	139	1.34
Z03	100	0.32
Z04	157	1.49
Z05	152	0.89
Z06	141	1.69
Z07	113	0.83
Z08	158	1.59
Z09	170	1.21
Z010	141	0.95
Z011	100	0.23
Z012	150	1.50
Z013	138	1.12
Z014	151	1.42
Z015	166	1.60
Z016	146	1.90
Z017	149	1.84
Z018	148	2.55
Z019	143	2.17
Z020	160	1.84
Z021	153	2.43
Z022	134	2.03
ROM 1	140	1.38
ROM 2	151	1.42

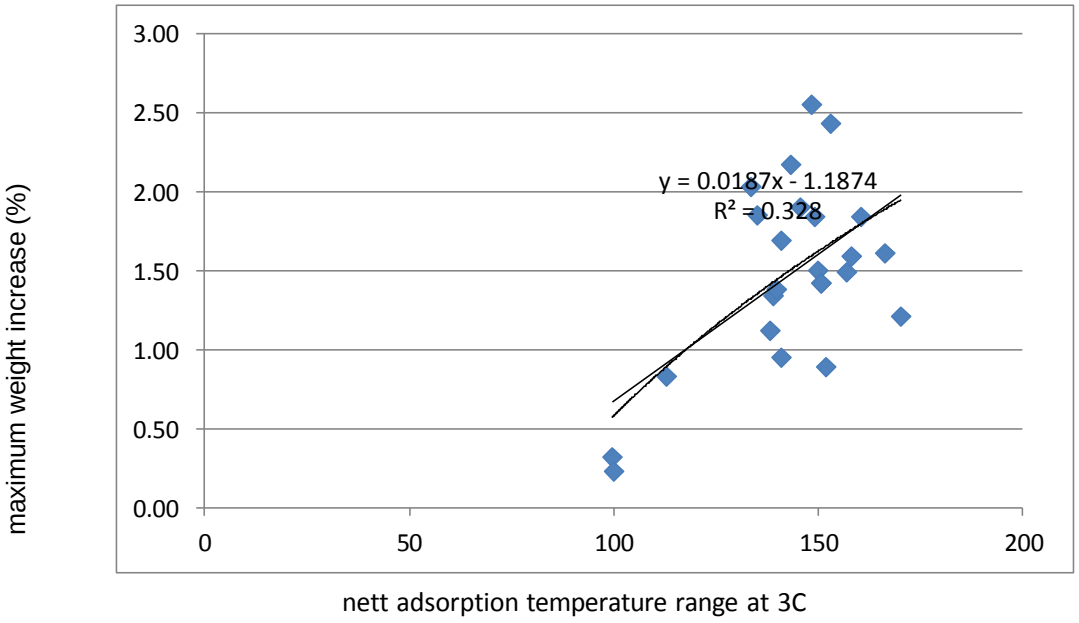


Figure 4.24: Correlation between %WT gain and net adsorption temperature range at 3C with poor correlation coefficient (Z01-Z24)

There is a weak positive correlation between temperature range and weight gain in this sample set.

4.3 Oxygen Absorption Test (Smith and Glasser)

The oxygen absorption (GLI) of the samples correlates fairly well with some of the thermal (T1 ,TR,WT) and chemical parameters (AS,C,CV,H,IM,N,VM).The oxygen adsorption rate was only determined on -100micron particles after a 2 hour period and results are shown in Figures 4.25-4.26. The mass change was also not recorded due to the simplicity of the experimental setup. The relative differences in oxygen absorption rates between the samples are still evident as well as the potential relationship to other variables (Table 4.6.)

Samples with air flush at ambient temperature showed no oxygen absorption even after several days. Samples flushed with oxygen and left at ambient temperature similarly showed no oxygen absorption. The addition of heat is therefore essential in laboratory testing to obtain relative sponcom liability of samples. McGeer (2015) demonstrated a particle size effect on oxygen absorption with smaller particle sizes having the strongest absorption rates (Figure 4.27).

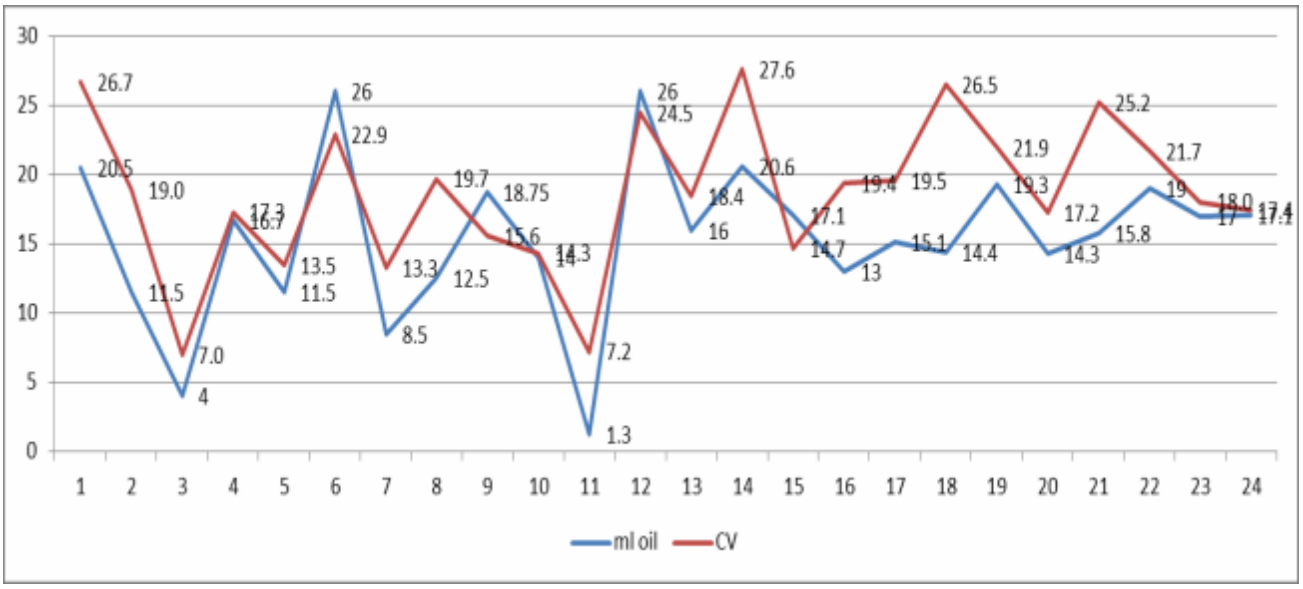


Figure 4.25: Relationship between CV and volume of oil displaced (oxygen adsorbed)

The higher CV samples (mostly S2 and S5 seam) showed the highest oxygen reactivity

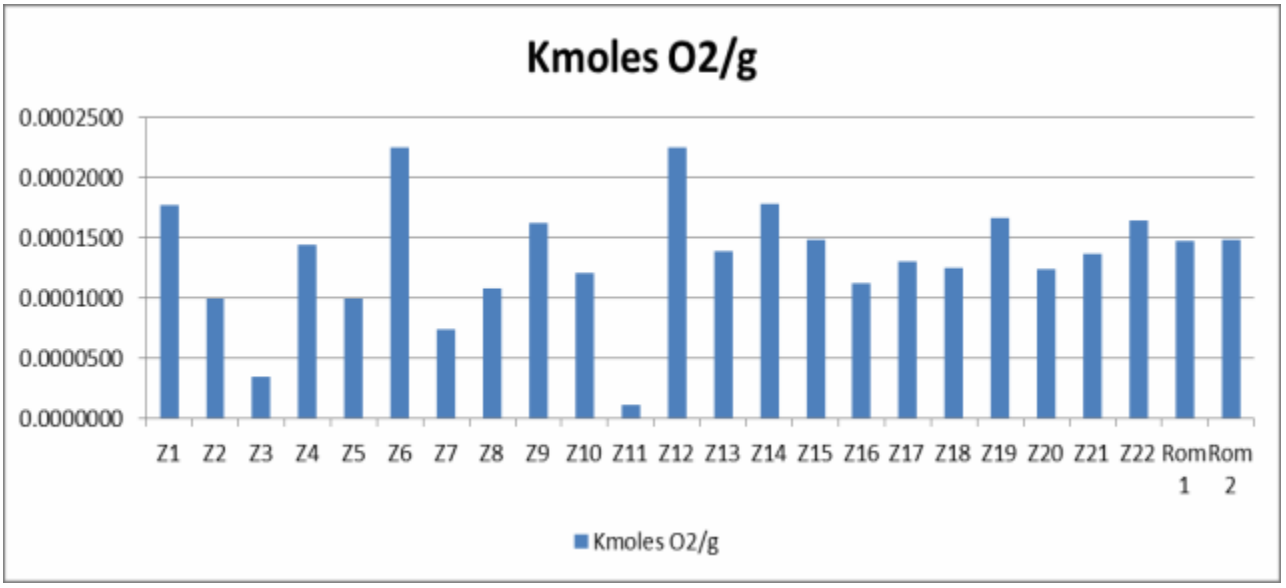


Figure 4.26: Oxygen absorption rate of the sample set from Boreholes 1 and 2

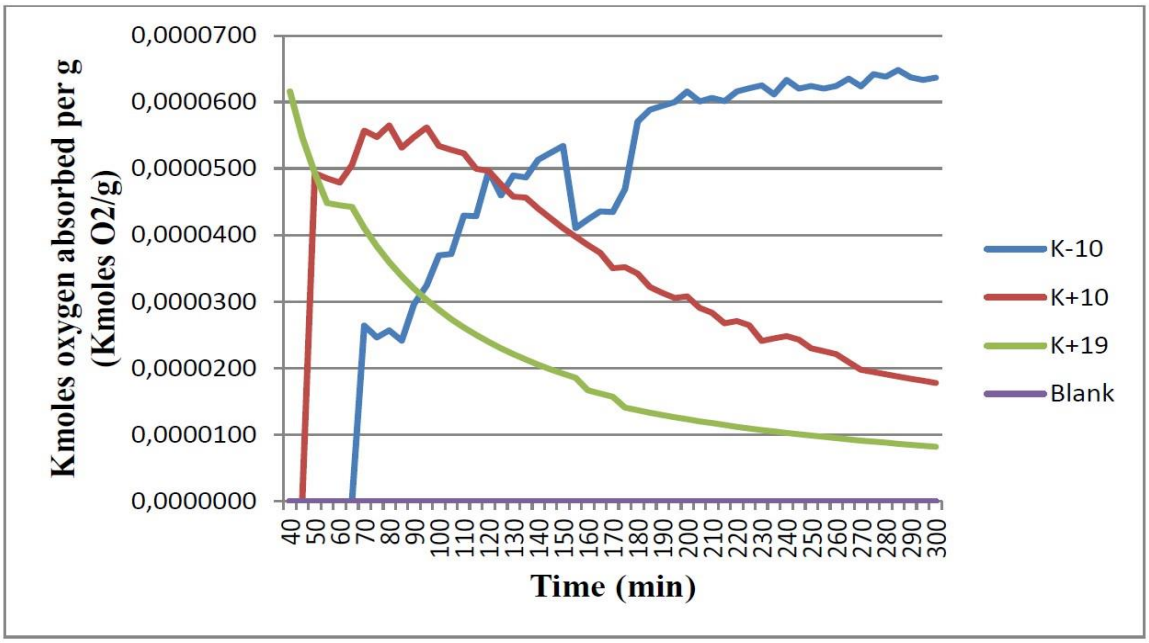


Figure 4.27: Effect of particle size on oxygen absorption rate (McGeer, 2015)

The -10mm sample shows the highest oxygen reactivity and the +19mm sample the lowest oxygen reactivity.

Table 4.6: Results of Smith-Glasser oxygen absorption

Sample	ml oil	CV	P oil	Time (min)	MWO_2	Mass (g)	Kmoles O2/g
Z1	20.5	26.7	0.934	120	18.0	50.0	0.0001773
Z2	11.5	19.0	0.934	120	18.0	50.0	0.0000995
Z3	4.0	7.0	0.934	120	18.0	50.0	0.0000346
Z4	16.7	17.3	0.934	120	18.0	50.0	0.0001444
Z5	11.5	13.5	0.934	120	18.0	50.0	0.0000995
Z6	26.0	22.9	0.934	120	18.0	50.0	0.0002249
Z7	8.5	13.3	0.934	120	18.0	50.0	0.0000735
Z8	12.5	19.7	0.934	120	18.0	50.0	0.0001081
Z9	18.8	15.6	0.934	120	18.0	50.0	0.0001622
Z10	14.0	14.3	0.934	120	18.0	50.0	0.0001211
Z11	1.3	7.2	0.934	120	18.0	50.0	0.0000112
Z12	26.0	24.5	0.934	120	18.0	50.0	0.0002249
Z13	16.0	18.4	0.934	120	18.0	50.0	0.0001384
Z14	20.6	27.6	0.934	120	18.0	50.0	0.0001782
Z15	17.1	14.7	0.934	120	18.0	50.0	0.0001479
Z16	13.0	19.4	0.934	120	18.0	50.0	0.0001124
Z17	15.1	19.5	0.934	120	18.0	50.0	0.0001306
Z18	14.4	26.5	0.934	120	18.0	50.0	0.0001245
Z19	19.3	21.9	0.934	120	18.0	50.0	0.0001669
Z20	14.3	17.2	0.934	120	18.0	50.0	0.0001237
Z21	15.8	25.2	0.934	120	18.0	50.0	0.0001366
Z22	19.0	21.7	0.934	120	18.0	50.0	0.0001643
Rom 1	17.0	18.0	0.934	120	18.0	50.0	0.0001470
Rom 2	17.1	17.4	0.934	120	18.0	50.0	0.0001479

The contour plans of oxygen reactivity (Figure 4.28-4.30) (expressed as volume of oil displaced) in the GLI test are shown below with a marked difference between the S5, S4U and S2 seams. The S4U seam showed the least reactivity and the S5 and S2 seams show clear zonation with higher oil volume displacement (oxygen reactivity) in areas of lower ash/higher CV.

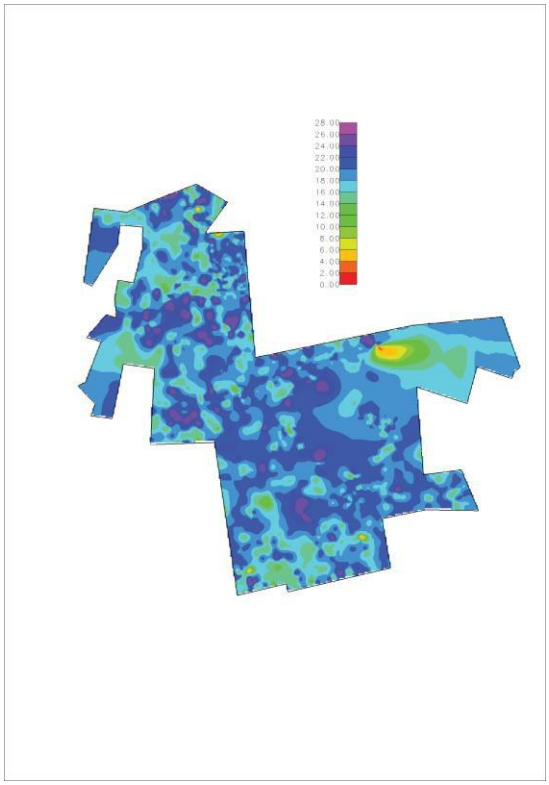


Figure 4.28: Volume oil displaced (oxygen reactivity) in S5 seam coal

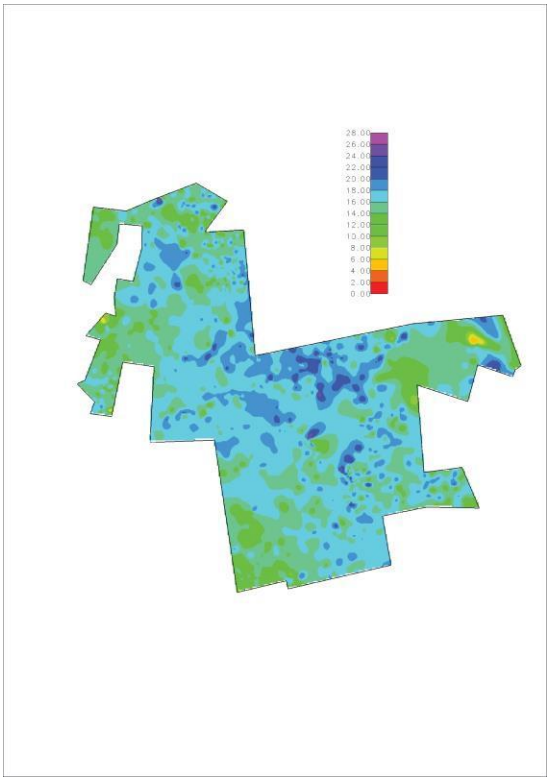


Figure 4.29: Volume oil displaced (oxygen reactivity) in S4U seam coal

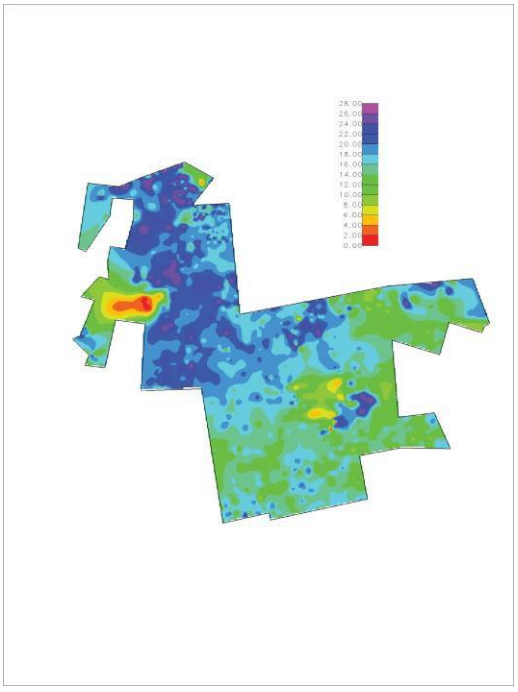


Figure 4.30: Volume oil displaced (oxygen reactivity) in S4U seam coal

The S5 seam reactivity is fairly uniform and relatively high with blue and purple shade widespread. The S4U seam reactivity is significantly less than in the S5 seam with green and pale blue shade dominant**.** Reactivity correlates well with higher CV areas in the north in the S2 seam plot.

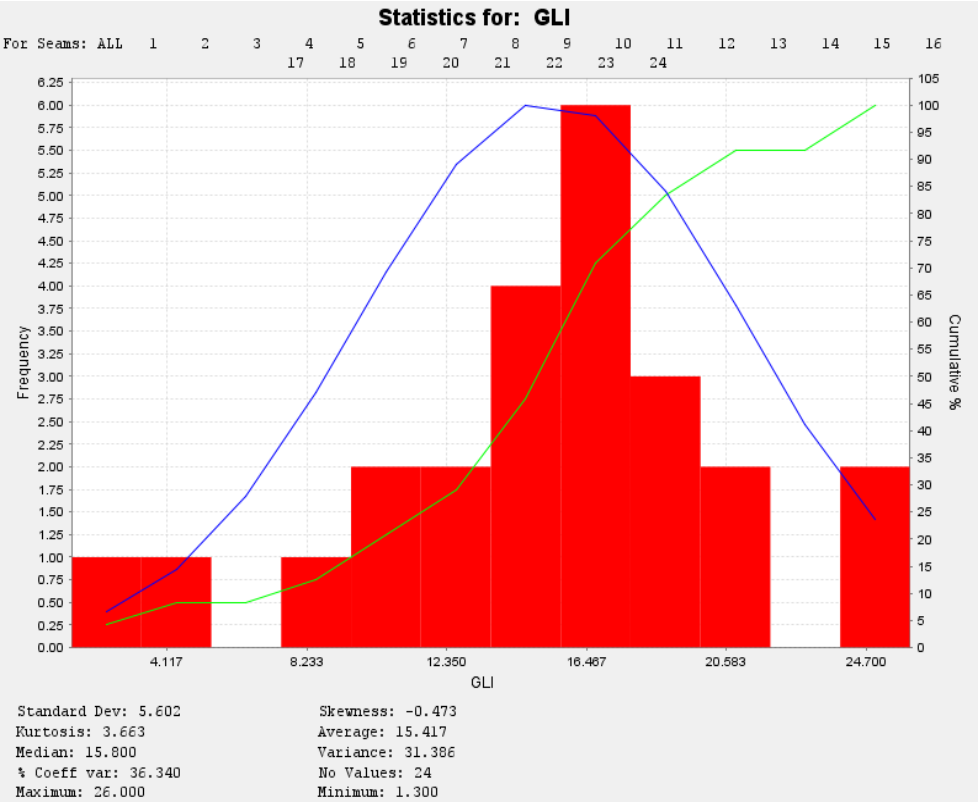


Figure 4.31: Volume of oil displaced in Smith-Glasser test for the sample dataset

The histograms for volume of oil displaced per seam are appended and the combined sample histogram is shown above. The variance is high with mean model values of 18.87, 16.55 and 16.7 for the S5, S4U and S2 seams respectively (Appendix A178-A180).

4.4 Chemical Analysis

The results of the ultimate and proximate analysis undertaken at an accredited external laboratory for the 24 samples are tabled below (Table 4.7). Ash analysis (Figure 4.34) was included as well as forms of sulphur (Figure 4.35) for each sample. Results are quoted on an air-dry basis.

Correlations between the chemical parameters are very good with no anomalies reported for the main elements.CV/AS and RD/AS correlation plots are shown in Figures 4.32-4.33.Self-heating potential can be calculated from proximate analysis but results can be variable (Wang and Luo,2015;Kaymakci and Didari,2002).If enough laboratory samples are available a plot can be derived and formulae used (multivariate regression) to assign sponcom test estimates(CPT,TGA etc.) to new boreholes drilled in the area.

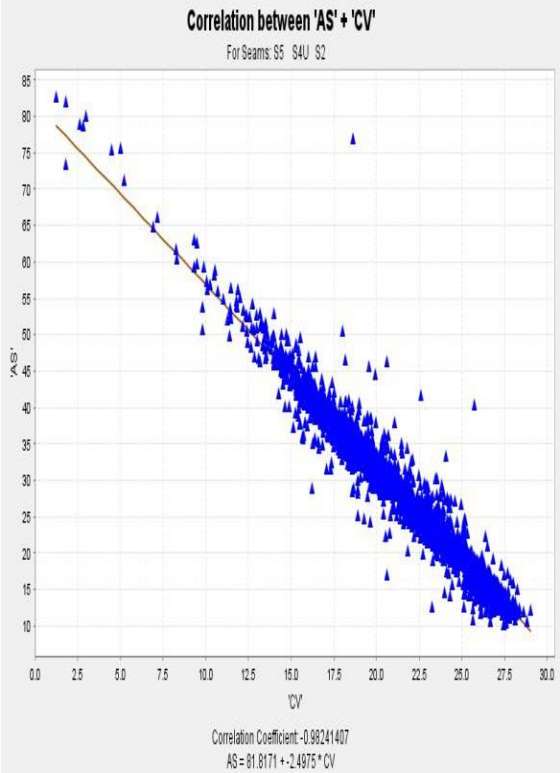


Figure 4.32: CV-AS correlation plot for combined seams

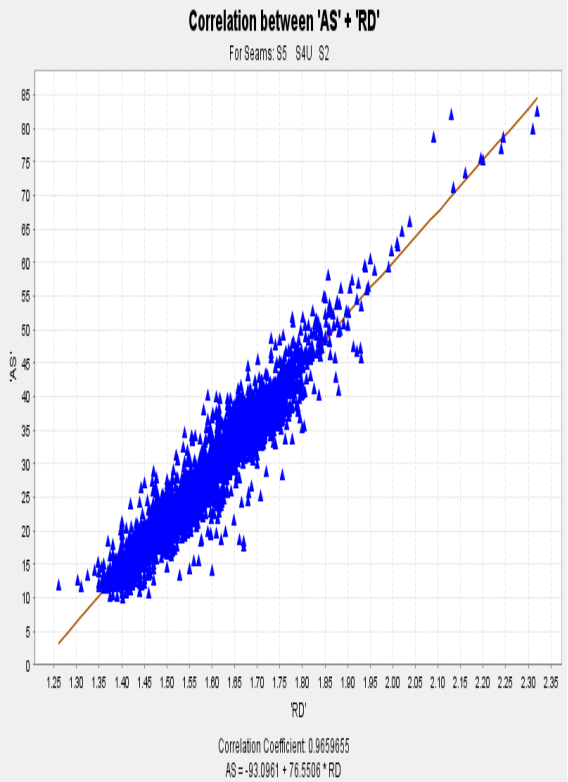


Figure 4.33: RD-AS correlation plot for combined seams

The CV-AS correlation and RD-AS correlation of the borehole database is acceptable although outliers have not been removed. These correlations prove the integrity of the borehole database and extrapolation of sponcom variables into this database can be regarded as reliable.

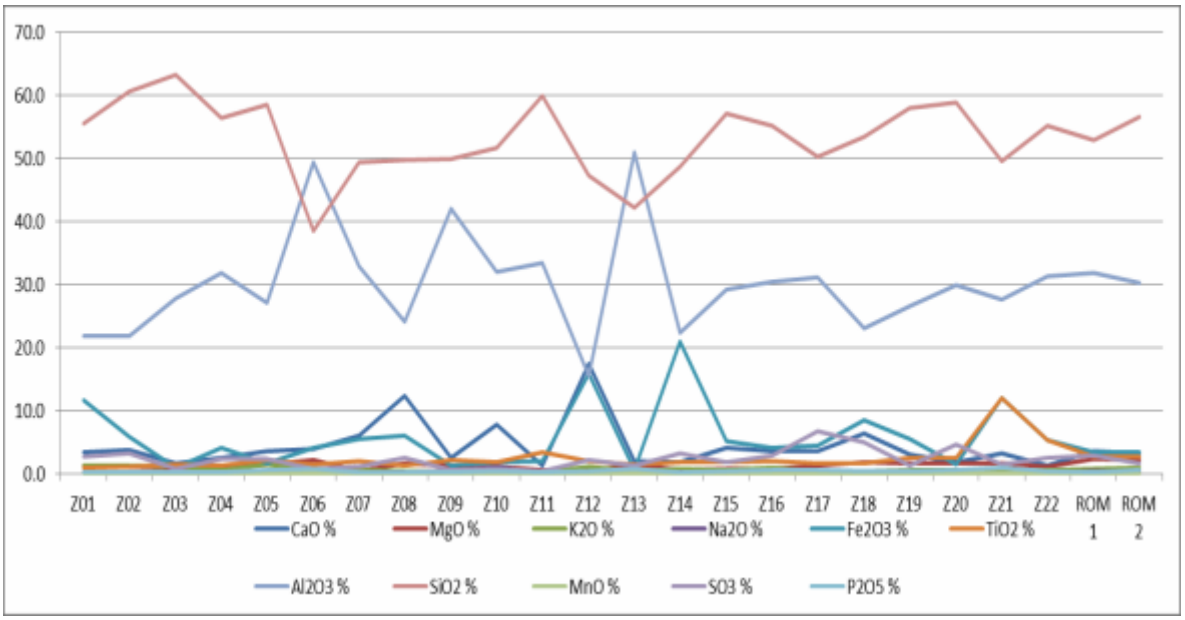


Figure 4.34: Ash analysis of the sample set

The metal oxides in the ash are dominated by Si and Al with Ca and Fe being prominent in the trace elements.Fe_2O_3 showed correlations with several chemical parameters (AS, CV, C, TR, VM), some of which may be anomalous. The other oxides did not show these correlations.

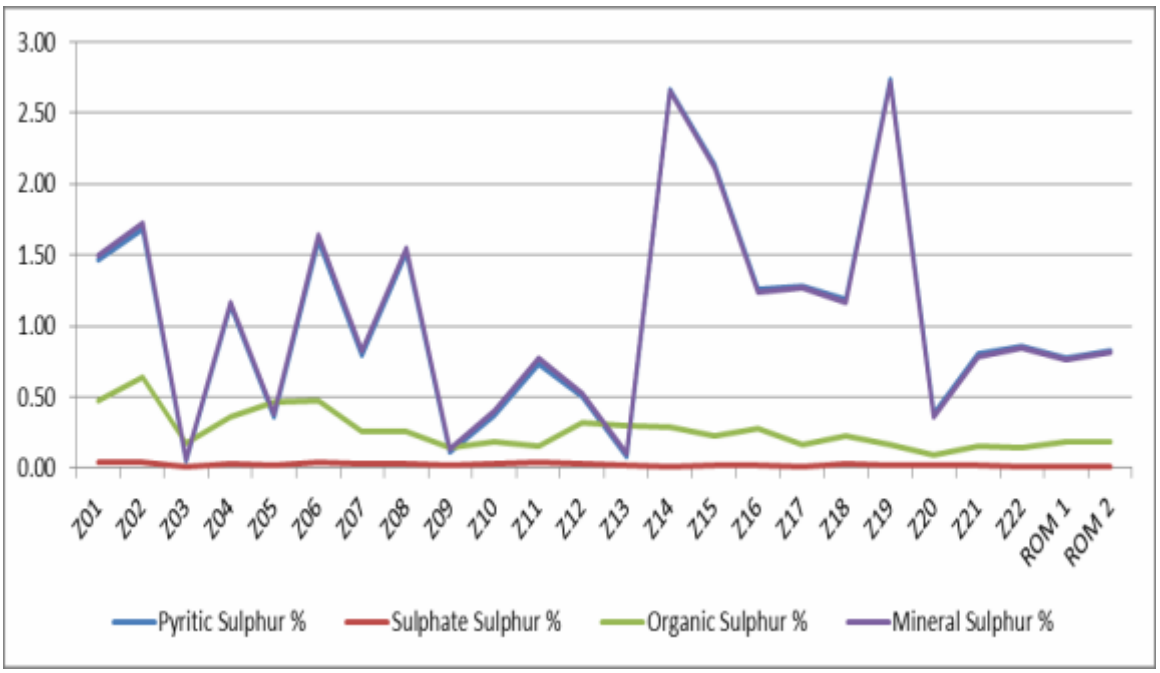


Figure 4.35: Forms of Sulphur of the sample set

SS, MS and PS showed some correlation to CPT but not to TGA or GLI. SS percentages are relatively low as is the OS%. Highest Sulphur values correlate to the S5 seam samples with the S4U having lowest Sulphur content.

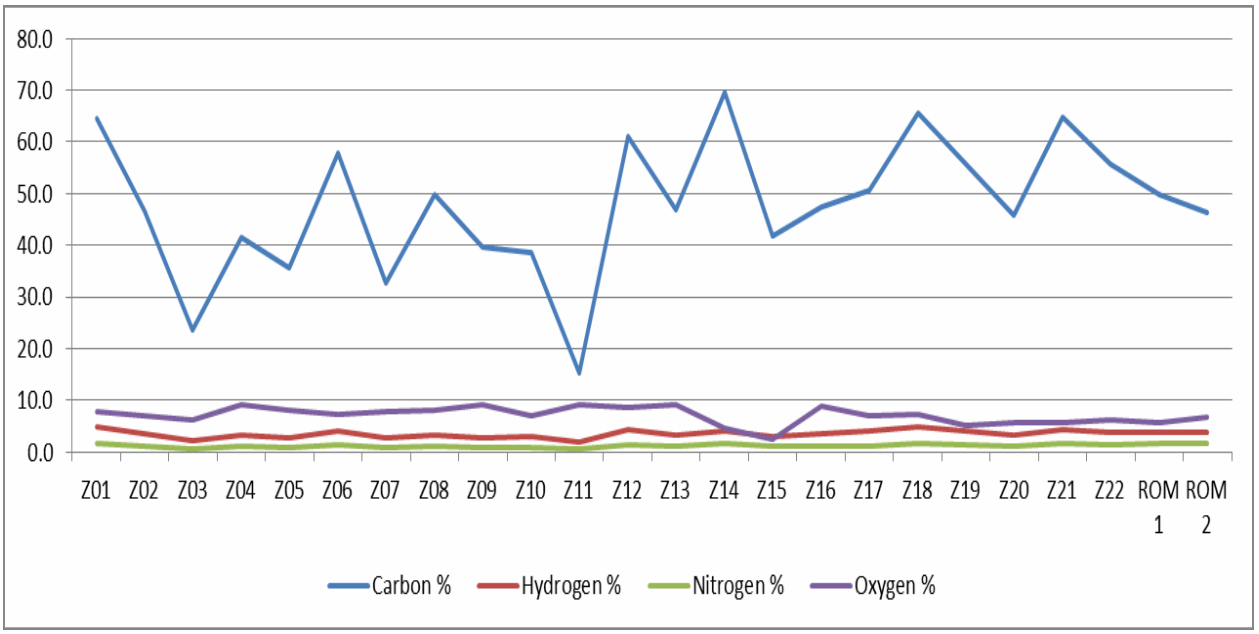


Figure 4.36: Ultimate analysis of the sample set

H, N and C showed correlation to several of the other sponcom variables. O showed no correlation to any of the other variables. Correlations are discussed in chapter 8.

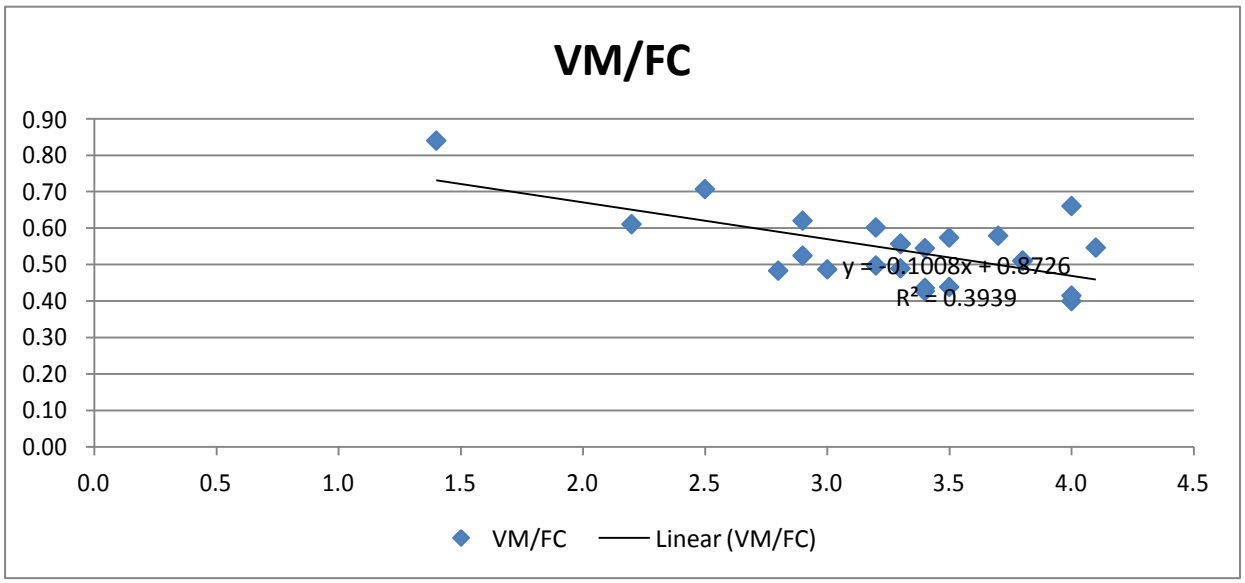


Figure 4.37: Fuel ratio and IM

The IM shows a negative relation with the fuel ratio and a positive relation to FC and VM, although Avila (2012) reports a negative relation between IM and FC in his samples.

Table 4.7: Proximate and Ultimate analysis of sample set (Air dry basis).

Sample	Raw air-dried qualities						Ultimate Analysis				Ash Analysis											Forms of Sulpur			
	Heat Value CV	Inherent Moisture	Ash	Volatile Matter	Fixed Carbon	Total Sulphur	Carbon	Hydrogen	Nitrogen	Oxygen	CaO	MgO	K_2O	Na_2O	Fe_2O_3	TiO_2	Al_2O_3	SiO_2	MnO	SO_3	P_2O_5	Pyritic Sulphur	Sulphate Sulphur	Organic Sulphur	Mineral Sulphur
	MJ/kg	%	%	%	%	%	%	%	%	%	%	%	%	%	%	%	%	%	%	%	%	%	%	%	%
Z01	26.7	4.0	15.3	32.1	48.6	1.97	64.4	4.8	1.7	7.8	3.3	1.2	1.4	0.2	11.5	1.0	21.8	55.4	0.015	2.7	0.210	1.46	0.04	0.47	1.50
Z02	19.0	3.2	36.1	22.8	37.9	2.36	46.5	3.6	1.2	7.1	3.7	1.2	1.3	0.1	5.9	1.1	21.8	60.5	0.009	3.2	0.200	1.68	0.04	0.64	1.72
Z03	7.0	2.5	64.9	13.5	19.1	0.23	23.5	2.3	0.5	6.1	1.6	1.0	1.1	0.1	0.9	1.5	27.8	63.1	0.005	0.8	0.160	0.05	0.01	0.17	0.06
Z04	17.3	3.3	40.2	20.2	36.3	1.53	41.6	3.3	1.1	9.0	2.6	1.1	0.6	0.2	4.1	1.3	31.7	56.3	0.013	2.3	0.210	1.14	0.03	0.36	1.17
Z05	13.5	3.5	48.2	17.6	30.7	0.84	35.6	2.8	0.8	8.2	3.6	1.5	1.5	0.2	1.7	2.1	27.1	58.4	0.009	2.3	0.500	0.36	0.02	0.46	0.38
Z06	22.9	4.1	23.2	25.7	47.0	2.11	57.7	4.1	1.5	7.3	3.8	2.1	0.5	0.3	4.0	1.4	49.4	38.5	0.026	0.8	0.720	1.60	0.04	0.47	1.64
Z07	13.3	2.2	52.7	17.1	28.0	1.08	32.6	2.7	0.8	7.9	6.1	0.5	0.5	0.1	5.4	1.9	32.9	49.3	0.052	1.1	0.240	0.79	0.03	0.26	0.82
Z08	19.7	4.0	31.9	18.3	45.8	1.81	49.8	3.3	1.2	8.0	12.3	1.5	0.4	0.3	6.0	1.3	24.0	49.6	0.014	2.5	0.240	1.52	0.03	0.26	1.55
Z09	15.6	3.5	43.7	16.1	36.7	0.27	39.6	2.8	1.0	9.2	2.5	1.3	0.3	0.4	1.2	2.1	42.0	49.8	0.014	0.5	0.240	0.11	0.02	0.14	0.13
Z10	14.3	3.3	46.7	17.9	32.1	0.58	38.6	2.9	0.9	7.1	7.8	1.1	0.8	1.1	1.8	1.8	31.9	51.6	0.012	0.8	0.400	0.37	0.03	0.18	0.40
Z11	7.2	1.4	71.0	12.6	15.0	0.92	15.2	1.9	0.5	9.1	1.3	0.5	0.2	0.1	2.0	3.4	33.3	59.8	0.000	0.5	0.200	0.73	0.04	0.15	0.77
Z12	24.5	3.8	20.1	25.7	50.4	0.85	61.1	4.2	1.4	8.5	17.4	0.4	1.0	0.2	15.8	1.9	15.4	47.3	0.023	2.1	0.450	0.50	0.03	0.32	0.53
Z13	18.4	4.0	35.3	17.8	42.9	0.40	46.8	3.2	1.1	9.2	2.0	1.5	0.3	0.2	0.6	1.5	50.9	42.1	0.012	1.2	0.790	0.08	0.02	0.30	0.10
Z14	27.6	3.7	13.4	30.4	52.5	2.95	69.7	4.1	1.7	4.5	1.9	0.6	0.8	0.2	21.0	1.8	22.4	48.6	0.006	3.3	0.270	2.66	0.01	0.29	2.65
Z15	14.7	3.0	46.3	16.6	34.1	2.36	41.8	3.1	1.0	2.5	4.1	0.7	0.6	0.1	5.1	1.9	29.1	57.0	0.011	1.8	0.360	2.13	0.02	0.23	2.11
Z16	19.4	3.4	34.2	22.0	40.4	1.54	47.4	3.4	1.1	8.9	3.5	0.7	0.9	0.2	4.1	2.0	30.4	55.2	0.014	2.8	0.630	1.26	0.02	0.28	1.24
Z17	19.5	3.3	32.5	21.1	43.1	1.44	50.6	3.9	1.2	7.1	3.6	1.2	0.4	0.3	4.4	1.6	31.1	50.1	0.018	6.8	0.510	1.28	0.01	0.16	1.27
Z18	26.5	3.8	15.5	27.3	53.4	1.42	65.5	4.8	1.6	7.3	6.3	1.7	0.3	0.1	8.5	1.7	23.0	53.4	0.040	4.9	0.350	1.19	0.03	0.23	1.16
Z19	21.9	3.4	27.4	20.7	48.5	2.89	55.6	4.0	1.4	5.3	3.0	1.7	0.5	0.1	5.4	2.5	26.5	57.8	0.008	1.2	0.470	2.73	0.02	0.16	2.71
Z20	17.2	2.8	40.7	18.4	38.1	0.47	45.9	3.3	1.1	5.7	1.9	1.6	0.5	0.1	1.4	2.5	29.8	58.8	0.007	4.6	0.640	0.38	0.02	0.09	0.36
Z21	25.2	3.4	19.2	23.5	53.9	0.95	64.7	4.4	1.6	5.7	3.1	1.6	0.5	0.1	11.9	11.9	27.6	49.6	0.012	1.4	0.860	0.80	0.02	0.15	0.78
Z22	21.7	2.9	29.2	26.0	41.9	1.00	55.6	3.7	1.3	6.3	1.3	1.1	0.5	0.1	5.3	5.3	31.3	55.2	0.002	2.4	0.430	0.86	0.01	0.14	0.85
ROM1	18.0	3.2	35.1	20.5	41.2	0.95	49.7	3.9	1.6	5.6	3.5	2.4	0.8	0.4	3.4	2.7	31.7	52.9	0.006	2.8	0.290	0.77	0.01	0.18	0.76
ROM2	17.4	2.9	37.8	20.4	38.9	1.00	46.2	3.8	1.6	6.7	3.2	2.1	0.8	0.3	3.3	2.7	30.2	56.5	0.009	1.6	0.640	0.82	0.01	0.18	0.81

4.5 Petrographic Analysis

4.5.1 Abnormal condition analysis

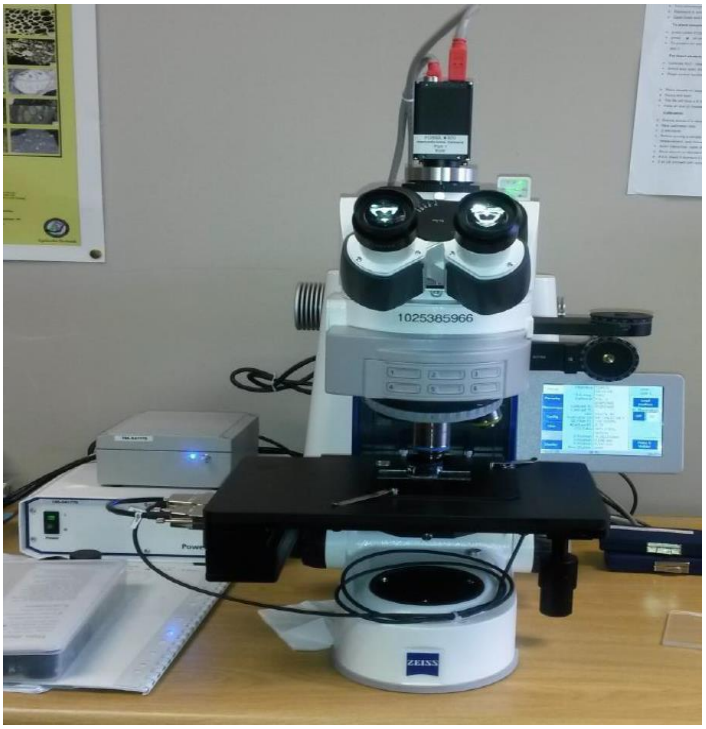


Figure 4.38: Zeiss Axiolmager reflectance light petrographic microscope

Contour plans of abnormal condition (AB) are shown in Figures 4.47 -4.49.The model averages for the S5, S4U and S2 seams are 30.64%, 31.22% and 31.13% respectively showing little variation between the seams for this parameter. The variance of AB on the S5 seam is higher at 4.19% vs 2.4% for the S4U and S2 seams.

The abnormal condition analysis is detailed in Table 4.8.Wagner (2015) notes that the samples show signs of weathering, mostly in terms of cracking and to a lesser extent fissuring. In many instances cracking is extensive, implying that the particles are potentially highly friable, and have an enhanced surface area. The samples commencing from Z01 through to Z12 show a gradual decrease in the proportion of particles exhibiting cracking and fissuring.

Certain samples, specifically Z03 and Z11, have a very high proportion of mineral matter, which has an influence on the abnormal condition data; minerals are counted as fresh particles unless alteration is noted, or cracking and fissuring within the mineral particle. Minerals are less prone to weathering / oxidation, and hence impacted on the total abnormal condition determination for that particle;

however, the organic matter in sample Z03 was highly cracked. The organic matter in Z11 was predominately fresh.

Pyrite content was variable between the samples, with sample Z02 reporting a very high proportion of pyrite determined in coal particles. The pyrite very rarely was observed in framboidal form, mostly as cell infilling, infilling of cracks, and small nodules. Sample Z04 reports a slightly enhanced reflectance range. Sample Z01 includes a fairly high proportion of porous fusinite, which may enhance the available surface area of the coal. Samples Z11 – Z13 contain large angular quartz particles (Wagner, 2015).

4.5.1.1 Micrographs

Below are some images of particles occurring in different samples (Figure 4.39-4.43). The cracking pattern was very consistent between all particles, in both vitrinite and inertinite. All photographs were taken at a magnification of x500, oil immersion lens, reflected white light, polarizer out. Scale bar is included on image, as well as the caption (Appendix A184-A189).

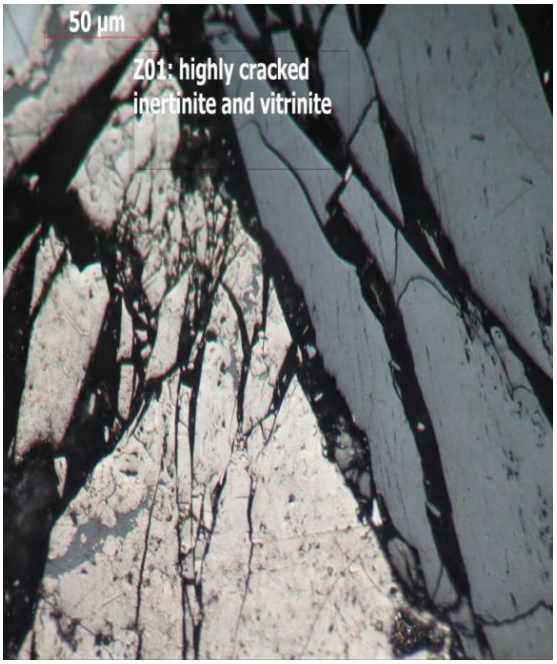


Figure 4.39: Sample Z01 showing cracked inertinite and vitrinite

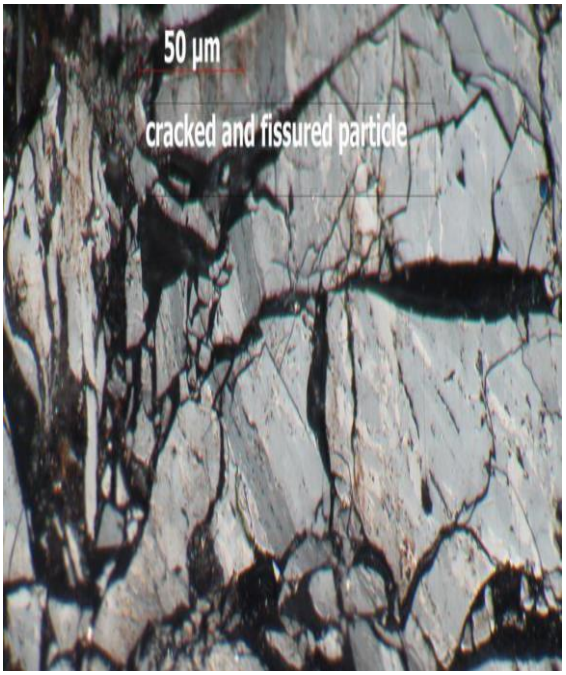


Figure 4.40: Sample Z01 showing cracked and fissure particle

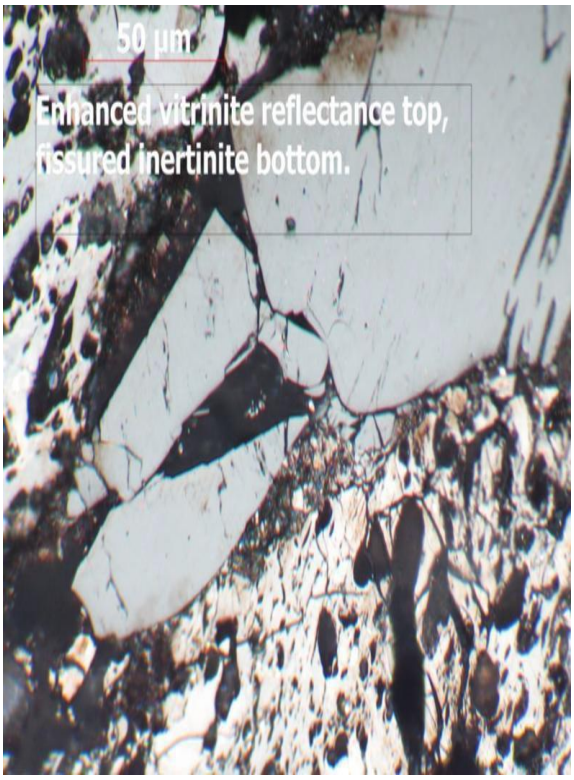


Figure 4.41: Sample Z01 showing enhanced vitrinite reflectance and fissured inertinite

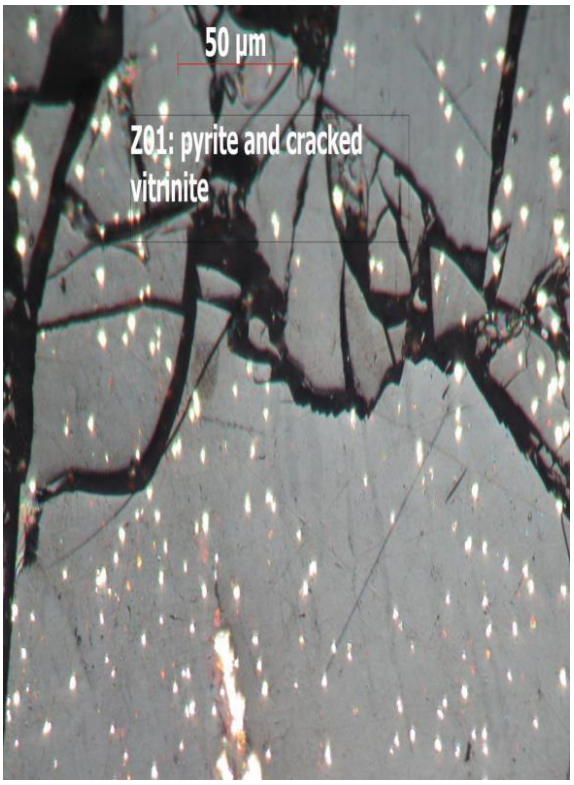


Figure 4.42: Sample Z01 showing pyrite and cracked vitrinite

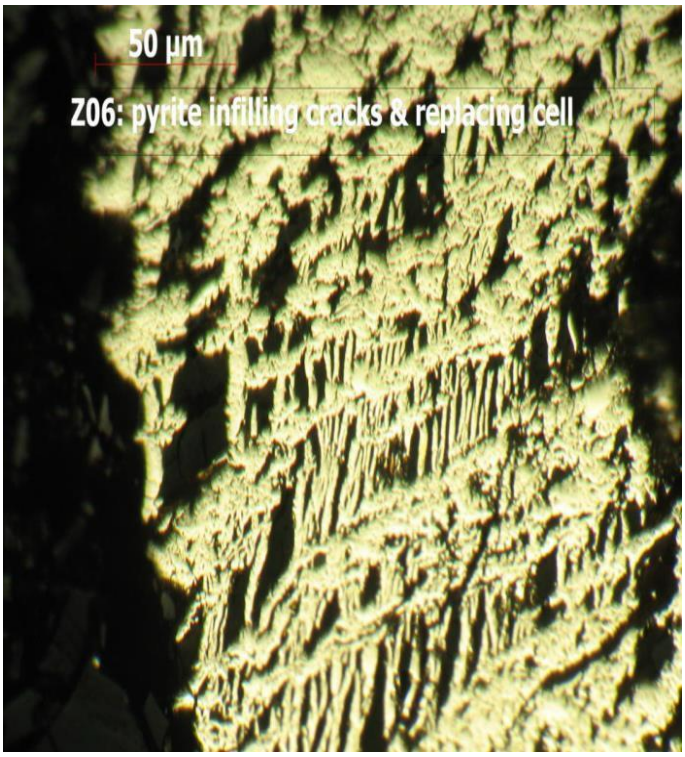


Figure 4.43: Sample Z06 showing pyrite infilling cracks

The geological setting of the samples is relatively undisturbed and intrusions or faulting would not contribute significantly to the abnormal condition of particles.

4.5.2 Maceral composition

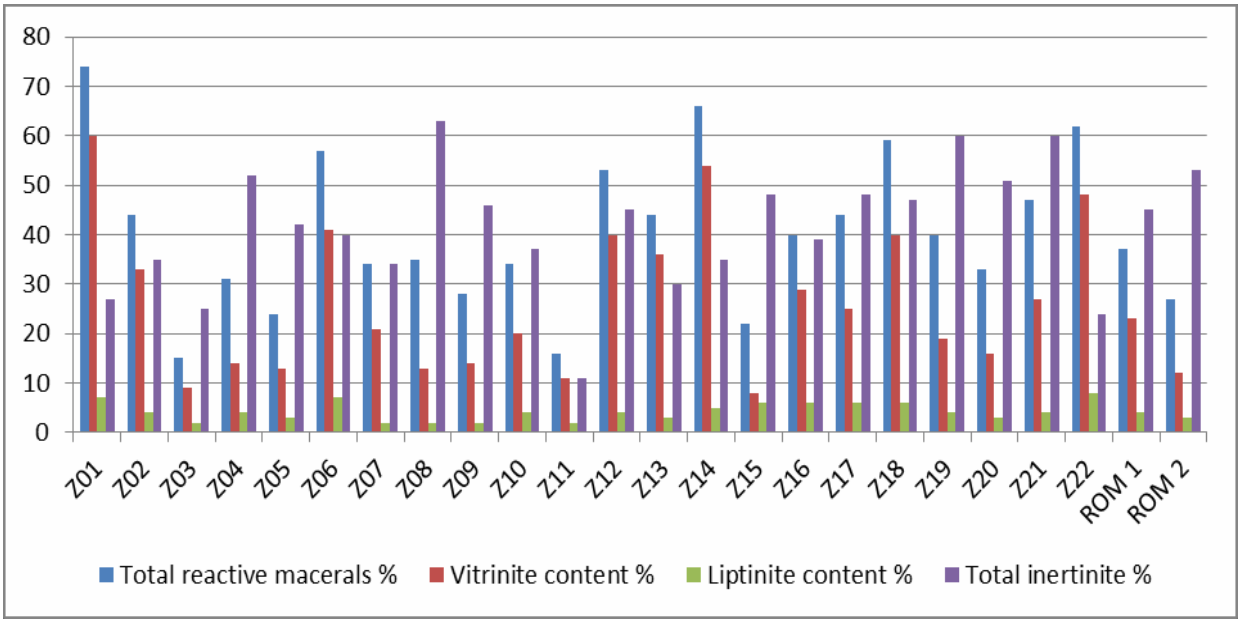


Figure 4.44: Maceral composition of the sample set

Liptinite content is low and compares with samples taken at nearby collieries within the Witbank coalfield. Inertinite is the dominant maceral group in the S2 and S4U samples. Vitrinite is dominant in the S5 seam samples and high CV bands in the lower seams.

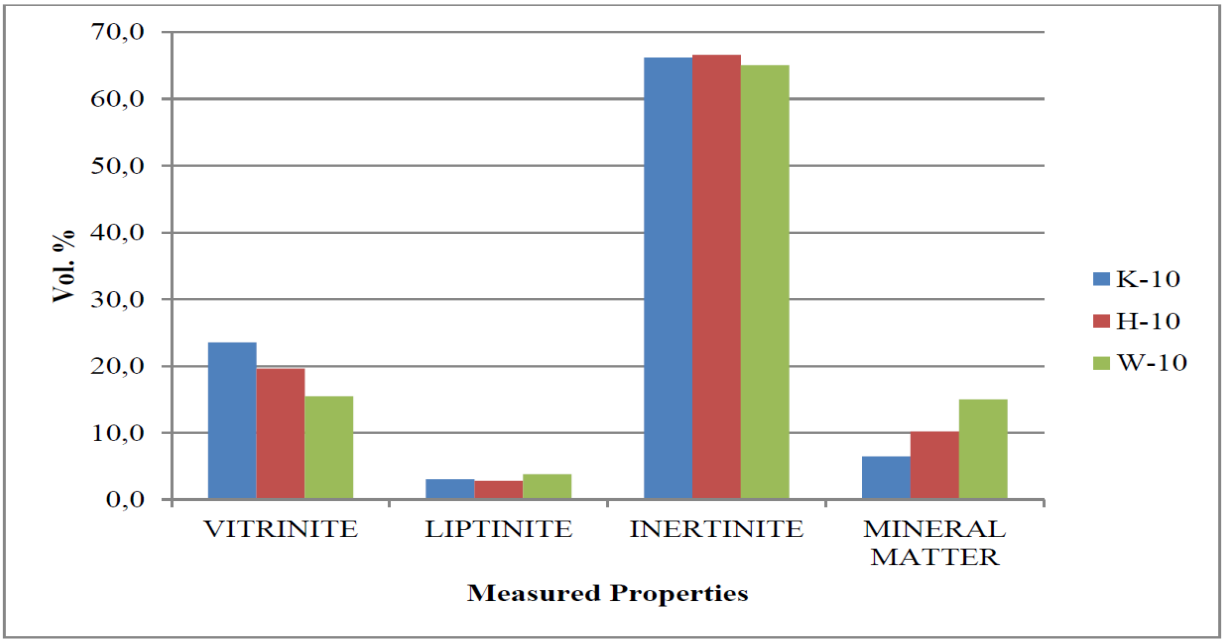


Figure 4.45: Maceral content from three nearby collieries within the Witbank Coalfield

The maceral composition of the sample set is shown in table 4.9.Total reactives are calculated from the addition of total vitrinite, total liptinite, reactive semifusinite and reactive inertodetrinite. Figures 4.50-4.52 show the TR% for each of the seams with a modelled average of 59.34% for the S5 (higher values in the south of the area). The S4U and S2 seams had TR values of 40.25% and 43.23%, significantly lower than the S5 seam.TR% was greater in the northern areas for the S4U and S2 seams.

4.5.3 Vitrinite reflectance

The mean random reflectance of vitrinite for the seam plies ranges between 0.67-0.85 (Figure 4.46).Sample Z04 from the S4U had the highest VR of all the seam plies. Contour plans of the modelled VR were similar for all the seams (0.71 -0.72).The S2 shows some zonation with lower VR in the northern areas although this zone also has the highest CV for the 2 seam.

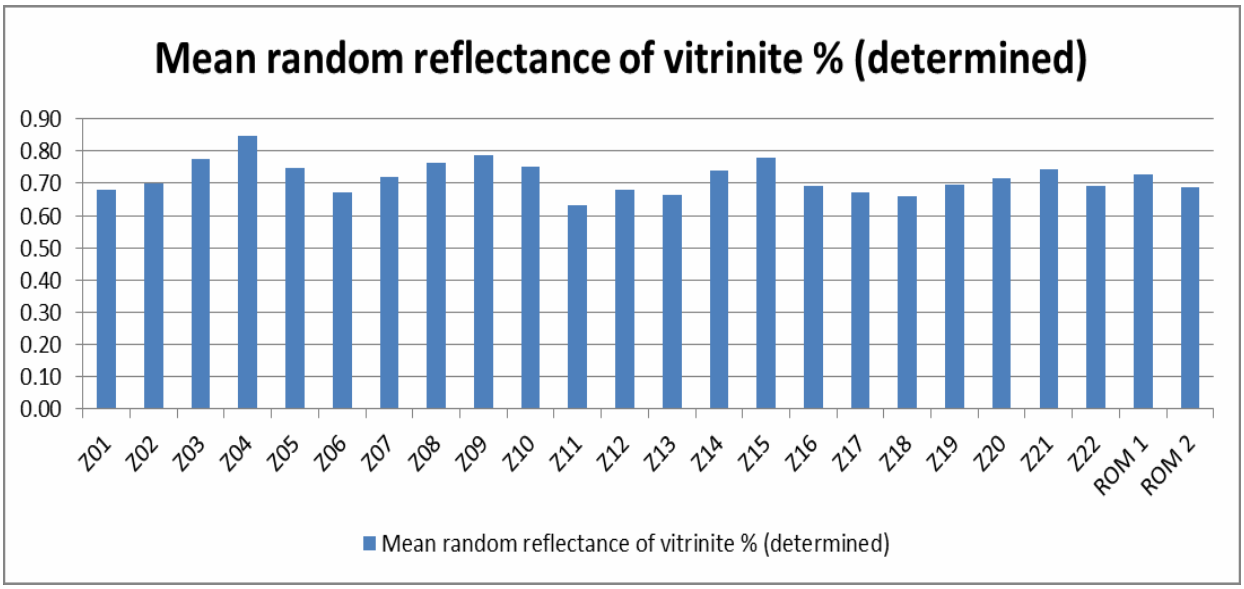


Figure 4.46: Vitrinite reflectance of sample set

In theory the vitrinite reflectance is believed by some to be more important than vitrinite content in determining sponcom liability (Mrs V du Caan, commentary).

Table 4.8: Abnormal particle analysis

Group	Condition	Sample ID														Sample									
		Z01	Z02	Z03	Z04	Z05	Z06	Z07	Z08	Z09	Z10	Z11	Z12	Z13	Z14	Z15	Z16	Z17	Z18	Z19	Z20	Z21	Z22	ROM 1	ROM 2
Fresh	**Total Fresh**	59.2	58.2	66.7	53.1	63.2	69	70.8	66.8	64.5	80.1	79.9	76	71.2	76	56.6	67.4	71.2	73.2	64.8	73.6	63.4	73.2	57.6	59
Fissures	**few**	3.7	2.4	5.8	5.9	3.9	3.8	2.5	4.9	6	2.7	1.6	3.3	2.3	7.6	10.2	6.6	8	7.6	10	8.8	13.6	7.4	12.6	13.6
	extensive	1	0.8	1.4	3.7	1.6	0.7	0.8	1.8	1.8	0.6	0	0.2	0	0	0	0	0	0.2	0	0	0.6	0	0.8	0
Cracks	**few**	15	9.7	5.4	10.7	12.3	9.3	9.8	9.5	13.5	8.6	5.3	11.2	12.3	9.4	8.8	6.4	10.2	12.6	15.8	6	13	8.6	13.6	10.2
	extensive	8.7	8.5	7.6	20.5	8	9.2	8.1	9.5	5.7	5.7	3.7	6.1	6.5	1	1.6	1	0.6	4	1.8	0.8	4	2.6	4.2	3.4
	dessicated	1.6	0	0	0	0	0.3	0.2	0	0	0	0	0.2	0	0.8	0	0	0.2	0	0	0	0.4	0.8	0	0
Holes	**inherent**	0.2	0.2	2.3	2.5	1.8	0.7	1.2	0.4	0.2	0	0	0.2	0	0	2.6	0.6	0.6	0.2	2	2.8	1.4	0	0.6	0.6
	leaching	0	0	0	0	0	0	0	0	0		0	0	0	0	0	0	0	0	0	0	0	0	0	0
Heat Affected	**organic**	0	0.2		0.8	0.2	0	0	0	0	0	0	0	0	0	0	0	0	0	0	0	0	0	0	0
	inorganic/minerals	0	0	0	0	0	0	0	0	0	0	0	0	0	0	0	0	0	0	0	0	0.4	0	0	0
Discoloration	**whole particle**	0	1.6	9.7	2.7	6.8	0.2	1	2	7.2	0.8	7.4	0.4	0.4	0	17.8	14.2	5.4	0.2	2	6.8	0	0.6	8.6	9.4
	dark zones	0	0	0	0	0	0	0	0	0	0	0	0	0	0	0	0	0	0	0	0	0	0	0	0
	light zones	0	0	0	0	0	0	0	0	0	0	0	0	0	0	0	0	0	0	0	0	0	0	0	0
	whole particle	0	0	0	0	0	0	0	0	0	0	0	0	0	0	0	0	0	0	0	0	0	0	0	0
Porous Fusinite	**fusinite**	6.2	3.2	0	0.4	1.2	3.5	2.5	1.4	0	0.4	0.4	2.4	2.3	2.8	1.2	1.6	1.4	1.6	3.2	0.8	2.8	4.6	1.8	0.4
Minerals	**alteration**	0	0.4	0	0	0.4	0	0	0	0	0	0	0	0.6	0	0	0	0	0	0	0	0	0	0	0
	pyrite	4.6	15	0.4	0.2	0.8	3.3	3.1	3.8	1.2	1.2	1.8	0	4.3	2.4	1.2	2.2	2.4	0.4	0.4	0.4	0.4	2.2	0.2	3.2
Total	**total abnormal condition**	41	42	33.4	46.8	36.8	31	29.2	33.3	35.6	20	20.2	24	28.7	24	43.4	32.6	28.8	26.8	35.2	26.4	36.6	26.8	42.4	41

The slightly higher AB for the ROM samples may be due to the cutting and crushing of these samples through the sampling plant. On a seam basis there appears to be no distinct separation on AB basis.

Table 4.9: Summary of major coal characteristics

Sample	Z01	Z02	Z03	Z04	Z05	Z06	Z07	Z08	Z09	Z10	Z11	Z12
RANK (degree of maturity)	Bituminous	Bituminous	Bituminous	Bituminous	Bituminous	Bituminous	Bituminous	Bituminous	Bituminous	Bituminous	Bituminous	Bituminous
ISO 11760-2005 Classification of Coals	Medium Rank C	Medium Rank C	Medium Rank C	Medium Rank C	Medium Rank C	Medium Rank C	Medium Rank C	Medium Rank C	Medium Rank C	Medium Rank C	Medium Rank C	Medium Rank C
Mean random reflectance of vitrinite % (determined)	0.68	0.70	0.78	0.85	0.75	0.67	0.72	0.76	0.79	0.75	0.63	0.68
Vitrinite-class distribution	V 5 to V 8	V 5 to V 8	V 5 to V 9	V 5 to V 11	V 5 to V 9	V 5 to V 8	V 5 to V 8	V 5 to V 9	V 6 to V 9	V 6 to V 8	V 5 to V 8	V 5 to V 7
Standard deviation s	0.062	0.056	0.088	0.095	0.075	0.063	0.071	0.072	0.061	0.061	0.060	0.055
Mean maximum reflectance of vitrinite % (calculated)	0.73	0.75	0.83	0.89	0.80	0.72	0.77	0.81	0.84	0.80	0.69	0.73
Abnormalities	None observed	None observed	None observed	None observed	None observed	None observed	None observed	None observed	None observed	None observed	None observed	None observed
PETROGRAPHIC COMPOSITION (% by volume)												
Maceral analysis (mineral matter basis)												
Total reactive macerals %	74	44	15	31	24	57	34	35	28	34	16	53
Vitrinite content %	60	33	9	14	13	41	21	13	14	20	11	40
Liptinite content %	7	4	2	4	3	7	2	2	2	4	2	4
Total inertinite %	27	35	25	52	42	40	34	63	46	37	11	45
Heat altered (coke, char etc.) %	0	0	0	0	0	0	0	0	0	0	0	0
Visible minerals %	6	28	64	30	42	12	43	22	38	39	76	11
Maceral analysis - Total %	100	100	100	100	100	100	100	100	100	100	100	100
Sample	**Z13**	**Z14**	**Z15**	**Z16**	**Z17**	**Z18**	**Z19**	**Z20**	**Z21**	**Z22**	**ROM1**	**ROM2**
RANK (degree of maturity)	Bituminous	Bituminous	Bituminous	Bituminous	Bituminous	Bituminous	Bituminous	Bituminous	Bituminous	Bituminous	Bituminous	Bituminous
ISO 11760-2005 Classification of Coals	Medium Rank C	Medium Rank C	Medium Rank C	Medium Rank C	Medium Rank C	Medium Rank C	Medium Rank C	Medium Rank C	Medium Rank C	Medium Rank C	Medium Rank C	Medium Rank C
Mean random reflectance of vitrinite % (determined)	0.67	0.74	0.78	0.69	0.67	0.66	0.70	0.72	0.74	0.69	0.73	0.69
Vitrinite-class distribution	V 5 to V 8	V 5 to V 8	V 5 to V 9	V 5 to V 8	V 5 to V 8	V 5 to V 8	V 5 to V 8	V 5 to V 8	V 5 to V 8	V 5 to V 8	V 5 to V 9	V 5 to V 9
Standard deviation s	0.054	0.080	0.098	0.073	0.609	0.060	0.078	0.063	0.064	0.063	0.074	0.078
Mean maximum reflectance of vitrinite % (calculated)	0.72	0.79	0.83	0.74	0.72	0.71	0.75	0.77	0.79	0.74	0.78	0.74
Abnormalities	None observed	None observed	None observed	None observed	None observed	None observed	None observed	None observed	None observed	None observed	None observed	None observed
PETROGRAPHIC COMPOSITION (% by volume)												
Maceral analysis (mineral matter basis)												
Total reactive macerals %	44	66	22	40	44	59	40	33	47	62	37	27
Vitrinite content %	36	54	8	29	25	40	19	16	27	48	23	12
Liptinite content %	3	5	6	6	6	6	4	3	4	8	4	3
Total inertinite %	30	35	48	39	48	47	60	51	60	24	45	53
Heat altered (coke, char etc.) %	0	0	0	0	0	0	0	0	0	0	0	0
Visible minerals %	31	6	38	26	21	7	17	30	9	20	28	32
Maceral analysis - Total %	100	100	100	100	100	100	100	100	100	100	100	100

There is no correlation between abnormal condition (AB) and known structures (figures 4.47-4.49). The S5 seam shows high variation with distinct zones of high AB and low AB. The S2 and S4U have more uniform AB plots and have few zones of high AB (>35%) as seen in the S5 seam plot.

The S5 seam has the highest % reactives (TR) with the southern area showing the highest values upwards of 60%.The S4U reactives generally range between 30-50% with the southern area being least reactive**.** The S2 reactives are similar to the S4U except in the north where values of 50-60% are noted**.**

The shade colour plot for the S5 seam shows the lowest vitrinite reflectance (VR) of the economic horizons. The S4U VR plot is fairly uniform and has higher values than the S5**.**The S2 plot has similar VR to the S5 seam with the lowest values correlating to highest CV areas.



Figure 4.47: S5 abnormal condition analysis (%)



Figure 4.48: S4U abnormal condition analysis (%)

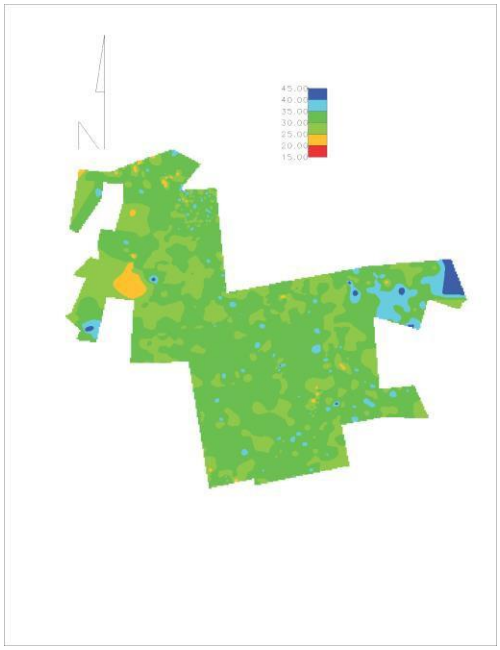


Figure 4.49: S2 abnormal condition analysis (%)

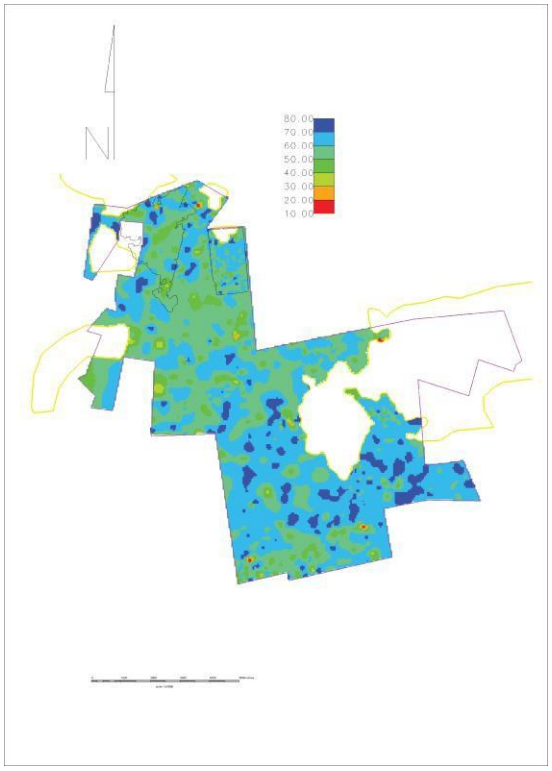


Figure 4.50: S5 Total reactives (%)

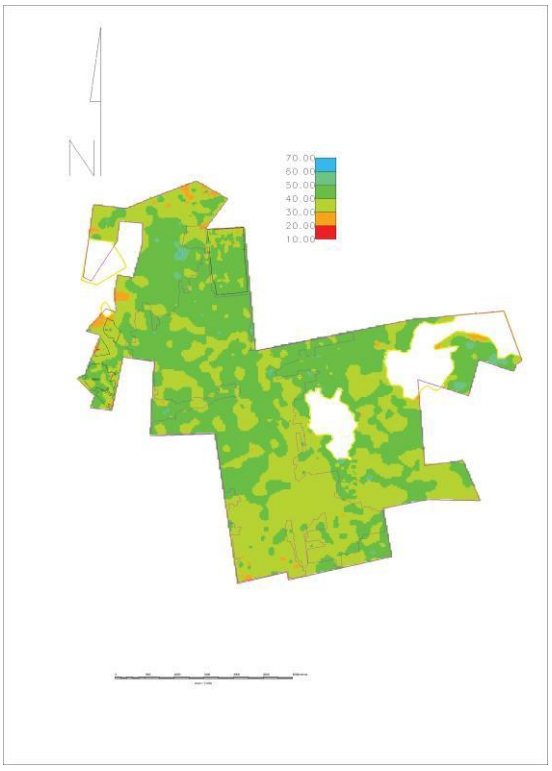


Figure 4.51: S4U total reactives (%)

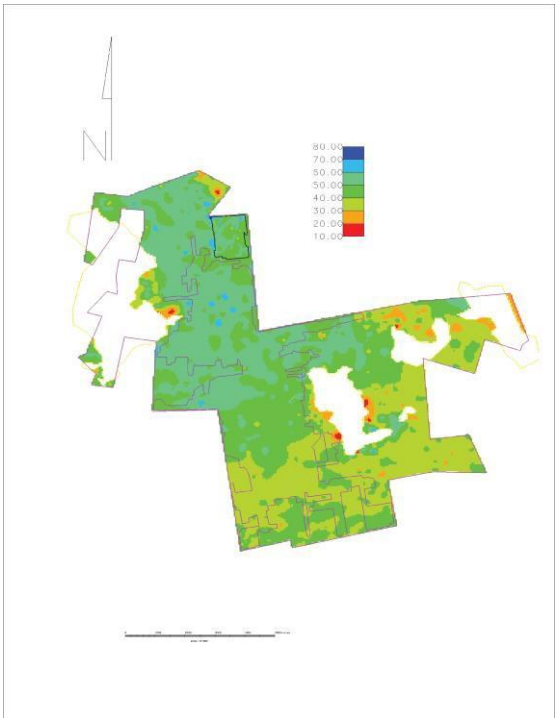


Figure 4.52: S2 total reactives (%)

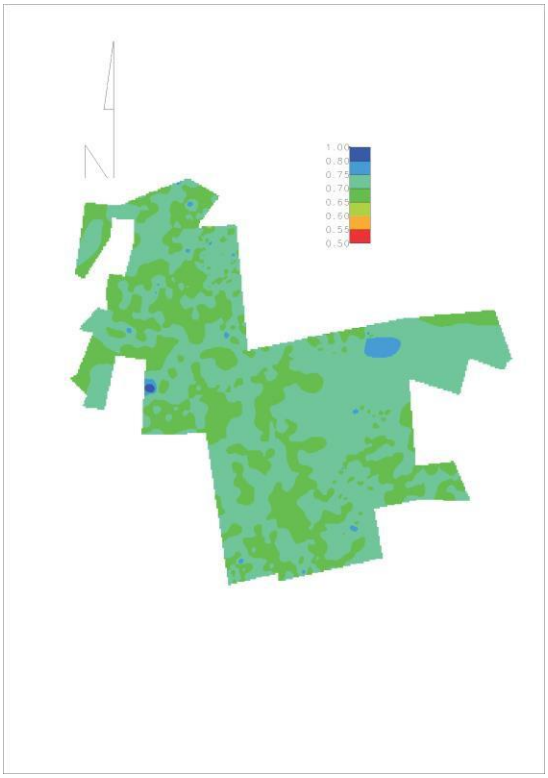


Figure 4.53: S5 seam VR

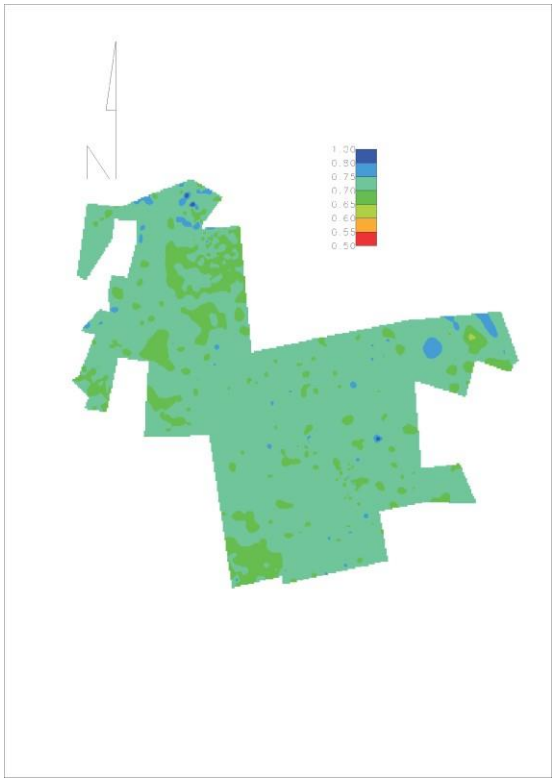


Figure 4.54: S4U seam VR

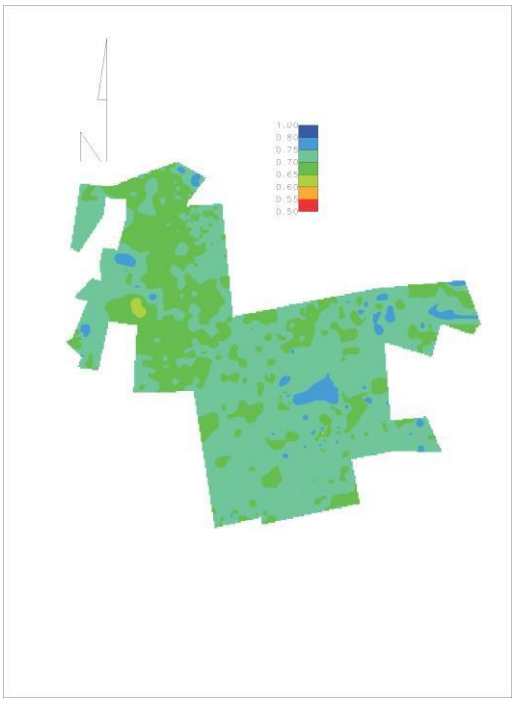


Figure 4.55: S2 seam VR

4.6 Geology

Geomorphological coal fire manifestations (sinkholes, depressions and subsidence etc.) are not present as there is no history of sponcom at Colliery X. The effect of carbonaceous roof and floor lithologies as well as in seam partings on sponcom is discussed in this section.

4.6.1 Mudstone roof and floor

Mudstone bands in the immediate roof and floor have been modelled for each seam. Although difficult to quantify, these lithologies are often associated with sponcom at different sites in the Witbank and other Coalfields. These units may have significant volatiles and carbon associated with them and typical values for sandstone and mudstone are tabled below (Table 4.10). Sulphur is not notably different from the coal seam values and could not be considered an additional factor to sponcom from these results.

From figures (4.56-4.58) below it can be seen that the S2 seam has relatively thick mudstone band in the roof (average 1.42m) that may contribute to self-heating. The S4U has a relatively thin mudstone layer in the immediate roof as does the S5 seam. The floor mudstone thicknesses for each seam are included in the appendix and range from 0.4m for the S4U to 0.2m for the S2.Roof or floor mudstone >2m is included in the risk matrix.

Table 4.10: Rock lithology qualities at Colliery X

Rock	RD	CV	IM	AS	VM	FC	TS	DAF
mud	2.02	8.3	2.6	63.0	15.7	18.8	0.67	46.9
sand	2.23	4.0	1.6	78.3	11.4	8.8	0.35	58.1
avg	2.12	6.2	2.1	70.6	13.5	13.8	0.51	52.5

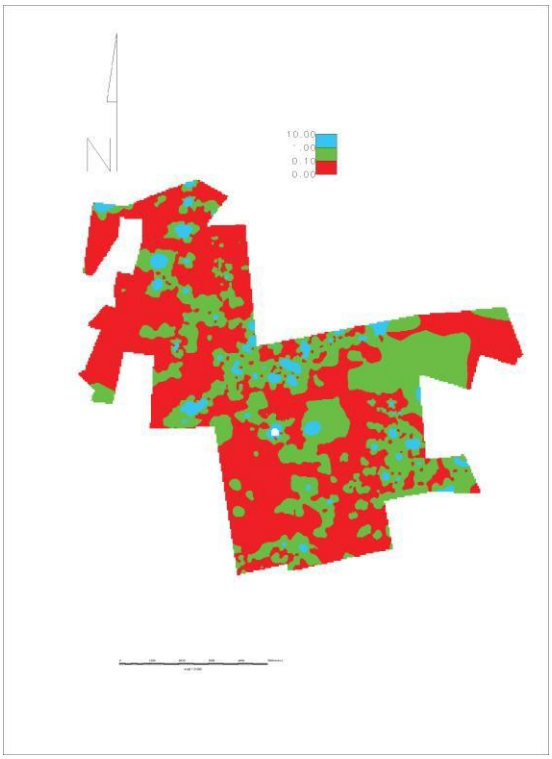


Figure 4.56: S5 seam roof mudstone



Figure 4.57: S4U seam roof mudstone

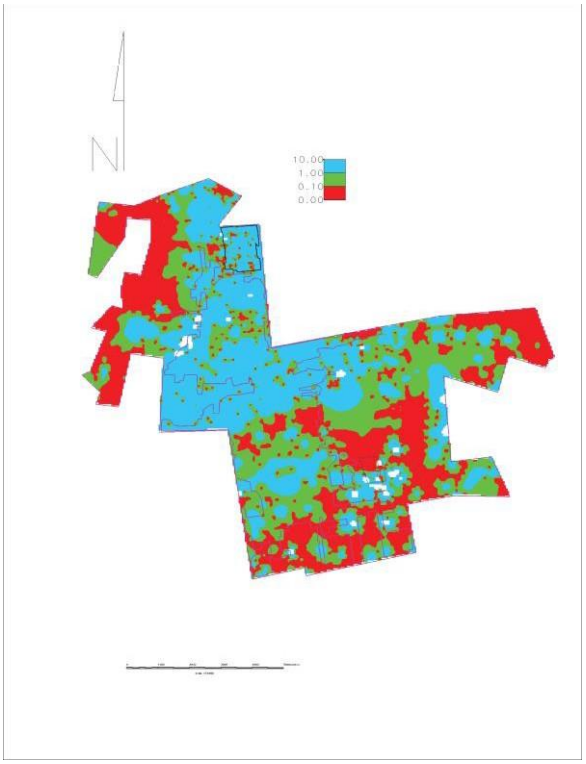


Figure 4.58: S2 seam roof mudstone thickness

4.6.2 In-seam partings

Mudstone parting thickness has been included in the risk matrix (Figures 4.59-4.60) as it may have some effect on sponcom liability (slows mining rate and possibly increases oxidation time). Sponcom is frequently observed to be associated with carbonaceous partings. The S5 seam does not have significant partings and only the S4U and S2 have been modelled**.** Lithologies are modelled according to % ash with 50-80% including mudstones and siltstones. Mudstones >2m in thickness were included in the risk matrix. Parting is more evident in the southern areas of the mine in both the S4U and S2 seams.

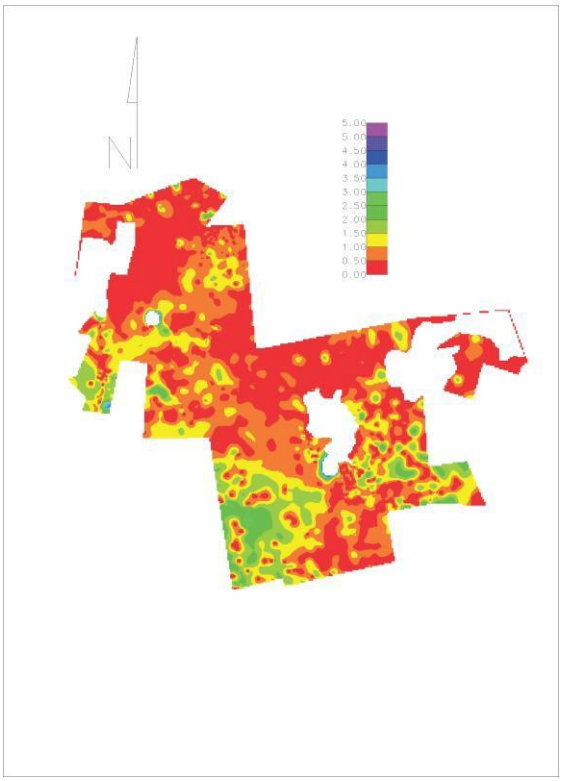


Figure 4.59: S4U mudstone parting thickness

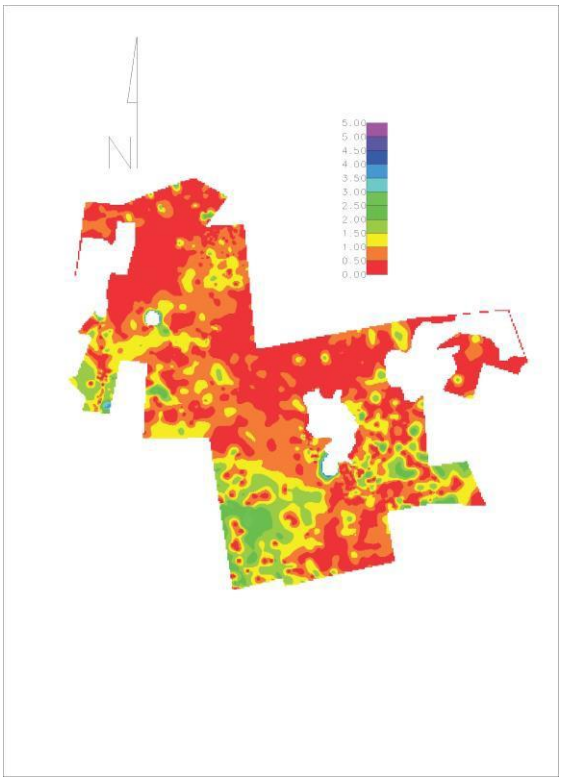


Figure 4.60: S2 mudstone parting thickness

5 DISCUSSION

5.1 Cross-Correlations

Cross correlation between each of 35 variables used in the sample dataset and model dataset are shown in tables 5.2-5.3 and meaningful correlation charts are included in the sub-sections.. Correlation coefficients for the laboratory data set are generally more linear than for the much larger model dataset that is skewed by CV distribution within each seam (figure 8.6 and 8.7). However the model dataset represents a spatial 2D picture of the sponcom liability of each seam and is more useful than when using laboratory data in isolation. Linear correlations between some of the chemical variables are to be expected (CV-AS, RD-AS etc.), and the potentially meaningful correlations are highlighted in these tables. The correlations are categorised as good (>80%), moderate (>70%) or low (>50%).

Table 5.1: Variables used in modelling and correlations.

Abreviation	Decription	Unit
AB	abnormal particles	%
Al2O3	Al2O3	%
Ash	ash	%
Carbon	total carbon	%
CaO	CaO	%
CPT	crossing point temperature	°C
CV	heat value	Mj/kg
Der Wt	derivative weight gain	
FC	fixed carbon	%
Fe2O3	Fe2O3	%
GLI	oxygen adsorption	
H	hydrogen	%
IM	inherent moisture	%
K2O	K2O	%
MGO	MgO	%
MNO	MnO	%
MS	mineral sulphur	%
N	nitrogen	%
Na2O	Na2O	%
O	oxygen	%
OS	organic sulphur	%
P2O5	P2O5	%
PS	pyritic sulphur	%
RD	relative density	g/cc
SiO2	SiO2	%
S03	S03	%
SS	sulphate sulphur	%
Tstart	start temperature TGA	°C
Tpeak	peak temperature TGA	°C
Ti02	Ti02	%
TR	total reactives	%
TS	total sulphur	%
VM	volatile matter	%
VR	vitrinite reflectance	%
WT	weight gain TGA	%

5.1.1 CPT (crossing point temperature) correlations

Notable correlations between CPT and CV,OS,TR and VM are shown in Figures 5.1-5.5.CPT generally correlates well with IM,AS and aliphacity (not measured in this investigation) and has frequently been shown to decrease with increase in IM,VM,FC.Higher ash values generally increase the CPT.Higher ranked coals usually show higher CPT. All of the seams in the study area are classed as bituminous medium rank C coal.Oxygen had a very high error coeficient with CPT (0.88).

CPT did not generally correlate well with the other sponcom (thermal) index tests(TGA and GLI).
The S5 had the lowest CPT of 196.6 ºC, followed by the S2 and S4U seams with CPT's of 207 ºC and 211.9 ºC. Based on some Indian CPT indexes (Pattanaik et al, 2011), none of these seams would be classed as highly susceptable to sponcom.The expected relationship between CPT and other sponcom variables are sometimes meaningful but not neccesarily linear.

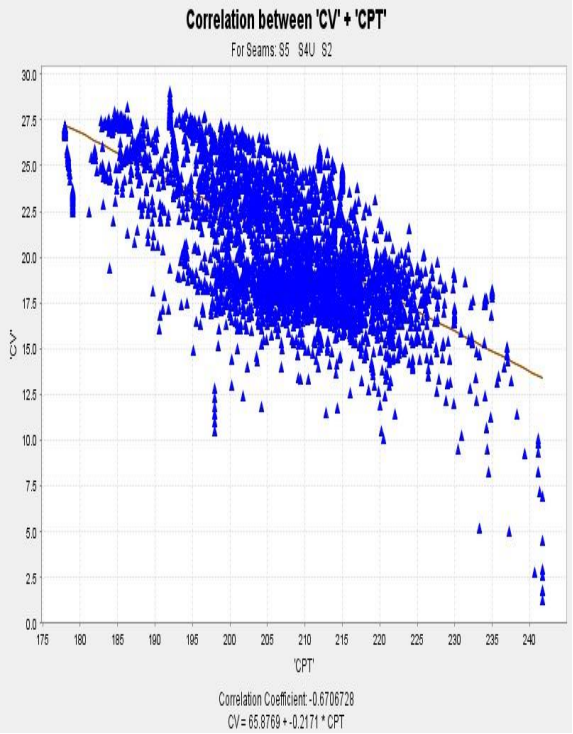


Figure 5.1: Correlation between CV and CPT for the model dataset

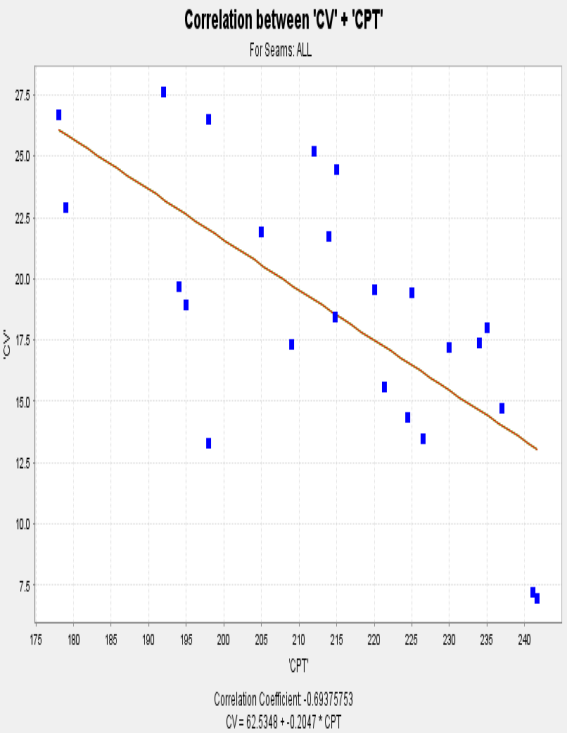


Figure 5.2: Correlation between CV and CPT for the sample dataset

The samples occur in as narrow rank range and the expected decrease in CPT with increasing CV is observable from both the datasets**.** The correlation coefficient is slightly higher for the laboratory sample dataset than the extrapolated modelling database**.**

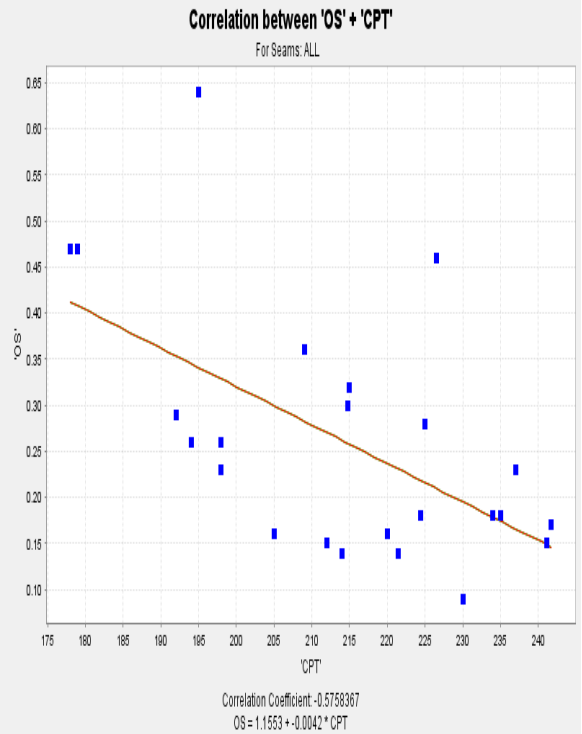


Figure 5.3: Correlation between OS and CPT for the sample dataset

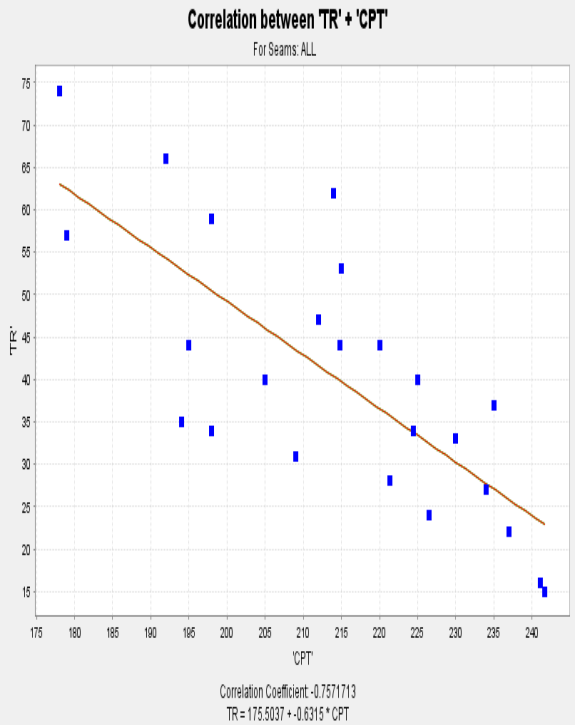


Figure 5.4: Correlation between TR (total reactives) and CPT for the sample dataset

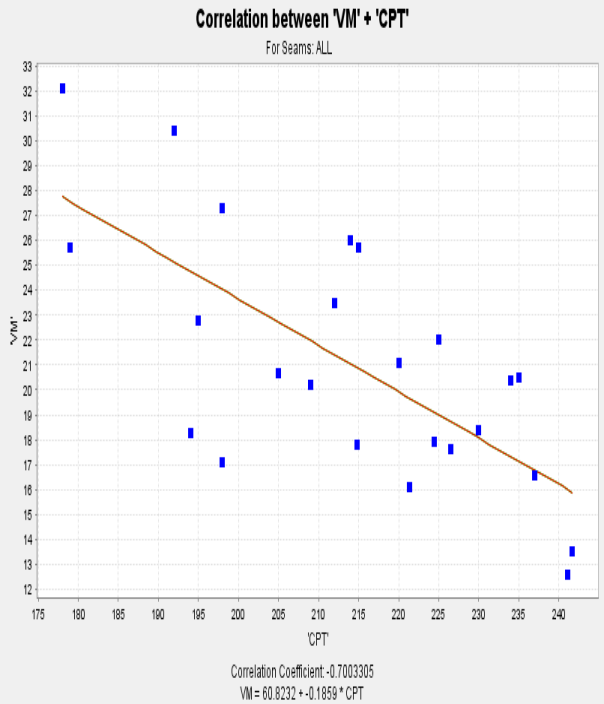


Figure 5.5: Correlation between VM (volatile matter) and CPT for the sample database

The OS had the highest correlation to CPT (-0.58) and PS the lowest correlation (-0.49).This agrees with theory that sulphur reduces CPT although, as expected, coefficients are not linear. Reactive macerals also reduce CPT with a clear trend visible. Volatile matter theoretically has the greatest influence on sponcom liability and clearly reduces CPT in the sample dataset.

5.1.2 TGA (thermogravimetric) correlations

T1, T2 and WT in the dataset under investigation show some correlations that are in contrast to popular theory. T1 shows moderate correlation with the proximate variables, WT and GLI, although T2 is more definitive as an indicator of sponcom. T2 should correlate negatively with vitrinite reflectance but the opposite relation is observed (Figure 5.6)

The WT gain in this particular dataset may be in the form of unstable peroxy complexes and not stable peroxy complexes. This implies that weight gain in some of these samples does not necessarily mean reduced sponcom liability, although theory generally points to the opposite argument (Avila et al., 2014).The WT correlates well with the proximate variables and moderately with GLI, T1 and TR (table 5.2 -5.3). The TGspi is found from the DER (derivative of weight gain) and is used in determining the low temperature reactivity of the sample. DER showed no correlation to the other variables but was highest for the S4U followed by the S2.

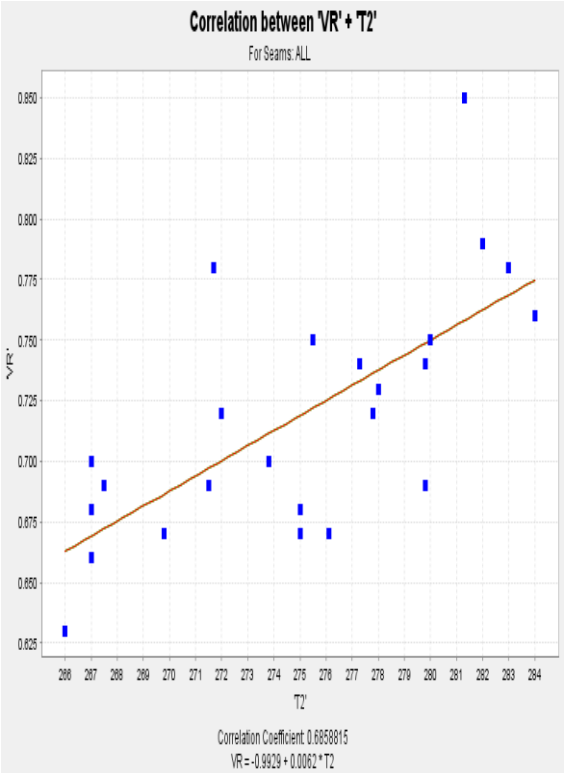


Figure 5.6: Sample dataset correlation of VR (vitrinite reflectance) and T2 (peak temperature)

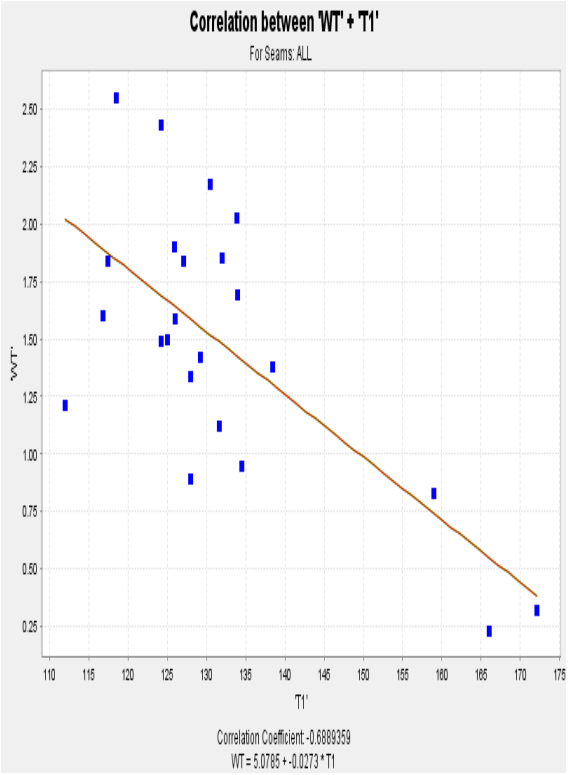


Figure 5.7: Sample dataset correlation of WT (weight gain %) and T1 (start temperature)

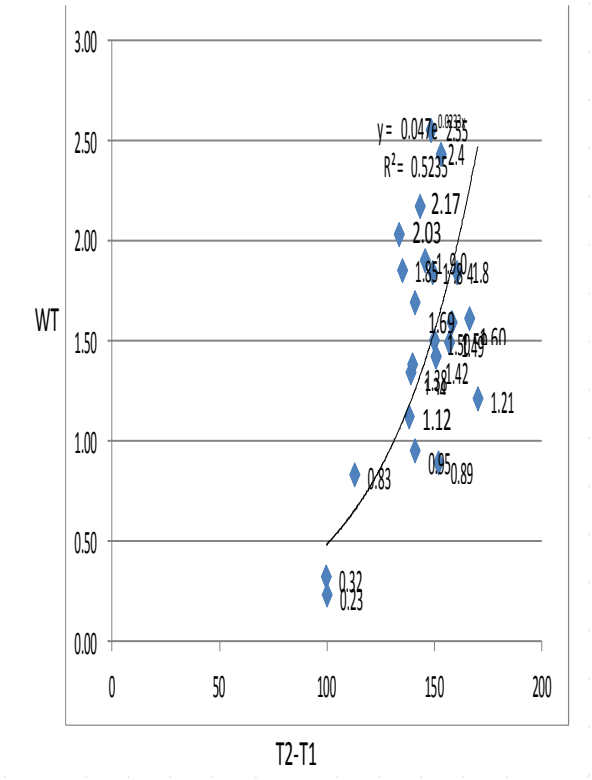


Figure 5.8: Sample dataset correlation WT and temperature differential

Peroxy-complexes formed at low initial temperature also have the highest WT. T2 and %WT gain showed very low correlation although a low T2 favours sponcom. Generally the net temperature range (T2-T1) (Figure 5.7) for the different heating rates does not vary much. The %WT gain decreases with increasing heating rates as exposure time to form oxy-complexes is reduced (figure 5.8). The lower temperature (3C) ramp is more indicative of the reactivity than high temperature gradients (5C-20C).

As the temperature range increase the weight gain of the stable (unstable) peroxy complex increases. Depending on the type of TGA profile obtained, the total mass gain, and the starting and the peak temperatures of the process, coals can be classified by their potential to undergo self-oxidation. Avila (2014) shows a relationship between the maximum weight increase and the temperature range in which this was observed, from which coals prone to spontaneous combustion can be clearly identified. The Colliery X set of results possibly indicates unstable compounds are formed in contrast to observations by Avilla.

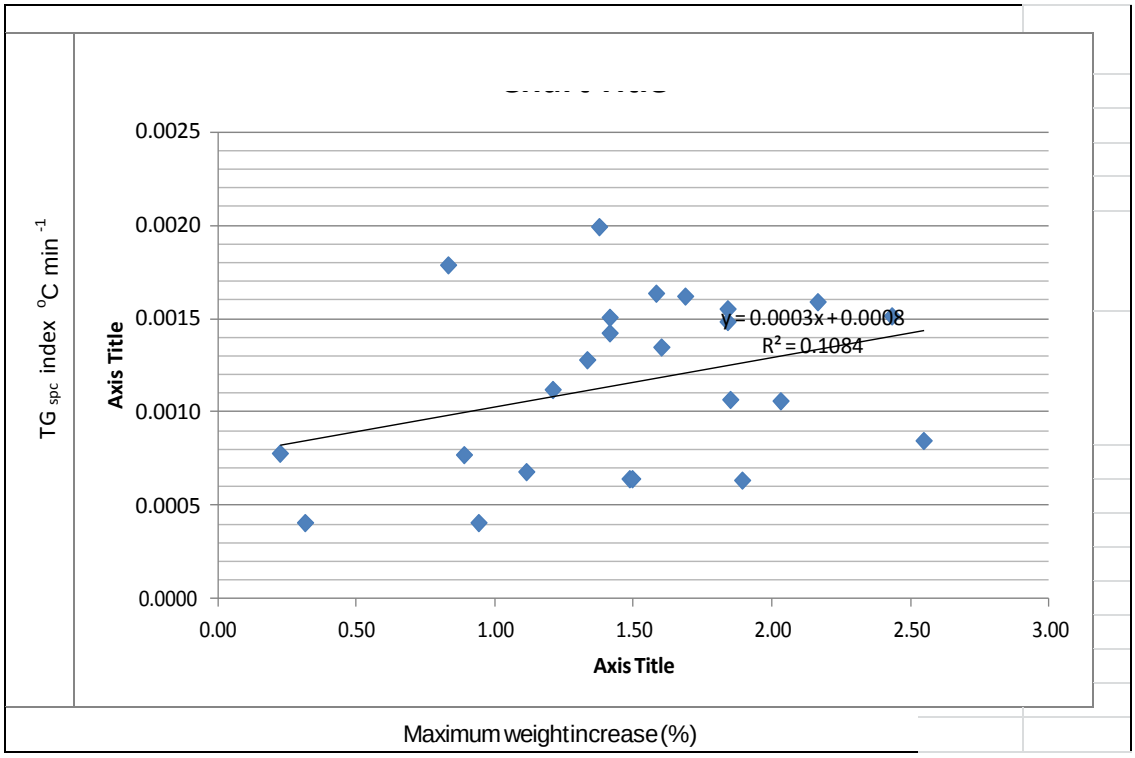


Figure 5.9: WT increase and TG spi correlation

WT and TGspi show positive correlation although the scatter is high. A negative correlation is more commonly described in theory i.e. higher reactive index values should correspond with low weight increase. The TGspi generally decrease with higher heating ramps showing reduced contact time with oxygen and a reduced coal ignition potential.

5.1.3 Oxygen absorption correlations

The oxygen absorption test (modified Smith and Glasser method) correlates fairly well with theoretical prediction. CPT results correlates well with VM, TR and IM. There is also a moderate correlation with T1 and WT. GLI and CPT showed a negative correlation and supports theory although the scatter is high. Oxygen content had an error coefficient of 0.84 with GLI. Theoretically the most significant regressor is always VM content followed by IM.VM represents the reactive component of the sample and IM acts as a proxy for the surface area of the coal. The GLI correlation coefficient with IM and VM was 0.71 and 0.67 respectively showing reasonable conformity with theory. Figures 5.10-5.13 show GLI correlation with selected variables.

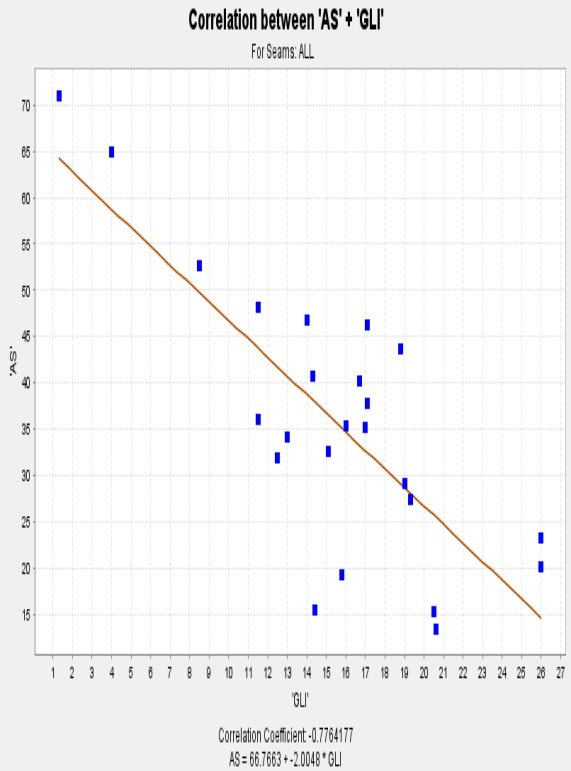


Figure 5.10: Correlation between AS and oxygen absorption GLI

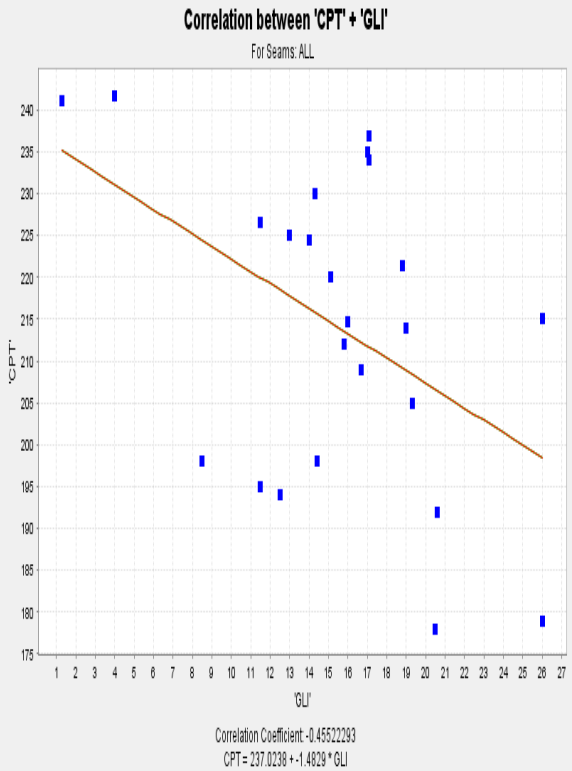


Figure 5.11: Correlation between CPT and oxygen absorption GLI

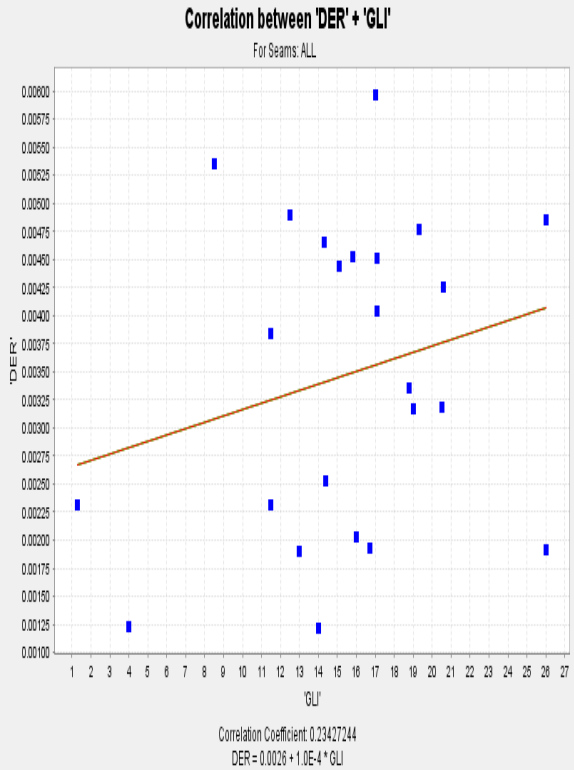


Figure 5.12: Correlation between (DER) and oxygen absorption (GLI)

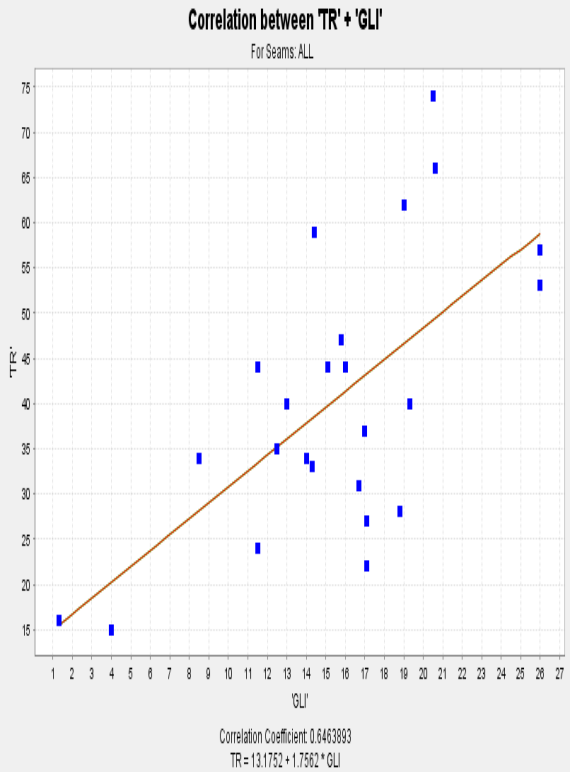


Figure 5.13: Correlation between derivative of TR and oxygen absorption (GLI)

As the ash content decreases oxygen reactivity increases with a clear negative relationship shown. As reactivity increases CPT decreases although scatter is high in this set of results. The derivative of weight gain has a poor correlation to GLI and the scatter is high. Total reactive macerals show a strong positive relation to oxygen absorption.

5.1.4 Chemical analysis correlations

Proximate, ultimate and ash elemental analysis were undertaken on all the samples. The CPT ,T1 ,WT,TR and GLI showed moderate to good correlation with the chemical variables.T2 and DER(derivative of weight gain) showed poor correlation to the chemical variables. The usual proximate-CV and ultimate relations were well defined (CV-AS, RD-AS) and the use of CV to correlate the sample dataset to the existing model database is reasonable and reliable.

Fe_2O_3 showed correlation to CV and TR. OS and SS also showed moderate correlation. The metal oxides however showed little relationship to one another or the thermal tests (CPT, TGA, GLI).Oxygen also showed no correlation to the other variables although some theory states ultimate oxygen to be related to sponcom liability. A weak negative correlation between DER and O (-0.45) suggests that less oxygen in the structural sites allows for more oxygen absorption. Hydrogen showed strong correlation to several of the thermal, chemical and petrographic variables.

Some of the correlations seen in the table are improbable and not noted in literature, but are marked for the purpose of comparison eg. N/VM, MnO/TS. Some of the relations of hydrogen and oxygen to other variables are shown in figures 5.14-5.16.

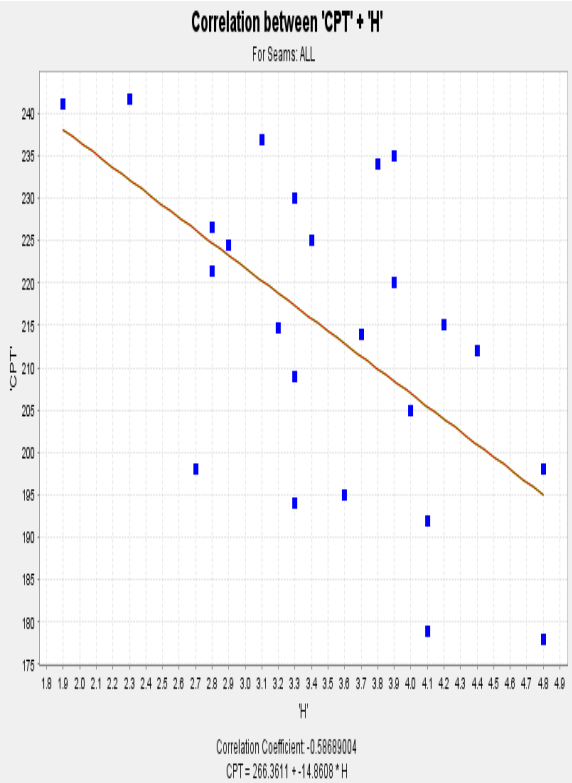


Figure 5.14: Correlation between CPT and H

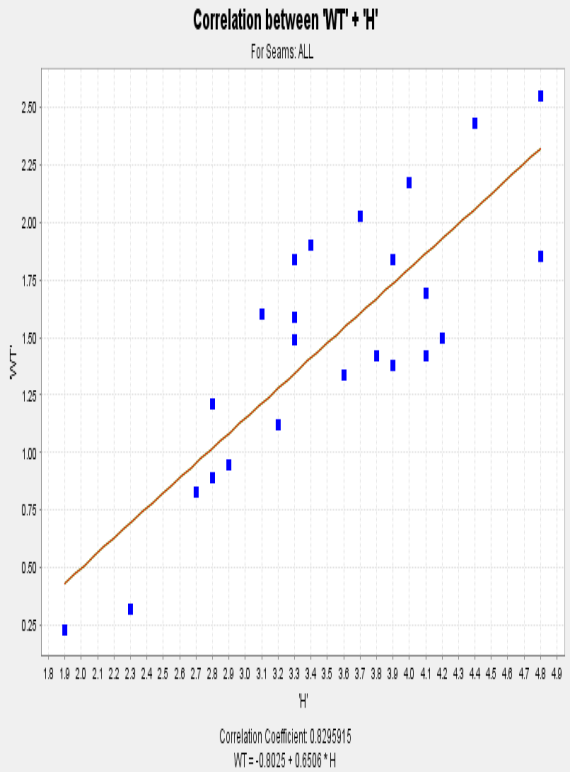


Figure 5.15: Correlation between WT and H

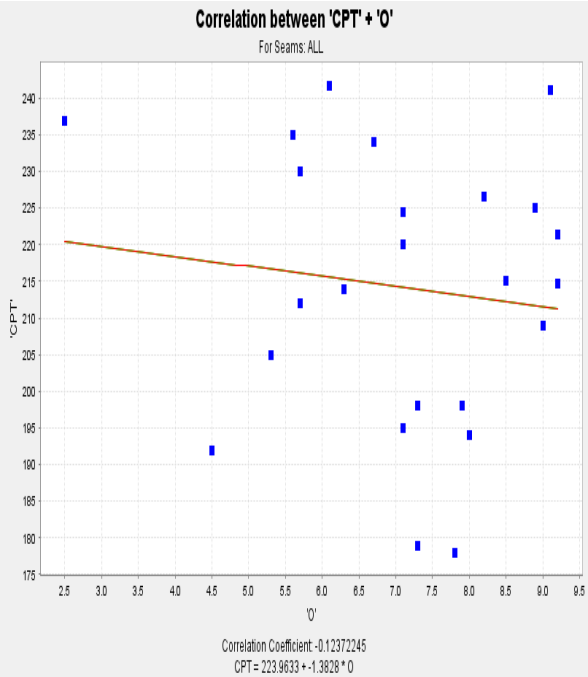


Figure 5.16: Correlation between CPT and O

Increasing hydrogen content significantly reduces CPT. The increase of % weight gain (WT) with hydrogen indicates unstable peroxy complexes rather than stable peroxy complexes are being formed. A very small negative relationship is seen between O and CPT.

A 'critical moisture content' (20-25%) is reported by some authors while some report a value of 7%. The IM in the study area ranges between 2-5% and shows a reduction in CPT as the IM increases. Below the 'critical moisture content' oxidation is increases with the formation of peroxides and above this temperature oxidation is reduced because oxygen molecules must diffuse through water. Higher disseminated mineral matter similarly acts as a barrier to oxidation as shown by the AS/CPT correlations.

5.1.5 Petrographic correlations

No correlation was observed between abnormal condition (AB) and any of the other 34 variables. The samples were not subject to rewetting and associated heat production and the laboratory results will not therefore simulate natural conditions (Rosemary Falcon, commentary)

Total reactives (TR) showed moderate to strong correlation with the chemical variables, GLI and CPT. Vitrinite reflectance only showed correlation with T2 (peak temperature).The correlation between Fe_2O_3 and TR was unique and possibly anomalous. None of the other ash oxides showed correlations to thermal or petrographic variables. Some of the petrographic correlations are shown in Figures 5.17-5.21.

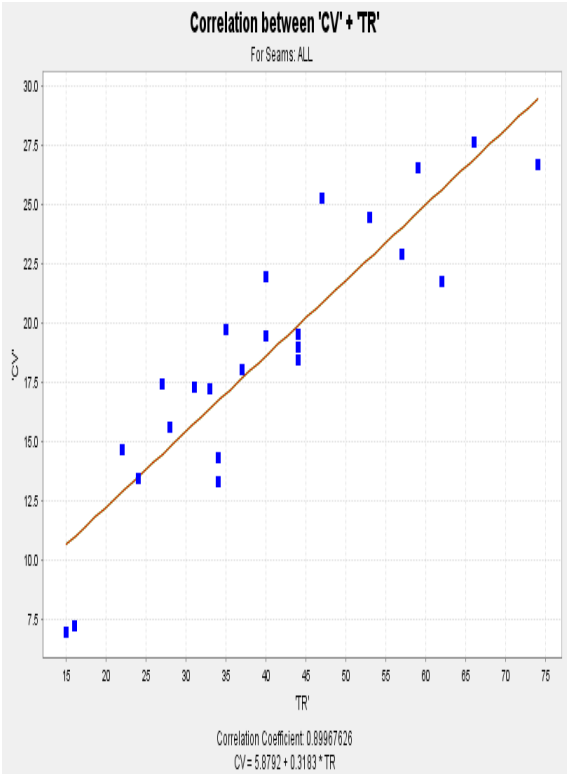


Figure 5.17: Correlation between CV and TR

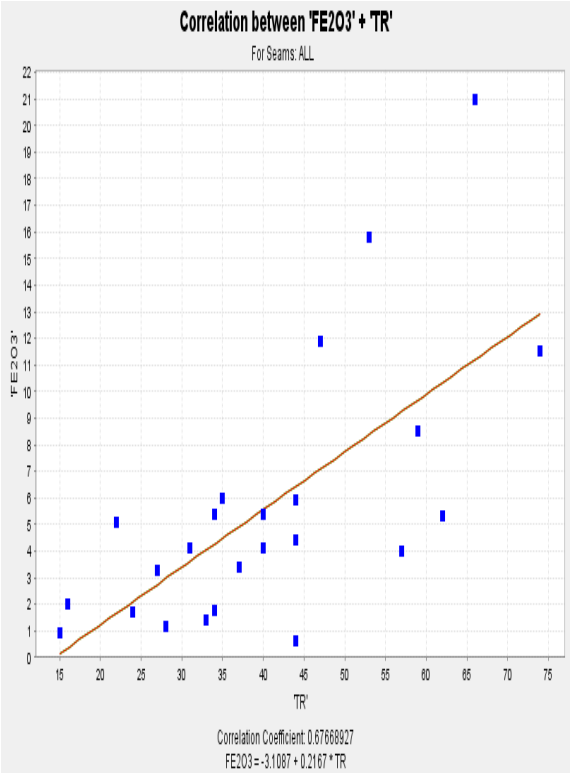


Figure 5.18: Correlation between Fe2O3 and TR

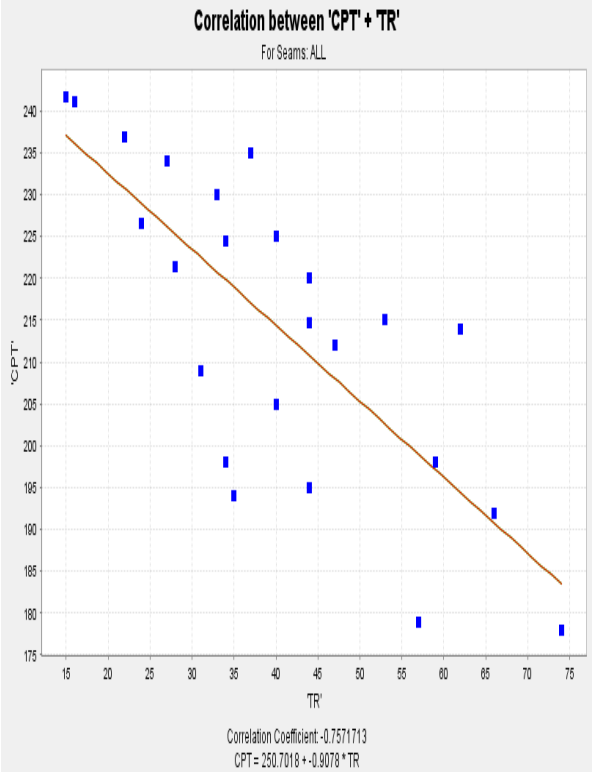


Figure 5.19: Correlation between CPT and TR

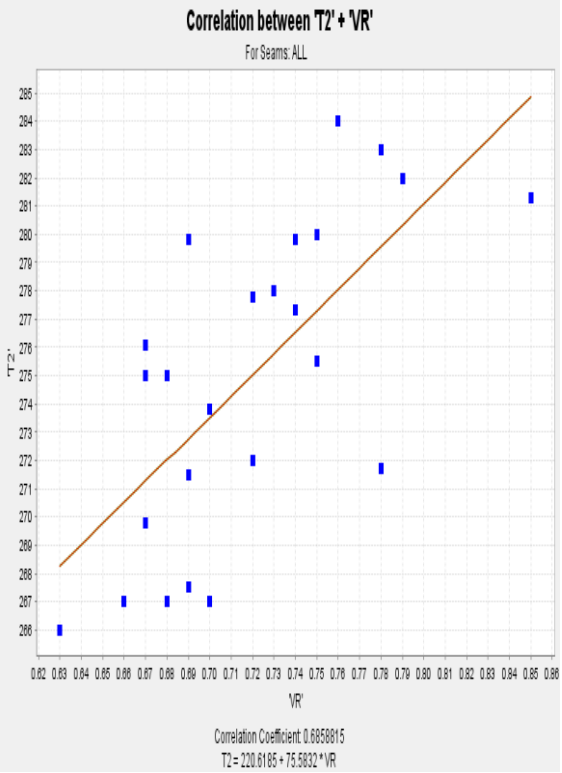


Figure 5.20: Correlation between T2 and VR

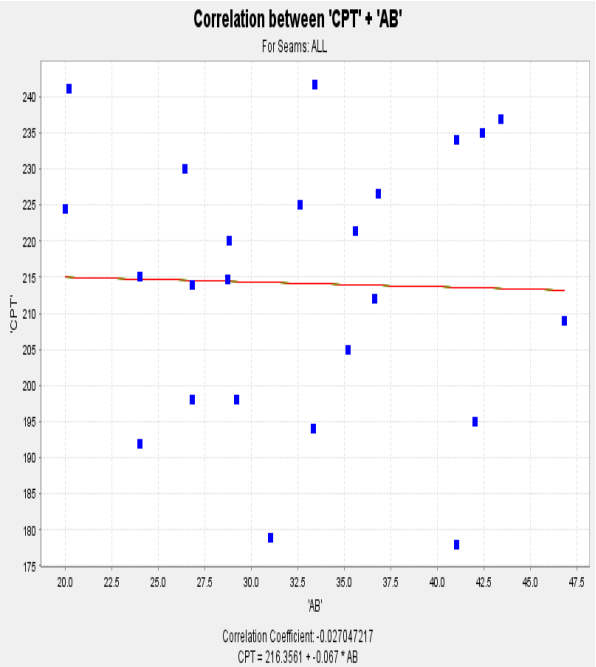


Figure 5.21: Correlation between CPT and AB

An almost linear relation is shown between reactive macerals and CV. The elemental Fe shows good positive correlation with TR. TR does not however correlate with the different forms of sulphur. Total reactive maceral content clearly reduces the CPT and promotes sponcom. Increasing VR appears to increase peak temperature and CPT although the scatter is high (thereby reduces sponcom liability). The vitrinite reflectance is thought to be more significant than the actual amount of vitrinite in determining sponcom liability. AB shows no correlation to CPT and could not be used as an indicator of sponcom liability.

5.1.6 Geological correlations

No correlation was found between geological and thermal or chemical factors (Figure 5.22-5.23). Thicker seams are more prone to sponcom as are shallow seams with structures connecting them to increased air-flow and oxygenation. Dykes and faults have not been included into the sponcom model but will likely have a localised self-heating effect on the coal seams when mining close to these features. The influence of partings and mudstone roof/floor bands can only be known once mining starts and no measurable correlations are possible between these geological features and sponcom liability.

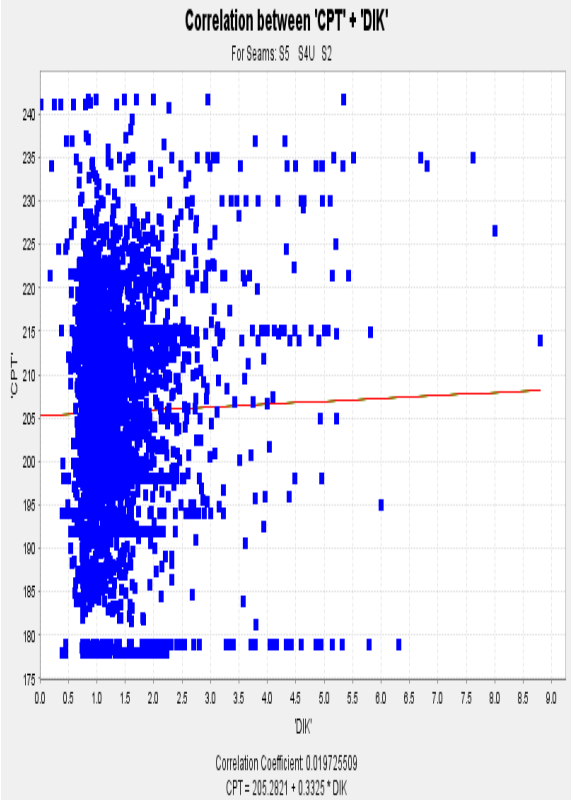


Figure 5.22: Correlation between CPT and seam thickness

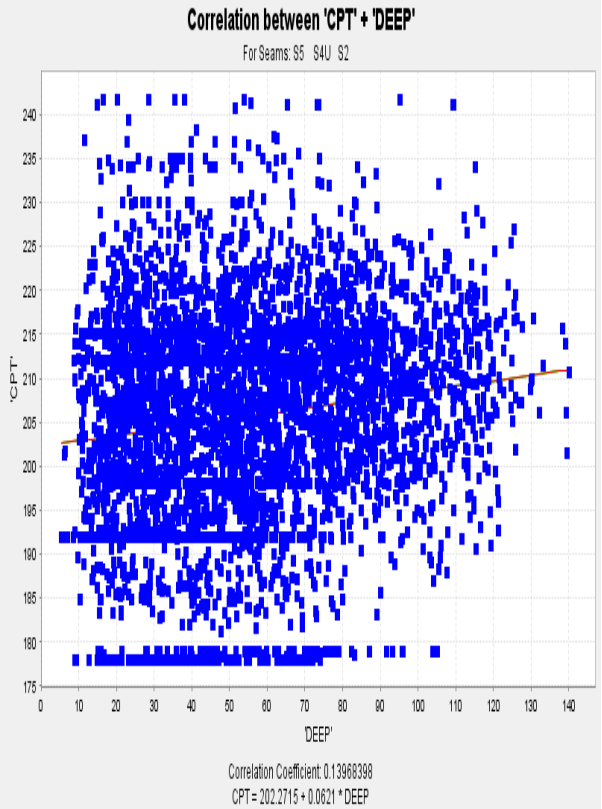


Figure 5.23: Correlation between CPT and seam depth

Thicker seams are more prone to sponcom but no correlation to thermal or chemical test results are evident. Seam thickness factor may only be significant when mining begins. Very deep seams (>400m) and shallow seams (<40m) are more prone to sponcom. As with seam thickness this factor may only become significant when mining begins.

Table 5.2: Cross correlation of all sample database variables - blue shade >80% correlation , green shade >70% correlation and yellow shade >50% correlation

		1	2	3	4	5	6	7	8	9	10	11	12	13	14	15	16	17	18	19	20	21	22	23	24	25	26	27	28	29	30	31	32	33	34	35	
		AB	Al2O3	Ash	Carbon	CaO	CPT	CV	Der Wt	FC	Fe2O3	GLI	H	IM	K2O	MGO	MNO	MS	N	Na2O	O	OS	P2O5	PS	RD	SiO2	SO3	SS	Tstart	Tpeak	TiO2	TR	TS	VM	VR	WT	
1	AB	1.00																																			1
2	Al2O3	-0.06	1.00																																		2
3	Ash	-0.05	0.26	1.00																																	3
4	Carbon	0.04	-0.28	-0.99	1.00																																4
5	CaO	-0.22	-0.43	-0.24	0.22	1.00																															5
6	CPT	-0.03	0.08	0.67	-0.63	-0.19	1.00																														6
7	CV	0.01	-0.28	-0.99	0.99	0.23	-0.69	1.00																													7
8	Der Wt	0.26	0.03	-0.27	0.30	-0.08	-0.26	0.27	1.00																												8
9	FC	0.06	-0.21	0.98	0.98	0.27	-0.61	0.97	0.32	1.00																											9
10	Fe2O3	-0.13	-0.59	-0.70	0.72	0.34	-0.51	0.73	0.14	0.64	1.00																										10
11	GLI	0.12	0.04	-0.78	0.77	0.26	-0.46	0.75	0.23	0.79	0.46	1.00																									11
12	H	0.16	-0.32	-0.95	0.95	0.19	-0.59	0.94	0.31	0.92	0.63	0.71	1.00																								12
13	IM	0.16	0.00	-0.78	0.74	0.33	-0.59	0.73	0.02	0.79	0.36	0.71	0.66	1.00																							13
14	K2O	0.35	-0.49	-0.05	0.04	0.09	-0.06	0.02	-0.24	-0.06	0.19	0.03	0.10	0.16	1.00																						14
15	MGO	0.36	0.30	-0.26	0.26	-0.20	-0.07	0.20	0.44	0.32	-0.31	0.25	0.37	0.35	-0.08	1.00																					15
16	MNO	-0.13	0.03	-0.20	0.17	0.40	-0.46	0.21	0.15	0.20	0.15	0.10	0.22	0.16	-0.18	-0.09	1.00																				16
17	MS	0.20	-0.31	-0.46	0.46	-0.04	-0.51	0.48	0.42	0.43	0.50	0.32	0.43	0.23	0.00	-0.06	0.00	1.00																			17
18	N	0.21	-0.22	-0.91	0.92	0.11	-0.53	0.91	0.45	0.89	0.62	0.75	0.94	0.62	0.05	0.46	0.10	0.45	1.00																		18
19	Na2O	-0.22	0.19	0.07	-0.08	0.24	0.09	-0.11	-0.18	-0.06	-0.20	0.13	-0.11	0.19	0.04	0.15	-0.05	-0.29	-0.04	1.00																	19
20	O	-0.17	0.26	0.16	-0.26	0.20	-0.12	-0.15	-0.45	-0.17	-0.26	-0.16	-0.29	0.08	-0.04	-0.12	0.23	-0.48	-0.27	0.22	1.00																20
21	OS	0.35	-0.11	-0.23	0.17	0.13	-0.58	0.23	-0.10	0.14	0.20	0.18	-0.21	0.41	0.61	-0.03	0.16	0.26	0.14	0.10	0.25	1.00															21
22	P2O5	-0.12	0.38	-0.32	0.33	-0.08	0.06	0.29	0.11	0.39	-0.07	0.34	0.29	0.29	-0.19	0.38	-0.01	-0.15	0.29	-0.09	-0.04	-0.14	1.00														22
23	PS	0.20	-0.31	-0.46	0.47	-0.04	-0.49	0.49	0.43	0.44	0.50	0.32	0.44	0.23	0.00	-0.05	-0.01	1.00	0.46	-0.12	-0.50	0.24	-0.22	1.00													23
24	RD	-0.07	0.25	0.99	-0.99	-0.25	0.67	-0.98	-0.27	0.98	-0.68	-0.78	0.94	-0.79	-0.05	-0.27	-0.20	-0.45	-0.91	0.22	0.16	-0.24	-0.34	-0.46	1.00												24
25	SiO2	0.28	-0.49	0.47	-0.44	-0.31	0.47	-0.45	-0.21	-0.51	-0.25	-0.57	-0.32	-0.56	0.37	-0.14	-0.43	-0.01	-0.37	-0.28	-0.21	-0.10	-0.42	0.00	0.47	1.00											25
26	SO3	-0.04	-0.37	-0.40	0.41	0.02	-0.12	0.40	0.20	0.38	0.22	0.09	0.46	0.21	0.02	0.09	0.11	0.21	0.34	-0.31	-0.15	0.02	0.02	0.22	-0.40	0.09	1.00										26
27	SS	-0.05	-0.02	0.00	-0.06	0.31	-0.50	0.05	-0.15	-0.05	0.04	-0.04	0.01	0.07	0.06	-0.17	0.34	0.11	-0.09	0.13	0.43	0.57	-0.22	0.09	0.00	-0.11	-0.21	1.00									27
28	Tstart	-0.25	0.08	0.60	-0.59	-0.17	0.21	-0.58	-0.15	-0.65	-0.20	-0.62	-0.51	-0.64	0.07	-0.26	-0.01	-0.22	-0.52	0.04	0.11	-0.09	-0.34	-0.27	0.63	0.22	-0.40	0.10	1.00								28
29	Tpeak	0.33	0.02	0.00	0.02	0.17	0.18	-0.05	0.31	0.10	0.00	0.26	-0.09	0.22	-0.07	0.19	-0.13	0.08	0.06	0.32	-0.26	-0.19	0.07	0.08	-0.02	-0.15	-0.03	-0.47	-0.44	1.00							29
30	TiO2	-0.01	-0.03	-0.15	0.20	-0.17	0.14	0.18	0.18	0.20	0.19	-0.01	0.17	-0.15	-0.21	0.12	-0.18	-0.14	0.20	-0.29	-0.22	-0.37	0.46	-0.12	-0.14	-0.03	-0.15	-0.27	-0.04	0.02	1.00						30
31	TR	-0.16	-0.18	-0.88	0.87	0.13	-0.76	0.90	0.14	0.79	0.68	0.64	0.83	0.61	0.09	0.06	0.24	0.38	0.76	-0.19	-0.05	0.32	0.15	0.38	-0.86	-0.46	0.35	0.04	-0.31	-0.34	0.06	1.00					31
32	TS	0.04	-0.09	-0.02	0.02	0.09	-0.46	0.06	0.45	-0.01	0.25	-0.06	0.02	-0.18	-0.04	-0.30	0.64	0.44	0.01	-0.15	-0.12	0.21	-0.24	0.43	-0.03	-0.14	-0.04	-0.03	0.24	-0.08	-0.14	0.13	1.00				32
33	VM	0.00	-0.35	-0.90	0.89	0.13	-0.70	0.92	0.14	0.80	0.75	0.67	0.89	0.59	0.25	0.08	0.18	0.46	0.84	-0.22	-0.13	0.37	0.11	0.46	-0.89	-0.30	0.39	-0.08	-0.37	-0.23	0.06	0.95	0.10	1.00			33
34	VR	0.47	-0.05	0.23	-0.21	-0.04	0.16	-0.26	-0.07	-0.18	-0.10	-0.04	-0.30	0.04	0.13	-0.05	-0.15	-0.06	-0.23	0.22	-0.18	-0.05	-0.32	-0.06	0.20	0.19	-0.21	0.53	-0.16	0.69	-0.01	-0.40	-0.03	-0.30	1.00		34
35	WT	0.16	-0.21	-0.81	0.82	0.07	-0.42	0.81	0.33	0.84	0.38	0.58	0.83	0.53	-0.18	0.34	0.18	0.42	0.75	-0.40	-0.28	-0.05	0.42	0.43	-0.82	-0.19	0.49	0.03	-0.68	0.02	0.33	0.62	-0.02	0.65	-0.16	1.00	35
		1	2	3	4	5	6	7	8	9	10	11	12	13	14	15	16	17	18	19	20	21	22	23	24	25	26	27	28	29	30	31	32	33	34	35	

Table 5.3: Cross correlation of all modelling database variables - blue shade >80% correlation , green shade >70% correlation and yellow shade >50% correlation

		1	2	3	4	5	6	7	8	9	10	11	12	13	14	15	16	17	18	19	20	21	22	23	24	25	26	27	28	29	30	31	32	33	34	35	
		AB	Al2O3	Ash	Carbon	CaO	CPT	CV	Der Wt	FC	Fe2O3	GLI	H	IM	K2O	MGO	MNO	MS	N	Na2O	O	OS	P2O5	PS	RD	SiO2	SO3	SS	Tstart	Tpeak	TiO2	TR	TS	VM	VR	WT	
1	AB	1.00																																			1
2	Al2O3	0.13	1.00																																		2
3	Ash	0.10	0.47	1.00																																	3
4	Carbon	-0.13	-0.49	-0.97	1.00																																4
5	CaO	-0.24	-0.37	0.03	-0.04	1.00																															5
6	CPT	-0.08	0.08	0.66	-0.62	0.16	1.00																														6
7	CV	-0.11	0.49	-0.98	0.99	-0.04	-0.67	1.00																													7
8	Der Wt	0.26	0.34	-0.03	0.05	-0.41	-0.25	0.03	1.00																												8
9	FC	-0.09	-0.36	-0.88	0.86	0.05	-0.57	0.88	0.05	1.00																											9
10	Fe2O3	-0.33	-0.69	-0.78	0.82	0.07	-0.45	0.80	-0.01	0.64	1.00																										10
11	GLI	-0.13	-0.08	-0.61	0.62	0.22	-0.45	0.62	-0.01	0.63	0.50	1.00																									11
12	H	0.09	-0.47	-0.91	0.92	0.00	-0.61	0.92	-0.06	0.81	0.62	0.55	1.00																								12
13	IM	0.00	-0.13	-0.37	0.28	0.01	-0.19	0.29	0.00	0.24	0.20	0.16	0.29	1.00																							13
14	K2O	0.32	-0.50	-0.27	0.27	0.08	-0.30	0.28	-0.25	0.18	0.40	0.35	0.33	0.05	1.00																						14
15	MGO	0.47	0.54	0.05	-0.05	-0.29	-0.07	-0.06	0.35	0.03	0.54	-0.11	0.14	0.03	-0.37	1.00																					15
16	MNO	-0.10	0.10	0.01	-0.03	0.41	-0.21	-0.02	-0.13	0.00	0.19	-0.03	0.16	0.05	-0.26	0.18	1.00																				16
17	MS	-0.14	-0.24	-0.56	0.56	-0.36	-0.64	0.57	0.40	0.45	0.62	0.30	0.38	0.12	0.20	-0.18	-0.26	1.00																			17
18	N	0.03	-0.42	0.94	0.96	-0.15	-0.64	0.96	0.16	0.83	0.75	0.60	0.93	0.27	0.31	0.09	-0.06	0.58	1.00																		18
19	Na2O	-0.06	0.28	0.22	-0.24	0.16	0.05	-0.23	-0.04	-0.17	-0.21	0.14	-0.28	-0.10	0.06	0.09	-0.08	-0.11	-0.19	1.00																	19
20	O	0.13	0.23	0.39	-0.49	0.49	0.12	-0.41	-0.46	-0.30	-0.54	-0.12	-0.27	-0.06	0.00	0.09	0.44	-0.66	-0.48	0.22	1.00																20
21	OS	0.25	0.00	-0.29	0.23	0.06	-0.70	0.29	-0.04	0.25	0.18	0.44	0.31	0.10	0.64	-0.03	0.15	0.34	0.28	0.10	0.21	1.00															21
22	P2O5	0.08	0.42	0.04	0.07	-0.04	0.21	0.03	0.19	0.15	-0.19	0.16	0.10	0.05	-0.35	0.46	0.04	-0.33	0.06	-0.09	-0.04	-0.24	1.00														22
23	PS	-0.15	-0.25	-0.56	0.57	-0.37	-0.63	0.58	0.40	0.45	0.63	0.29	0.38	0.13	0.19	-0.18	-0.26	1.00	0.58	-0.12	-0.68	0.31	-0.32	1.00													23
24	RD	0.11	0.48	0.97	-0.95	0.04	0.65	-0.96	-0.02	-0.84	-0.78	-0.58	-0.89	-0.35	-0.27	0.06	0.01	-0.55	-0.92	0.22	0.39	-0.27	-0.02	-0.56	1.00												24
25	SiO2	0.31	-0.42	0.26	-0.27	-0.20	0.37	-0.26	-0.28	-0.31	-0.19	0.58	-0.13	-0.07	0.24	-0.09	-0.28	-0.12	-0.23	-0.28	-0.04	-0.25	-0.42	-0.11	0.25	1.00											25
26	SO3	-0.26	-0.58	-0.53	0.56	-0.05	-0.28	0.54	-0.16	0.42	0.46	0.00	0.55	0.16	0.11	-0.09	0.11	0.39	0.51	-0.31	-0.32	0.02	-0.36	0.40	-0.53	0.28	1.00										26
27	SS	0.30	0.17	0.05	-0.16	0.33	-0.37	-0.07	-0.19	-0.01	-0.33	0.07	0.11	0.05	0.17	0.25	0.52	-0.23	-0.11	0.13	0.67	0.60	-0.02	-0.25	0.05	-0.12	-0.20	1.00									27
28	Tstart	-0.04	0.31	0.58	-0.58	-0.17	0.13	-0.58	0.11	-0.58	-0.33	-0.39	-0.54	-0.19	0.06	-0.14	-0.04	-0.10	-0.52	0.04	0.15	0.07	-0.19	-0.11	0.55	0.10	-0.41	0.10	1.00								28
29	Tpeak	-0.10	0.05	0.07	-0.02	0.10	0.18	-0.06	0.47	-0.04	0.20	0.12	-0.29	-0.07	-0.17	-0.12	-0.34	0.20	-0.04	0.32	-0.36	-0.25	0.13	0.20	0.06	-0.36	-0.21	-0.47	-0.20	1.00							29
30	TiO2	0.10	0.01	0.13	0.16	-0.17	0.27	0.12	0.22	0.14	0.06	-0.14	0.15	0.07	-0.27	-0.21	-0.20	-0.26	0.14	-0.29	-0.27	-0.50	0.69	-0.25	-0.12	-0.01	-0.24	-0.27	-0.15	0.12	1.00						30
31	TR	-0.12	-0.39	-0.88	0.88	0.15	-0.78	0.90	-0.05	0.76	0.72	0.62	0.85	0.25	0.44	-0.14	0.00	0.57	0.86	-0.19	-0.31	0.47	-0.16	0.57	-0.86	-0.21	0.52	0.04	-0.31	-0.31	-0.10	1.00					31
32	TS	-0.05	-0.26	-0.52	0.81	-0.08	-0.39	0.55	0.03	0.37	0.44	0.31	0.51	0.15	0.15	-0.02	0.00	0.33	0.53	-0.15	-0.24	0.16	-0.02	0.34	-0.53	-0.12	0.32	-0.03	-0.29	-0.07	0.06	0.51	1.00				32
33	VM	-0.10	-0.47	-0.83	0.80	-0.12	-0.57	0.82	-0.01	0.48	0.73	0.40	0.75	0.30	0.29	-0.12	-0.02	0.52	0.79	-0.22	-0.38	0.24	-0.09	0.53	-0.82	-0.12	0.51	-0.08	-0.40	-0.08	0.07	0.76	0.59	1.00			33
34	VR	0.15	-0.04	0.21	-0.13	-0.15	0.23	-0.19	0.35	-0.22	0.10	-0.20	-0.36	-0.12	-0.05	-0.17	-0.42	0.10	-0.17	0.22	-0.38	-0.34	-0.09	0.10	0.19	0.05	0.20	0.53	-0.07	0.78	0.24	0.34	-0.12	-0.13	1.00		34
35	WT	0.16	-0.25	-0.65	0.67	-0.08	-0.30	0.65	0.03	0.64	0.23	0.20	0.78	0.24	-0.15	0.43	0.21	0.10	0.64	-0.40	-0.24	-0.13	0.39	0.12	-0.63	0.02	0.45	0.03	-0.64	-0.28	0.47	0.48	0.36	0.48	-0.26	1.00	35
		AB	Al2O3	Ash	Carbon	CaO	CPT	CV	Der Wt	FC	Fe2O3	GLI	H	IM	K2O	MGO	MNO	MS	N	Na2O	O	OS	P2O5	PS	RD	SiO2	SO3	SS	Tstart	Tpeak	TiO2	TR	TS	VM	VR	WT	

5.2 Combined Risk Matrix

The overall risk matrix was calculated on a full seam basis by combining the following 15 variable scores (Table 5.4), each variable having a score of 0, 1 or 2 (low-mod-high probability). Banerjee (1981) evaluated sponcom risk by the equation:

Risk = geological factor * mining factor *coal factor

The risk rating at this stage is biased toward coal and geological factors with mining factor excluded until this data becomes available. Risk rating is relative and results cannot be compared or extrapolated to other collieries without a significantly increased laboratory database. The sponcom risk for the current pillar area and total mine areas are compared in Table 5.5-5.6 and the results do not differ significantly. This comparison is included as the future resources may be mined by bord and pillar and then extracted by opencast methods.

Table 5.4: Variables used in risk matrix model

Coal factor			Geological factor	Mining factor
Chemical	Petrographic	Thermal	Geological	Mining
AS	AB	CPT	ST	not used
VM	TR	T2	TO	
IM	VR	GLI	MST	
TS		WT		

The risk matrix values for the pillar area and total mine are shown in tables 8.6 and 8.7 below.

Table 5.5: Risk matrix values for the total mine area on a seam basis.

Total Mine Risk Matrix					
Seam	Coal Factor			Geological Factor	
	Thermal Matrix	Chemical Matrix	Petrographic Matrix	Geological Matrix	Total Matrix
S5	4.56	6.8	3.66	0.43	15.41
S4U	3.63	2.6	2.68	1.15	10.05
S2	3.84	2.85	2.86	1.12	10.61

Table 5.6: Risk matrix values for the pillar area on a seam basis.

Pillar Area Risk Matrix					
Seam	Coal Factor			Geological Factor	
	Thermal Matrix	Chemical Matrix	Petrographic Matrix	Geological Matrix	Total Matrix
S5	4.56	6.76	3.62	0.29	15.2
S4U	2.77	2.59	2.59	1.12	10.05
S2	3.84	3.08	2.87	1.21	10.96

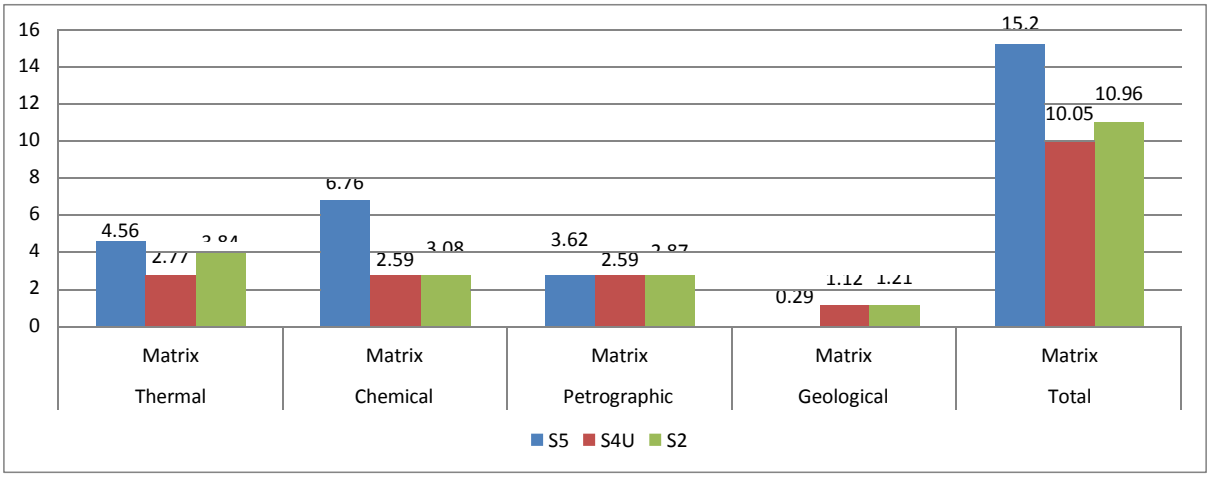


Figure 5.24: Histogram of matrix scores per sponcom factor and seam in the mined out pillar area

The S5 seam has the highest overall risk rating of the 3 seams for the pillar area and unmined areas. The high VM and TS resulted in a high score (6.76) from the chemical variables. Petrographic factors were also high in the S5 (3.62) as were the thermal factors (4.56).The geological factors however had the lowest influence on the S5 seam due to the general absence of parting and the seam being relatively thin. When mining proceeds it is thought that the mining factor will also be less influential for the S5 seam as there has been no previous underground mining. Other factors such as ventilation, mining rate and fines etc. will be more evident when mining the S4U and S2. Figure 5.25 indicates widespread and fairly even sponcom liability in the S5 seam.

The S4U seam ranks lowest on the overall sponcom matrix score at 10.05 points and only has a higher rating on the geological scale compared to the S5 seam. The S4U seam has the highest ash content of the seams and scores relatively low on the thermal and chemical tests. Thick mudstone bands are common in the SE areas of the mine and these will likely impact the sponcom liability during mining. Figure 5.26 shows slightly localized increase in sponcom liability of the S4U seam in the north-central corner of the lease area. The remaining S4U areas show relatively low sponcom liability.

The S2 seam ranked second in sponcom liability after the S5 seam and shows distinct zoning between the northern and southern areas of the mine (Figure 5.27). This is linked mainly to the thermal and chemical indices. The unmined areas have a similar risk rating to the mined out areas for all the seams.

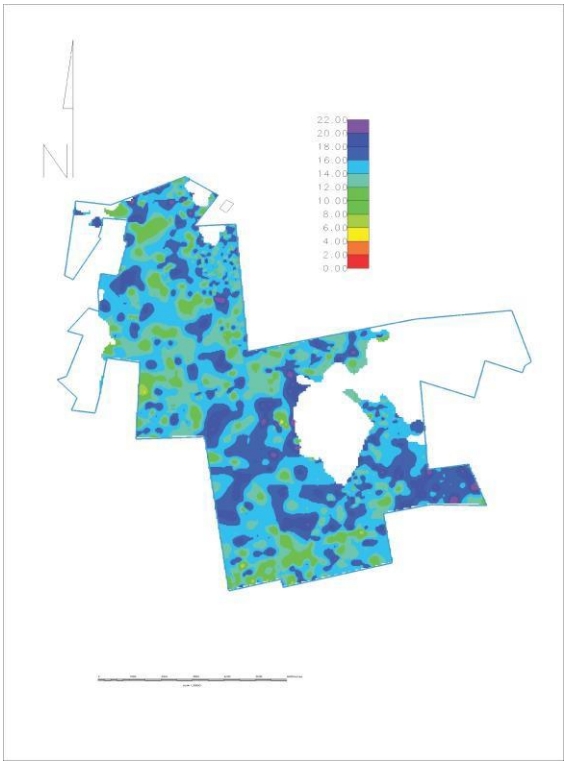


Figure 5.25: No.S5 seam combined factor sponcom risk matrix

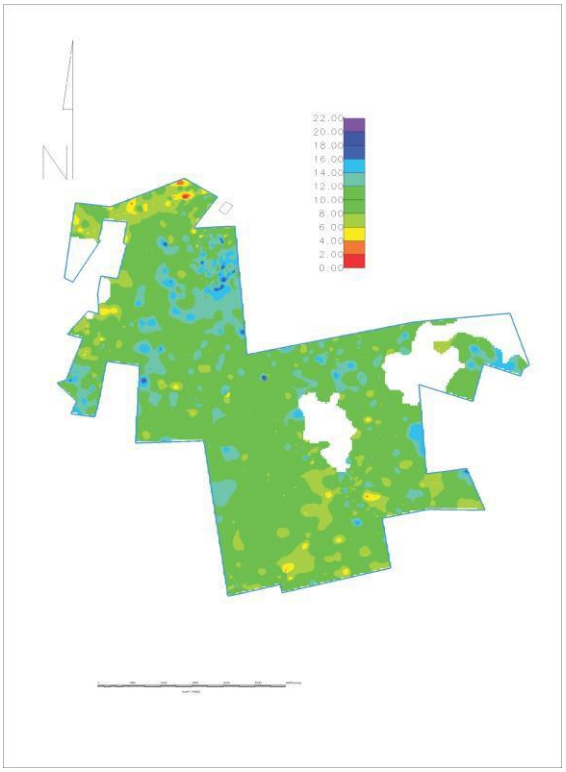


Figure 5.26: No.S4U seam combined factor sponcom risk matrix

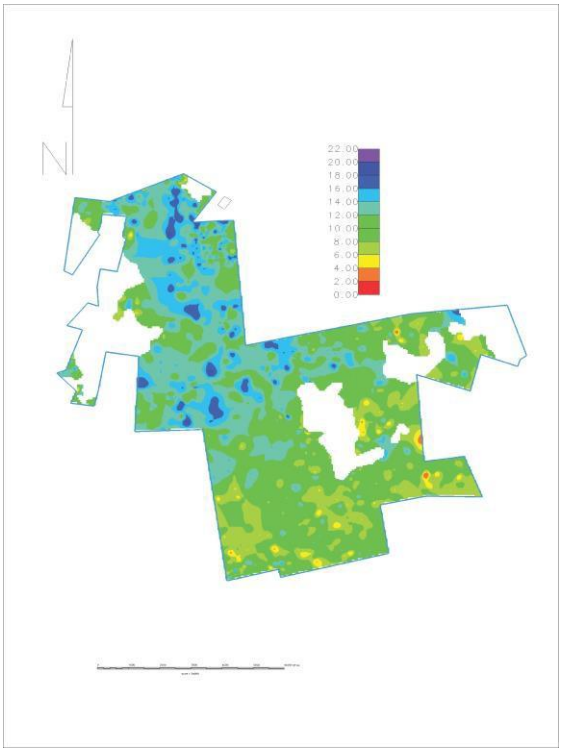


Figure 5.27: No. S2 seam combined factor sponcom risk matrix

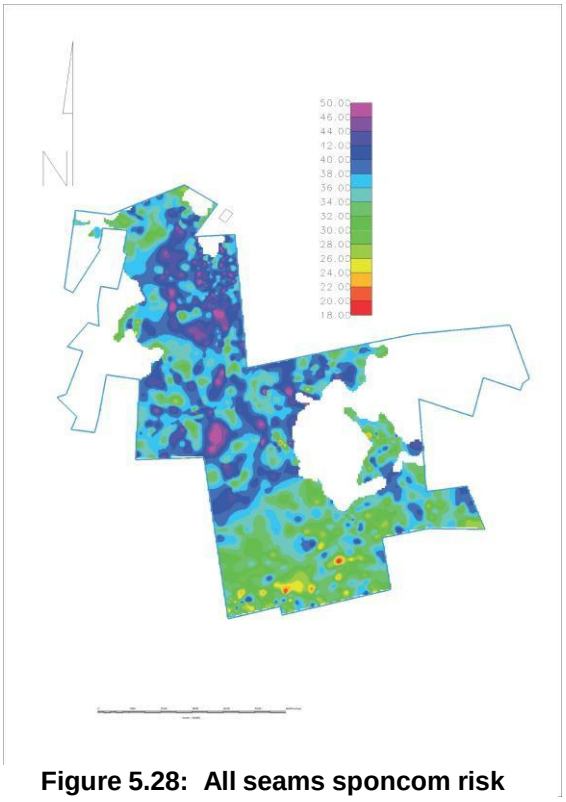


Figure 5.28: All seams sponcom risk matrix

The scale is relative and dark blue shade is widespread indicating high sponcom liability. A significant reduction in sponcom liability is noted with uniform green shades covering the area. The northern area of the S2 seam shows sponcom liability similar to that of the S5 seam whereas the southern area resembles the S4U seam index rating. The northern and central portions of the mine are most at risk for sponcom. The strip ratios are lower in these regions compared to the southern areas where seams are 120-140m deep.

In summary the results that have been acquired have been presented in a new way and possibly take the elusive problem of sponcom prediction another step closer. A protocol that is possible of making reliable sponcom predictions is certainly assisted by a more graphical approach and the method used enables sponcom to be modelled in a similar fashion to a coal resource.

6 CONCLUSION

6.1 General Conclusions

The prediction of sponcom in a mining environment remains a challenge but can be a useful tool and add value to collieries where this phenomenon occurs. No exact methodology or standard exists to predict self-heating of coal but many tests are available that can be used in isolation or in combination with each other to create indices that vary in complexity. The fact that sponcom is multifactorial in its origins suggests that by using a wide variety of testing methods a more meaningful evaluation of its occurrence is possible. This was the purpose of this investigation.

Based on the results of the work undertaken the following main conclusions can be made. This particular case study made use of 2 exploration boreholes placed in the North and South of the area. Extensive physical, chemical and petrographic analysis was undertaken on 22 subsamples and 2 ROM samples. The results were extrapolated to the existing samples in the geological model enabling a “sponcom model” analogous to a “geological model” to be created. The method used in this study is not known to have been used on other collieries in the Witbank Coalfield and all results are interpreted in a relative manner. The slight bias to using coal factors in the indices’ means that the model can be expanded and improved on when the mining and geological factors are better understood.

Cross correlations between 35 thermal and chemical variables are tabled in the text. Some correlations are not logical or meaningful but those that are established in theory were used for modelling of the sponcom liability index. A total of 15 variables were modelled including some geological factors to produce contour plans of individual and combined variables. Ultimately a two dimensional sponcom risk-matrix was created that shows spatial variation for each seam.

6.2 Predictive methods to estimate the potential of coal to spontaneous combustion

6.2.1 Thermal properties

Three thermal testing methods were used to determine sponcom liability of drillcore samples. CPT results were more consistent than in the other methods. TGA produced some results that are contrary to theory, especially regarding the percentage weight gained. The oxygen absorption tests provide a simple and rapid method of obtaining sponcom potential and could be applied at site laboratories with minimal cost. Only Fe_2O_3 from the ash analysis showed a weak correlation with CPT and GLI. The correlation between the thermal methods was generally poor but the thermal methods generally correlated well with the chemical variables known to effect sponcom.

The thermal tests if performed at one laboratory may have produced more conformable results and some of the variations, notably from TGA theory may be justifiable.

6.2.2 Chemical properties

The chemical variables known to effect sponcom i.e. AS, VM, IM, and TS correlated fairly well with CPT and GLI, but moderately with TGA (T1 and WT). Ultimate oxygen slightly decreased oxygen absorption (GLI) and CPT confirming theory that if chemically bound to the coal structure it reduces the chance of further oxidation. The pyrite theory has many opponents and proponents in literature. The current dataset suggests that TS does reduce CPT and T2, although not significantly. TS has a negligible effect on GLI or WT. All the forms of S showed moderate correlation with CPT but not GLI or TGA tests.

Nitrogen has been found by (Kaymackci and Didari, 2000) to be important in multivariate regression. N_2 shows contradictory results and promotes oxygen absorption (GLI) and reduces CPT, thereby favouring sponcom. In the TGA test N_2 increases with WT and reduces sponcom liability according to theory.

6.2.3 Petrographic properties

The No.2 and No.4 seams are enriched in inertinite and oxidation of aromatic compounds is unlikely to progress at low temperatures. The No.5 seam is vitrinite rich with high aromaticity, and may form oxygenated complexes that will decompose and liberate heat to drive spontaneous combustion.
Liptinite and vitrinite are both reactive macerals and support spontaneous combustion. The dataset occurs in a narrow rank band and increasing vitrinite content would support increasing sponcom liability as the rank of the samples are similar.

The reactivity of coals of similar rank is related to differences in ash and inertinite contents. As rank increases combustion reactivity decreases and vitrinite reflectance increases, although the relationship is not linear. AB did not correlate with any of the other test variables but in theory would indicate the presence of intrusion or ground movement that would increase sponcom propensity.

6.2.4 Mining and Geological factors

The geological factors had no significant correlation to the thermal or chemical variables. The shallow seams <40m are very limited in area and connection paths with the surface allowing air and moisture to migrate to mined-out areas has a minimal influence on the overall sponcom index. Roof and floor mudstones >2m, as well as in-seam mudstone partings >2m were modelled and given a weighting slightly lower than the chemical and thermal variables. Thick carbonaceous bands are known to be associated with burning coal seams but the exact mechanism is not understood. A possible explanation is the fairly high content of volatiles (12-17%) and FC (10-18%) in some rocks. Secondary porosity may also be enhanced by mining activity.

Extrinsic effects such as the mine ambient temperature, relative humidity of the air and the as-mined moisture content of the coal change continuously and their incorporation into a sponcom index still needs to be though out. The generation of fines during mining and friction created by machinery can also contribute to sponcom and are difficult to quantify.

In conclusion, it appears that the acceptability of a method for determining spontaneous heating characteristics of coal mainly depends upon how closely it predicts the spontaneous heating behaviour in the field conditions. The chemical reaction between coal and oxygen at low temperature is complex and remains not well understood despite many years of research. However, in summary, the current research has shown the following:

- The overall results from this research produced potentially useful contour plans of different geological and coal factors effecting sponcom of coal using single variable and combined variable datasets.
- The method is easily reproducible and applicable; the only requirements are a geological modelling package and a sufficient borehole database to which laboratory testing can be extrapolated and modelled.
- The results produced generally tie in with sponcom theory although some of the methods, notably TGA, produced mixed results
- The model is biased to coal factor influences but the model can easily be expanded to include mining factors and is not limited by number of variables that can be modelled

It is hoped that the results obtained could be of use in future mining operations when applied to mines with the potential of extracting (by opencast methods) previously mined underground pillars. The method could be applied to different mines within the Witbank, Highveld and Ermelo Coalfields with a history of sponcom (Klein kopje Colliery, New Vaal Colliery, Middelburg Mines, Landau Colliery and ATCOM Colliery, to name a few).

6.3 RECOMMENDATIONS:

1. Further work should be undertaken to establish the applicability of the approach taken in this research to other coal mining areas, especially those seams with different qualities and different geological factors.

2. The impact of mining factors should be added to the model and formulae derived from these investigations to establish the impact of those factors.

3. Alternative thermal methods could be applied in future studies to possibly reduce inconsistencies in results. The added inputs of professionals in the statistical and physical chemistry disciplines will also assist in interpretation of results.

References

1 A coal mine on fire". The Argus. 1902-04-02

2 Adamus,A.,2002.Reveiw of the use of nitrogen in mine fires.Trans.Inst.Metall.,Sect. A; Number 2:Min.Tech.,111,.A89-A98.

3 Androutsopoulos GP, Linardos ThJ. ,1986.Powder Technol 1986;47:9–15.

4 Ashley,G.H., 1928.Bituminous Coal Fields of Pennsylvania. Pensylvania Geological Series, Fourth Series, Bulletin M6,Part 1.

5 ASTM,2005.D388-05 Standard Classification of Coals by Rank. American Society for Testing and Materials, Book of Standards v 05.06-Gaseous fuels; Coal and Coke. ASTM, West Conshohocken ,PA

6 Avila,C., Wu.,T and Lester,E.,2014.Estimating the spontaneous combustion potential of coals using thermogravimetric analysis, Department of Chemical and Environmental engineering, University of Nottingham, University Park, Nottingham, UK, Energy Fuels 2014 ,28,1765-1773

7 Avila,C.R., 2012. Predicting self-oxidation of coal/biomass blends using thermal and optical methods. Thesis submitted to The University of Nottingham for the degree of Doctor of Philosophy, app 1.

8 Axelson D. E. (1987) Solid state carbon-13 nuclear magnetic resonance, study of Canadian coals. Fuel Process. Technol. 16, 257-278

9 Axelson D. E. (Ed.) (1985) ~3C CP MAS FT NMR spectrum of fossil fuels general survey. In Solid State Nuclear Magnetic Resonance of Fossil Fuels: an Experimental Approach, pp. 181-221. Multiscience, Montreal.).

10 Bailey, J.G., Tate, A., Diessel, C.F.K. and Wall,T.F.,1990.A char morphology system with application to coal combustion. T.F., Fuel, 1990,69, 225-239.

11 Bakker,P.,Church,D.J.,Feuchtwanger,T.F.,Grootenboer,J.,Lee,C.A.,Longshaw,T.G.,1978.Some practical applications of thermal infrared linescanning,Min.Mag.October,398-399,401,403,405,407,409,411,and 413

12 Banerjee SC, Nandy DK, Banerjee DD, Chakravorty RN,1972.. Classification of coal with respect to their susceptibility to spontaneous combustion. Transactions of the Mining Geological and Metallurgical Institute of India 1972;59(2):15-31)

13 Banerjee, N.G. (1975) advances in the science and technology of high temperature carbonization. Journal of Mines, Metals & Fuels, 23 (6). pp. 271-279. ISSN 0022-2755

14 Banerjee, S.C., 1981. Spontaneous combustion of coal and mine fires. Oxford and IBH, Calcutta, New Delhi, 165pp

15 Banerjee, S.C., 1981. Spontaneous combustion of coal and mine fires. Oxford and IBH, Calcutta, New Delhi, 52pp.

16 Banerjee,S.C,(1982),A theoretical design to determination of risk index of spontaneous fires in coal mines. J.Mines, Metals and Fuels,August,p.399.

17 Banerjee,S.C.,1985,Spontaneous combustion of coal and mine fires,CH4,80-85.

18 Banerjee,S.C.,Nandy,D.K.,Banerjee,D.D.,Sen.S.K,(1988) Spontaneous fire risk rating of a colliery proposed to be developed by short wall method of mining, Proc IV International Mine Ventilation Congress, Brisbane, Queensland, Australia, July.

19 Banerjee,SC.,1985.Spontaneous Combustion of Coal and Mine Fires. Oxford and IBH Publishing Company, New Delhi,168 p

20 Banerjee.S.C.,1985.Spontaneous combustion of coal and mine fires p301-320

21 Barve SD, Mahadevan V.,1994. Prediction of spontaneous heating liability of Indian coals based on proximate constituents. In: Proceedings of the 12th International Coal Preparation congress. Cracow, Poland; 1994: p. 557-62

22 Barber,J.,2012.Geological modelling, Gemcom Minex-white paper.

23 Behera.P, and Mohanty.P.G ,2009.Peroxy Complex and Crossing Point Temperature of Talcher Coals - An Adducer to Assess the Spontaneous Combustibility Character #P. G. Department of Geology, Utkal University, Bhubaneswar-751004, India †Department of Mathematics, Sambalpur University, Burla-768019, India (†703, Rameswarpatna, Bhubaneswar-751002, India) Received 24 October, accepted in revised form 7 December 2008J.Sci.Res.1(1),55-60(2009)

24 Bell, F.G., 1996. Dereliction: colliery spoil heaps and their rehabilitation.Environ.Eng.Geoscience.,2, 85-96

25 Bell, F.G., Donnelly, L.J., 2006.Mining and its impact on the environment. Taylor and Francis, Oxford, England, 547p

26 Bell,F.G (a), Bullock, S.E.T. (b),. Ha¨lbich ,T.F.J (c) ,Lindsay, P. (d),2001. Environmental impacts associated with an abandoned mine in the Witbank Coalfield, South Africa.a Department of Geology and Applied Geology, UniÍersity of Natal, Durban, 4041, South Africa b Anglogold, Corporate Field SerÍices, PriÍate Bag X5010, Vaal Reef, 2621, South Africac Gold Fields Ltd., Kloof DiÍision, P.O. Box 190, Western Area, 1780, South Africad CRL Energy Research and Testing, P.O. Box 29415, Christchurch, New Zealand International Journal of Coal Geology 45 _2001. 195–216

27 Berkowitz , N.1979. An introduction to coal technology, New York, Academic Press , 1979, pp.70-75.

28 Berkowitz, N., 1957, On the differential thermal analysis of coal: Fuel, v. 36,no. 3, p. 355–373.

29 Berkowitz,N and Schein,H.G (1950-51) Heat of wetting and spontaneous ignition of coal,Fuel,vol.30,no.4,pp.94-96.

30 Berkowitz,N.(1979) An introduction to coal technology, New York: Academic Press.

31 Bhattacharyya, K.K., 1982. “D” system classification of coals in respect of spontaneous combustion, Journal of Mines, Metals and Fuels, April 1982, PP.185-186

32 Bhattacharyya,K.K.,Hodges,D.J. and Hinsley,F.B. (1969) The influence of humidity on the initial stages of spontaneous heating of coal, The Mining Engineer,Feb.1969,pp.274-284.

33 Bowes, P. C., 1984. Self-heating: Evaluating and Controlling the Hazards, London: Department of the Environment, Building Research Establishment PP. 330-333

34 Brown, M. E., Dollimore, D. and Galwey, A. K. (1980) Reactions in the Solid State, Comprehensive Chemical Kinetics, Vol. 22, (eds. C. H. Bamford and C. F. H. Tipper), Elsevier, Amsterdam.

35 Bullock, S.E.T., Bell, F.G.,(1997) Some problems associated with past mining in the Witbank Coalfield, South Africa.Environ.Geol.,33,61-71

36 Bunnett, R., Burke, P.J., Czechowski, F., 1987. Metalloporphyrins in lignite, coal, and calcite. In: Filby, R.H., Branthaver, J.F. (Eds.), Metal Complexes in Fossil Fuels Geochemistry, Characterization, and Processing. American Chemical Society, Washington, D.C., pp. 173–185.:;

37 Burdukov,A.P., a,b, Popov V.I.,a,b, YusupovT.S., a,c, Chernetskiy,M.Yu. ,b,,. Hanjalic K.,a,d ,a. Novosibirsk State University, Novosibirsk, Russia,b Kutateladze Institute of Thermophysics, SB RAS, Novosibirsk, Russia, c Institute of Geology, SB RAS, Novosibirsk, Russia, d Delft University of Technology, Chem. Eng. Dept., Delft, Autothermal combustion of mechanically-activated micronized coal in a 5 MW pilot-scale combustor. The Netherlands, Fuel 122 (2014) 103–111

38 C.Kim,A.G. (1977) Laboratory studies on spontaneous heating of coal, U.S. Bureau of Mines,(Information Circular 8756)

39 Cadle A.B., Cairncross B., Christie A.D.M. and Roberts D.L.1993 The Karoo Basin of South Africa: type basin for the coal-bearing deposits of southern Africa. International Journal of Coal Geology, 23 (1993) 117-157.

40 Cairncross,B. ,1988. Paleodepositional environments and tectonosedimentary controls of the postglacial Permian coals, Karoo Basin, South Africa. International Journal of Coal Geology, 12 (1989) 365-380.

41 Cairncross,B. ,1990. Tectono-sedimentary settings and controls of the Karoo Basin Permian coals, South Africa. International Journal of Coal Geology, 16 (1990) 175-178

42 Cao, D., Fan, X., Guan, H., Wu, C., Shi, X., Jai, Y., 2007. Geological models of spontaneous combustion in the Wuda coalfield, Inner Mongolia, China. In: Stracher, G.B. (Ed.),Geology of Coal Fires: Case Studies from Around the World: Geological Society of America Reviews in Engineering Geology00802018, XVIII, pp. 23–30..

43 Carr ,A. D. and Williamson, J. E.1990.The relationship between aromaticity, vitrinite reflectance and maceral composition of coals: Implications for the use of vitrinite reflectance as a maturation parameter. British Gas plc, London Research Station, Research and Technology Division, Michael Road, Fulham, London SW6 2AD, U.K.(Received 26 October 1989; accepted 23 April 1990) Advances in Organic Geochemistry 1989Org. Geochem. Vol. 16, Nos 1-3, pp. 313-323, 1990

44 Cassels,C.J.C.,1998.Thermal modeling of underground coal fires in northwest China: University of Dundee, Scotland, Thesis: The Netherlands, International Institute for Geo-Information Science and Earth Observation (ITC) publication 51 (CD-ROM,ITC library)

45 Chaiken, R.F,.Heat balance in in-situ combustion. 1977, U.S Bureau of Mines, RI 8221,11 p.)

46 Chaiken,R.F., Singer,J.M., and Lee,C.K.(1979) Model Coal Tunnel Fires in ventilation flow. U.S. Bureau of Mines Report of Investigations, RI 8355

47 Chandra, D. and Prasad, Y.V.S., 1990. Effect of coalification on spontaneous combustion of coals.Int. J. Coal Geol., 16: 225-229

48 Chandra, D., Behera, P. and Niyogi, C., 1993. Coal petrology and systematics of Gondwana coals in relation to spontaneous combustion. In: Birbal Sahni Centenary Nat. Symp. Gond. Geol. Mag.,Spec. Vol., pp. 262-274

49 Chandra, D., Prasad, Y.V.S., Acharya, H.B., Samsuddin, A.K. and Banerji, K.C., 1987. Spontaneous combustion of the coal seams of the Raniganj coalfieldla thermal study. In: R.M. Singh (Editor), Proc. Nat. Sem. Coal Res. India. Tara Printing Works, Varanasi, pp. 206-214.

50 Chauvin,R.;Lodel,R. and Phillipe,J.L.(1985) Spontaneous combustion of coal, Proceedings 21st International conference of Safety in Mines Research Institutes, Sydney: A.A.Balkema.)

51 Cloke M, Lester E. ,1994.Characterization of coals for combustion using petrographic analysis: a review. Fuel 1994;73:315±20.

52 Coal seam fire.From Wikipedia, the free encyclopedia

53 Coalazi,G.J.,2004.Prevention ,control and /or extinguishment of coal seam fires using cellular grout. In: Stracher,G.B.(Ed).,Coal fires burning around the world :a global catastrophe. Int.J.Coal Geol.44,49-68

54 Philips, H., Uludag, S., Chalebi, K. Prevention and control of spontaneous combustion. Best practice guidelines for surface coal mines in South Africa. Coaltech 2011.p5

55 Cooper,G.,1996.Vitrinite reflectance: Petroleum Exploration Society of Australia

56 Coward, H.F., 1957; "Research on spontaneous combustion in mines-a review",London: Safety in Mines Research Establishment, Ministry of Power,Research Report no, 142.

57 Cray,D., 2010. "Deep Underground, Miles of Hidden Wildfires Rage". Time Magazine.

58 Criddle, S.J (1961) The CO/CO2 ratio and spontaneous combustion, Colliery Guardian, VOL.202, no.5224, June 1961, pp.664-666.

59 Cudmore, J.F. and Sanders, R.H.(1984) Spontaneous combustion of coal, mine fires and interpretation of analyses of mine gases-a literature review, Australian Coal Industry Research Laboratories, Report 84-10

60 Dalla Torre,M.,Mahlmann,R.F.,Ernst,W.G.,1997.Experimental study on the pressure dependence of vitrinite maturation.Geochim.Cosmochim.Acta61,2921-2928

61 Dalverny.L.E and Chaiken,R.F.,1991.Mine fire diagnostics and implementation of WIFE at Renton, PA.US Bureau of Mines,R19363, 42 p.

62 Davidson R. M. (1986) Nuclear magnetic resonance studies of coal. Report No. ICTIS/TR32, IEA, Coal Research, London

63 Didari,V and Kaymakc,I (2000).Relations between Coal Properties and Spontaneous Combustion Parameters.Department of Mining Engineering, Zonguldak Karaelmas University, Turkish J. Eng. Env. Sci.26 (2002) , 59 { 64.

64 Discover,1999.China's on fire. R&D news 20(10),20.

65 Durie, R.A. (Ed.), 1991. The Science of Victorian Brown Coal: Structure, Properties and Consequences for Utilization. Butterworth-Heinemann, Oxford. 750 pp

66 Elbeyli I.Y., Piskin S., 2006.Combustion and pyrolysis characteristics of Tuncbilek lignite; Journal of Thermal Analysis and Calorimetry, Vol.83, 2006. p.721 726

67 Elick, J.M., 2011. Mapping the coal fire at Centralia using thermal infrared imagery. International Journal of Coal Geology (ISSN: 01665162) 87, 197–203

68 Elick,J.M, 2013. The effect of abundant precipitation on coal fire subsidence and its implications in Centralia. Earth and Environmental Sciences, Susquehanna University, 514 University Ave., Selinsgrove, PA 17870, United States International Journal of Coal Geology 105 (2013) 110–119.

69 Ellyett, C.D.,Flemming,A.D.,1974.Thermal infrared imagery of the burning mountain fire. Remote Sens.Environ.3,79-86.

70 Eroglu, H.N. (1992). Factors affecting the spontaneous combustion index, Johannesburg: PH.D. thesis, University of the Witwatersrand

71 Eroglu,H.N.,Gouws, M.J. and Phillips,H.R., 1991. Spontaneous combustion liability contours, Proceedings 12th Scientific and Technical Mining Congress of Turkey, pp. 41-51,Ankara, Turkey.)

72 Faill, R.T., 1999. Paleozoic. In: Schultz, C.H. (Ed.), The Geology of Pennsylvania, Pennsylvania Geological Survey, Special Publication, 1. ISBN: 0818202270, pp. 419–433

73 Falcon, R.M.S., 1989. Macro- and micro-factors affecting coal-seam quality and distribution in southern Africa with particular reference to the No. 2 seam, Witbank coalfield, South Africa. In: P.C. Lyons and B. Alpern (Editors), Peat and Coal: Origin, Facies, and Depositional Models. International Journal of Coal Geology, 12: 681-731.

74 Falcon,R.M.,1986.Spontaneous combustion of the organic matter in discards from the Witbank Coalfield.JS Afr.Inst.Min.Metall.86,243-250

75 Feng,K.K.,Chakravorty,R.N, and Cochraine ,T.S.,(1973) Spontaneous combustion, a coal mining hazard, CIM Bulletin,66(138),October,pp.75-84.

76 Ferrari, B., 1938. Die Entstehung von Grubenbranden nach Untersuchungen auf kohlenpetrographischer Grundlage. Gluckauf, 74: 765-774.

77 Filby, R.H., van Berkel, G.J., 1987. Geochemistry of metal complexes in petroleum, source rocks and coals: an overview. In: Filby, R.H., Branthaver, J.F. (Eds.), Metal Complexes in Fossil Fuels: Geochemistry, Characterization, and Processing. American Chemical Society, Washington, D.C., pp. 2–39..

78 GAI Consultants Inc., 1983. Centralia mine fire assessment drilling and diagnostic monitoring final report. Office of Surface Mining, United States Department of the Interior. (153 pp. (OSM/TR-3/83)).

79 Galle, E. 1910-11 Centralb. f. Bakteriol., Abt. 11, 28, 461-73.

80 Gangopadhyay ,P.K.,2007.Application of remote sensing in coal-fire studies and coal-fire-related emissions, In: Stracher,G.B.(Ed),Geology of coal fires: case studies from around the world ,Reviews in Engineering Geology XVIII. Geological Society of America,Boulder,CO,pp.239-248.the problem becomes how to measure the differences.

81 Gielisch,H.,2007.Detecting concealed coal fires. In: Stracher,G.B.(Ed.),Geology of Coal Fires: Case studies from around the world. Reviews in Engineering Geology XVIII. Geological Society of America,Boulder,pp.199-210.

82 Given, P.H., Miller, R.N., 1987a. The association of major, minor and trace inorganic elements with lignite. II. Minerals, and major and minor elements profiles, in four seams. Geochimica et Cosmochimica Acta 51, 1311–1322

83 Given, P.H., Miller, R.N., 1987b..The association of major, minor and trace elements with lignites. III. Trace elements in four lignites and general discussion of all data from this study. Geochimica et Cosmochimica Acta 51, 1843–1853.,

84 Glasser.D. and Itay.M.,1988.The low temperature oxidation of coal taken near a dolerite intrusion. Department of chemical engineering, University of the Witwatersrand, Johannesburg, Wits. Fuel processing technology,18(1988) 201-208.

85 Glenn B Stracher, Tammy P Taylor, 2004. Coal Fires Burning around the World: a Global Catastrophe International Journal of Coal Geology Volume 59, Issues 1–2, 12 July 2004, Pages 7–1

86 Goldammer, J.G.; Seibert, B. (1989): Natural rain forest fires in Eastern Borneo during the Pleistocene and Holocene, Naturwissenschaften, November 1989, Volume 76, Issue 11, p. 518-520

87 Goodarzi,F.1994.Optical properties of carbonized sporinite in vitrinite/sporinite blends. Fuel 1984,63,820.

88 Gouws , M.J (1987) Crossing-point characteristics and differential thermal analysis of South African coals, Johannesburg: MSc. (Eng) dissertation, University of the Witwatersrand.

89 Gouws, M. ,1992.A spontaneous combustion liability index based on ignition temperature tests and adiabatic calorimetry, Johannesburg: PH.D. thesis, University of the Witwatersrand

90 Graham, J.I., 1914-15. The absorption of oxygen by coal. Part V: The influence on temperature on rates of absorption by different parts of the Barsley Bed. Trans Inst Mine Eng. 48: 521-549

91 Graham,J.I. and Jones.T.D.(1924-25).Spontaneous combustion in the South Wales coalfields,Trans.Inst.Min.Eng.,vol.69,pp.413-427

92 Guan, H.Y. and Zhang, J.M., 1999. Project report, as a contribution to the Sino-Dutch Coal Fire Research Initiative “Coal Fire Environmental Investigations in Rujigou Coalfield of Ningxia Autonomous Region, P.R. China.” Beijing Remote Sensing Corporation (BRSC), Beijing, P.R. China and Shenhua Group Corporation Limited, Beijing, P.R. China.

93 Guney, M, 1971. An adiabatic study of the influence of moisture on the spontaneous heating of coal, CIM Bulletin, 64:138-146.

94 Guney,M.(1968) Oxidation and spontaneous combustion of coal-a review of individual factors part I,Colliery Gaurdian,Jan.26 1968,pp.105-110.

95 Gupta,R.P and Prakash,A.,1998.Reflection aureoles associated with thermal anomalies due to subsurface mine fires in the Jharia Coalfield, India.Int.J. Remote Sens.19(14),2619-2622.

96 Hadden,R. and Rein,G., 2010.Burning and suppression of smoldering coal fires, coal and peat fires, a global perspective,vol1,Chapter 18,pp.319-327.

97 Haiyan.G.,2005. International Research for Sustainable Control and Management. Spontaneous Coal Seam Fires: Mitigating a Global Disaster. International Conference.Beijing,P.R.China,2005,p67-80

98 Hampattsoumiana,E., Nimmo’.W. , Rosenbergb,P., Thomsen,B., and Williamsa,A,1998. Evaluation of the chemical properties of coals and their maceral group constituents inrelation to combustion reactivity using multi-variate analyses. Fuel Vol. 71, No. 7, pp. 135-148, 1998.

99 Hansen,I..C.,Hodges,J.E.,Redmond,K.M.,1990.Determining the effectiveness of past mine fire surface seal abatement methods.US Bureau of mines research contract report J0278004,235p

100 Harris,L. (1981) the use of nitrogen to control spontaneous combustion heatings, The Mining Engineer, June 1981,PP.883-892.

101 Hatcher,P.G. and Clifford,D.J.,1997.The organic chemistry of coal: from plant materials to coal.Org.Geochem.27,251-274

102 Hessley,R.K. and Riley,J.T.,1986.Coal Science, John Wiley and Sons, New York,269 p.

103 Hill CR.,1986. Particle size and moisture effects on the low-temperature oxidation of coal. MSc Dissertation, University of the Witwatersrand; 1986.

104 Hirsch,P.B.,1954.Infra-Red and -X-ray studies of coal.Proc.Soc.Ser.A 1954,226,143)201a

105 Holland, M.J., Cadle, A.B., Pinheiro, R. and Falcon, R.M.S., 1989. Depositional environments and coal petrography of the Permian Karoo Sequence: Witbank Coalfield, South Africa. International Journal of Coal Geology.,11: 143-169.

106 Hower,J.C. and Gayer,R.A.,2002.Mechanisms of coal metamorphism: case studies from Palaeozioc coalfields. Int.J.Coal Geol.50,215-245.

107 Internet publication.2012.Unreferenced.Mine fires (India)". Retrieved 15 June 2012.

108 Itay M, Hill CR, Glasser D.,1989.A study of the low temperature oxidation of coal. Fuel Process Technol 1989;21:81–97.

109 Itay M. ,1983. The low temperature oxidation of coal; its kinetics and the implication for spontaneous combustion. PhD Thesis, University of the Witwatersrand; 1983.

110 J. Zhang,J.,. Wagner, N., Prakash,A., Mehl,H., Voigt,S., (2004). "Detecting coal fires using remote sensing techniques". International Journal of Remote Sensing 25 (16): 3193–3220. doi:10.1080/01431160310001620812.

111 Jakarta post,2004.“Haze thickens in Sumatra and Kalimantan, affects Malaysia.” 2004. Jakarta Post 16 October, 1

112 Johnson,W.,Miller,G.,1979.Abandoned coal-mined lands: nature, extent and cost reclamation. USBM Special publication 6-79,29p

113 Jones R. B., Robertson S. D., Claque A. D. H., Wind R. A., Duijvestijn M. J., Van Der Lugt. C., Vriend J. and Smidt J. (1986) Dynamic nuclear polarization 13C n.m.r. of coal. Fuel 65, 520-525.

114 Jones,R.F., and Townend,D.T.A.,1949.The oxidation of coal, J. Soc. Chem. Industr. 68, 197 (1949). doi:10.1002/jctb.5000680701

115 Khandelwal,M., (a),*and Singh,T.N.,(b). Prediction of macerals contents of Indian coals from proximate and ultimate analyses using artificial neural networks a Department of Mining Engineering, College of Technology and Engineering, Maharana Pratap University of Agriculture and Technology, Udaipur 313 001, Indiab Department of Earth Sciences, Indian Institute of Technology Bombay, Powai, Mumbai 400 076, India

116 Kadioglu Y, Varamaz M.,2003. The effect of moisture content and air-drying on spontaneous combustion characteristics of two Turkish lignites. Fuel 2003;82(13):1685-93]

117 Kaji, R., Hishinuma, Y., and Nakamura, Y., 1985, Low temperature oxidationof coals: Effects of pore structure and coal composition: Fuel, v. 64, no. 3,p. 297–302, doi: 10.1016/0016-2361(85)90413-2

118 Kanury,A.M., 1975. Gordon and Beach Science Publishers.. Introduction to Combustion Phenomena. Gordon and Breach Science Publishers, New York. 411 p.

119 Kaymakci, E. and Didari, V., 2002."Relations between coal properties and spontaneous combustion parameters." Turkish Journal of Engineering and Environmental Science 26, 59-64.

120 Kim, A.G., 1977. Laboratory studies on spontaneous heating of coal. US Bur. Mines Inform. Circ.,8756: 1-13

121 Kim, A.G., 2007. Greenhouse gases generated in underground coal-mine fires. In: Stracher, G.B. (Ed.), Geological Society of America Reviews in Engineering Geology00802018, XVIII, pp. 1–13

122 Kim, A.G., Chaiken,R.F.,1993.Fires in abandoned coal mines and waste banks.US bureau of Mines,IC9352,58p.

123 Kim,A.G., and Dalverny,L.E.,1994,Mine fire diagnostics at the Large mine site, in proceedings of the international land reclamations and mine drainage conference. Pitsburgh Pennsylvania. U.S Bureau of Mines special publication SP 06D-94V4p139-147.

124 Kim,A.G.,Chaiken,R.F.,1993.Fires in abandoned coal mines and waste banks.US Bureau of Mines,IC9352, p279

125 Kim,T (a).,, Choi.,G (a),* Kim,D.,(b).(2013).Thermochemical and combustion behaviors of coals of different ranks and their blends for pulverized-coal combustion. Cheoreon Moon (a), Yonmo Sung (a), Seongyool Ahn.a School of Mechanical Engineering, Pusan National University, 30 Jangjeon-dong, Geumjeong-ku, Busan 609-735, Republic of Koreab Pusan Clean Coal Center, Pusan National University, 30 Jangjeon-dong, Geumjeong-ku, Busan 609-735, Republic of Korea. Applied Thermal Engineering 54 (2013) 111-119.G.

126 Kiss, L.T., 1982. Chemistry of Victorian brown coals. Australian Coal Geology 4, 153–168

127 Kok M.V. ,2006. An investigation into the thermal behaviour of coals; Energy Sources 2002;24(10):899 906.

128 Krishnaswamy S, Bhat S, Gunn RD, Agarwal PK.,1996. Fuel 1996;75(3): 333–43

129 Küçük, A., Kadioğlu, Y., and Gülaboğlu, M.S., 2003, A study of spontaneous combustion characteristics of a Turkish lignite: Particle size, moisture of coal, humidity of air: Combustion and Flame, v. 133, no. 3, p. 255–261,doi: 10.1016/S0010-2180(02)00553-9.

130 LaNoMat/ Laboratory of New Materials for Electrochemical Systems and Energy / Ecole Polytechnique de Montreal

131 Lawn, C. J., Street, P. J., and Baum, M. M.,1981: in Eighteenth Symposium (International) on Combustion, The Combustion Institute, Pittsburgh, 1981, pp. 731–740.],

132 Leicht,R.D,1940.Some information on extinguishing refuse bank fires near Mahonoy City, PA.US Bureau of Mines,IC7104,p16

133 Li,S.H. and Parr,S.W.(1926) The oxidation of pyrites as a factor in the spontaneous combustion of coal,Ind. and Eng.Chem., vol.18,no.12,pp.1299-1304.

134 Li,Z., Colin, R. , Ward,C.R., Lila,W.,2010. Occurrence of non-mineral inorganic elements in macerals of low-rank coals Gurba School of Biological, Earth and Environmental Sciences, University of New South Wales, Sydney, 2052, Australia International Journal of Coal Geology 81 (2010) 242–250

135 Limpitlaw,D.,Aiken,M., Lodewijks,H & Viljoen,M., (2005). "Sustainable Development in the life of coal mining in South Africa" (PDF). The South African Institute of Mining and Metallurgy. p. 3.

136 Liotta,R.,Brons,G.,and Isaacs,J.,1983. Oxidative weathering of Illinious No 6 coal. Fuel 62:781-91.

137 Malumbazo (a),, Wagner,N.J. (b),. Bunt,J.R(c).,2013.The impact of particle size and maceral segregation on char formation in a packed bed combustion unitN. a Council for Geoscience, Mineral Resources Development, 280 Pretoria Street, Silverton, Pretoria 0001, South Africa. b School of Chemical and Metallurgical Engineering, Private Bag X3, University of the Witwatersrand, Johannesburg 2050, South Africac School of Chemical and Minerals Engineering, Private Bag X6001, North-West University, Potchefstroom 2520, South AfricaFuel 111 (2013) 350–356

138 Marevich, N.V. and Travin, A.B., 1953. Tendency towards spontaneous combustion of petrographic types of coal from Prokop'evsk deposit of Kuzbass. Izv. Akad. Nauk SSSR Otd. Tekh. Nauk, pp.1110-1117

139 Marinov VN.,1977. Self-ignition and mechanisms of interaction of coal with oxygen at low temperatures. Fuel 1977;56:153–70.

140 McCullogh,C.M.,Diamond,W.P.,Bench,B.M.,Deal,M.,1975.Selected geological factors affecting mining of the Pittsburgh coalbed, US Bureau of Mines,R18093,72p.

141 McGeer,B(2015). A laboratory based study of the spontaneous combustion of coal: Properties and factors that will reduce or enhance the effect of spontaneous combustion liability of coal.

142 Michael H.S., Mille,R.O, and Whitehouse,A.E. 2000. "The Continuing Fire Threat in Southeast Asia." Environmental Science & Technology 34(February): 82A-85A).

143 Michalski,S.R., and Gray,R.E.,2001.Ash disposal-mine fires-environment:anIndiandilemma.Bull.Eng.Geol.Environ.,60,23-90.

144 Michalski,S.R..Winsched,L.J., and Gray,R.E,R1997.Fires in abandoned coal mines. Bulletin of association of engineering geologists,v27,p479-495

145 Misra,B.K, Bhagwan ,D.,Singh,B.D,(1994). Susceptibility to spontaneous combustion of Indian coals and lignites: an organic petrographic autopsy Department of Biodiagenesis, Birbal Sahni Institute of Palaeobotany, 53, University Road, Lucknow-226 007, India (Received June 15, 1992; revised version accepted October 11, 1993) International Journal of Coal Geology2 5 (1994) 265-286

146 Morris, R., (1986) An historical note of the research into the causes of spontaneous combustion prior to 1750 ,Journal of the Mine Ventilation Society of South Africa,Dec.1986,pp.168-170.

147 Morris,R. and Atkinson,T.(1988) An analysis of underground fires in South African coal mines from 1970 to 1985,J.Mine Vent.Soc.of S.A.,Vol.40,No.10,pp.134-139.

148 Moxon, N.T. and Richardson, S.B., 1985. The assessment of chemical inhibitors of self-heating in coal. In: Proc. Int. Conf. Coal Sci. (Sydney, N.S.W., Australia), pp. 487-490

149 Murchison,D.G.,1990.,Petrographic aspects of coal structure: reactivity of macerals in laboratory and natural environments. Newcastle Research Group in Fossil Fuels and Environmental Geochemistry (NRG), FUEL, 1991, Vol 70, March,

150 Myles A. Smith,M.A.,a,*, David Glasser,D.,b,2005.Spontaneous combustion of carbonaceous stockpiles. Part II. Factors affecting the rate of the low-temperature oxidation reaction.a)Department of Chemical Engineering, University of South Africa, Room 403F, Private Bag X6, Florida 1710, South Africab)School of Process and Materials Engineering, University of the Witwatersrand, P.O. Box 3, Wits 2050, South Africa.Fuel 84 (2005) 1161–1170

151 Nandy DK, Banerjee DD, Chakravorty RN. ,1972.Application of crossing point temperature for determining the spontaneous heating characteristics of coal. Journal of Mines, Metals and Fuels 1972;20:41-8.

152 Nandy, D.K., Banerjee, D.D. and Chakravorty, R.N., 1972. Application of crossing point temperature for determining the spontaneous heating characteristics of coal. J. Mines Met. Fuels, 20 (2):41-48.

153 Nandy,D.K., Banerjee,D.D, and Chakravorty,R.N.,1967. Effect of Inherent Moisture on the self heating of coal Coal, J.Mines, Metals and Fuels,October,1967,p297

154 Nandy,D.K., Banerjee,D.D, and Chakravorty,R.N.,1972. Application of Crossing Point Temperature for Determining the Spontaneous Heating Characteristics of Coal, J.Mines, Metals and Fuels,February,1972,p41.

155 Nelson,M.,Chen,X.,2007. Geology of coal fires: case studies from around the world: The Geological Society of America:Boulder,CO,2007,pp 31-83.

156 Nolter, M.A., Vice, D.H., 2004. Looking back at the Centralia coal fire; a synopsis of its present status. International Journal of Coal Geology (ISSN: 01665162) 59, 99–106

157 Nordon P, Bainbridge NW, Young BC.,1979. Some properties of char affecting the self-heating reaction in bulk. Fuel 1979;58(6):443–64.

158 Nugroho, Y. S., McIntosh, A. C., & Gibbs, B. M. (2000). Low-temperature oxidation of single and blended coals. Fuel, 79, 1951-1961

159 Nugroho,Y.S., McIntosh,A.C., and Gibb,B.M.,.USING THE CROSSING POINT METHOD TO ASSESS THE SELF-HEATING BEHAVIOR OF INDONESIAN COALS Department of Fuel and Energy Leeds University Leeds LS2 9JT, UK

160 Ohlson, K., 2010. Earth on Fire, Discover Magazine. 3 pp. (ISSN: 02747529)).,
161 Oreshko,W.F.1961 ,Coal, Typology, Chemical and Physical Constitution. Elsevier (1961), p. 243
162 Parr, S.W. and Kressman, F.W., 1910. The spontaneous combustion of coal. Ill. Exp. Stn. Bull., 149.
163 Pattanaik.D.S.(1), Behera.P.(2), Bijay Singh,B(3)., 2011. Spontaneous Combustibility Characterisation of the Chirimiri Coals, Koriya District, Chhatisgarh, India.1,2P.G. Department of Geology, Utkal University, Bhubaneswar, Orissa, India 3University Department of Geology, Ranchi University, Ranchi, Jharkhand, India International Journal of Geosciences, 2011, 2, 336-347
164 Petrakis,L. and Grandy,D.W.,1980,Coal analysis, characterisation and petrography,J.Chem,Educ,57,689-694.
165 Pietrzak R, Wachowska H.,2003. Low temperature oxidation of coals of different rank and different sulphur content. Fuel 2003;82(6):705.
166 Polat S, Harris IJ.,1984.Low temperature oxidation of Victorian brown coal. Fuel 1984;63:669–72
167 Porter,H.C. and Ovitz,F.K.(1912) Deterioration and spontaneous heating of coal, U.S.B.M. Technical paper no.16.
168 Primer on spontaneous heating and pyrophoricity. US Department of Energy; 1994
169 PurserD.A.,2002.Toxicity assessment of combustion products, In: Beyler, C.L., Custer, R.L.P., Walton, W.D., Watts, J.M., Drysdale, D.,Hall,J.R.,Jr., Dinenno, P.J (Eds.), SFPE Handbook of Fire Protection Engineering, third ed. National Fire protection Association, Quincy, MA, pp. 2.83-2.171. Rein, G., 2009.Smouldering combustion phenomena in science and technology. Int. Rev. Chem. Eng. 1(1),3-18,)
170 Purshall, B.R and Ghosh, S.K (1965) Early detection of spontaneous heating using using chromatographic gas analysis, The Mining Engineer, June 1965, PP.511-526.
171 Rathmore,C.S.,.Wright,R.,1993.Monitoring environmental impacts of coal mining. Int.J.Remote Sens.14 (6),1021-1042.
172 Ratnasthein, B., 1985. Spontaneous ignition temperature of northern Thailand coals. In: Proc. Int. Conf. Coal Sci. (Sydney, N.S.W., Australia), pp. 463-466.
173 Ren, T.X., Edwards, J.S., and Clarke, D., 1999, Adiabatic oxidation study on the propensity of pulverised coals to spontaneous combustion: Fuel, v. 78,p. 1611–1620, doi: 10.1016/S0016-2361(99)00107-6.
174 Rennie, D. (2002). "How China's scramble for 'black gold' is causing a green disaster". The Daily Telegraph (London). Retrieved 30 April 2010
175 Ressler, D.E.,Markel, E., 2006.Weeds and Wildfires. Soil Temperature and CO2 Affect Plant Diversity at a Mine Fire: 18thWorld Congress of Soil Science14390108, 18, p. 159.,
176 Rojas-Gonzales,A.F.,2013.Volatile matter release and thin and thick char formation as a function of vitrinite content, coal rank, time and temperature devolatilization.Inicio,vol.15,num 2.2013,1-10.
177 Russell N. J., Wilson M. A., Pugmire R. J. and Grant D. M. (1983) Preliminary studies on the aromaticity of Australian coals. Fuel 62, 601-605.
178 Sanyal, S.P., 1984. Petrology of natural coke associated with igneous intrusives in parts of the Raniganj coalfield. Mem. Geol. Surv. India, 117: 1-106
179 Saraf,A.K.,Prakash,A.,Sengupta,S.,Gupta,R.P.,1995.Landsat TM data for estimating ground temperature and depth of subsurface coal fire in Jharia coal field ,India.Int.J.Remote Sens.16(12),2111-2124
180 Saranchuk VI, Galushko LYa, Paschenko LV, Luk'yanenko LV. ,1978.Solid,Fuel Chem 1978;12(91):9-12
181 Saxena, R., Navale, G.K.B., Chandra, D. and Prasad, Y.V.S., 1990. Spontaneous combustion of some Permian coal seams of India: an explanation based on microscopic and physico-chemical properties. In: K.P. Jain and R.S. Tiwari (Editors) Proc. Symp. Vistas in Indian Palaeobotany. Palaeobotanist,38: 58- 82
182 Schmidt, L.D., 1945. In: Lowry, H.H. (Ed.), Chemistry of Coal Utilization, Vol. I. John Wiley and Sons, New York, NY, Ch. 18.
183 Schowengerdt, R. A. (2007). In Wikipedia: Remote sensing: models and methods for image processing (3rd ed.). Academic Press. p. 2. ISBN 978-0-12-369407-2.

184 Schweinfurth, S., 2009. Chapter C: An Introduction to Coal Quality. In: Pierce, B.S., Dennen, K.O. (Eds.), The National Coal Resource Assessment Overview. U.S. Geological Survey Professional Paper 1625–F. 10449612U.S. Department of the Interior U.S. Geological Survey (16 pp.).;

185 Serio, M. A., Bassilakis, R. and Solomon, P. R.,1996. "Use of TG-FTIR analysis for the characterization of fuels and resources," ACS Div. of Fuel Chem. Prepr. 41 (1), 43–50 (1996)

186 Sevenster PG. Fuel 1961;40:7–17.

187 Shallenberger,J.P.,1993.The use of remote sensing to track the progression of the underground coal mine fire at Centralia, PA. The Pennsylvania State University ,unpublished senior thesis, State College,Pennsylvania,77p

188 Singh, A.K., Singh, R.V.K., Singh, M.P., Chandra, H., Shukla, N.K., 2007. Mine fire gas indices and their application to Indian underground coal mine fires. International Journal of Coal Geology 69, 192–204.)(12=34)

189 Singh,R.N.,Demiirbilek,S and Aziz,N.I.(1985),An approach to safe design of mine workings against the risk of spontaneous combustion,Proc.21st International conference of Sferty in Mine Research.Sydney.21-25 October.

190 Singh,R.V.K., 2013. The 9th Asia-Oceania Symposium on Fire Science and Technology Spontaneous heating and fire in coal mines , Mine Fire Division, CSIR-Central Institute of Mining & Fuel Research, Barwa Road, Dhanbad, 826015, Jharkhand, India. Procedia Engineering 62 (2013) 78 – 90

191 Singh.S.K.,2012.,OPTIMIZATION OF HEATING RATE OF CROSSING POINT TEMPERATURE APPARATUS. A THESIS SUBMITTED IN PARTIAL FULFILLMENT OF THE REQUIREMENTS FOR THE DEGREE OF BACHELOR OF TECHNOLOGY INMINING ENGINEERING,108MN023,DEPARTMENT OF MINING ENGINEERING,NATIONAL INSTITUTE OF TECHNOLOGY,ROURKELA – 769008

192 Sinnatt, F.S., Stern, H. and Bailey, F., 1920. Does fusain cause mine and bin fires, spoil coke and aid explosions. Coal Age, 18: 384

193 Skorupska, N.M. and Marsh, H., Proc. Con& on Applied Energy Research, Swansea, UK, 161-181London.The Institute of Energy, 1989Nandi, B.N., Brown, T.D. and Lee, G.K., Fuel, 1977, 56,125-130

194 Smith, A. C. and Lazzara, C. P., 1987. Spontaneous Combustion Studies of U. S. Coals. U.S. Bureau of Mines, Report of Investigation 9079,p.2,

195 Smith,M.A(a),*, David Glasser,D(b).,2002.Spontaneous combustion of carbonaceous stockpiles. Part I: the relative importance of various intrinsic coal properties and properties of the reaction system. Fuel 84 (2005) 1151–1160, (a)Department of Chemical Engineering, University of South Africa, Room 403F, Private Bag X6, Florida 1710, South Africa (b)School of Process and Materials Engineering, University of the Witwatersrand, P.O. Box 3, Wits 2050, South Africa Received 26 June 2002; received in revised form 19 November 2004; accepted 9 December 2004 Available online 1 February 2005.

196 Smith.M.A.,(a),*, Glasser.D(b).,2002..Spontaneous combustion of carbonaceous stockpiles. Part I: the relative importance of various intrinsic coal properties and properties of the reaction system. Fuel 84 (2005) 1151–1160. b) a)Department of Chemical Engineering, University of South Africa, Room 403F, Private Bag X6, Florida 1710, South Africa b School of Process and Materials Engineering, University of the Witwatersrand, P.O. Box 3, Wits 2050, South Africa Received 26 June 2002; received in revised form 19 November 2004; accepted 9 December 2004 Available online 1 February 2005

197 Sondreal, E.A. and Ellman, R.C., 1974. Laboratory determination of factors affecting storage of North Dakota Lignite. Report of investigation 7887, Bureau of Mines, United States Department of the Interior

198 Stach, E., Mackowsky, M.-Th., Teichmfiller, M., Taylor, G.H., Chandra, D. and Teichmiiller, R., 1982. Stach's textbook of coat petrology. Borntraeger, Stuttgart, 3rd ed., 535pp.

199 Stott, J.B. (1956) An isothermal micro-calorimeter, Journal of Scientific Instruments,vol.33, Feb.1956, pp.58-63.

200 Stott, J.B., and Baker, O.J., 1953, Differential thermal analysis of coal: Fuel,v. 32, no. 4, p. 415–427.

201 Stracher,GB.,2011.Coal and Peat Fires: A Global Perspective. Edited by Glenn B. Stracher, Anumpa Prakash and Ellina V.Sokol,2011Chapter 3,p48-60

202 Stracher GB; Prakash A; Sokot EV.,2011 Coal and Peat Fires: A Global Perspective Volume 1-Geology and Combustion.2011:20-21.)

203 Sua,S.,*, Pohla,J.H., Holcombeb,D.,. Hart,J.2000.A proposed maceral index to predict combustion behavior of coal.aDepartment of Chemical Engineering, The University of Queensland, Brisbane, Qld 4072, AustraliabACIRL Limited, 1 ACIRL St., Riverview, Qld 4303, AustraliacCRC for Black Coal Utilization, The University of Newcastle, University Drive, Callaghan, NSW 2308, Australia Received 20 December 1999; accepted 25 July 2000 Fuel 80 (2001) 699±706

204 Swann, P.D., Allardice, D.J., and Evans, D.G., 1974, Low-temperature oxidation of brown coal. 1: Changes in internal surface due to oxidation: Fuel,v. 53, no. 2, p. 85–87, doi: 10.1016/0016-2361(74)90060-X.

205 Taraba,B, (a),, Pavelek,Z,(b). ,2014. Investigation of the spontaneous combustion susceptibility of coal using the pulse flow calorimetric method: Fuel 125 (2014) 101–105. 25 years of experience a) University of Ostrava, Faculty of Science, Institute of Environmental Technologies, 30. dubna 22, 701 03 Ostrava 1, Czech Republic. b) OKD, HBZS, a.s., Ostrava-Radvanice, Czech Republic

206 Teichmuller,M. and Teichmuller,R.,1967.Diagenisis of coal (coalification).In:Larson,G., and Chilingar,G.V (Ed8),Diagenesis in Sediments,Elsevier,Amsterdam,pp,391-415.

207 Terry,R.C.,1987.Terminating persistent underground coal fires.US Patent No.4641711,February 10,1987.

208 Thomas GC, Gosnell ME, Shibaoka M. 1996.Combustion kinetics of coal maceral particles using a laser nanoreactor mass analyser, CET/IR 487. CSIRO Division of Coal and Energy Technology, Sydney, 1996

209 Thomas R.J and Kim,A,G., 1988. Mine Fire Diagnostics to Locate and Monitor Abandoned Mine Fires p. 348-355 in: Proceedings of 1988 Mine Drainage and Surface Mine Reclamation Conference. (Pittsburgh, PA)

210 Thomas, C.G., Gosnell, M.E., Gawronski, E., Phonganant, D. and Shibaoka, M., 1993. The behavior of inertinite macerals under pulverised fuel combustion conditions.Org. Geochem., 1993, 20,779-795..

211 Tobin-Janzen, T., Shade, A., Marshall, L., Torres, K., Belbo, C., Janzen, C., Lenig, J., Martinez, A., Ressler, D., 2005. Nitrogen Changes and Domain Bacteria Ribotype Diversity in Soils Overlying the Centralia CoalMine Fire. Soil Science (ISSN: 0038075X) 170, 1–11

212 USBM,1993.In: Kim,A.G, Chaiken.R.F., Fires in abandoned coal mines and waste banks.IC9352 ,Washington, D.C, USA. Department of the Interior.USBM,1993.

213 USBM-study and control of fires in abandoned mines and waste banks.

214 Vaimakis,T. C., Thermogravimetry (TG).Chemistry Department, University of Ioannina, P. O. Box 1186, Ioannina 45110, Greece,undated.p10

215 Varga,E. (1967) New factors in the self ignition of coals,Colliery Guardian,Jan.13 1967,pp.55-60

216 Vice,D.H.,2007.Application of airborne thermal infrared imagery to geothermal exploration. Geitherm. Resour. Council Trans.31,369-372

217 Wade, L. (1988) The propensity of South African Coals to spontaneously combust, Johannesburg: PH.D. thesis, University of the Witwatersrand.)

218 Wade, L.,Phillips, H.R and Gouws, M.J. ,1986. Spontaneous combustion of South African coals, Procedings. Symposium. Underground Mining Methods and Technology, edited by A.B.Szwiliski and M.J Richards, Elsevier Science Publishers B.V.,Amsterdam (1987), pp.65-73.

219 Wagner,N.,2015.Abnormal Condition Analysis, Coal Samples For Spont Comb Potential. Internal report. UnpublishedA/Prof Nikki Wagner (ICCP accredited, SACNAS, FFF, Geol Soc) 20 Nielson Drive, Blairgowrie, 2194 0828539780 / Nicola.wagner@wits.ac.za Report by :

220 Wang,C., Liu,Y, Zhang,X. , Che, D.,2011.A study on coal properties and combustion characteristics of blended coals in North western China, Energy Fuels 25 (2011) 3634-3645.

221 Wang,X and Luo,Y 2015.Study on correlation of quantified coal rank with self-heating temperature. Mining Engineering, 2015, Vol. 67, No. 11, pp. 54-60.

222 Watson, J.R.,(1977) Opening of a sealed area at Northfield Colliery. Fires in Collieries and Gold Mines, A.M.M.S.A. and M.V.S.S.A., Chamber of Mines of South Africa, Johannesburg, pp.45-57.

223 White,E.M.,1973.Fires and explosion. In Cassidy,S.M (Ed.),Elements of Practical Coal Mining. Coal division, SME-AIME, New York,pp.227-258

224 Whitehouse, A; Mulyana, A. S. (2004). "Coal Fires in Indonesia". International Journal of Coal Geology (Amsterdam: Elsevier) 2012 (1–2): 91–97 [p. 95].

225 Wikipedia,the free online encyclopedia

226 Winmill, T.F. (1915-16) The atmospheric oxidation of iron pyrites , Transactions of the Institute.Mineralagy.E.,vol.51, pp.500-509

227 www.groupes.polymtl.ca/lanomat/modules/facilities/index.php?cat_id...

228 Xie, KC.,2002. Coal structure and its reactivity. Beijing: Science Press; 2002.

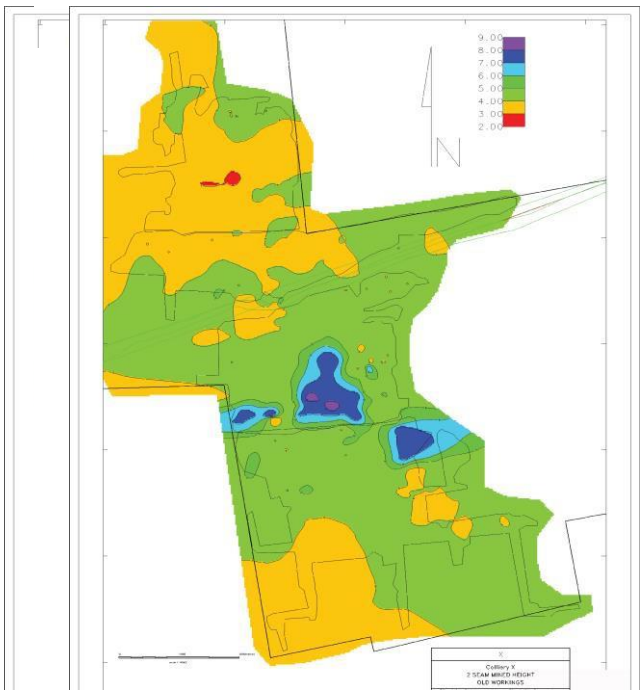
229 Yohe.,G. R. and Harman,C. A.,(1941). J. Am. Problems of oxygen stoichiometry in analysis of coal. Chem. Soc. 63, 555 (1941). doi:10.1021/ja01847a055

230 Zheng, J.A. Kozinski,2000. Thermal events occurring during the combustion of biomass residue, Fuel 79 (2000) 181-192.

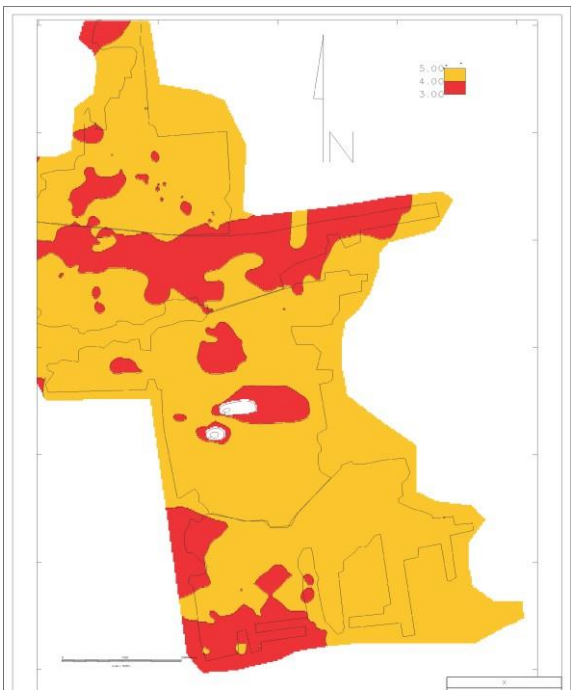
231 Zilm K. W., Pugmire R. J., Larter S. R., Allan J. and Grant D. M. (1981) Carbon-13 CP/MAS spectroscopy of coal macerals. Fuel 60, 717-722.

APPENDIX

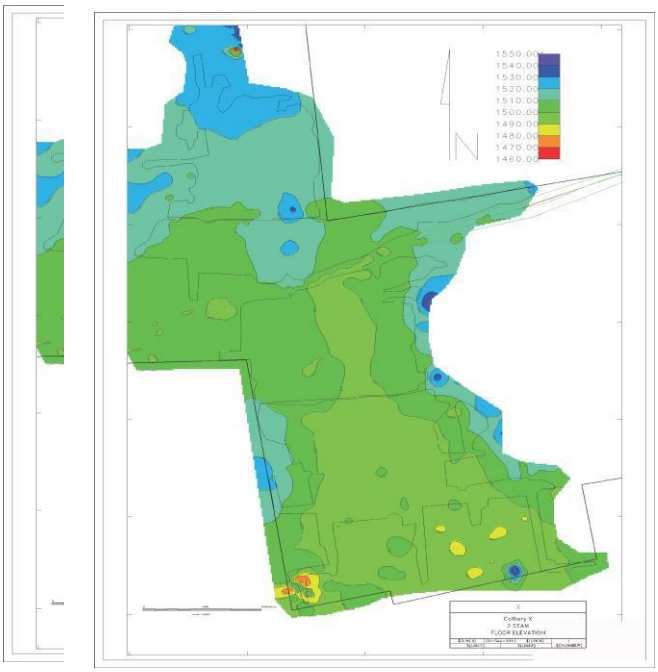
Appendix 2: No S2 seam mined height of pillars - excludes bottom coal



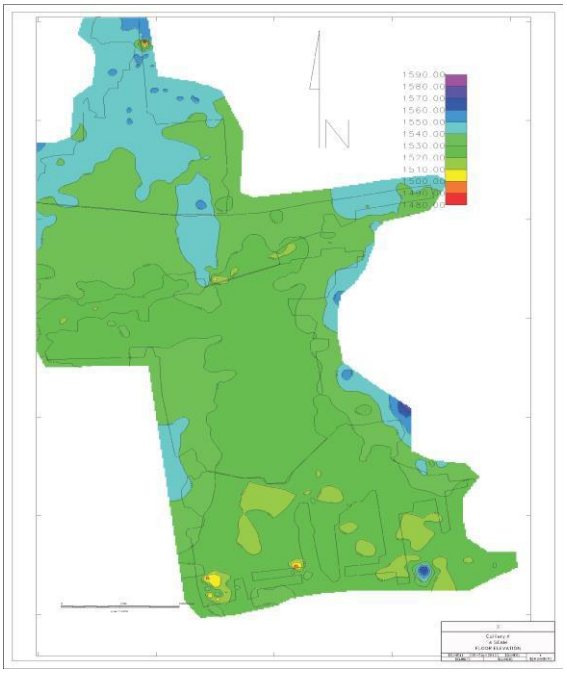
Appendix 1: No S4U seam mined height of pillars - excludes top coal



Appendix 4: No.S2 seam floor elevation



Appendix 3: No.S4U seam floor elevation



Sample Identification	Sampe Number	CROSSOVER TEMPERATURE °c	COMMENTS
SP32814 - Z01	216943	178	
SP32814 - Z02	216944	195	
SP32814 - Z03	216945	-	No cross over temperature
SP32814 - Z04	216946	209	
SP32814 - Z05	216947	-	No cross over temperature
SP32814 - Z06	216948	179	
SP32814 - Z07	216942	198	
SP32814 - Z08	216949	194	
SP32814 - Z09	216950	-	No cross over temperature
SP32814 - Z10	216951	-	No cross over temperature
SP32814 - Z11	216952	-	No cross over temperature
SP32814 - Z12	216953	215	
SP32814 - Z13	216954	-	No cross over temperature

Appendix 6: Crossing point temperatures for samples Z13-Z22

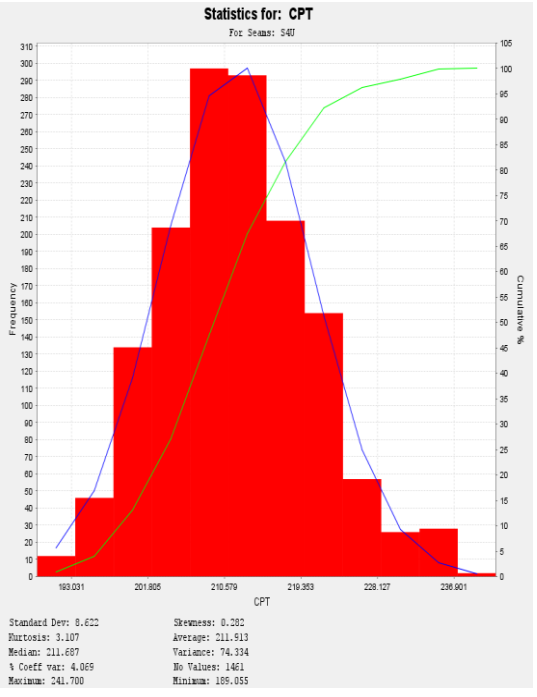
Date analysed	Sample Identification	Sampe Number	*CROSSOVER TEMPERATURE		COMMENTS
			Original	Duplicate	
			°c	°c	
02/12/2014	S10014-Z14	197738	192	194	1 degree/minute
06/01/2015			214	210	2 degree/minute
03/12/2014	S10014-Z15	197739	237	245	1 degree/minute
06/01/2015			257	245	2 degree/minute
04/12/2014	S10014-Z16	197740	225	218	1 degree/minute
07/01/2015			227	220	2 degree/minute
08/12/2014	S10014-Z17	197741	220	220	1 degree/minute
08/01/2015			220	217	2 degree/minute
09/12/2014	S10014-Z18	197742	198	200	1 degree/minute
09/01/2015			205	209	2 degree/minute
10/12/2014	S10014-Z19	197743	205	205	1 degree/minute
12/01/2015			230	221	2 degree/minute
12/12/2014	S10014-Z20	197744	230	220	1 degree/minute
12/01/2015			246	247	2 degree/minute
17/12/2014	S10014-Z21	197745	212	220	1 degree/minute
13/01/2015			214	250	2 degree/minute
18/12/2014	S10014-Z22	197746	214	232	1 degree/minute
14/01/2015			223	225	2 degree/minute

Appendix 7: Crossing point temperatures for samples ROM1 and ROM2

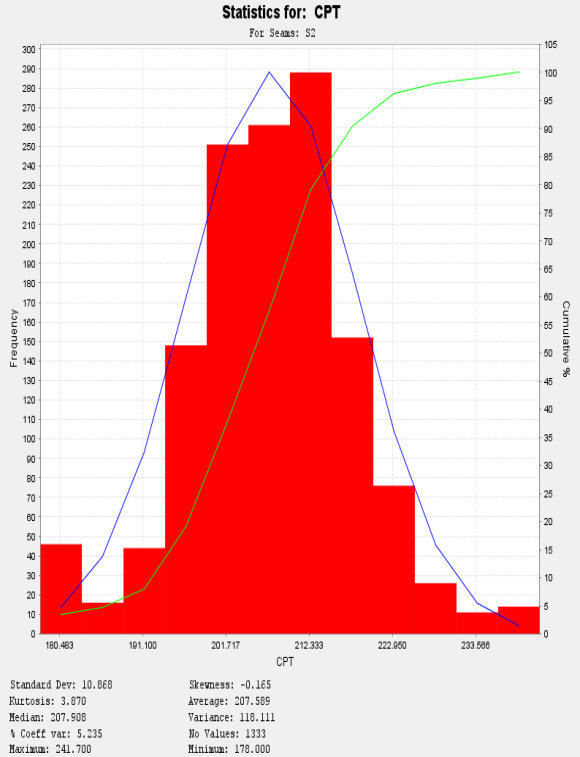
Date analysed	Sample Identification	Sampe Number	*CROSSOVER TEMPERATURE		COMMENTS
			Original	Duplicate	
			°c	°c	
19/12/2014	ROM 27/11/2014	198116	235	230	1 degree/minute
15/01/2015			239	250	2 degree/minute
20/12/2014	ROM 28/11/2014	198117	234	238	1 degree/minute
15/01/2015			247	258	2 degree/minute

Appendix 8: Crossing point temperature histogram for No.S5 seam

Appendix 9: Crossing point temperature histogram for No.S4U seam



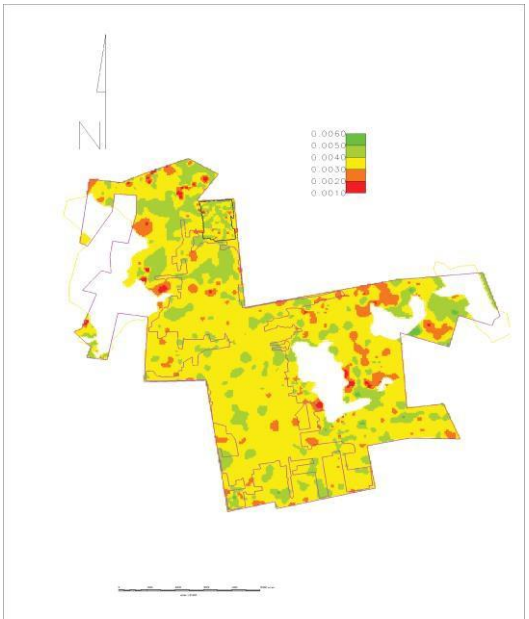
Appendix 10: Crossing point temperature histogram for No.S2 seam



Appendix 11: Derivative of weight gain No.S2 seam (TGA)



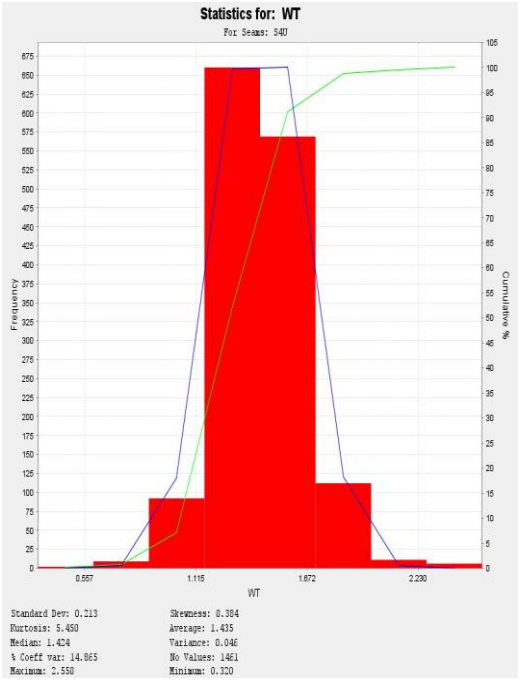
Appendix 12: Derivative of weight gain No.S4Useam (TGA)



Appendix 13: Histogram of weight gain (%) No.S2seam (TGA)

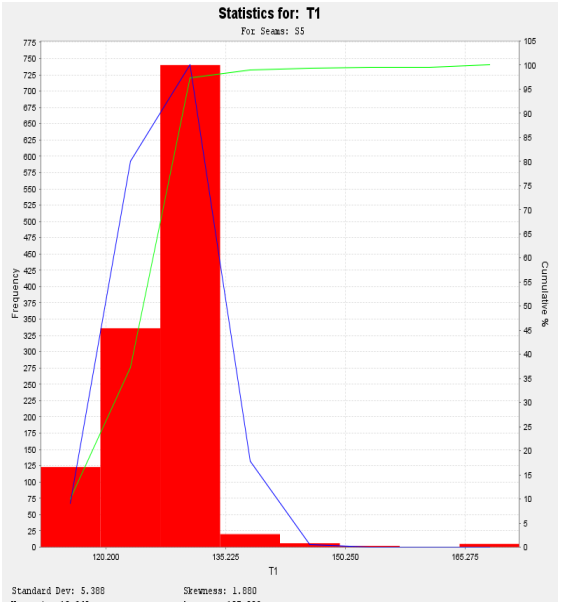


Appendix 14: Histogram of weight gain (%) No.S4U seam (TGA)



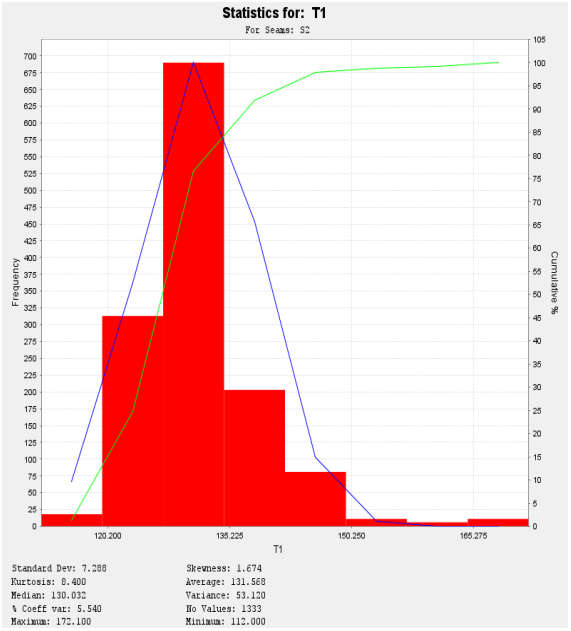
Appendix 15: Histogram WT (%) No.S5 seam (TGA)

Appendix 16: Histogram of T1 of No.S5 seam (TGA)



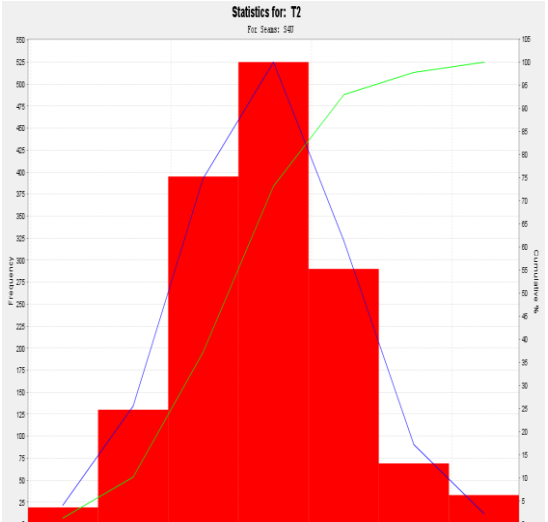
Appendix 17: Histogram of T1 of No.S4U seam (TGA)

Appendix 18: Histogram of T1 of No.S2 seam



Appendix 19: Histogram of peak temperature of No.S5 seam (TGA)

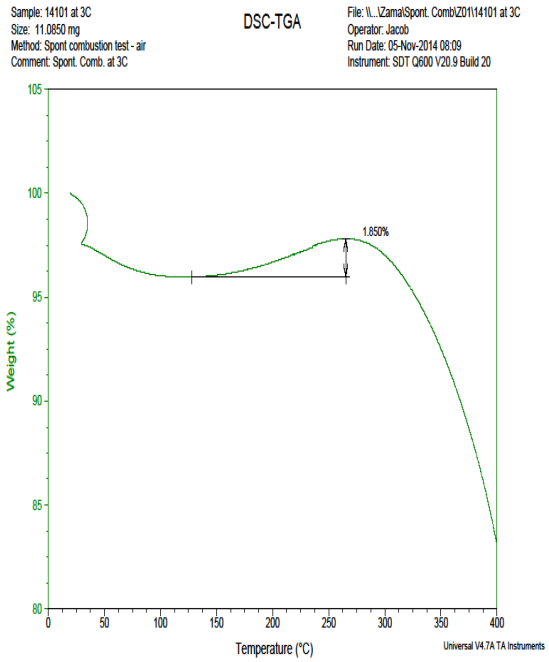
Appendix 20: Histogram of peak temperature of No.S5 seam (TGA)



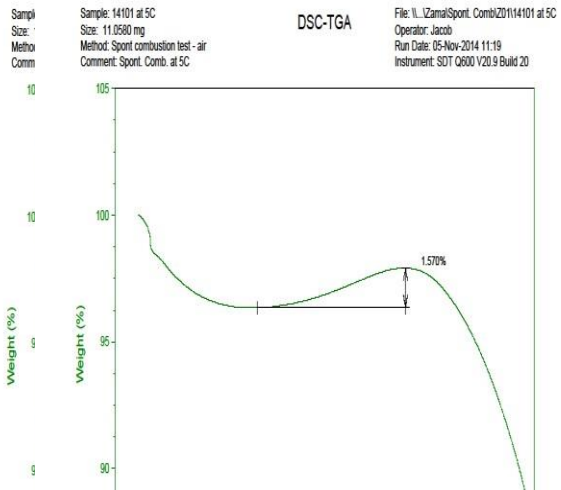
Appendix 21: Histogram of peak temperature of No.S2 seam (TGA



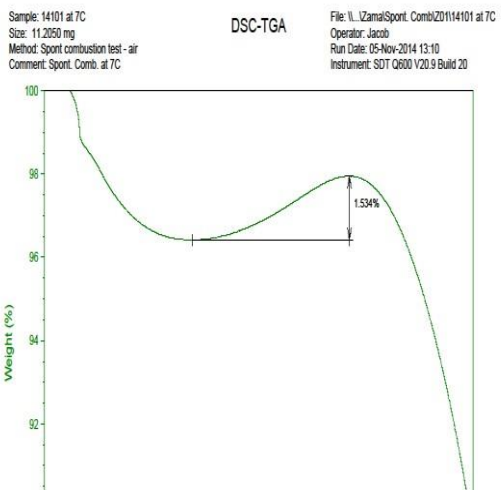
Appendix 22: Oxygen absorption for sample Z01 at 3 degree C ramp (TGA



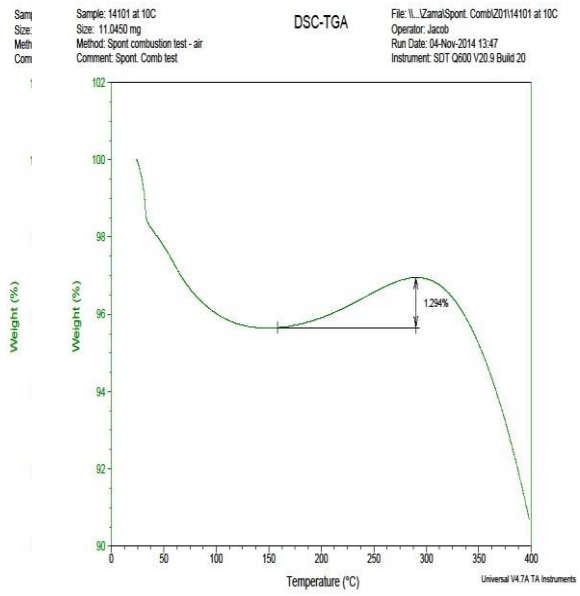
Appendix 23: Oxygen absorption for sample Z01 at 5 degree C ramp (TGA)



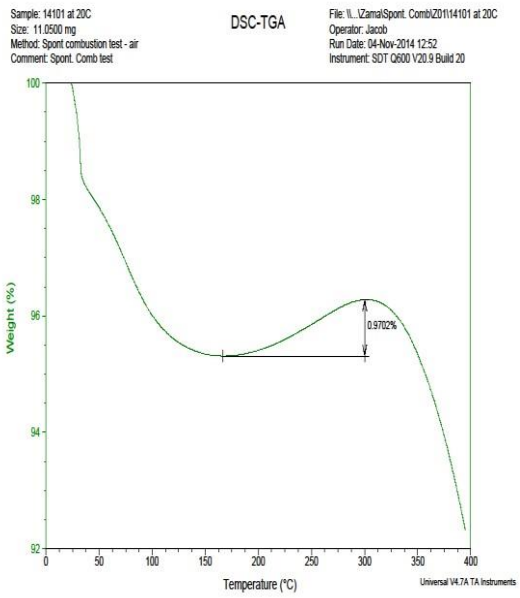
Appendix 24: Oxygen absorption for sample Z01 at 7 degree C ramp (TGA)



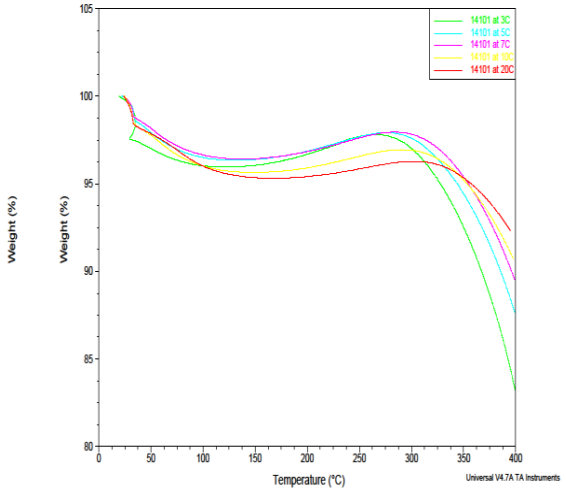
Appendix 25: Oxygen absorption for sample Z01 at 10 degree C ramp (TGA)



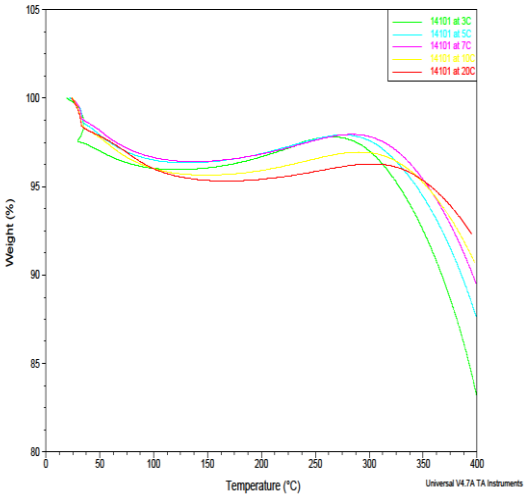
Appendix 26: Oxygen absorption for sample Z01 at 20 degree C ramp (TGA)



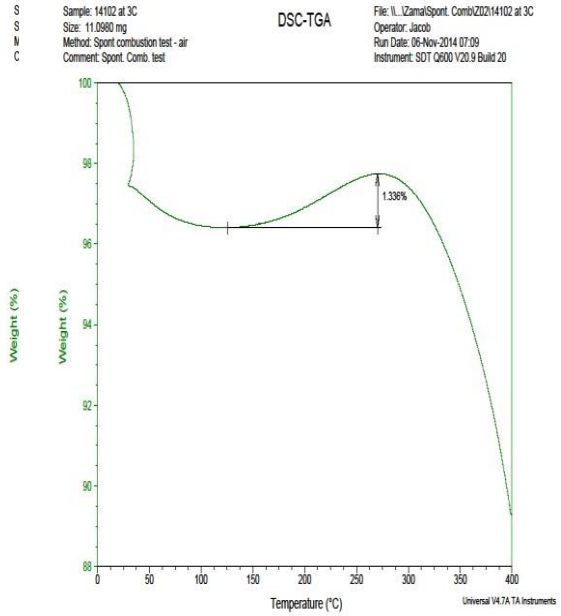
Appendix 27: Oxygen absorption mix for sample Z01 (TGA)



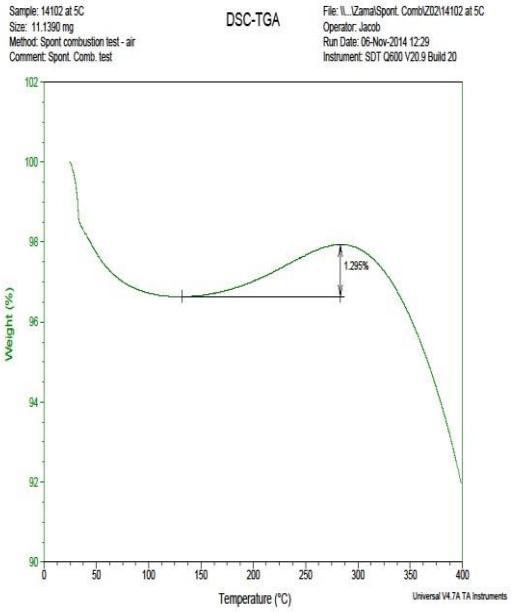
Appendix 28: Ignition test mix for sample Z01(TGA)



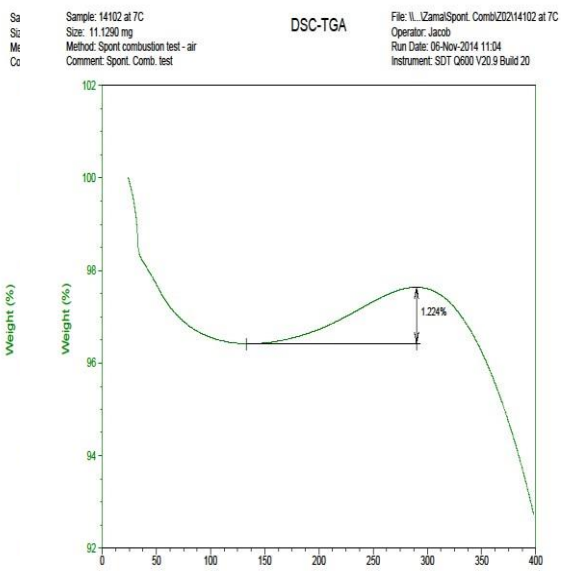
Appendix 29: Oxygen absorption for sample Z02 at 3 degree C ramp (TGA)



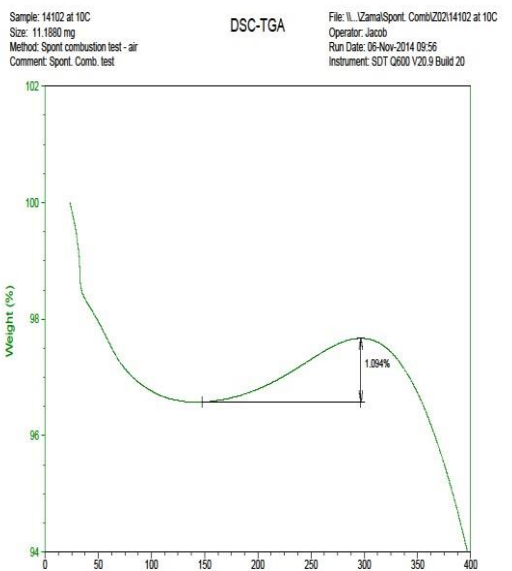
Appendix 30: Oxygen absorption for sample Z02 at 5 degree C ramp (TGA)



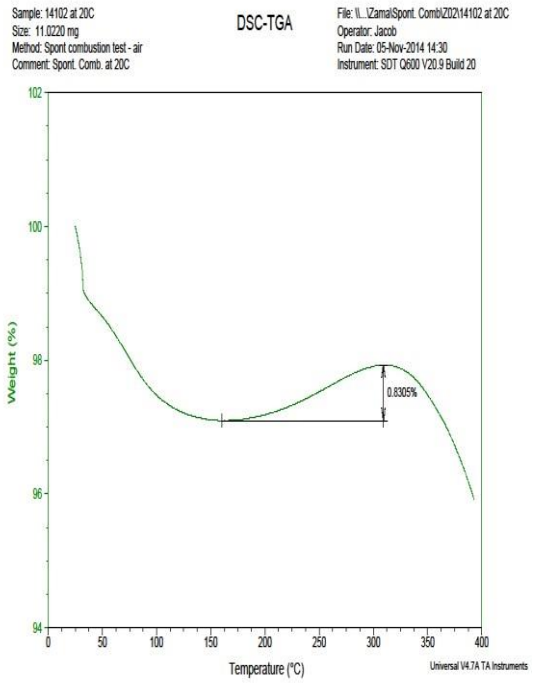
Appendix 31: Oxygen absorption for sample Z02 at 7 degree C ramp (TGA)



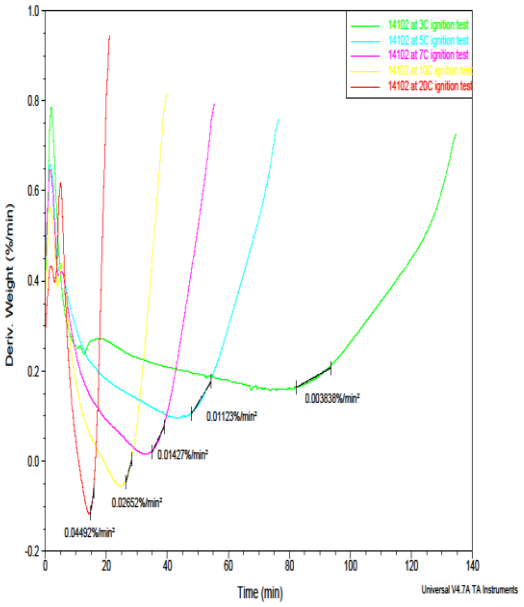
Appendix 32: Oxygen absorption for sample Z02 at 10 degree C ramp (TGA)



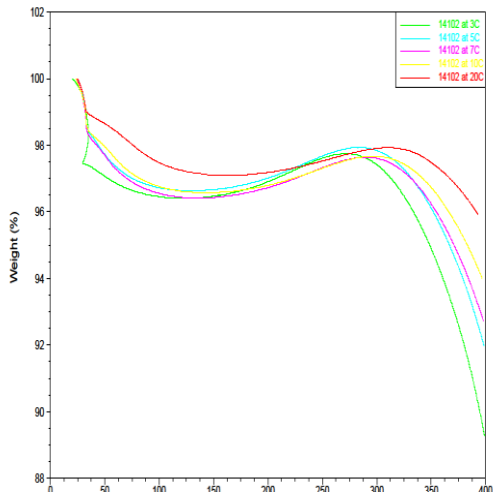
Appendix 33: Oxygen absorption for sample Z02 at 20 degree C ramp (TGA)



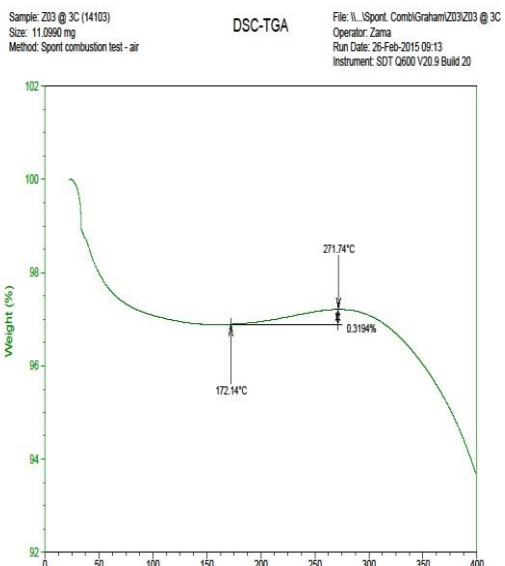
Appendix 34: Oxygen absorption mix for sample Z02 (TGA)



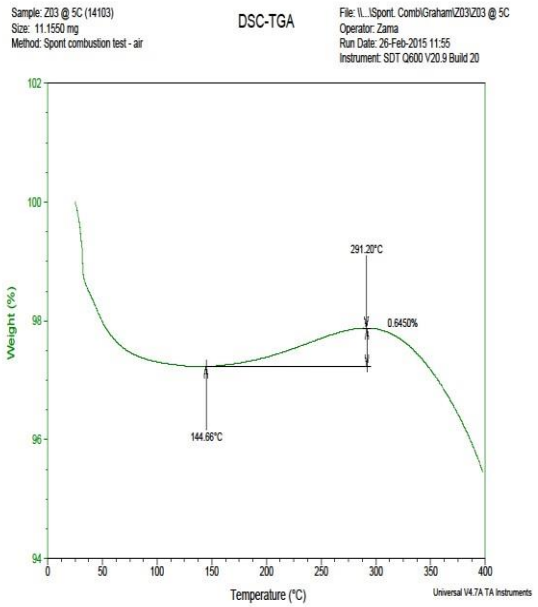
Appendix 35: Ignition test mix for sample Z02(TGA)



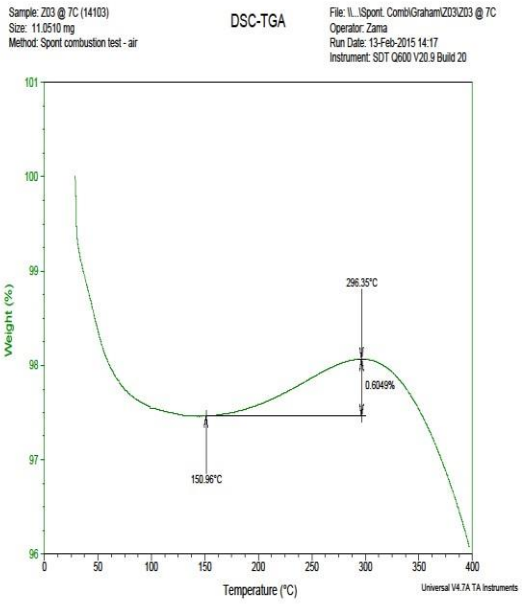
Appendix 36: Oxygen absorption for sample Z03 at 3 degree C ramp (TGA)



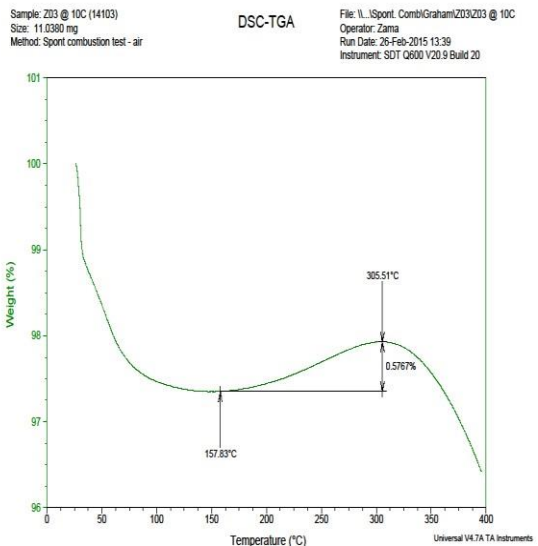
Appendix 37: Oxygen absorption for sample Z03 at 5 degree C ramp (TGA)



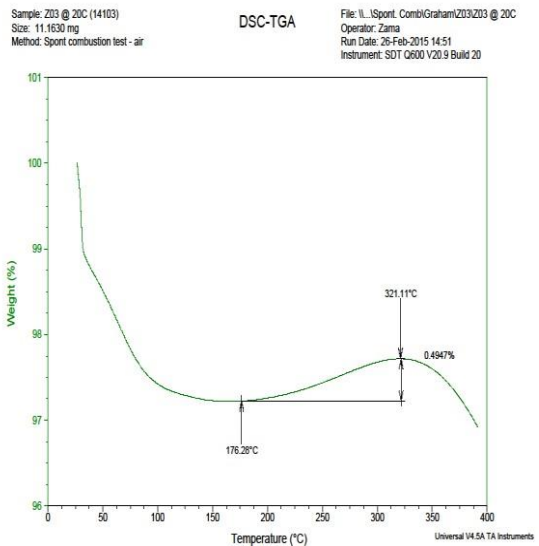
Appendix 38: Oxygen absorption for sample Z03 at 7 degree C ramp (TGA)



Appendix 39: Oxygen absorption for sample Z03 at 10 degree C ramp (TGA)

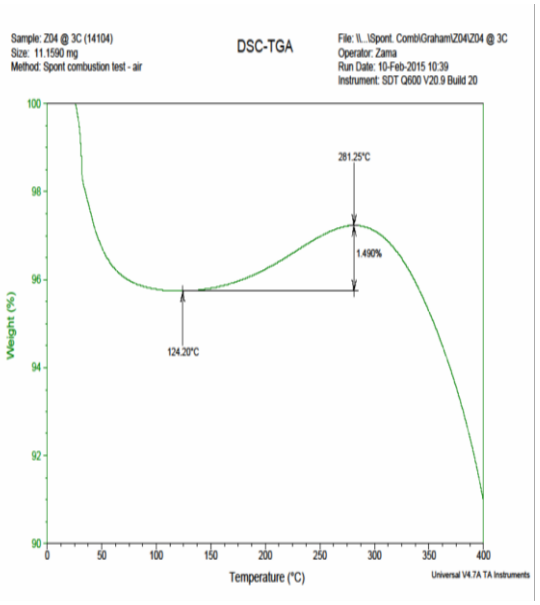


Appendix 40 Oxygen absorption for sample Z03 at 20 degree C ramp (TGA)

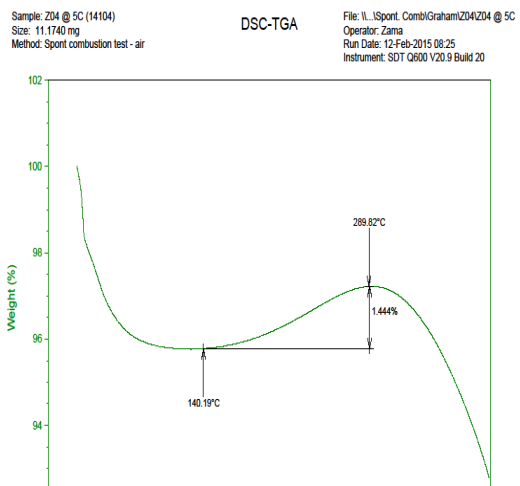


Appendix 41: Ignition test mix for sample Z03 (TGA)

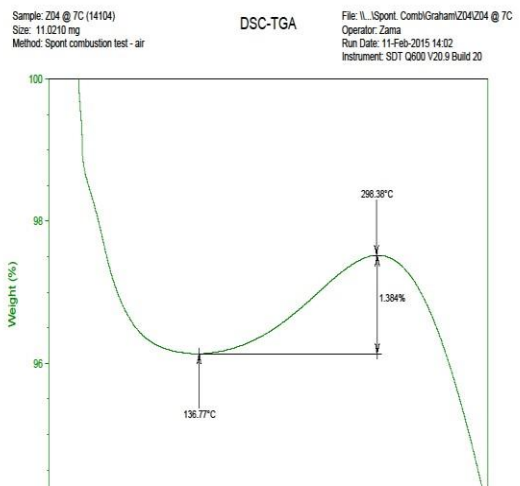
Appendix 42: Oxygen absorption for sample Z04 at 3 degree C ramp (TGA)



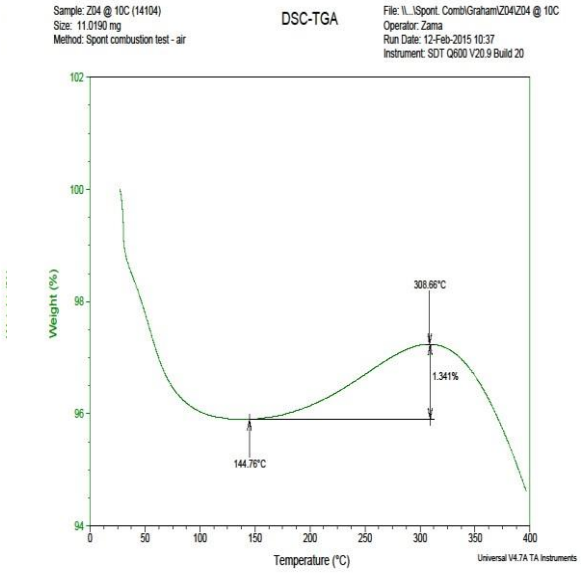
Appendix 43: Oxygen absorption for sample Z04 at 5 degree C ramp (TGA)



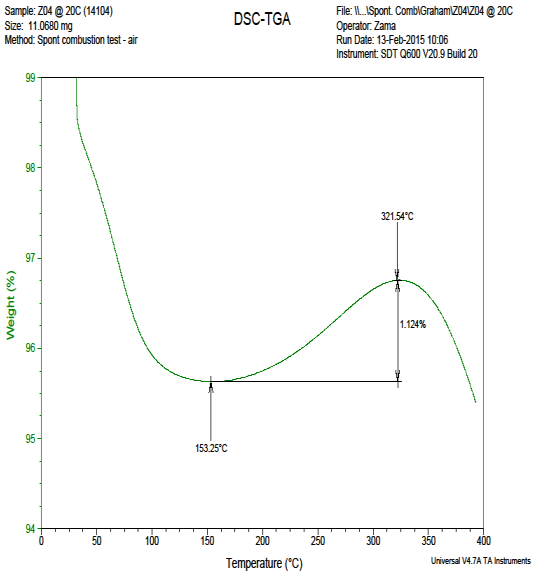
Appendix 44: Oxygen absorption for sample Z04 at 7 degree C ramp (TGA)



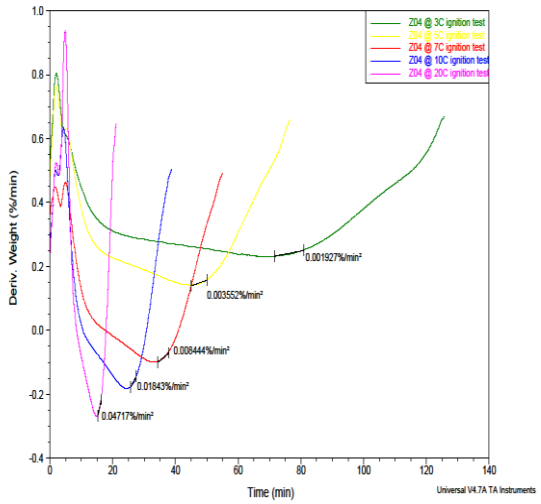
Appendix 45: Oxygen absorption for sample Z04 at 10 degree C ramp (TGA)



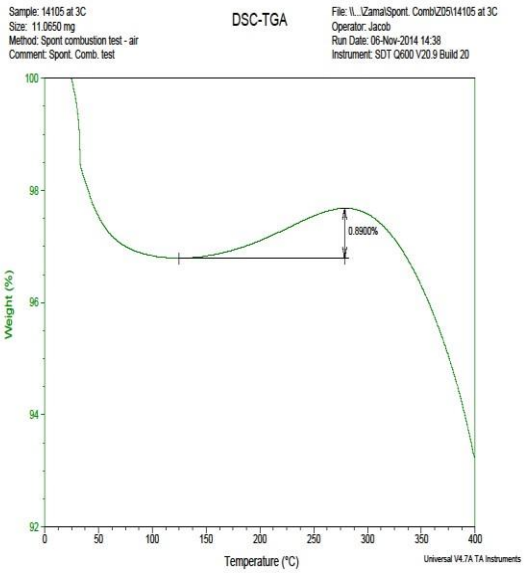
Appendix 46: Oxygen absorption for sample Z04 at 20 degree C ramp (TGA)



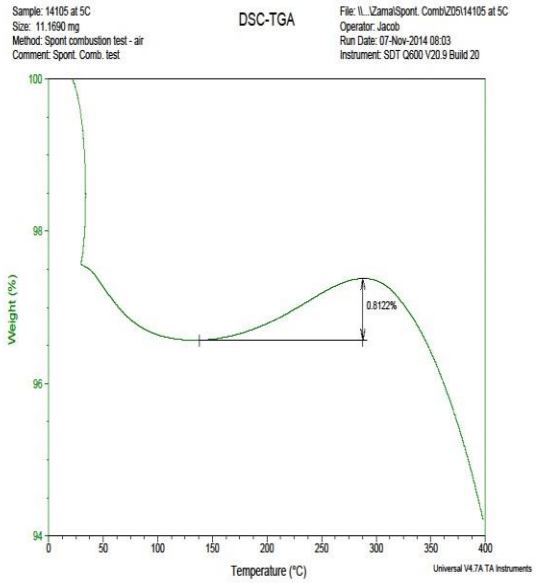
Appendix 47: Ignition test mix for sample Z04 (TGA)



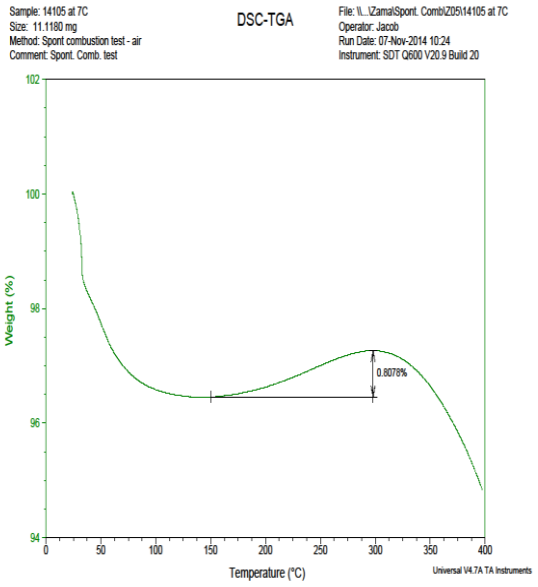
Appendix 48: Oxygen absorption for sample Z05 at 3 degree C ramp (TGA)



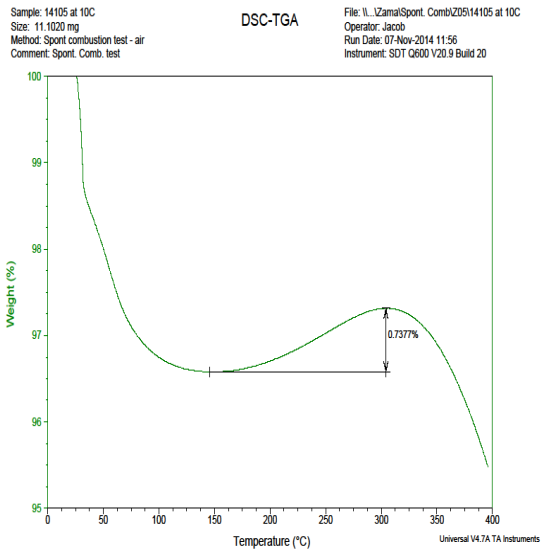
Appendix 49: Oxygen absorption for sample Z05 at 5 degree C ramp (TGA)



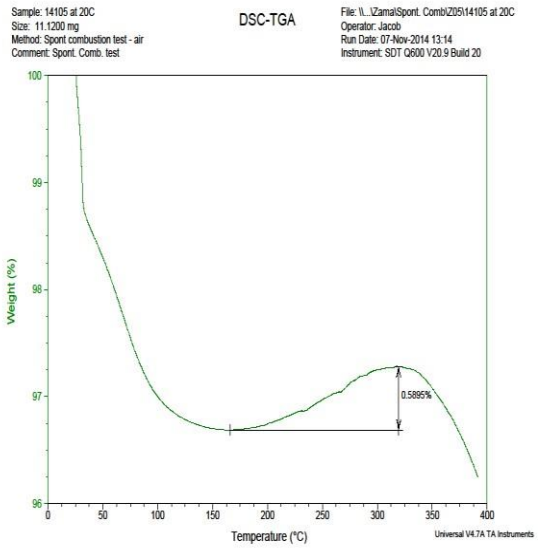
Appendix 50: Oxygen absorption for sample Z05 at 7 degree C ramp (TGA)



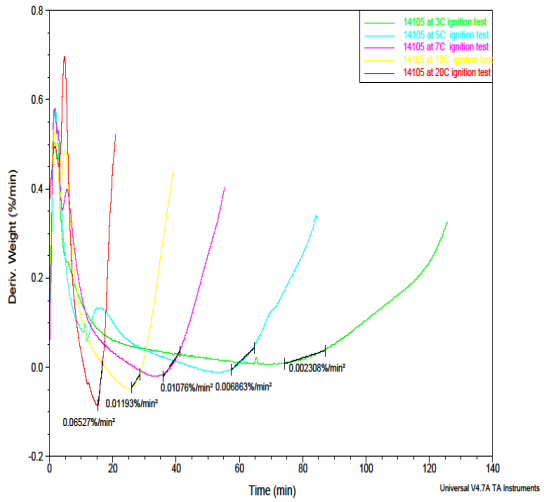
Appendix 51: Oxygen absorption for sample Z05 at 10 degree C ramp (TGA)



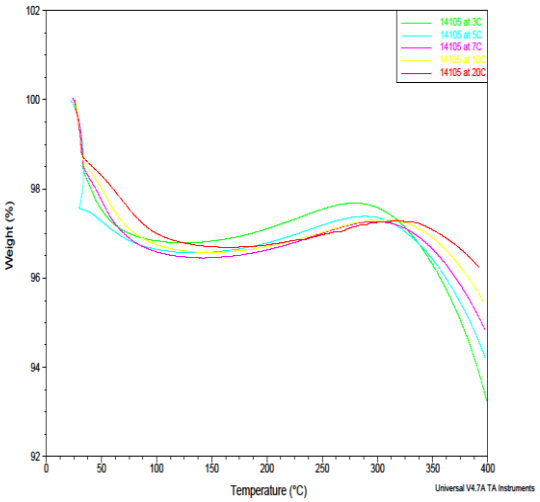
Appendix 52: Oxygen absorption for sample Z05 at 20 degree C ramp (TGA)



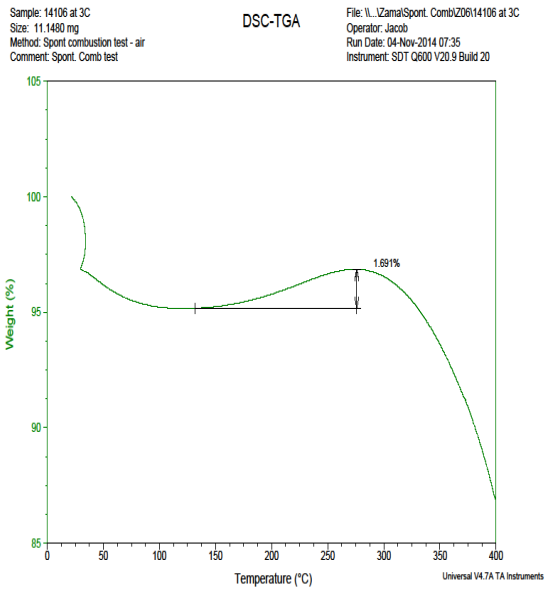
Appendix 53: Ignition test mix for sample Z05 (TGA)



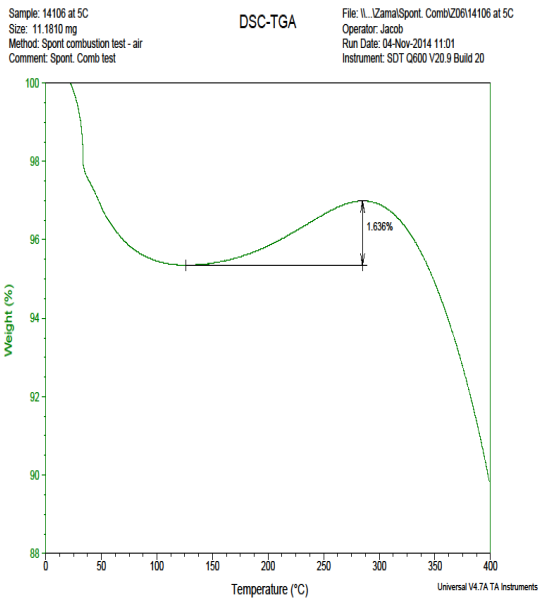
Appendix 54: Oxygen absorption mix for sample Z05 (TGA)



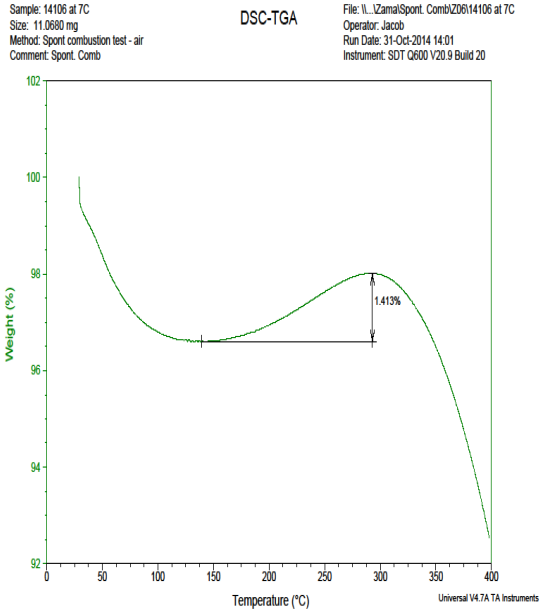
Appendix 55: Oxygen absorption for sample Z06 at 3 degree C ramp (TGA)



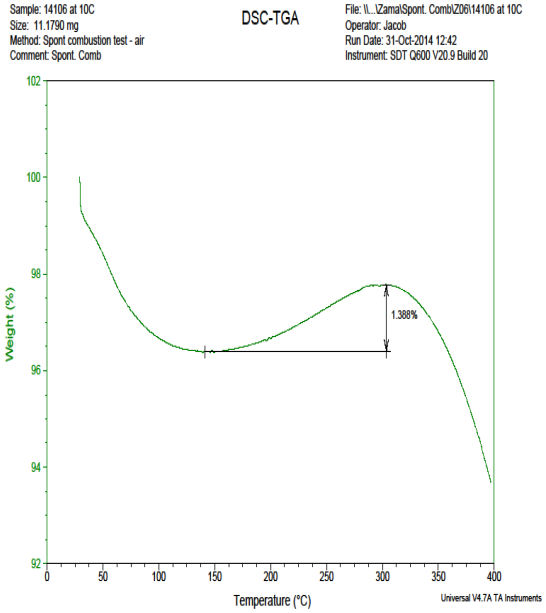
Appendix 56: Oxygen absorption for sample Z06 at 5 degree C ramp (TGA)



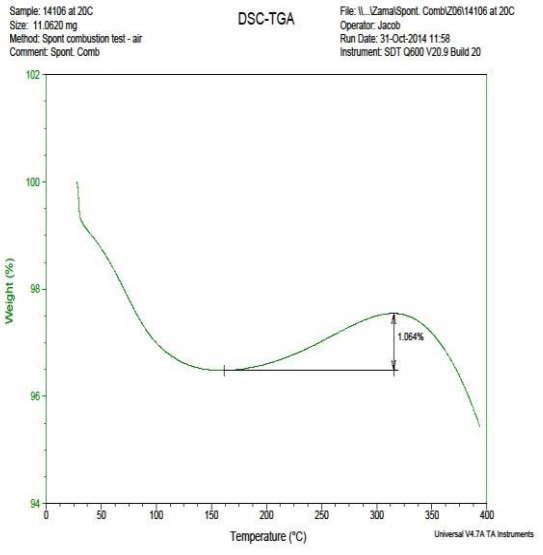
Appendix 57: Oxygen absorption for sample Z06 at 7degree C ramp (TGA)



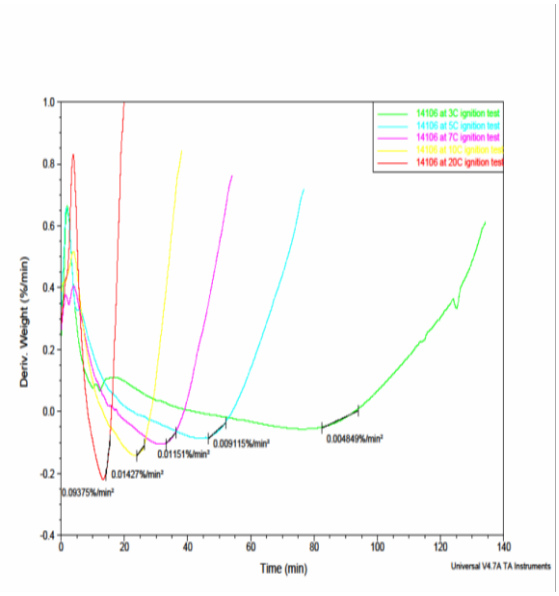
Appendix 58: Oxygen absorption for sample Z06 at 10 degree C ramp (TGA)



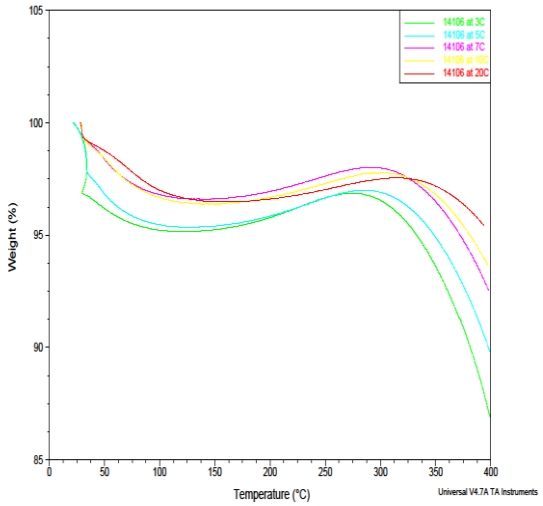
Appendix 59: Oxygen absorption for sample Z06 at 20 degree C ramp (TGA)



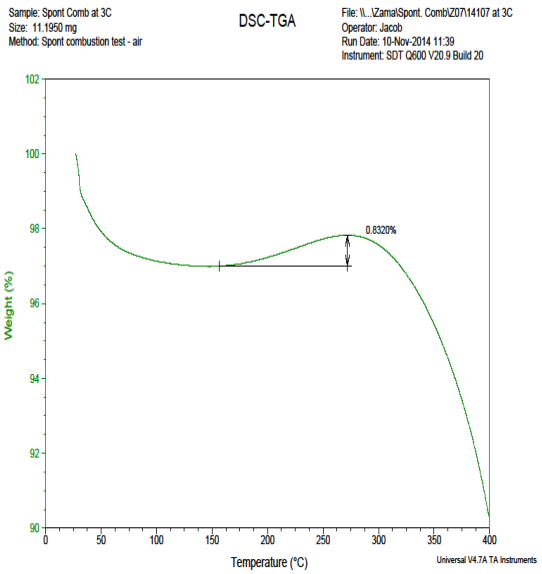
Appendix 60: Ignition test mix for sample Z06 (TGA)



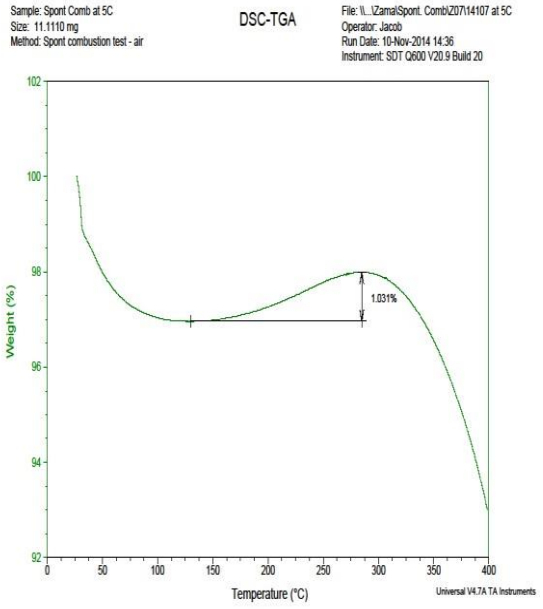
Appendix 61: Oxygen absorption mix for sample Z06 (TGA)



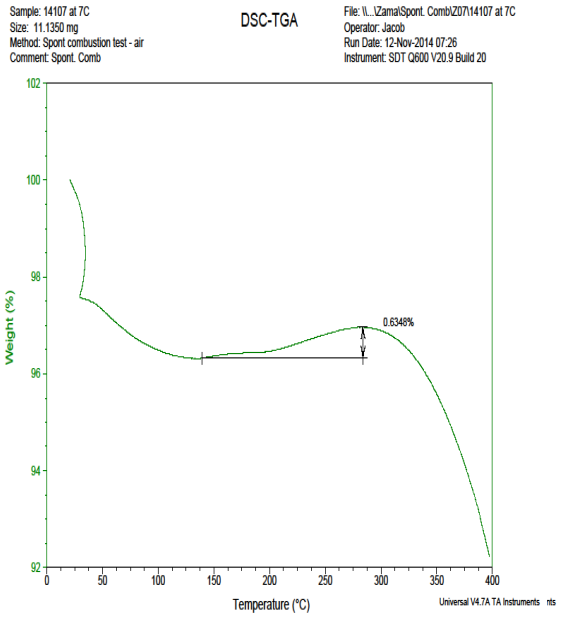
Appendix 62: Oxygen absorption for sample Z07 at 3 degree C ramp (TGA)



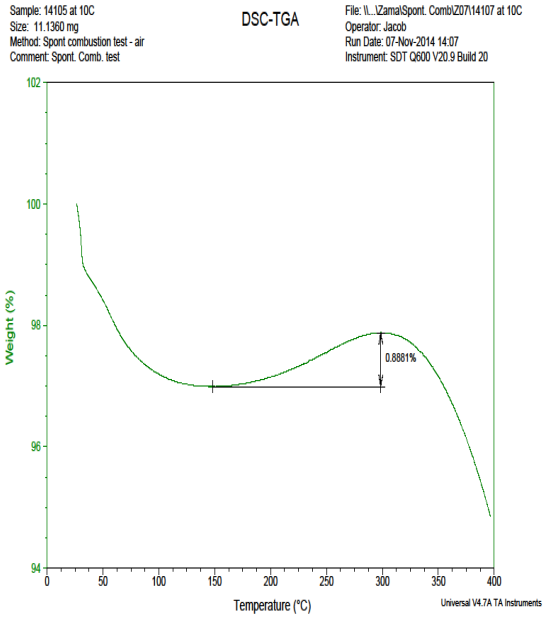
Appendix 63: Oxygen absorption for sample Z07 at 7 degree C ramp (TGA)



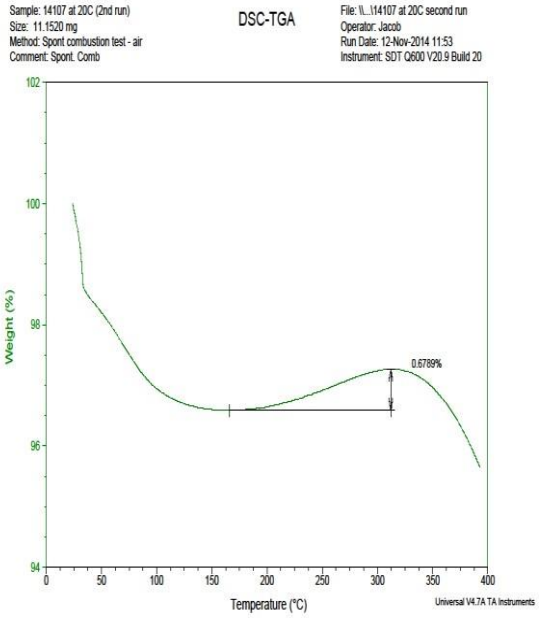
Appendix 64: Oxygen absorption for sample Z07 at 5 degree C ramp (TGA)



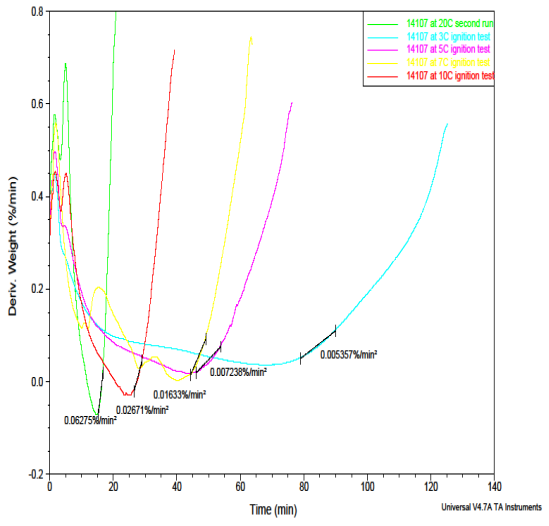
Appendix 65: Oxygen absorption for sample Z07 at 10 degree C ramp (TGA)



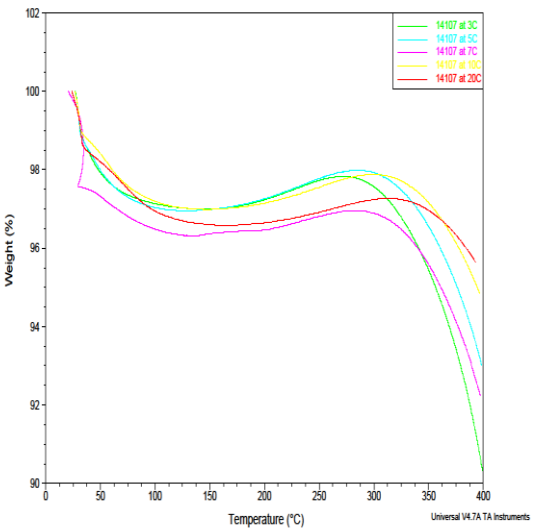
Appendix 66: Oxygen absorption for sample Z07 at 20 degree C ramp (TGA)



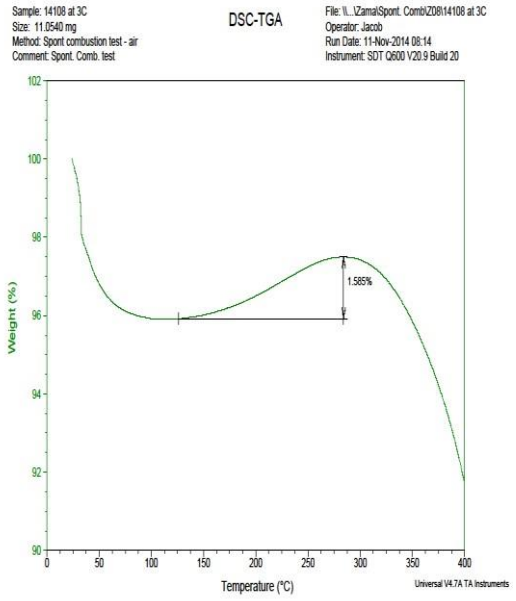
Appendix 67: Ignition test mix for sample Z07 (TGA)



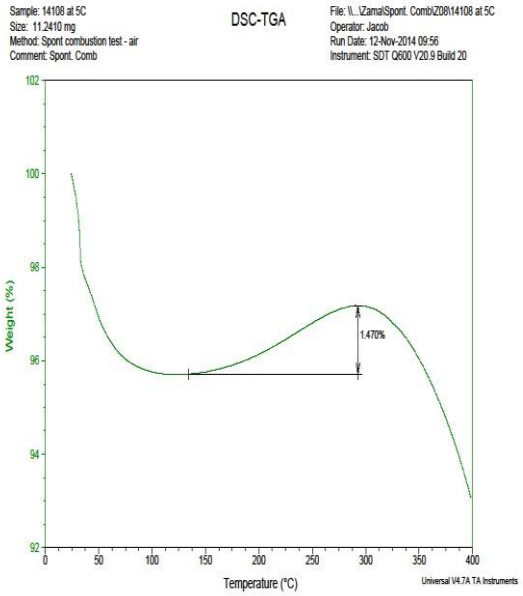
Appendix 68: Oxygen absorption mix for sample Z07 (TGA)



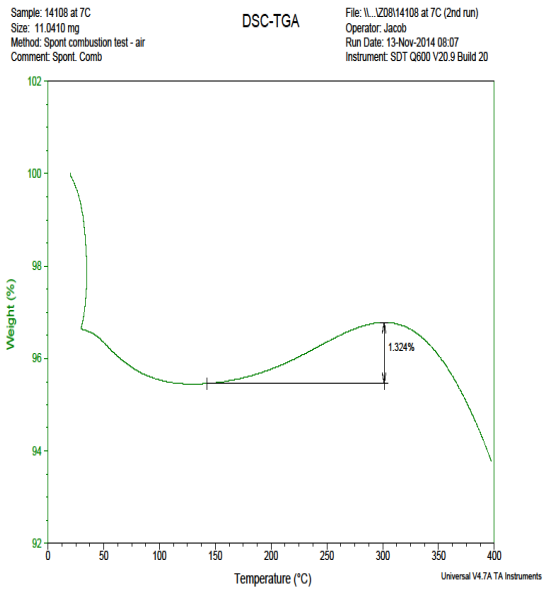
Appendix 69: Oxygen absorption for sample Z08 at 3 degree C ramp (TGA)



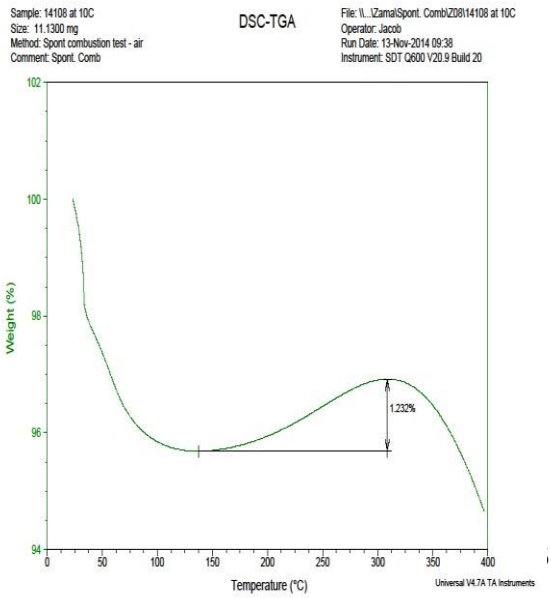
Appendix 70: Oxygen absorption for sample Z08 at 5 degree C ramp (TGA)



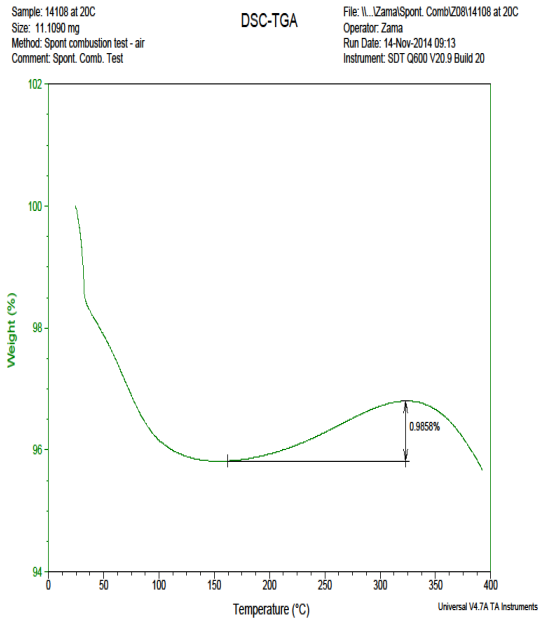
Appendix 71: Oxygen absorption for sample Z08 at 7 degree C ramp (TGA)



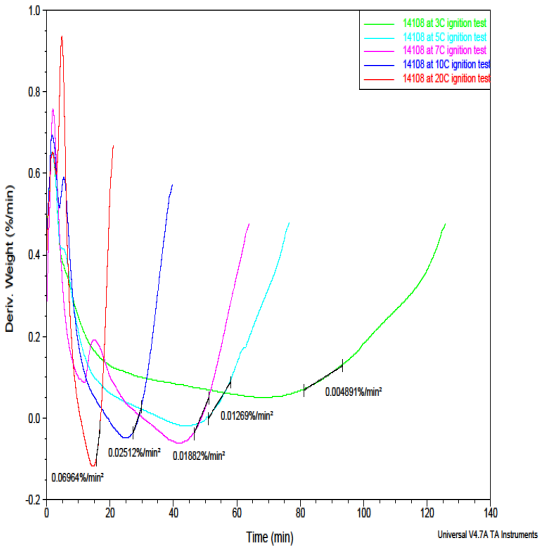
Appendix 72: Oxygen absorption for sample Z08 at 10 degree C ramp (TGA)



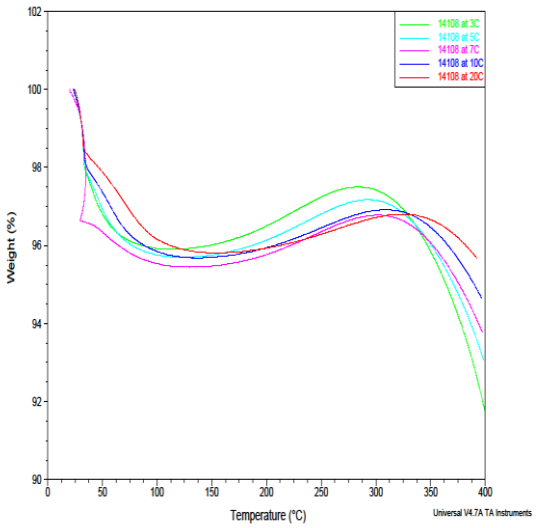
Appendix 73: Oxygen absorption for sample Z08 at 20 degree C ramp (TGA)



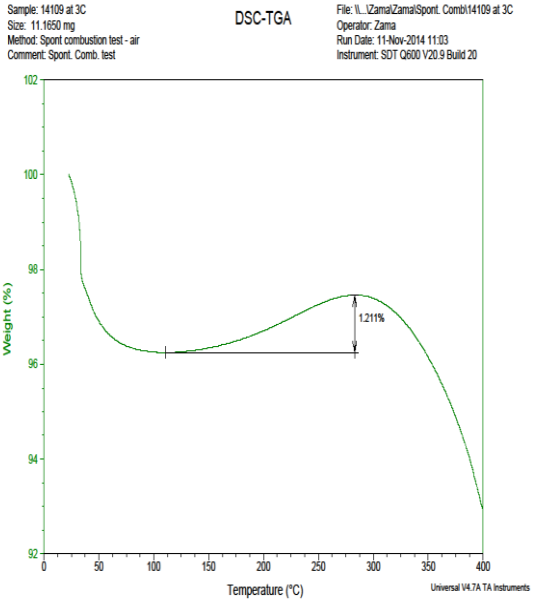
Appendix 74: Ignition test mix for sample Z08 (TGA)



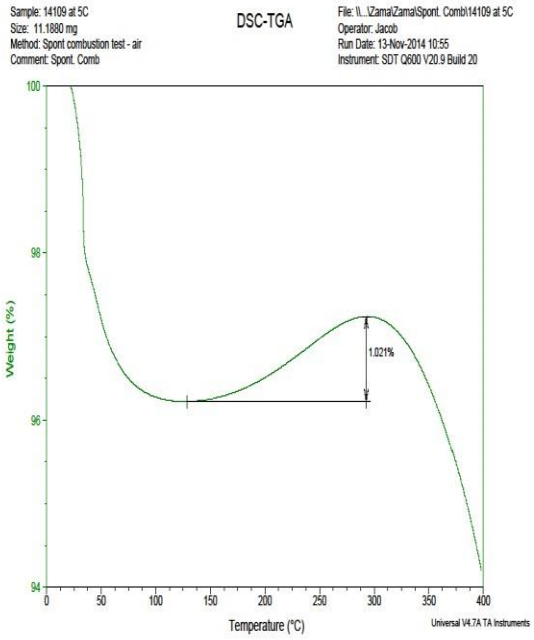
Appendix 75: Oxygen absorption mix for sample Z08 (TGA)



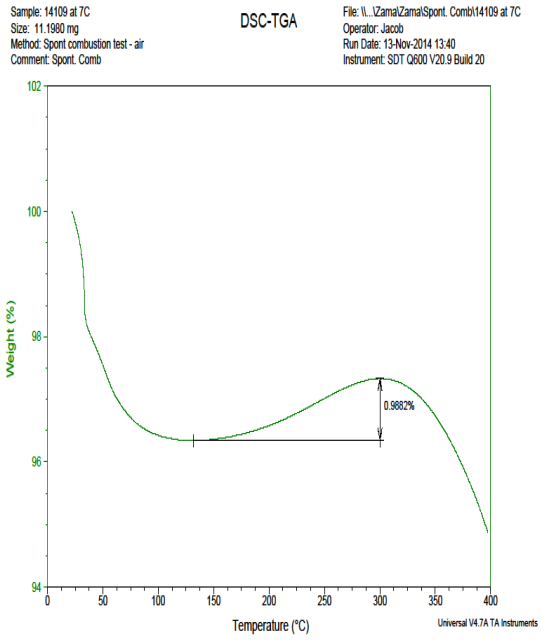
Appendix 76: Oxygen absorption for sample Z09 at 3 degree C ramp (TGA)



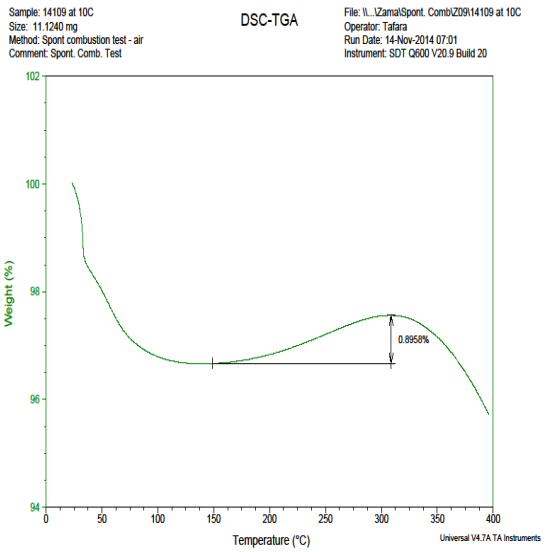
Appendix 77: Oxygen absorption for sample Z09 at 5 degree C ramp (TGA)



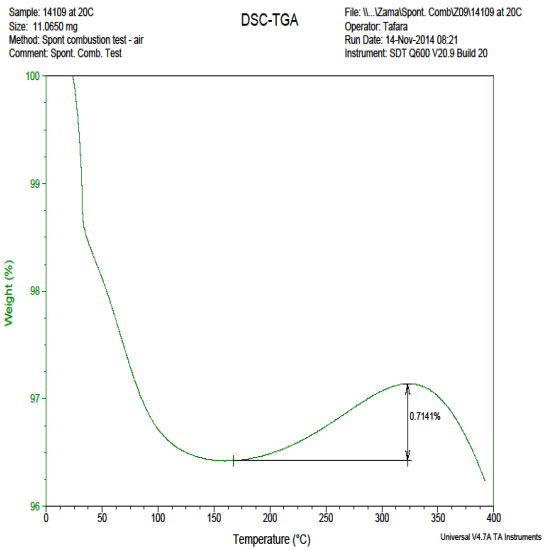
Appendix 78: Oxygen absorption for sample Z09 at 7 degree C ramp (TGA)



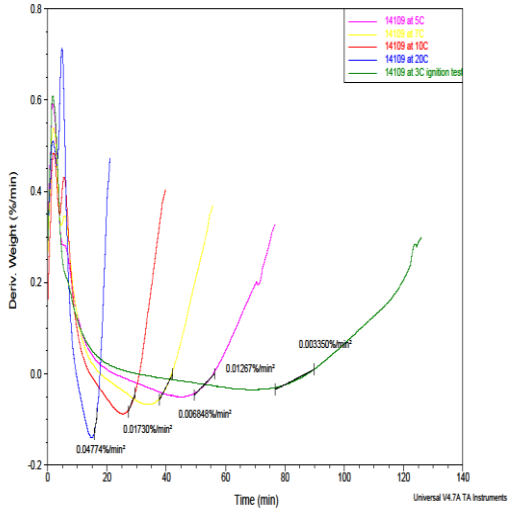
Appendix 79: Oxygen absorption for sample Z09 at 10 degree C ramp (TGA)



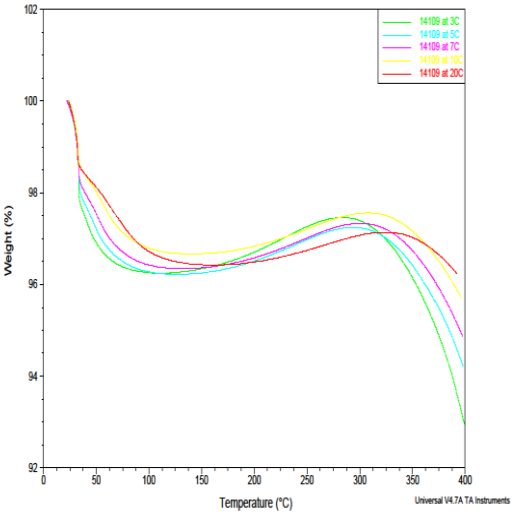
Appendix 80: Oxygen absorption for sample Z09 at 20 degree C ramp (TGA)



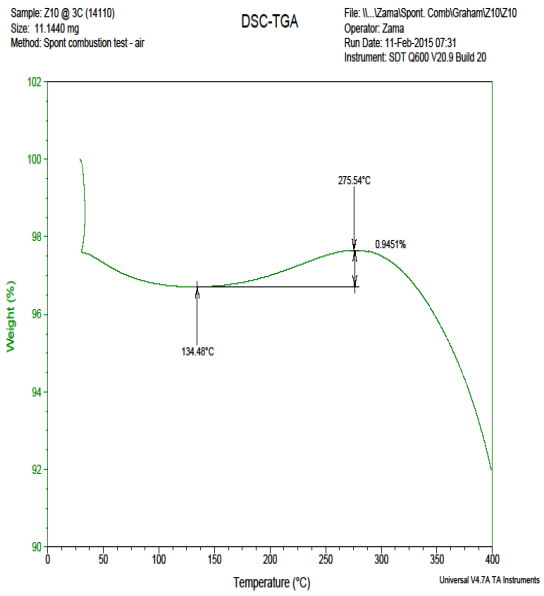
Appendix 81: Ignition test mix for sample Z09 (TGA)



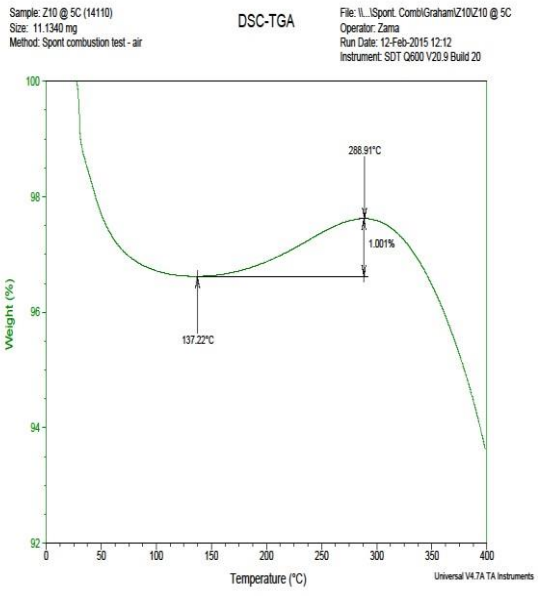
Appendix 82: Oxygen absorption mix for sample Z09 (TGA)



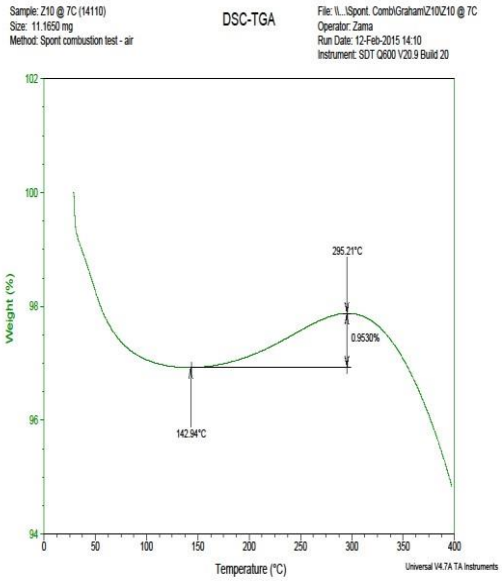
Appendix 83: Oxygen absorption for sample Z10 at 3 degree C ramp (TGA)



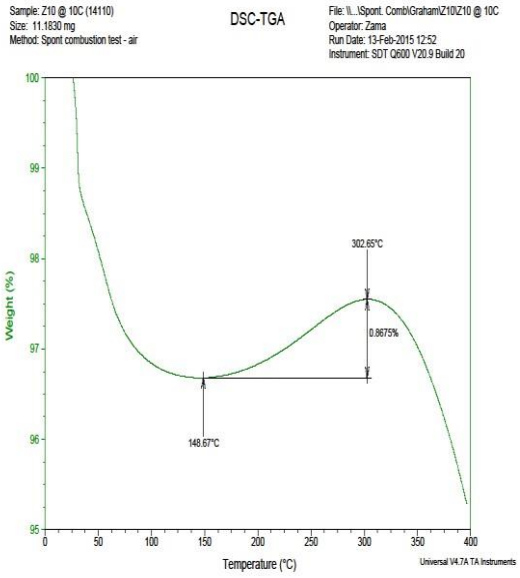
Appendix 84: Oxygen absorption for sample Z10 at 5 degree C ramp (TGA)



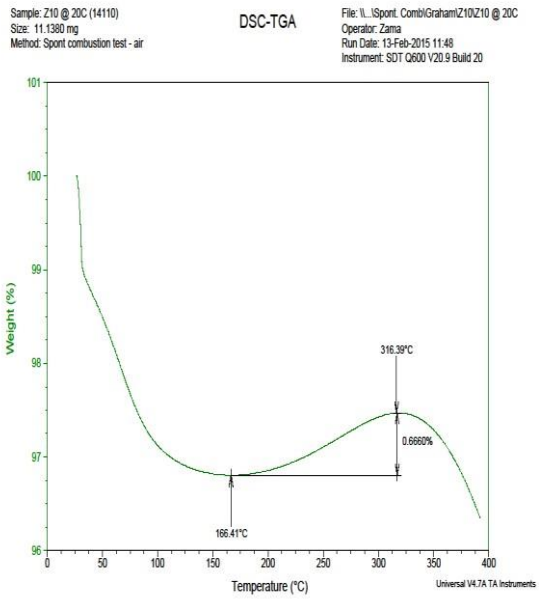
Appendix 85: Oxygen absorption for sample Z10 at 7 degree C ramp (TGA)



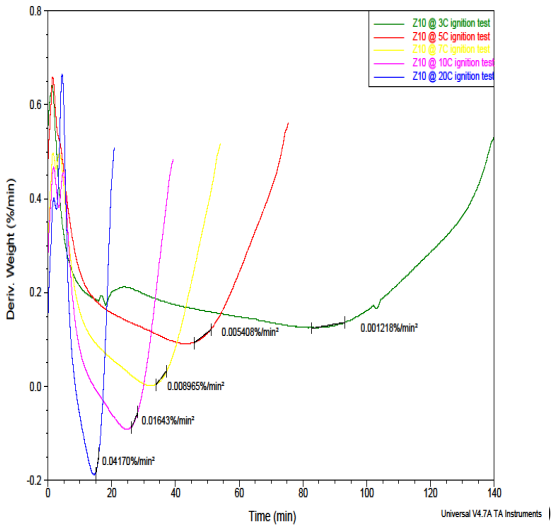
Appendix 86: Oxygen absorption for sample Z10 at 10 degree C ramp (TGA)



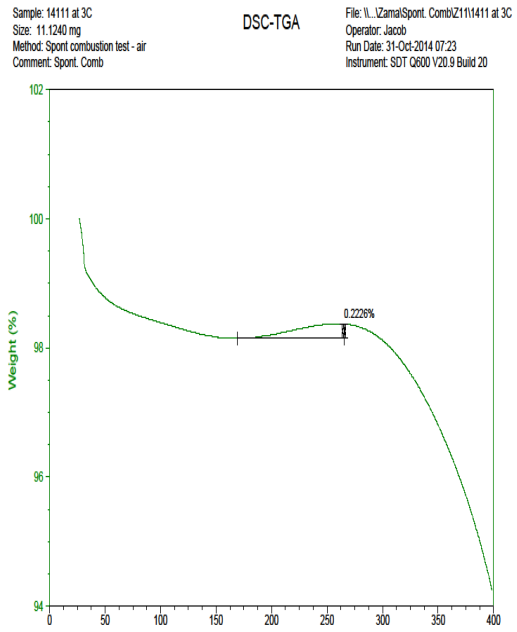
Appendix 87: Oxygen absorption for sample Z10 at 20 degree C ramp (TGA)



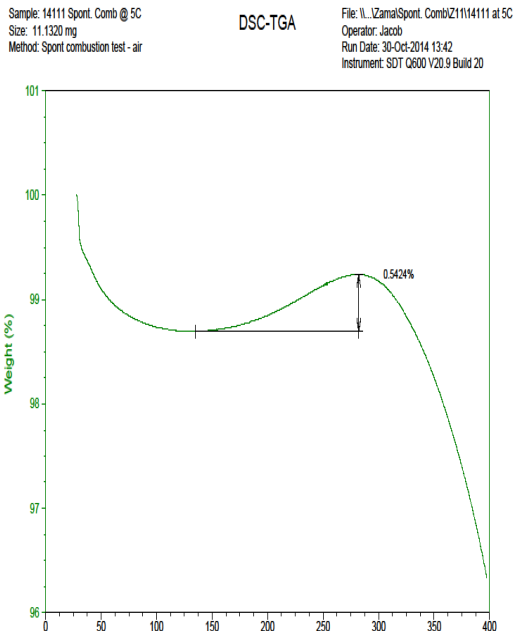
Appendix 88: Ignition test mix for sample Z10 (TGA)



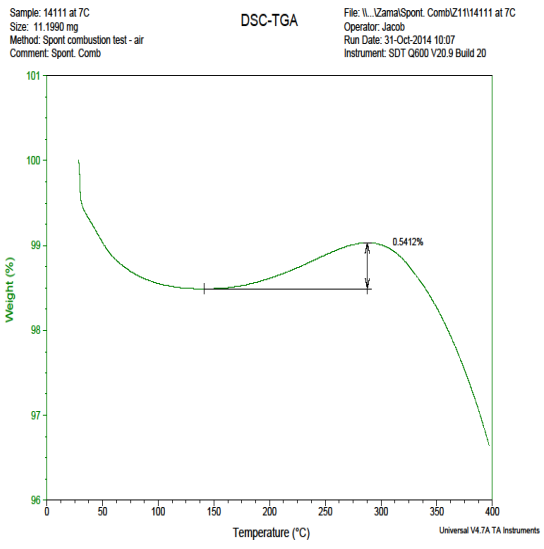
Appendix 89: Oxygen absorption for sample Z11 at 3 degree C ramp (TGA)



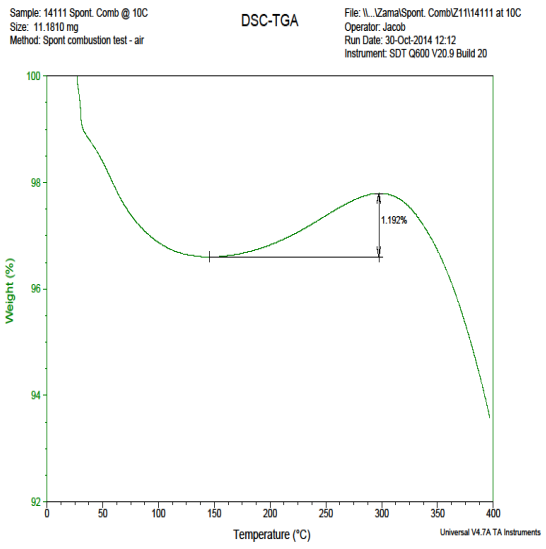
Appendix 90: Oxygen absorption for sample Z11 at 5 degree C ramp (TGA)



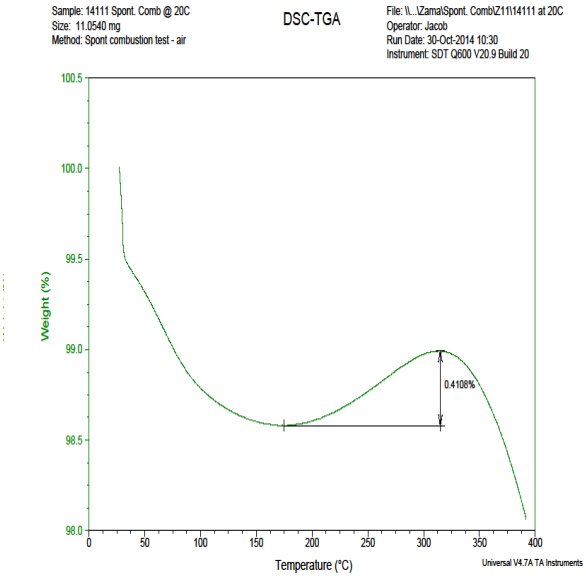
Appendix 91: Oxygen absorption for sample Z11 at 7 degree C ramp (TGA)



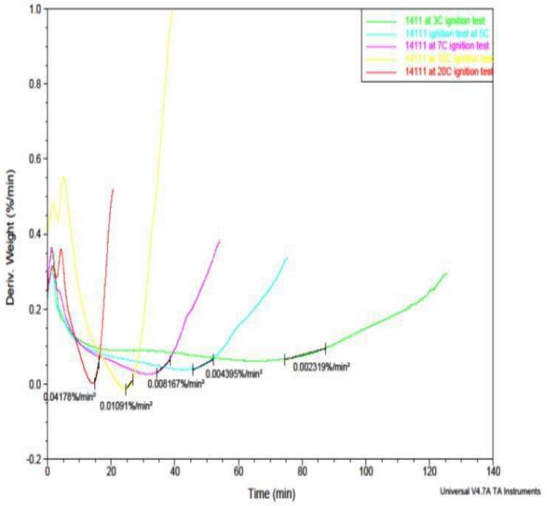
Appendix 92: Oxygen absorption for sample Z11 at 10 degree C ramp (TGA)



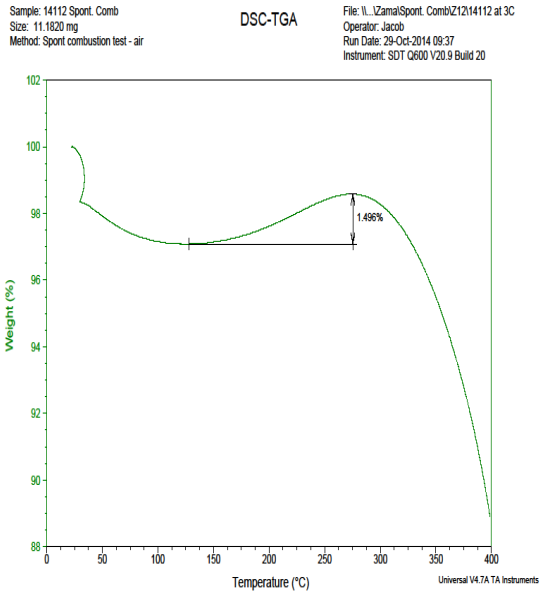
Appendix 93: Oxygen absorption for sample Z11 at 20 degree C ramp (TGA)



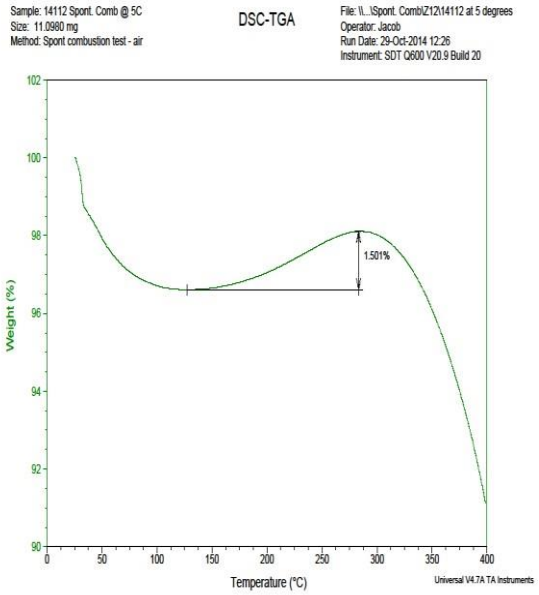
Appendix 94: Ignition test mix for sample Z11 (TGA)



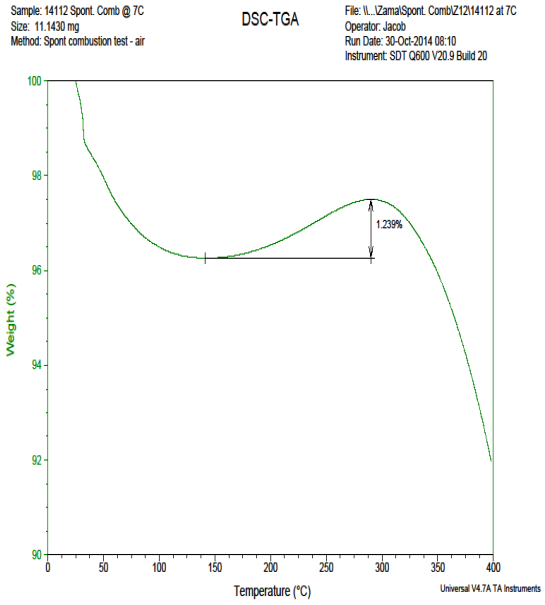
Appendix 95: Oxygen absorption for sample Z12 at 3 degree C ramp (TGA)



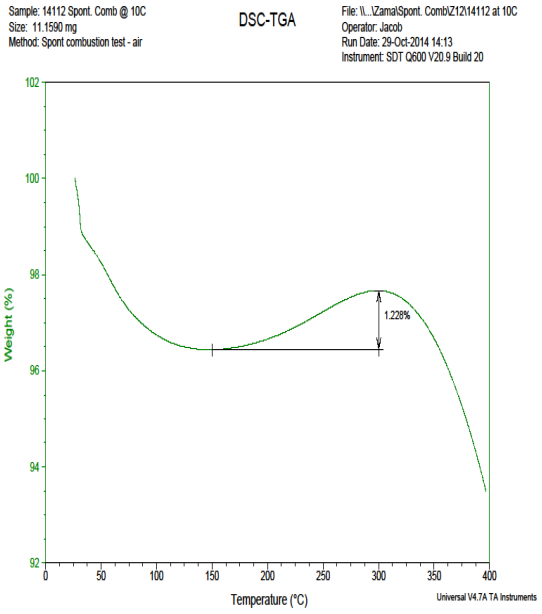
Appendix 96: Oxygen absorption for sample Z12 at 5 degree C ramp (TGA)



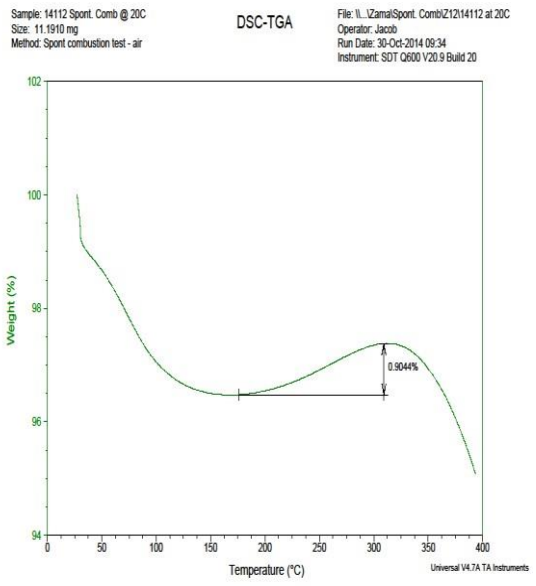
Appendix 97: Oxygen absorption for sample Z12 at 7 degree C ramp (TGA)



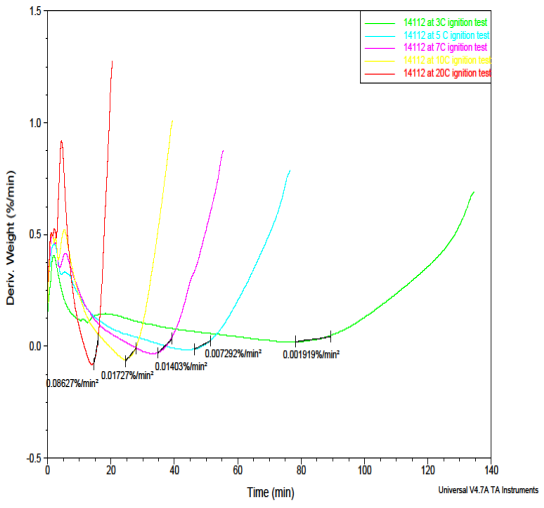
Appendix 98: Oxygen absorption for sample Z12 at 10 degree C ramp (TGA)



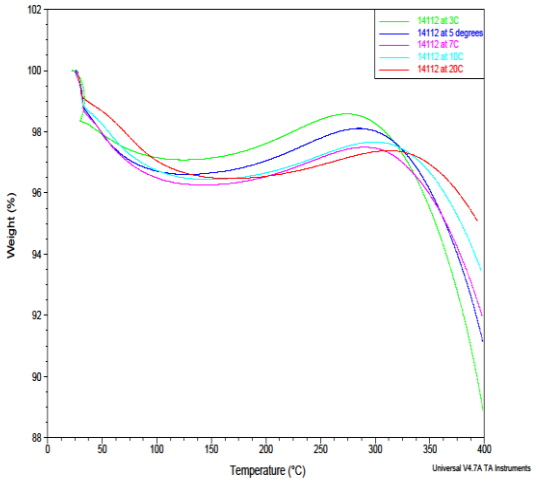
Appendix 99: Oxygen absorption for sample Z12 at 20 degree C ramp (TGA)



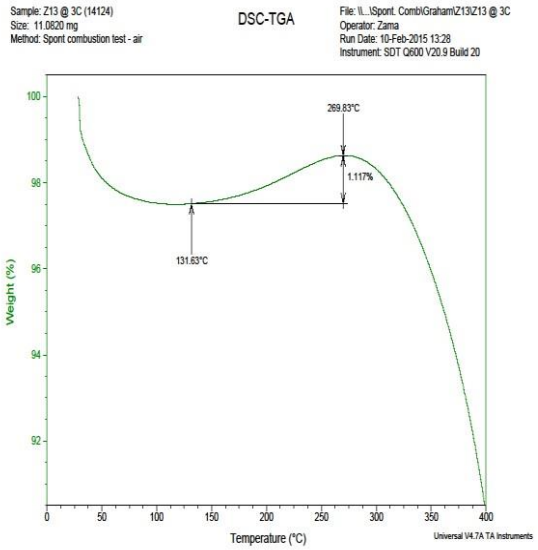
Appendix 100: Ignition test mix for sample Z12 (TGA)



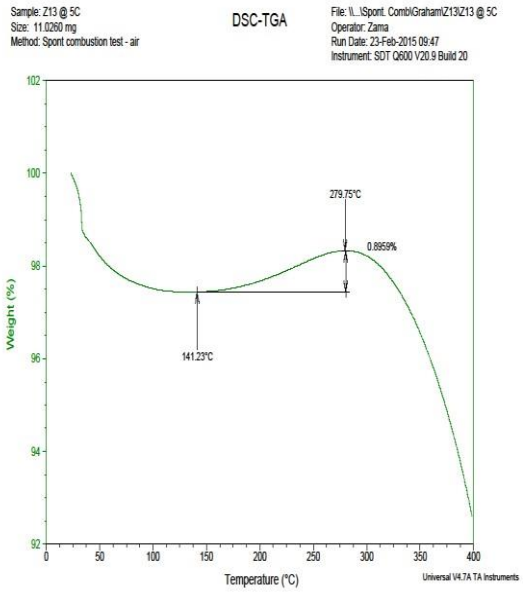
Appendix 101: Oxygen absorption mix for sample Z12 (TGA)



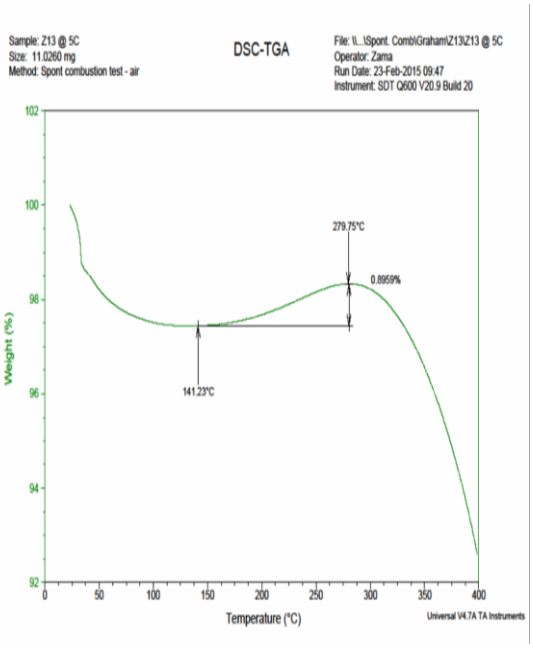
Appendix 102: Oxygen absorption for sample Z13 at 3 degree C ramp (TGA)



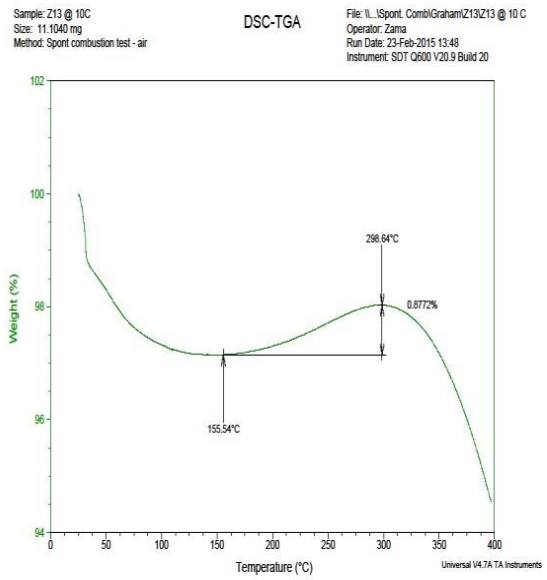
Appendix 103: Oxygen absorption for sample Z13 at 5 degree C ramp (TGA)



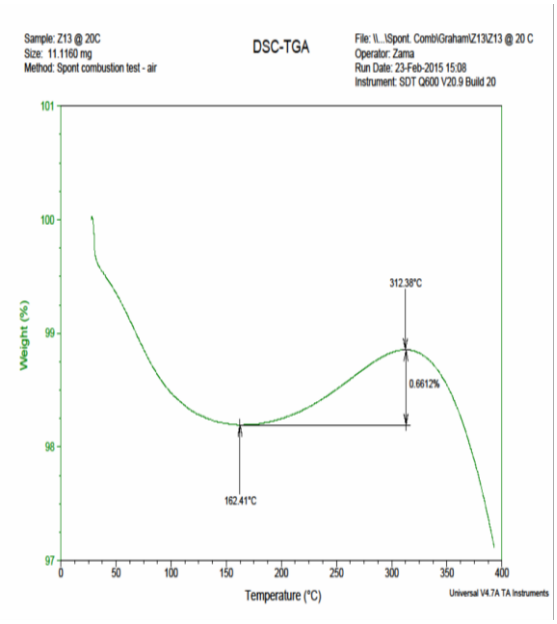
Appendix 104: Oxygen absorption for sample Z13 at 7 degree C ramp (TGA)



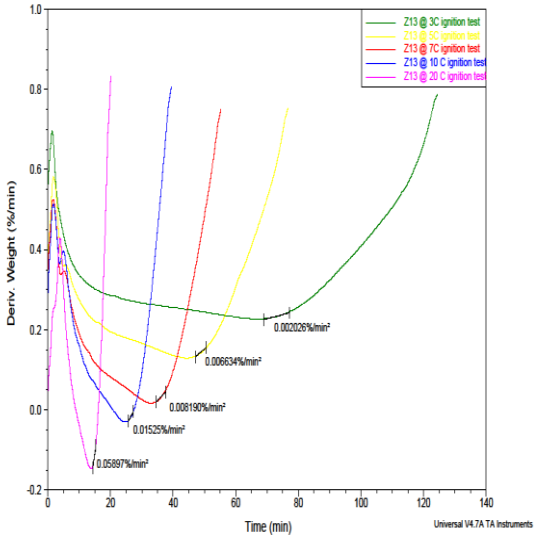
Appendix 105: Oxygen absorption for sample Z13 at 10 degree C ramp (TGA)



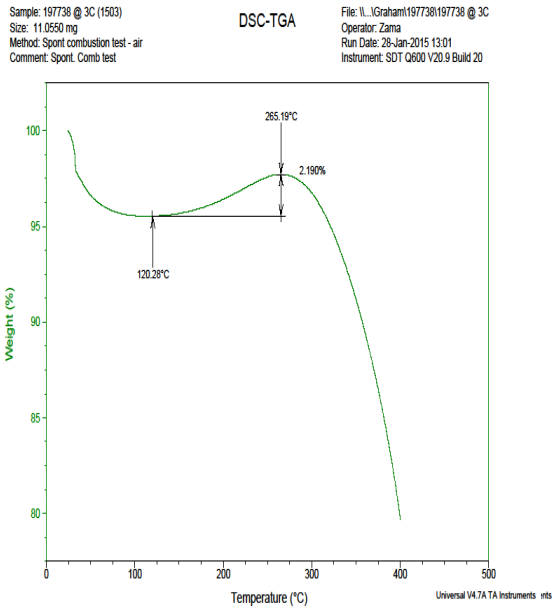
Appendix 106: Oxygen absorption for sample Z13 at 20 degree C ramp (TGA)



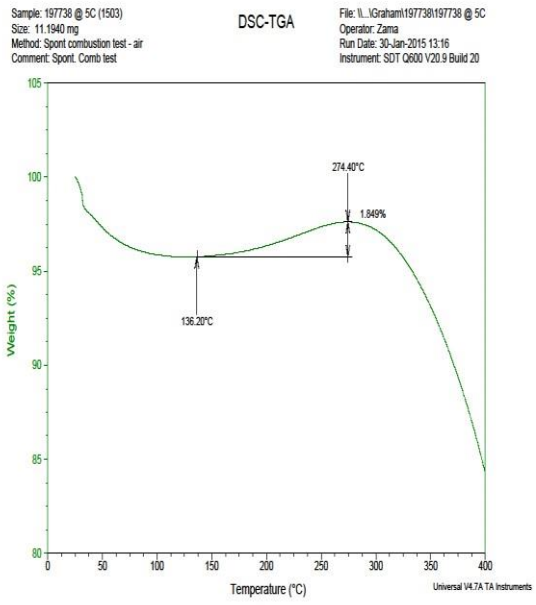
Appendix 107: Ignition test mix for sample Z13 (TGA)



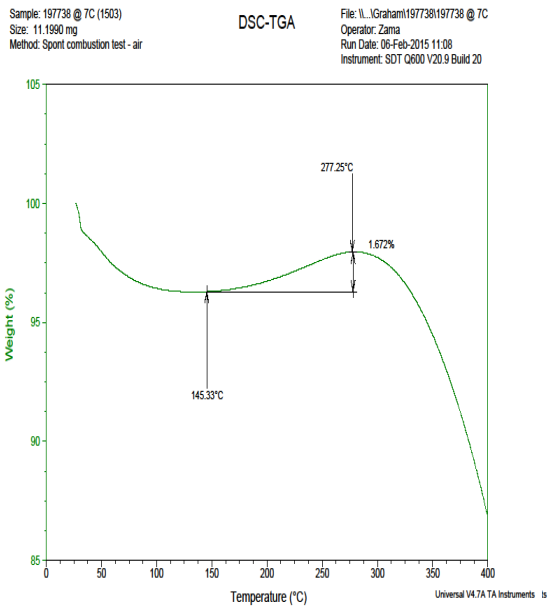
Appendix 108: Oxygen absorption for sample Z14 at 3 degree C ramp (TGA)



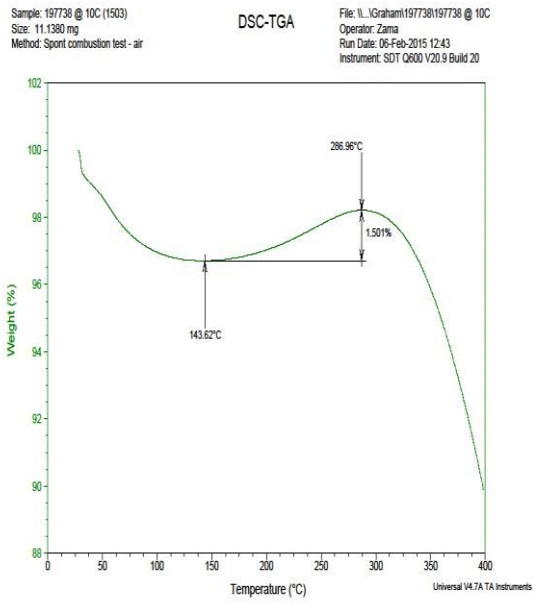
Appendix 109: Oxygen absorption for sample Z14 at 5 degree C ramp (TGA)



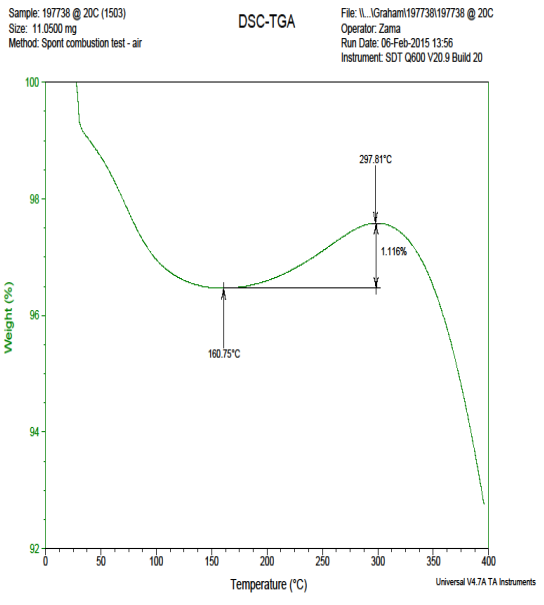
Appendix 110: Oxygen absorption for sample Z14 at 7 degree C ramp (TGA)



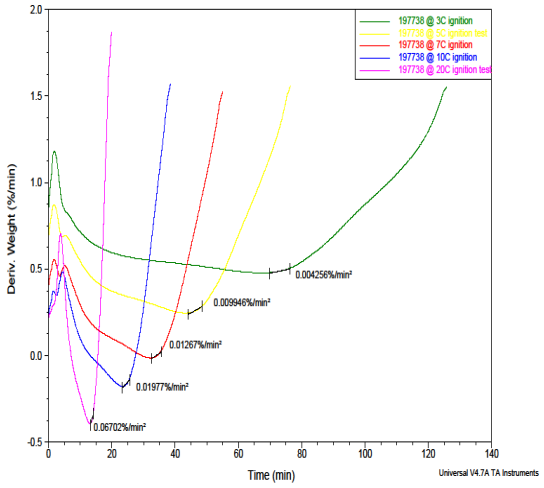
Appendix 111: Oxygen absorption for sample Z14 at 10 degree C ramp (TGA)



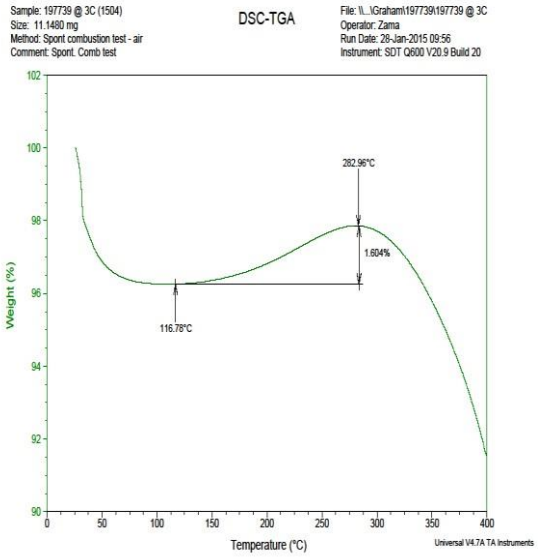
Appendix 112: Oxygen absorption for sample Z14 at 20 degree C ramp (TGA)



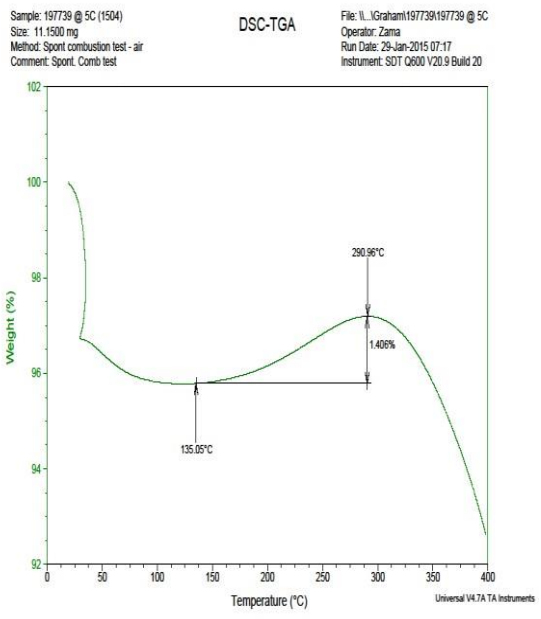
Appendix 113: Ignition test mix for sample Z14 (TGA)



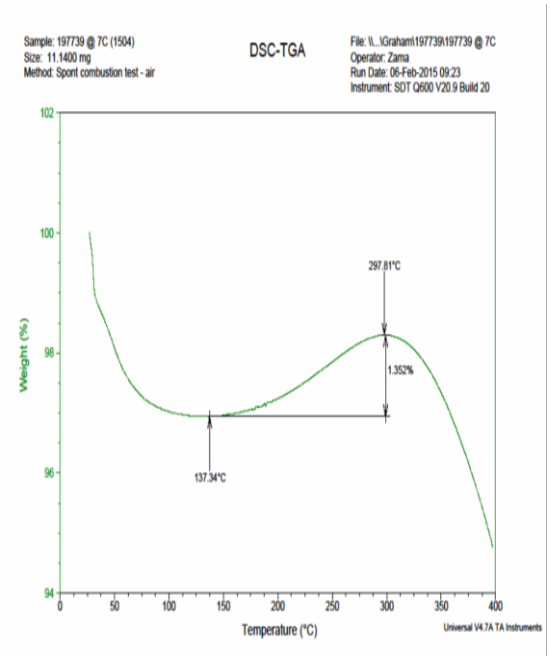
Appendix 114: Oxygen absorption for sample Z15 at 3 degree C ramp (TGA)



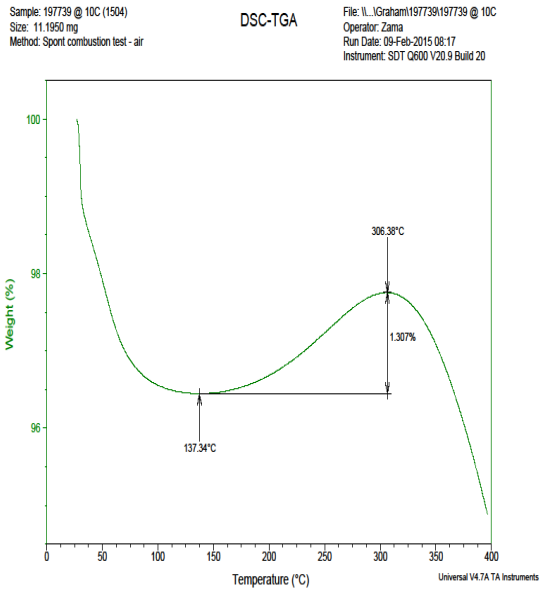
Appendix 115: Oxygen absorption for sample Z15 at 5 degree C ramp (TGA)



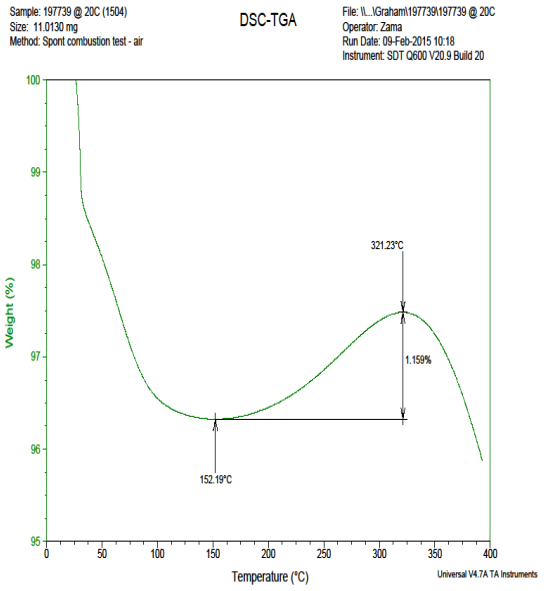
Appendix 116: Oxygen absorption for sample Z15 at 7 degree C ramp (TGA)



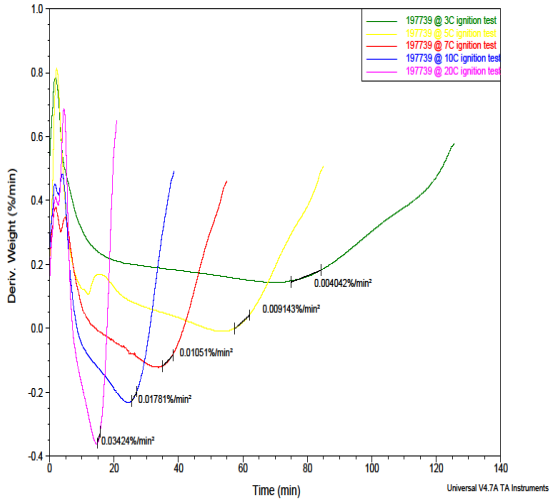
Appendix 117: Oxygen absorption for sample Z15 at 10 degree C ramp (TGA)



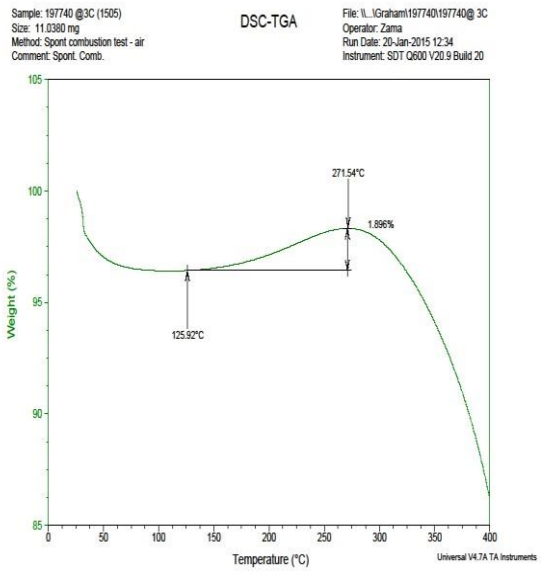
Appendix 118: Oxygen absorption for sample Z15 at 20 degree C ramp (TGA)



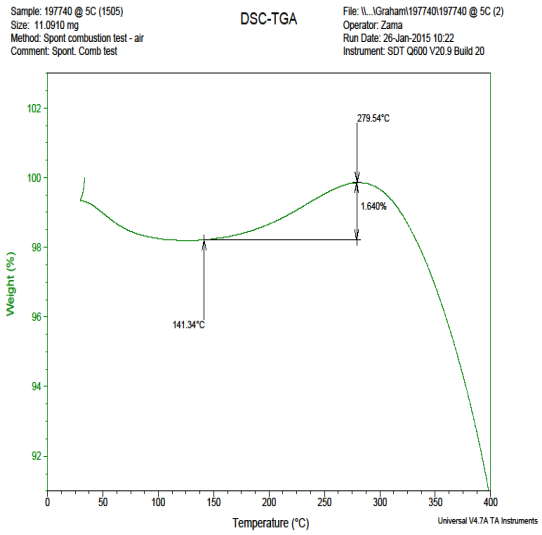
Appendix 119: Ignition test mix for sample Z15 (TGA)



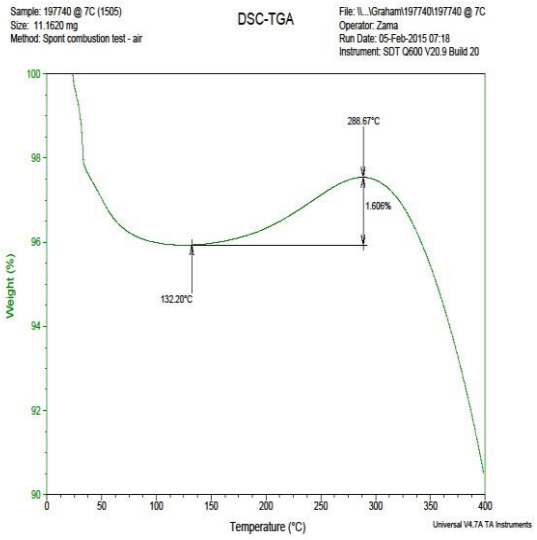
Appendix 120: Oxygen absorption for sample Z16 at 3 degree C ramp (TGA)



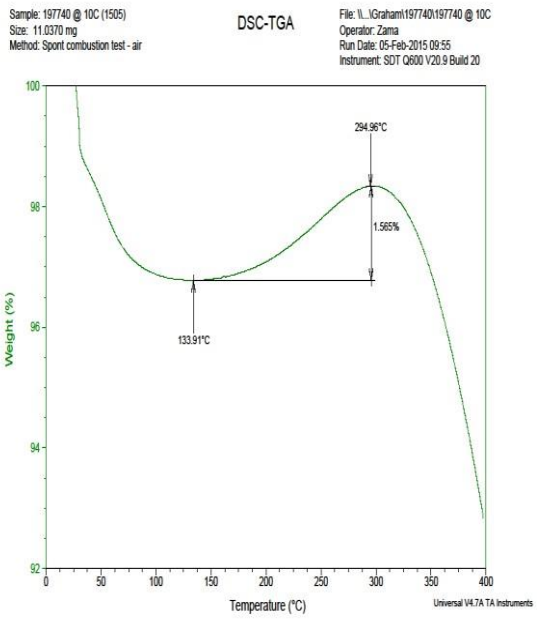
Appendix 121: Oxygen absorption for sample Z16 at 5 degree C ramp (TGA)



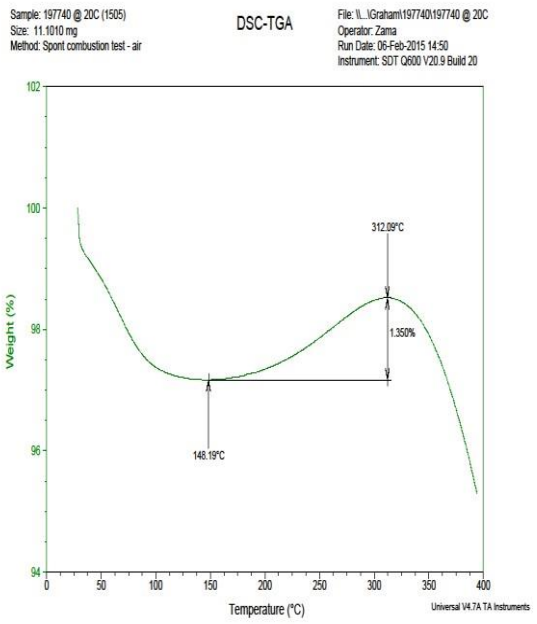
Appendix 122: Oxygen absorption for sample Z16 at 7 degree C ramp (TGA)



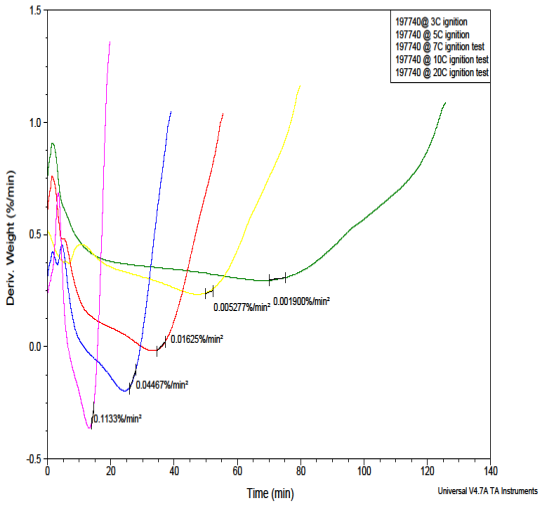
Appendix 123: Oxygen absorption for sample Z16 at 10 degree C ramp (TGA)



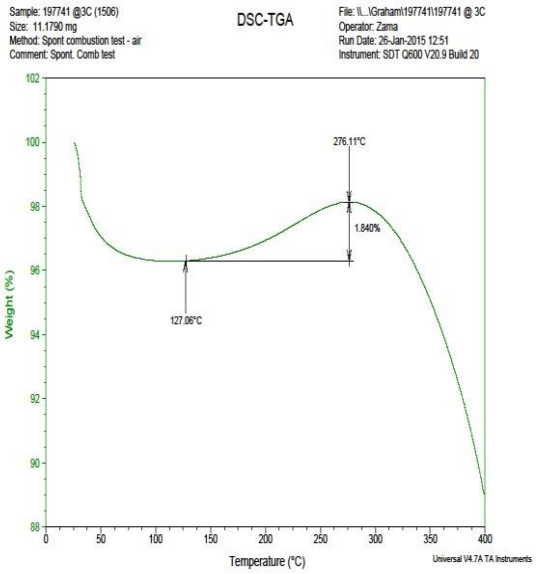
Appendix 124: Oxygen absorption for sample Z16 at 20 degree C ramp (TGA)



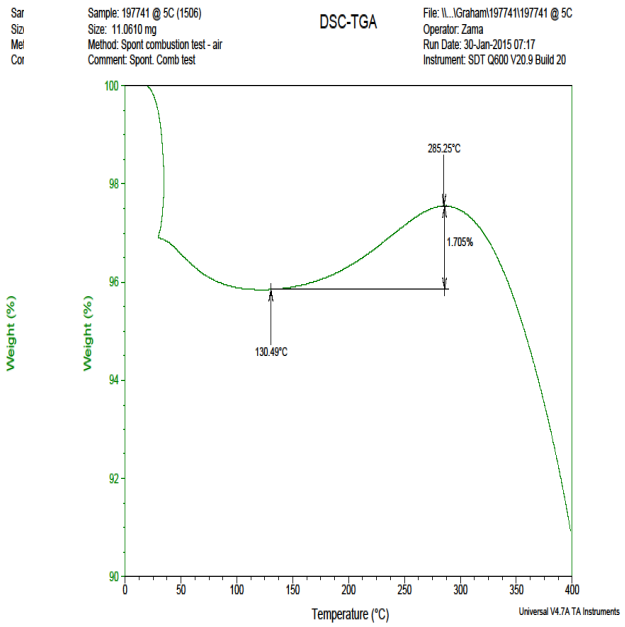
Appendix 125: Ignition test mix for sample Z16 (TGA)



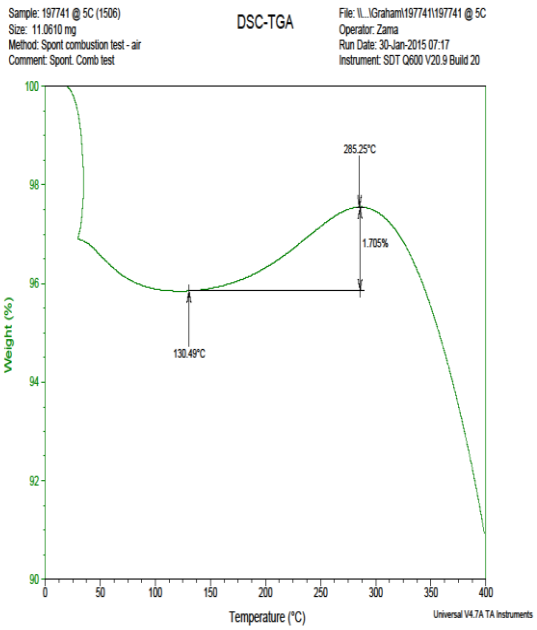
Appendix 126: Oxygen absorption for sample Z17 at 3 degree C ramp (TGA)



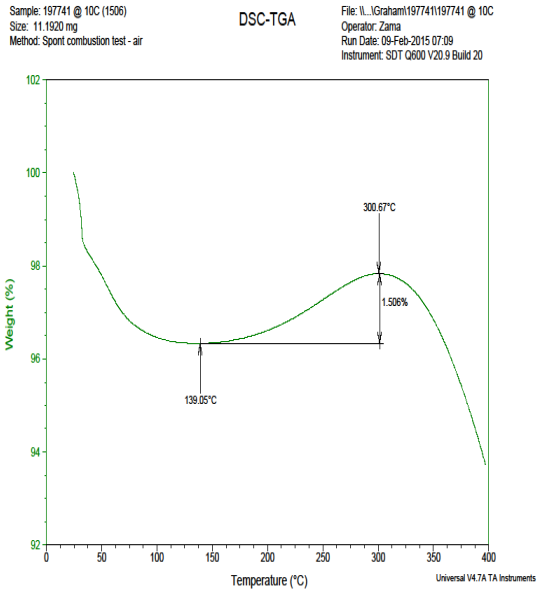
Appendix 127: Oxygen absorption for sample Z17 at 5 degree C ramp (TGA)



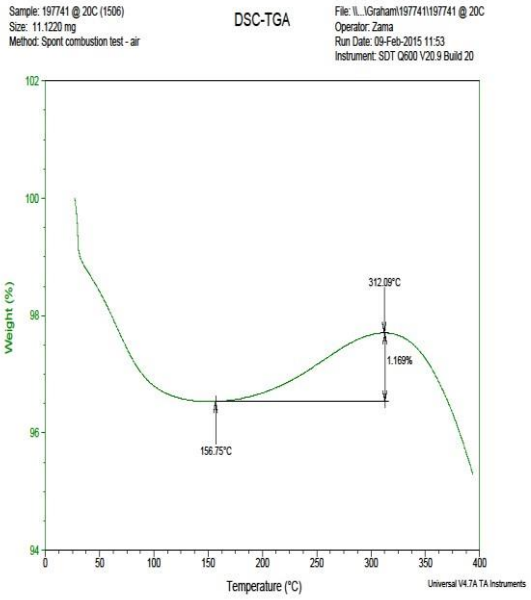
Appendix 128: Oxygen absorption for sample Z17 at 7 degree C ramp (TGA)



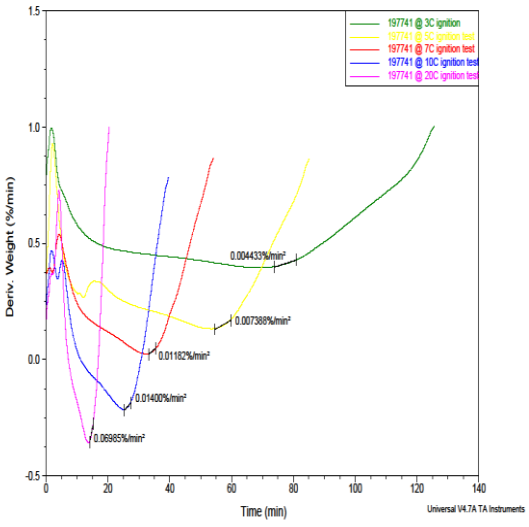
Appendix 129: Oxygen absorption for sample Z17 at 10 degree C ramp (TGA)



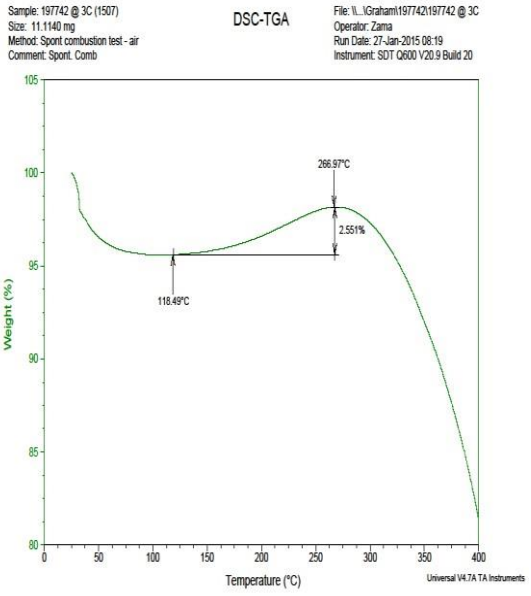
Appendix 130: Oxygen absorption for sample Z17 at 20 degree C ramp (TGA)



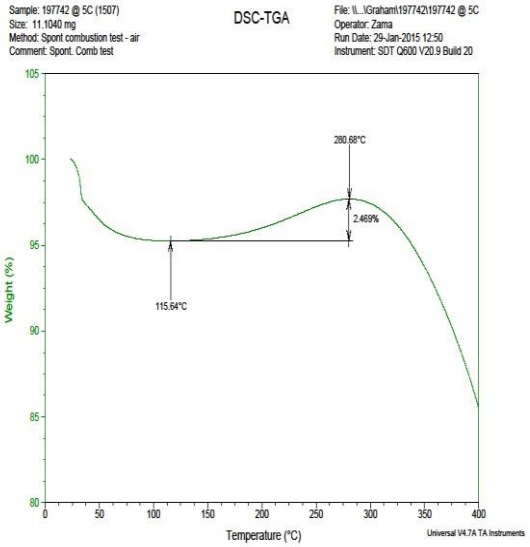
Appendix 131: Ignition test mix for sample Z17 (TGA)



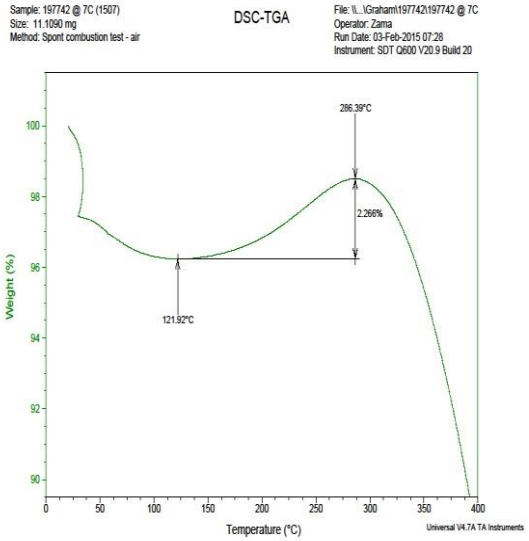
Appendix 132: Oxygen absorption for sample Z18 at 3 degree C ramp (TGA)



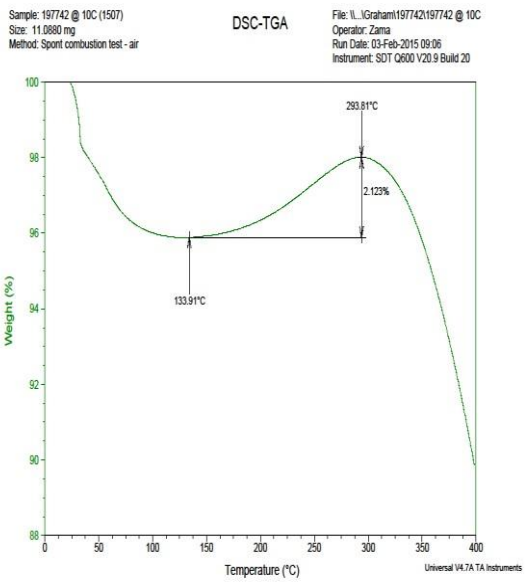
Appendix 133: Oxygen absorption for sample Z18 at 5 degree C ramp (TGA)



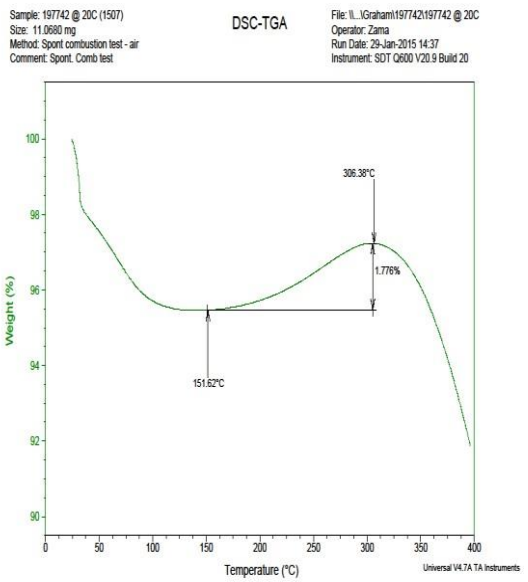
Appendix 134: Oxygen absorption for sample Z18 at 7 degree C ramp (TGA)



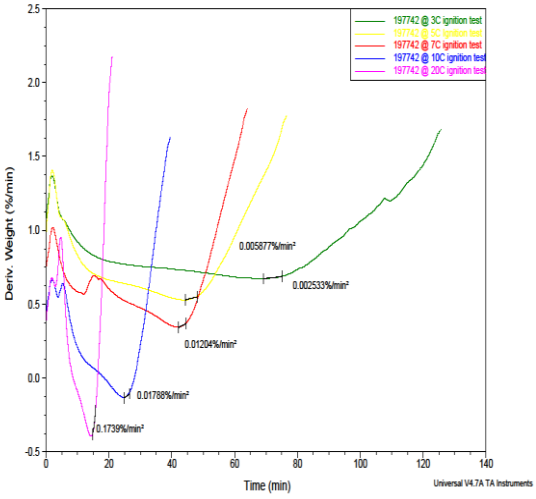
Appendix 135: Oxygen absorption for sample Z18 at 10 degree C ramp (TGA)



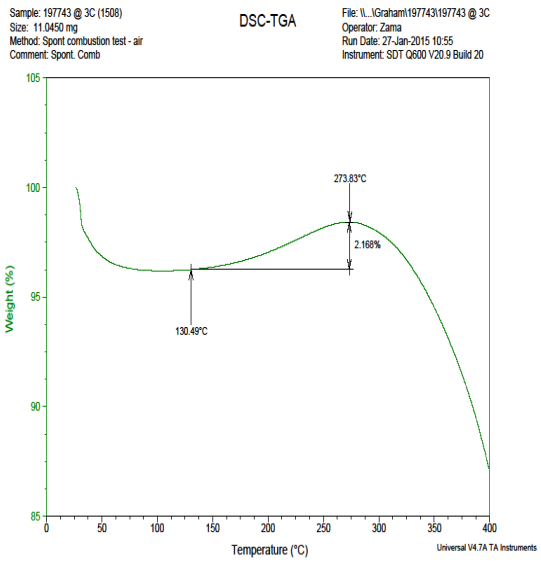
Appendix 136: Oxygen absorption for sample Z18 at 20 degree C ramp (TGA)



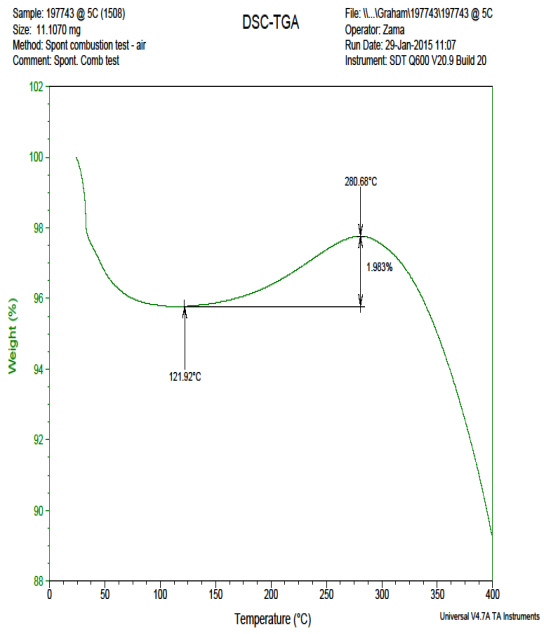
Appendix 137: Ignition test mix for sample Z18 (TGA)



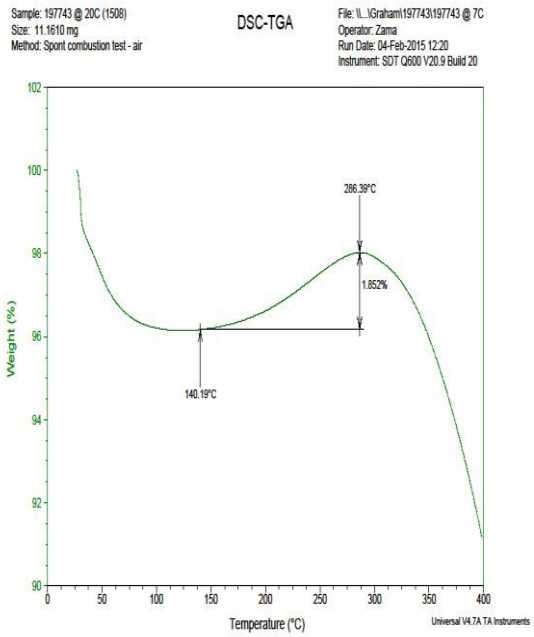
Appendix 138: Oxygen absorption for sample Z19 at 3 degree C ramp (TGA)



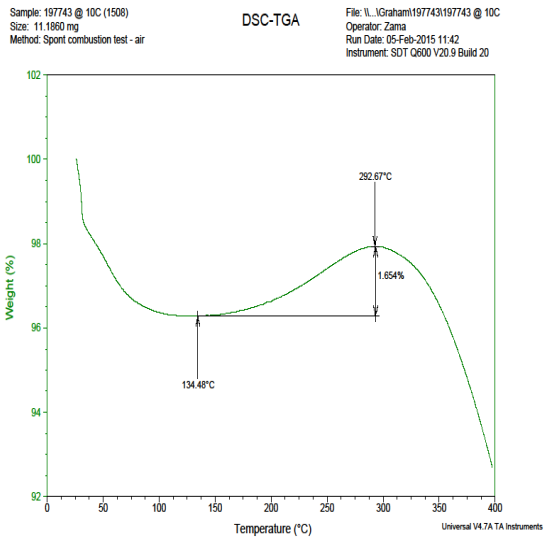
Appendix 139: Oxygen absorption for sample Z19 at 5 degree C ramp (TGA)



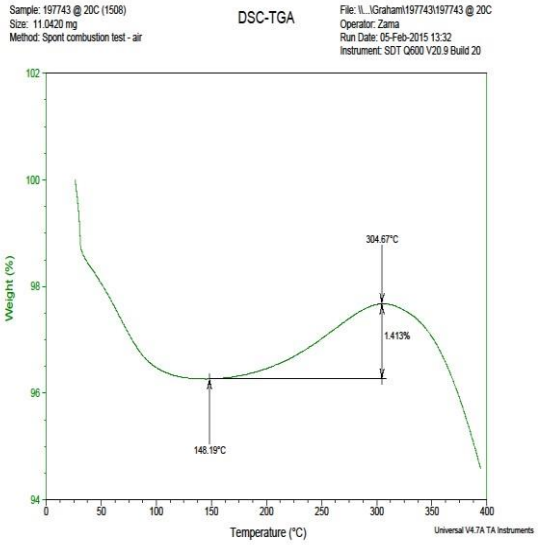
Appendix 140: Oxygen absorption for sample Z19 at 7 degree C ramp (TGA)



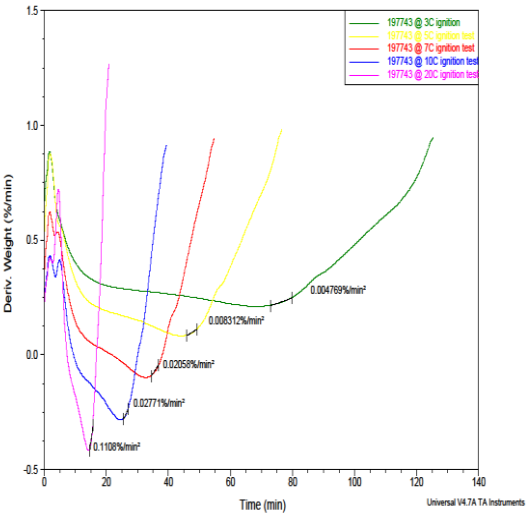
Appendix 141: Oxygen absorption for sample Z19 at 10 degree C ramp (TGA)



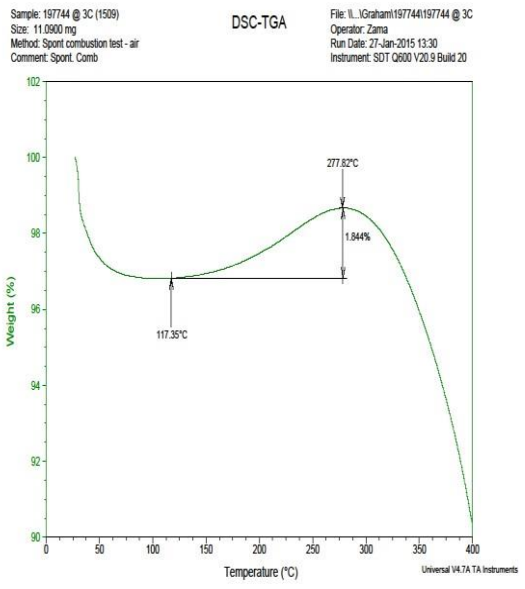
Appendix 142: Oxygen absorption for sample Z19 at 20 degree C ramp (TGA)



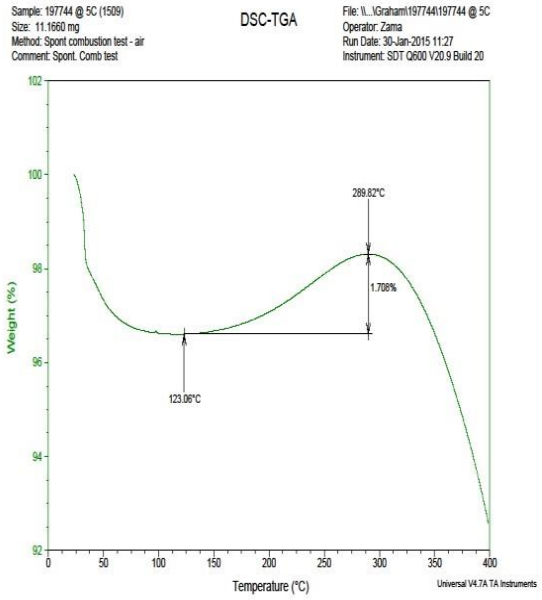
Appendix 143: Ignition test mix for sample Z19 (TGA)



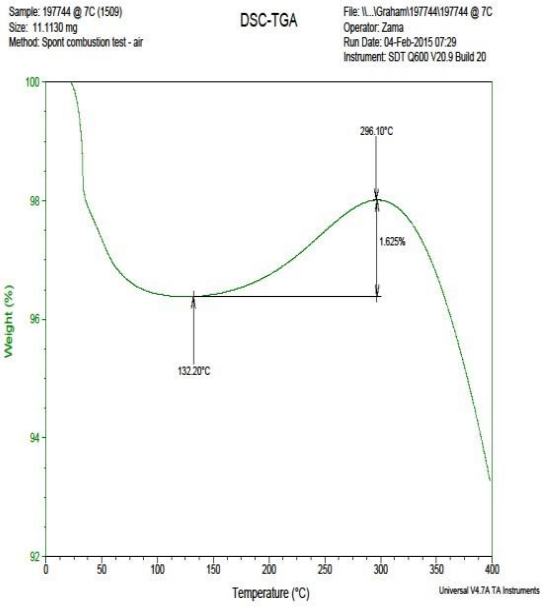
Appendix 144: Oxygen absorption for sample Z20 at 3 degree C ramp (TGA)



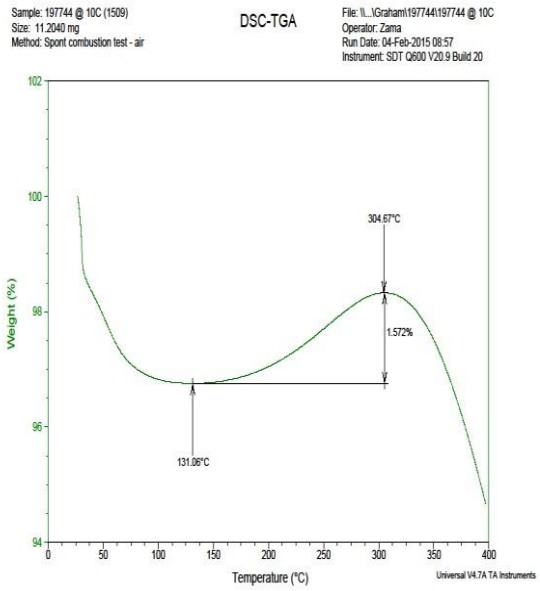
Appendix 145: Oxygen absorption for sample Z20 at 5 degree C ramp (TGA)



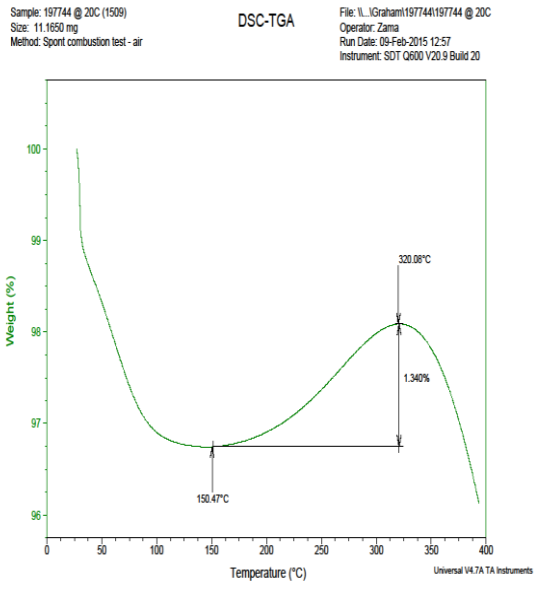
Appendix 146: Oxygen absorption for sample Z20 at 7 degree C ramp (TGA)



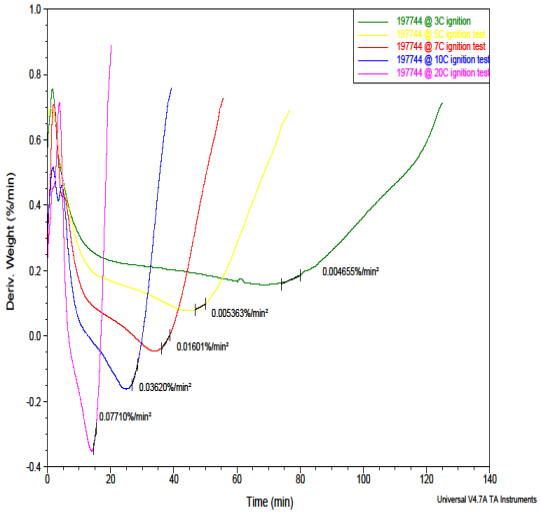
Appendix 147: Oxygen absorption for sample Z20 at 10 degree C ramp (TGA)



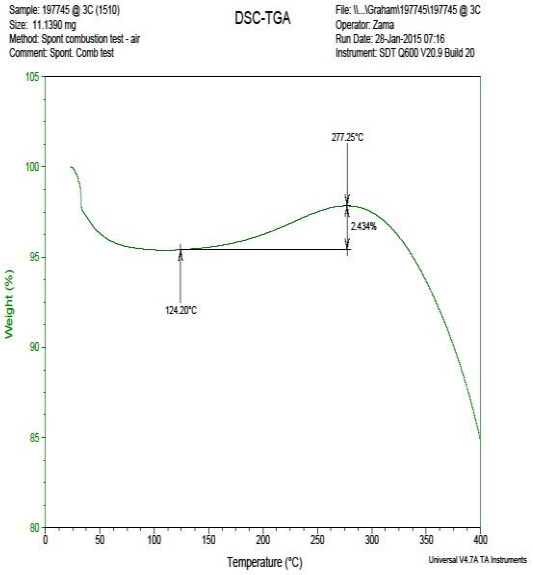
Appendix 148: Oxygen absorption for sample Z20 at 10 degree C ramp (TGA)



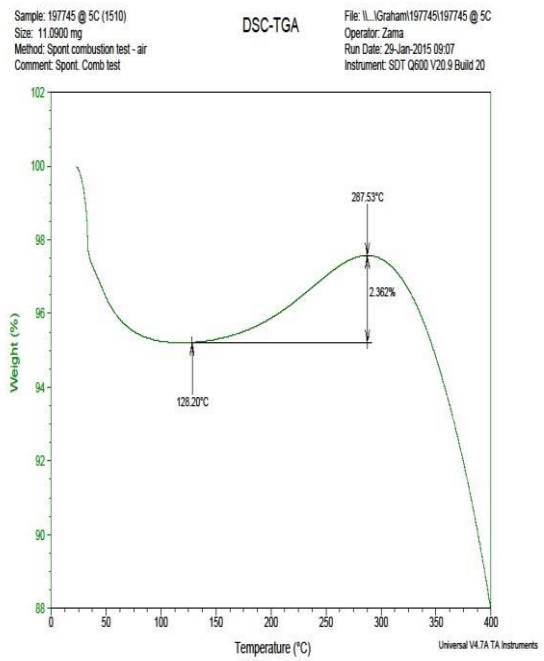
Appendix 149: Ignition test mix for sample Z20 (TGA)



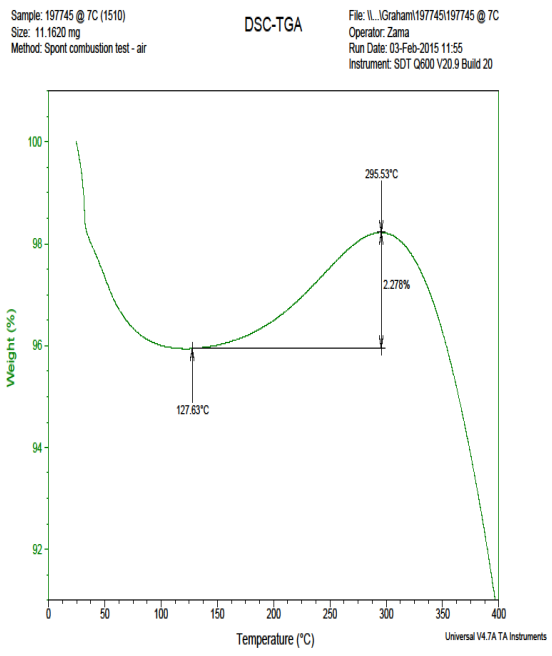
Appendix 150: Oxygen absorption for sample Z21 at 3 degree C ramp (TGA)



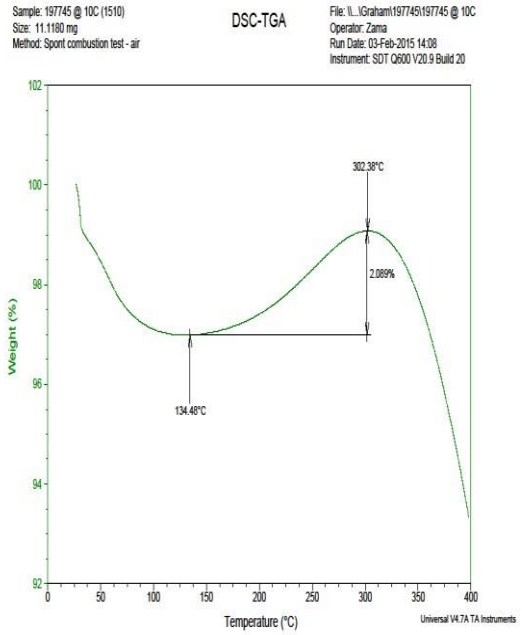
Appendix 151: Oxygen absorption for sample Z21 at 5 degree C ramp (TGA)



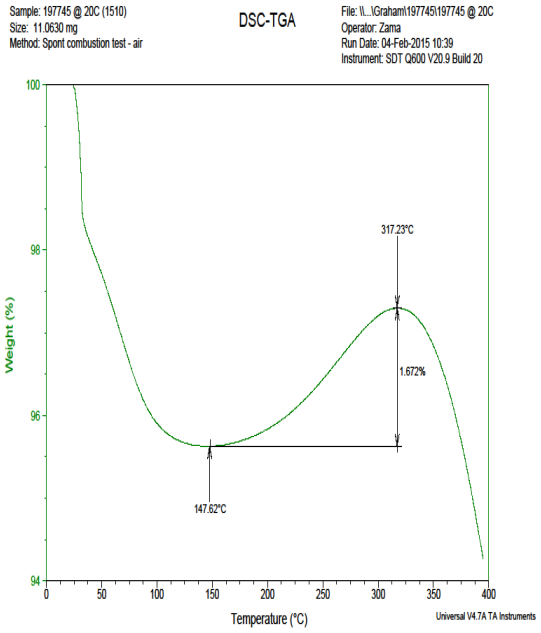
Appendix 152: Oxygen absorption for sample Z21 at 7 degree C ramp (TGA)



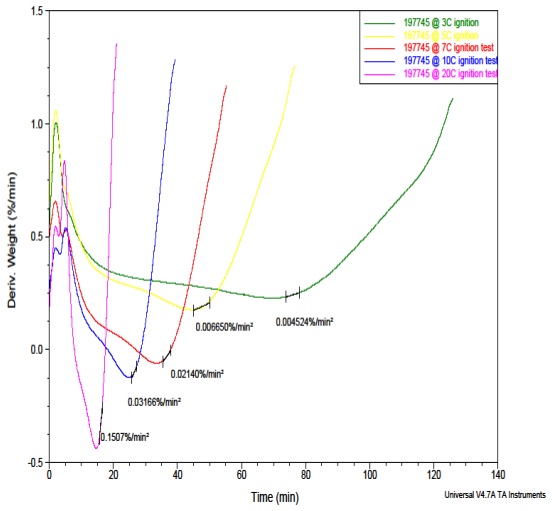
Appendix 153: Oxygen absorption for sample Z21 at 10 degree C ramp (TGA)



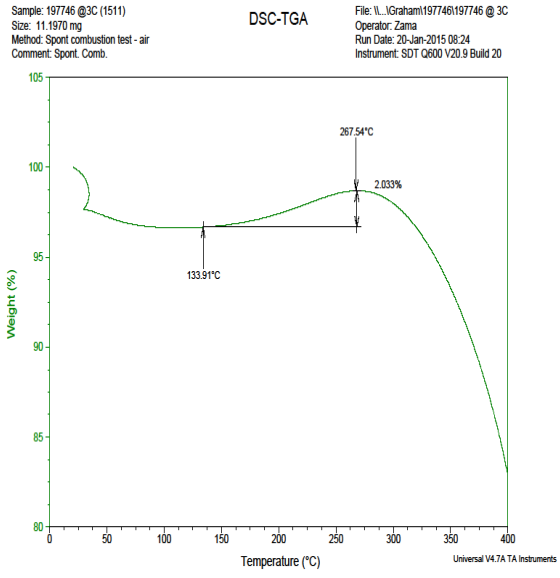
Appendix 154: Oxygen absorption for sample Z21 at 20 degree C ramp (TGA)



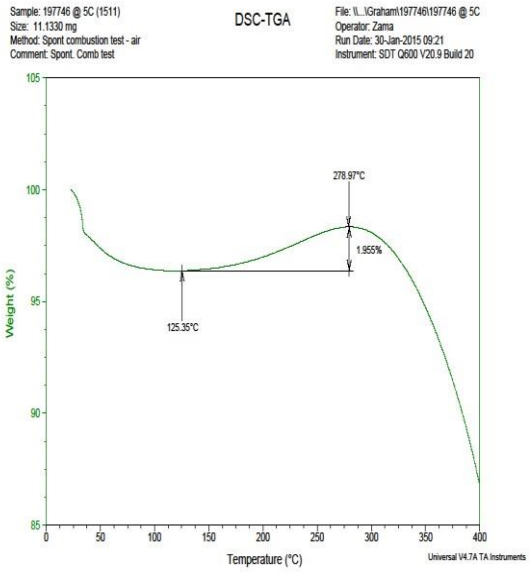
Appendix 155: Ignition test mix for sample Z21 (TGA)



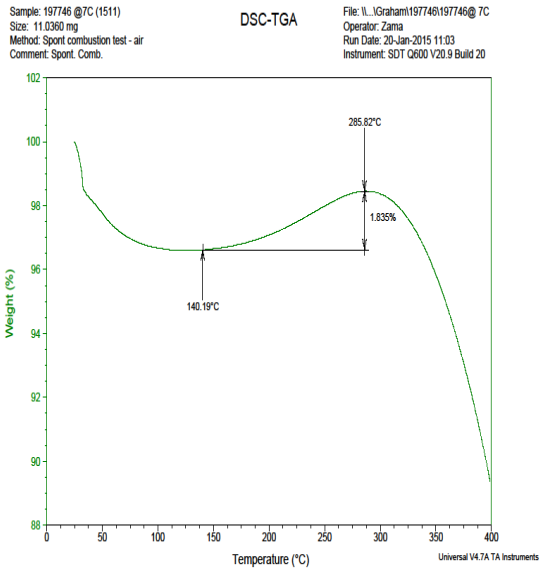
Appendix 156: Oxygen absorption for sample Z22 at 3 degree C ramp (TGA)



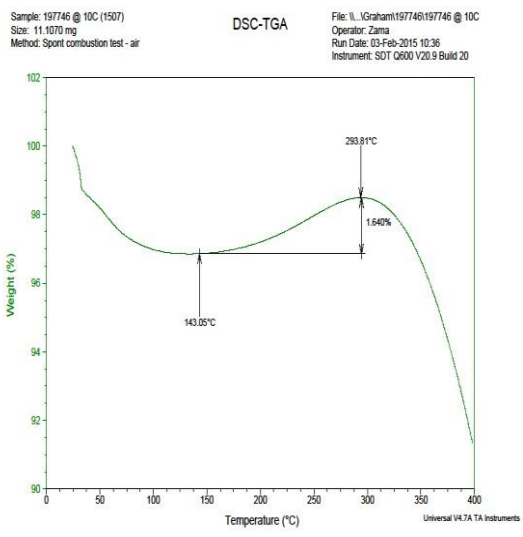
Appendix 157: Oxygen absorption for sample Z22 at 5 degree C ramp (TGA)



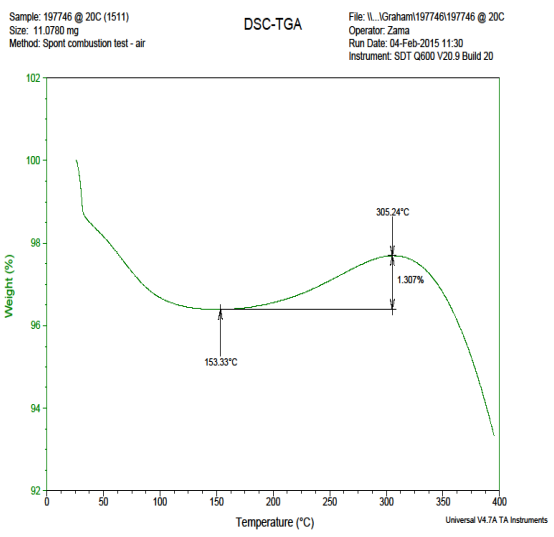
Appendix 158: Oxygen absorption for sample Z22 at 7 degree C ramp (TGA)



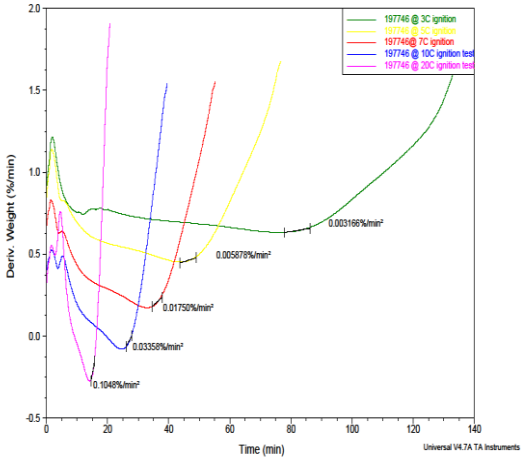
Appendix 159: Oxygen absorption for sample Z22 at 10 degree C ramp (TGA)



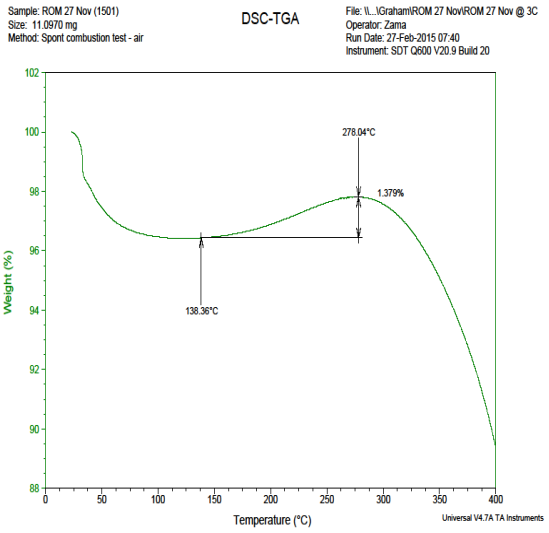
Appendix 160: Oxygen absorption for sample Z22 at 20 degree C ramp (TGA)



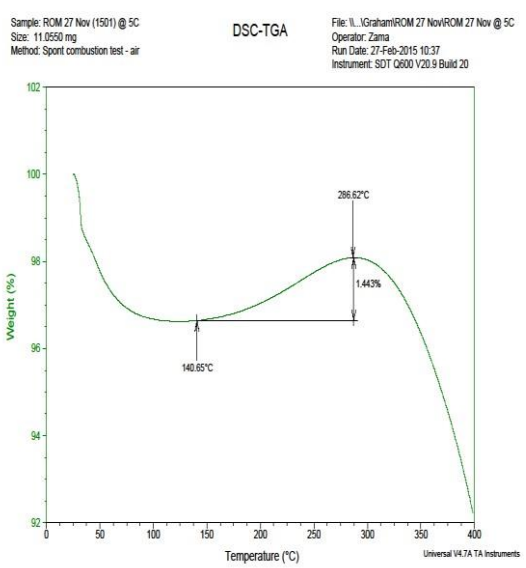
Appendix 161: Ignition test mix for sample Z22 (TGA)



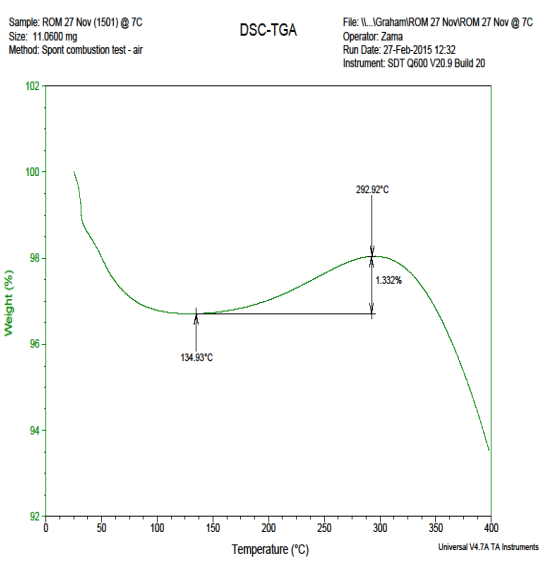
Appendix 162: Oxygen absorption for sample ROM1 at 3 degree C ramp (TGA)



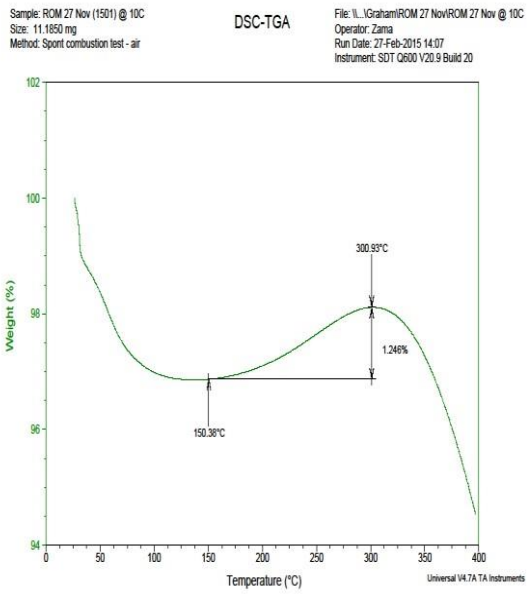
Appendix 163: Oxygen absorption for sample ROM1 at 5 degree C ramp (TGA)



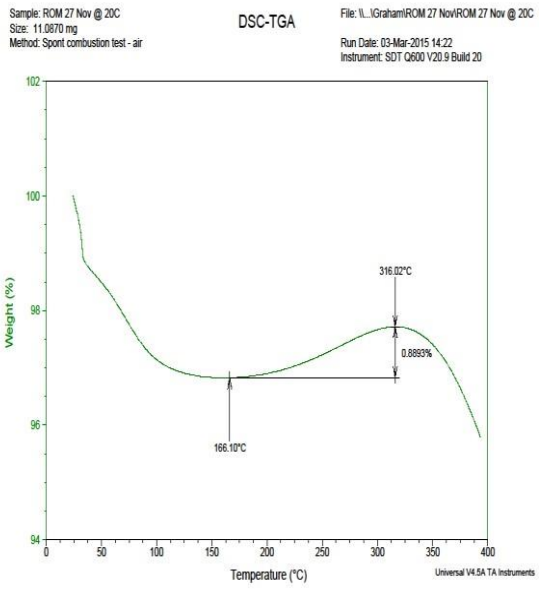
Appendix 164: Oxygen absorption for sample ROM1 at 7 degree C ramp (TGA)



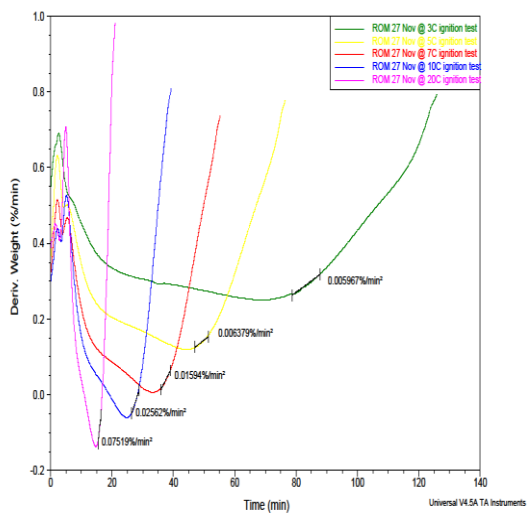
Appendix 165: Oxygen absorption for sample ROM1 at 10 degree C ramp (TGA)



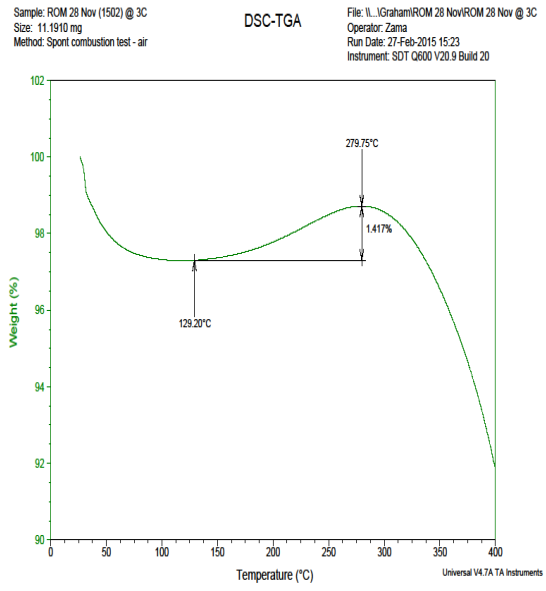
Appendix 166: Oxygen absorption for sample ROM1 at 20 degree C ramp (TGA)



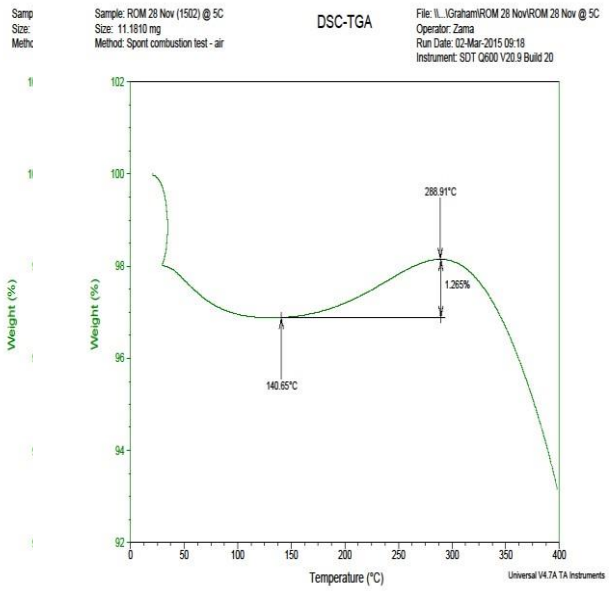
Appendix 167: Ignition test mix for sample ROM1 (TGA)



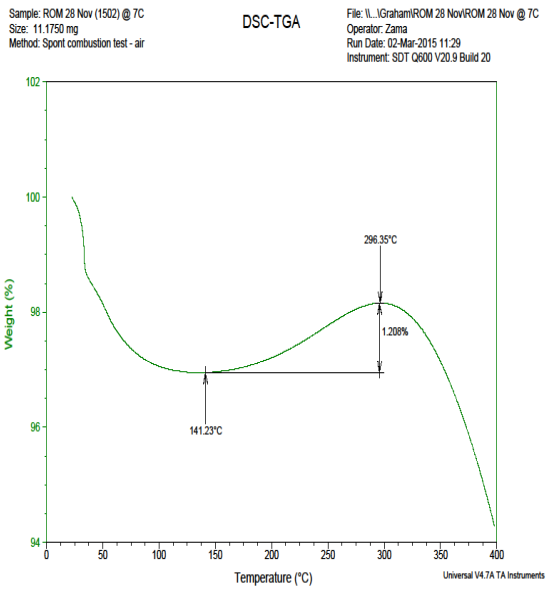
Appendix 168: Oxygen absorption for sample ROM2 at 3 degree C ramp (TGA)



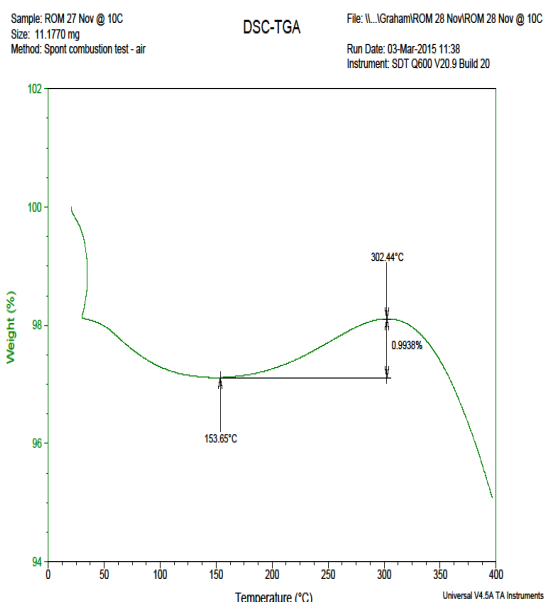
Appendix 169: Oxygen absorption for sample ROM2 at 5 degree C ramp (TGA)



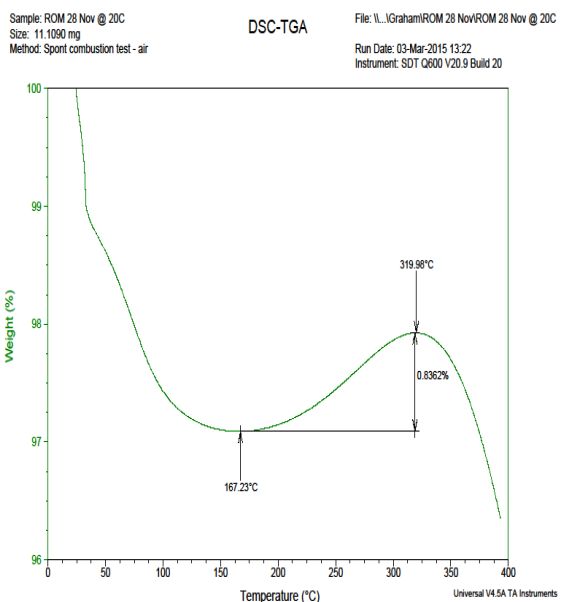
Appendix 170: Oxygen absorption for sample ROM2 at 7 degree C ramp (TGA)



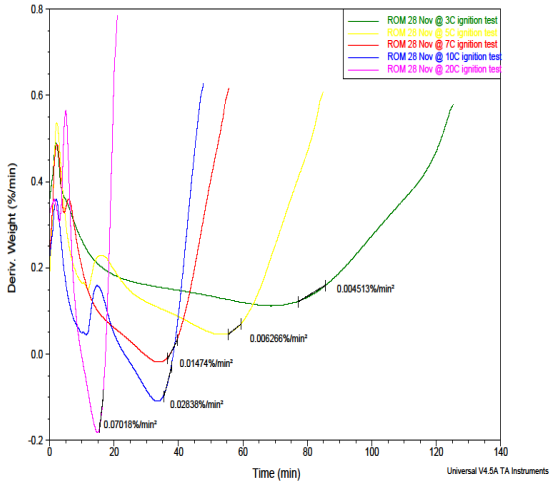
Appendix 171: Oxygen absorption for sample ROM2 at 10 degree C ramp (TGA)



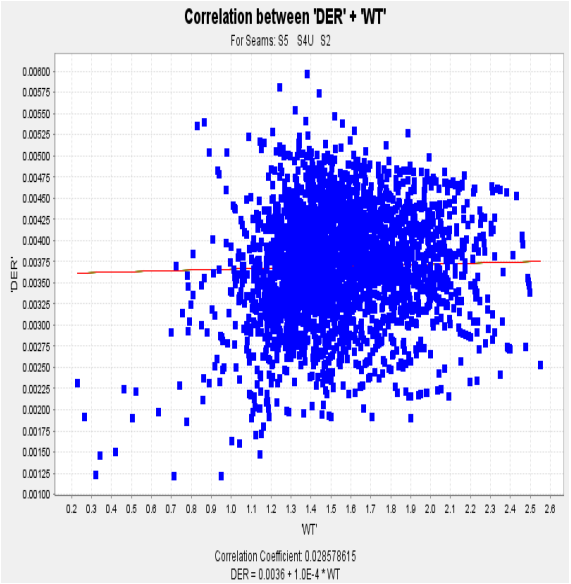
Appendix 172: Oxygen absorption for sample ROM2 at 20 degree C ramp (TGA)



Appendix 173: Ignition test mix for sample ROM2 (TGA)

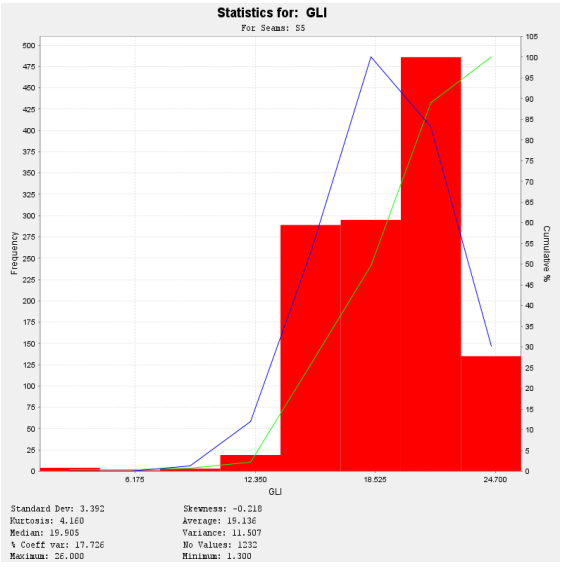


Appendix 174: Correlation between derivative of weight gain and % weight gain (TGA)

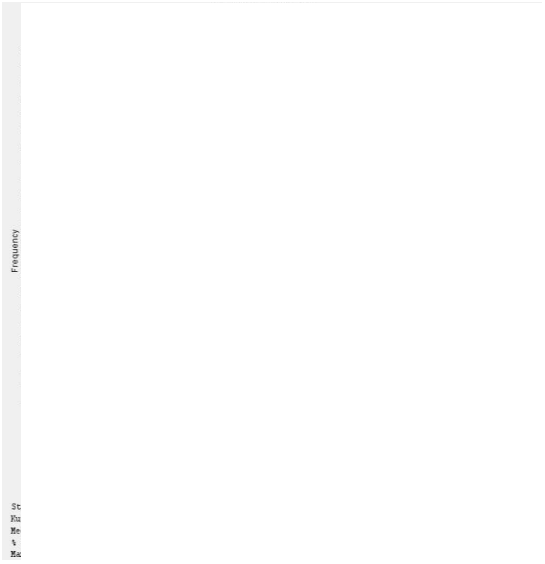


Appendix 175: Correlation between % oxygen (ultimate) and % weight gain (TGA)

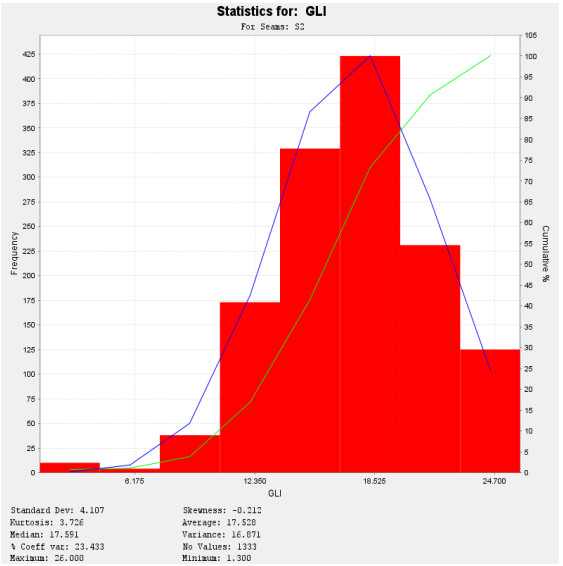
Appendix 176: Histogram of oxygen absorption test for No.5 seam (Smith-Glasser)



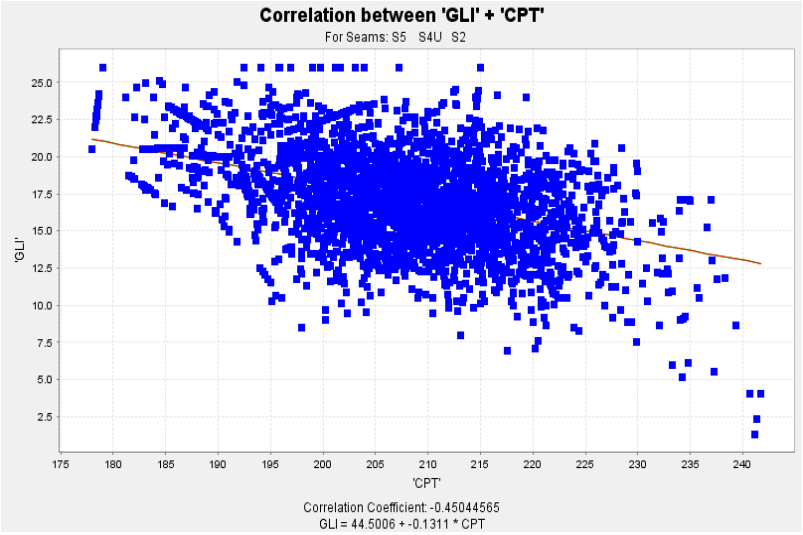
Appendix 177: Histogram of oxygen absorption test for No.4U seam (Smith-Glasser)



Appendix 178: Histogram of oxygen absorption test for No.2 seam (Smith-Glasser)



Appendix 179: Correlation between of oxygen absorption and crossing point temperature for combined seams



Appendix 180: Chemical analysis of samples Z1-Z22, ROM1-2 from SGS laboratories

Address	4 Paul Kruger Road Trichardt 2311
Tel:	017 638 0871 017 638 0438
Contact Persons	

Test Report

Bore Hole					SP32814						
Sample unique number					Z01	Z02	Z03	Z04	Z05	Z06	Z07
Thickness(m)					1.85	1.30	0.50	0.80	1.04	2.20	0.96
Laboratory number					216943	216944	216945	216946	216947	216948	216942
	Analysis		Unit	Method / Standard							
Analysis on air dry basis	Calorific Value	In Coal	MJ/kg	ISO 1928	26.66	18.95	6.98	17.30	13.45	22.91	13.31
	Inherent Moisture	In Coal	%	ISO 5068-2	4.00	3.2	2.5	3.3	3.5	4.1	2.2
	Ash	In Coal	%	ISO 1171:1997(E)	15.30	36.1	64.9	40.2	48.2	23.2	52.7
	Volatile	In Coal	%	ISO 562	32.10	22.8	13.5	20.2	17.6	25.7	17.1
	Fix Carbon	In Coal	%	By Calculation	48.60	37.9	19.1	36.3	30.7	47.0	28.0
	Total Sulphur	In Coal	%	ASTM D 4239	1.97	2.36	0.23	1.53	0.84	2.11	1.08
Analysis on air dry basis	Carbon	In Coal	%	ASTM D 5373-08	64.40	46.50	23.50	41.60	35.63	57.70	32.60
	Hydrogen	In Coal	%	ASTM D 5373-08	4.83	3.57	2.25	3.25	2.82	4.06	2.74
	Nitrogen	In Coal	%	ASTM D 5373-08	1.73	1.21	0.52	1.08	0.80	1.51	0.81
	Oxygen	In Coal	%	By Calculation	7.77	7.06	6.10	9.04	8.21	7.32	7.87
	Chlorine	In Coal	%	ISO 587							
	Phosphorous	In Coal	%	By XRF							
Analysis of the ash	CaO	In Ash	%	IN HOUSE METHOD By XRF	3.30	3.74	1.60	2.56	3.60	3.84	6.08
	MgO	In Ash	%		1.20	1.17	0.97	1.11	1.47	2.12	0.46
	K_2O	In Ash	%		1.35	1.31	1.09	0.59	1.46	0.50	0.52
	Na_2O	In Ash	%		0.15	0.14	0.14	0.18	0.20	0.33	0.11
	Fe_xO_3	In Ash	%		11.53	5.87	0.87	4.08	1.69	4.03	5.41
	TiO_2	In Ash	%		0.99	1.10	1.52	1.30	2.14	1.42	1.93
	Al_2O_3	In Ash	%		21.80	21.80	27.80	31.70	27.10	49.38	32.91
	SiO_2	In Ash	%		55.40	60.50	63.10	56.30	58.40	38.53	49.27
	MnO	In Ash	%		0.015	0.009	0.005	0.013	0.009	0.026	0.052
	SO_3	In Ash	%		2.71	3.16	0.76	2.32	2.26	0.78	1.05
	P_2O_5	In Ash	%		0.21	0.20	0.16	0.21	0.50	0.72	0.24
Ash Fusion Temperature	Atmosphere / Reducing										
	Deformation temperature	In Ash	°C	ED 540							
	Softening temperature	In Ash	°C								
	Hemisphere temperature	In Ash	°C								
	Flow temperature	In Ash	°C								
Analysis on air dry basis	Calorific Value			ISO 1928							
	Gross CV	In Coal	MJ/kg								
	Gross CV	In Coal	kcal/kg								
	Net CV	In Coal	kcal/kg								
	HGI	In Coal	Unit	ISO 5074							
	Total Moisture	In Coal	%	ISO 589							
FORMS OF SULPHUR	Pyritic sulphur	In Coal	%		1.46	1.68	0.05	1.14	0.36	1.60	0.79
	Sulphate sulphur	In Coal	%		0.04	0.04	0.01	0.03	0.02	0.04	0.03
	Organic Sulphur	In Coal	%		0.47	0.64	0.17	0.36	0.46	0.47	0.26
	Mineral Sulphur	In Coal	%		1.50	1.72	0.06	1.17	0.38	1.64	0.82
FORMS OF SILICA	Free	In Coal	%								
	Combined	In Coal	%								

Test Report

Bore Hole					SP32814						
Sample unique number					Z08	Z09	Z10	Z11	Z12	Z13	
Thickness(m)					1.00	0.90	1.10	1.00	2.00	1.10	
Laboratory number					216949	216950	216951	216952	216953	216954	
	Analysis		Unit	Method / Standard							
Analysis on air dry basis	Calorific Value	In Coal	MJ/kg	ISO 1928	19.70	15.61	14.34	7.22	24.47	18.41	
	Inherent Moisture	In Coal	%	ISO 5068-2	4.00	3.5	3.3	1.4	3.8	4.0	
	Ash	In Coal	%	ISO 1171:1997(E)	31.90	43.7	46.7	71.0	20.1	35.3	
	Volatile	In Coal	%	ISO 562	18.30	16.1	17.9	12.6	25.7	17.8	
	Fix Carbon	In Coal	%	By Calculation	45.80	36.7	32.1	15.0	50.4	42.9	
	Total Sulphur	In Coal	%	ASTM D 4239	1.81	0.27	0.58	0.92	0.85	0.40	
Analysis on air dry basis	Carbon	In Coal	%	ASTM D 5373-08	49.80	39.60	38.60	15.20	61.10	46.80	
	Hydrogen	In Coal	%	ASTM D 5373-08	3.26	2.76	2.89	1.94	4.22	3.17	
	Nitrogen	In Coal	%	ASTM D 5373-08	1.21	0.98	0.88	0.47	1.40	1.08	
	Oxygen	In Coal	%	By Calculation	8.03	9.19	7.06	9.07	8.53	9.25	
	Chlorine	In Coal	%	ISO 587							
	Phosphorous	In Coal	%	By XRF							
Analysis of the ash	CaO	In Ash	%	IN HOUSE METHOD by XRF	12.29	2.53	7.78	1.29	17.42	2.02	
	MgO	In Ash	%		1.54	1.32	1.06	0.52	0.37	1.47	
	K2O	In Ash	%		0.44	0.29	0.81	0.22	1.01	0.33	
	Na_2O	In Ash	%		0.27	0.39	1.06	0.08	0.16	0.21	
	Fe_2O_3	In Ash	%		6.04	1.20	1.79	1.95	15.80	0.63	
	TiO_2	In Ash	%		1.28	2.11	1.84	3.36	1.90	1.46	
	Al_2O_3	In Ash	%		24.02	42.02	31.91	33.29	15.43	50.88	
	SiO_2	In Ash	%		49.59	49.83	51.57	59.81	47.27	42.11	
	MnO	In Ash	%		0.014	0.014	0.012	0.000	0.023	0.012	
	SO_3	In Ash	%		2.53	0.53	0.82	0.45	2.13	1.24	
	P_2O_5	In Ash	%		0.24	0.24	0.40	0.20	0.45	0.79	
Ash Fusion Temperature	Atmosphere / Reducing			ISO 540							
	Deformation temperature	In Ash	°C								
	Softening temperature	In Ash	°C								
	Hemisphere temperature	In Ash	°C								
	Flow temperature	In Ash	°C								
Analysis on air dry basis	Calorific Value			ISO 1928							
	Gross CV	In Coal	MJ/kg								
	Gross CV	In Coal	kcal/kg								
	Net CV	In Coal	kcal/kg								
	HGI	In Coal	Unit	ISO 5074							
	Total Moisture	In Coal	%	ISO 589							
FORMS OF SULPHUR	Pyritic sulphur	In Coal	%		1.52	0.11	0.37	0.73	0.50	0.08	
	Sulphate sulphur	In Coal	%		0.03	0.02	0.03	0.04	0.03	0.02	
	Organic Sulphur	In Coal	%		0.26	0.14	0.18	0.15	0.32	0.30	
					1.55	0.13	0.40	0.77	0.53	0.10	
FORMS OF SILICA	Free	In Coal	%								
	Combined	In Coal	%								

Test Report

Bore Hole					S100-14						
Sample unique number					Z14	Z15	Z16	Z17	Z18	Z19	Z20
Laboratory number					197738	197739	197740	197741	197742	197743	197744
	Analysis		Unit	Method / Standard							
Analysis on air dry basis	Calorific Value	In Coal	MJ/kg	ISO 1928	27.62	14.69	19.42	19.54	26.50	21.94	17.22
	Inherent Moisture	In Coal	%	ISO 5068-2	3.7	3.0	3.4	3.3	3.8	3.4	2.8
	Ash	In Coal	%	ISO 1171:1997(E)	13.4	46.3	34.2	32.5	15.5	27.4	40.7
	Volatile	In Coal	%	ISO 562	30.4	16.6	22.0	21.1	27.3	20.7	18.4
	Fix Carbon	In Coal	%	By Calculation	52.5	34.1	40.4	43.1	53.4	48.5	38.1
	Total Sulphur	In Coal	%	ASTM D 4239	2.95	2.36	1.54	1.44	1.42	2.89	0.47
Analysis on air dry basis	Carbon	In Coal	%	ASTM D 5373-08	69.7	41.8	47.4	50.6	65.5	55.6	45.9
	Hydrogen	In Coal	%	ASTM D 5373-08	4.11	3.08	3.44	3.94	4.81	4.04	3.34
	Nitrogen	In Coal	%	ASTM D 5373-08	1.67	1.01	1.12	1.17	1.64	1.41	1.05
	Oxygen	In Coal	%	By Calculation	4.47	2.45	8.90	7.05	7.33	5.26	5.74
Analysis of the ash	SiO2	In Ash	%	IN HOUSE METHOD by XRF	48.55	56.97	55.20	50.14	53.40	57.84	58.81
	Al2O3	In Ash	%		22.37	29.13	30.41	31.08	22.98	26.49	29.80
	Fe2O3	In Ash	%		20.98	5.10	4.06	4.40	8.50	5.39	1.43
	CaO	In Ash	%		1.86	4.14	3.51	3.55	8.33	2.96	1.85
	MgO	In Ash	%		0.64	0.71	0.69	1.21	1.74	1.69	1.56
	Na2O	In Ash	%		0.16	0.13	0.15	0.31	0.13	0.11	0.10
	K2O	In Ash	%		0.81	0.62	0.85	0.43	0.31	0.51	0.54
	P2O5	In Ash	%		0.27	0.36	0.63	0.51	0.35	0.47	0.64
	TiO2	In Ash	%		1.81	1.87	1.95	1.57	1.70	2.45	2.45
	MnO	In Ash	%		0.01	0.01	0.01	0.02	0.04	0.01	0.01
	SO3	In Ash	%		3.25	1.79	2.77	6.78	4.91	1.24	4.61
FORMS OF SULPHUR	Mineral Sulphur	In Coal	%	ISO 157	2.66	2.13	1.26	1.28	1.19	2.73	0.38
	Sulphate sulphur	In Coal	%	ISO 157	0.01	0.02	0.02	0.01	0.03	0.02	0.02
	Organic Sulphur	In Coal	%	ISO 157	0.29	0.23	0.28	0.16	0.23	0.16	0.09
	Pyritic sulphur	In Coal	%	ISO 157	2.65	2.11	1.24	1.27	1.16	2.71	0.36

Test Report

Bore Hole					S100-14						
Sample unique number					Z21	Z22					
Laboratory number					197745	197746					
	Analysis		Unit	Method / Standard							
Analysis on air dry basis	Calorific Value	In Coal	MJ/kg	ISO 1928	25.22	21.72					
	Inherent Moisture	In Coal	%	ISO 5068-2	3.40	2.9					
	Ash	In Coal	%	ISO 1171:1997(E)	19.20	29.2					
	Volatile	In Coal	%	ISO 562	23.5	26.0					
	Fix Carbon	In Coal	%	By Calculation	53.9	41.9					
	Total Sulphur	In Coal	%	ASTM D 4239	0.95	1.00					
Analysis on air dry basis	Carbon	In Coal	%	ASTM D 5373-08	64.7	55.6					
	Hydrogen	In Coal	%	ASTM D 5373-08	4.44	3.71					
	Nitrogen	In Coal	%	ASTM D 5373-08	1.57	1.32					
	Oxygen	In Coal	%	By Calculation	5.74	6.27					
Analysis of the ash	SiO2	In Ash	%	IN HOUSE METHOD by XRF	49.56	55.19					
	Al2O3	In Ash	%		27.63	31.32					
	Fe2O3	In Ash	%		11.92	5.31					
	CaO	In Ash	%		3.11	1.29					
	MgO	In Ash	%		1.62	1.05					
	Na2O	In Ash	%		0.12	0.10					
	K2O	In Ash	%		0.47	0.54					
	P2O5	In Ash	%		0.86	0.43					
	TiO2	In Ash	%		2.48	2.79					
	MnO	In Ash	%		0.01	0.00					
	SO3	In Ash	%		1.36	2.43					
FORMS OF SULPHUR	Mineral Sulphur	In Coal	%	ISO 157	0.80	0.86					
	Sulphate sulphur	In Coal	%	ISO 157	0.02	0.01					
	Organic Sulphur	In Coal	%	ISO 157	0.15	0.14					
	Pyritic sulphur	In Coal	%	ISO 157	0.78	0.85					

TABLE 1: ABNORMAL CONDITION ANALYSIS (VOLUME %)

CLIENT:	GRAHAM GEMMELL
PROJECT:	MSC INVESTIGATION INTO SPONTANEOUS COMBUSTION
DATE:	28-Feb-15
JOB / SAMPLE NUMBERS:	
ANALYST:	Dr NJ Wagner
ICCP ACCREDITATION:	ICCP/SCAP-056/AB ; ICCP/CBAP/056; ICCP/DOMVR/056

THESE RESULTS RELATE ONLY TO THE SAMPLES ANALYSED

		SAMPLE NUMBER / ID												
GROUP	**CONDITION**	**Z01**	**Z02**	**Z03***	**Z04**	**Z05**	**Z06**	**Z07**	**Z08**	**Z09**	**Z10**	**Z11***	**Z12**	**Z13**
FRESH	**total fresh**	59.2	58.2	66.7	53.1	63.2	69	70.8	66.8	64.5	80.1	79.9	76	71.2
FISSURES	few	3.7	2.4	5.8	5.9	3.9	3.8	2.5	4.9	6	2.7	1.6	3.3	2.3
	extensive	1	0.8	1.4	3.7	1.6	0.7	0.8	1.8	1.8	0.6	0	0.2	0
CRACKS	few	15	9.7	5.4	10.7	12.3	9.3	9.8	9.5	13.5	8.6	5.3	11.2	12.3
	extensive	8.7	8.5	7.6	20.5	8	9.2	8.1	9.5	5.7	5.7	3.7	6.1	6.5
	desiccated	1.6	0	0	0	0	0.3	0.2	0	0	0	0	0.2	0
HOLES	inherent	0.2	0.2	2.3	2.5	1.8	0.7	1.2	0.4	0.2	0	0	0.2	0
	leaching	0	0	0	0	0	0	0	0	0	0	0	0	0
HEAT AFFECTED	organic	0	0.2	0.8	0.2	0	0	0	0	0	0	0	0	0
	inorganic / minerals	0	0	0	0	0	0	0	0	0	0	0	0	0
DISCOLOURATION	whole particle	0	1.6	9.7	2.7	6.8	0.2	1	2	7.2	0.8	7.4	0.4	0.4
	dark zones	0	0	0	0	0	0	0	0	0	0	0	0	0
	light zones	0	0	0	0	0	0	0	0	0	0	0	0	0
	due to heat	0	0	0	0	0	0	0	0	0	0	0	0	0
POROUS FUSINITE	fusinite	6.2	3.2	0	0.4	1.2	3.5	2.5	1.4	0	0.4	0.4	2.4	2.3
MINERALS	alteration	0	0.4	0	0	0.4	0	0	0	0	0	0	0	0.6
	pyrite	4.6	15	0.4	0.2	0.8	3.3	3.1	3.8	1.2	1.2	1.8	0	4.3
TOTAL	**total abnormal condition**	**41**	**42**	**33.4**	**46.8**	**36.8**	**31**	**29.2**	**33.3**	**35.6**	**20**	**20.2**	**24**	**28.7**

* high mineral matter, counted as fresh particles. Z03 most OM was cracked; Z11 most OM was fresh

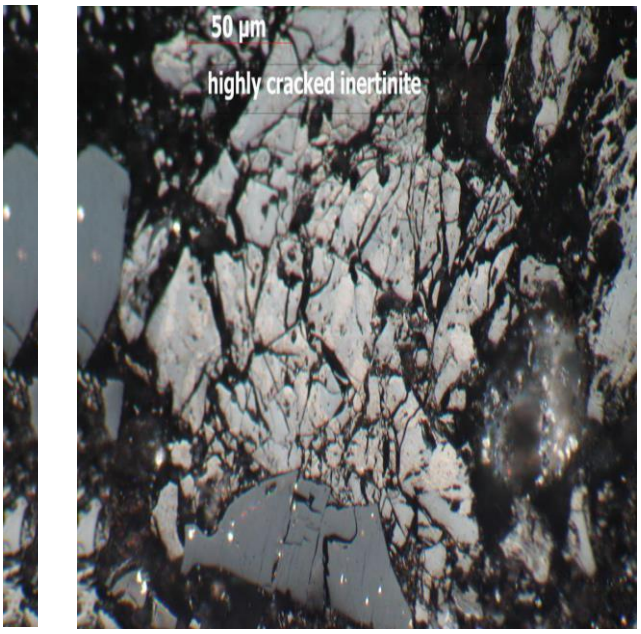
TABLE 1: ABNORMAL CONDITION ANALYSIS (VOLUME %)

CLIENT:	GRAHAM GEMMELL
PROJECT:	MSC INVESTIGATION INTO SPONTANEOUS COMBUSTION; Khutala coals
DATE:	
JOB / SAMPLE NUMBERS:	
ANALYST:	Prof NJ Wagner
ICCP ACCREDITATION:	ICCP/SCAP-056/AB ; ICCP/CBAP/056; ICCP/DOMVR/056

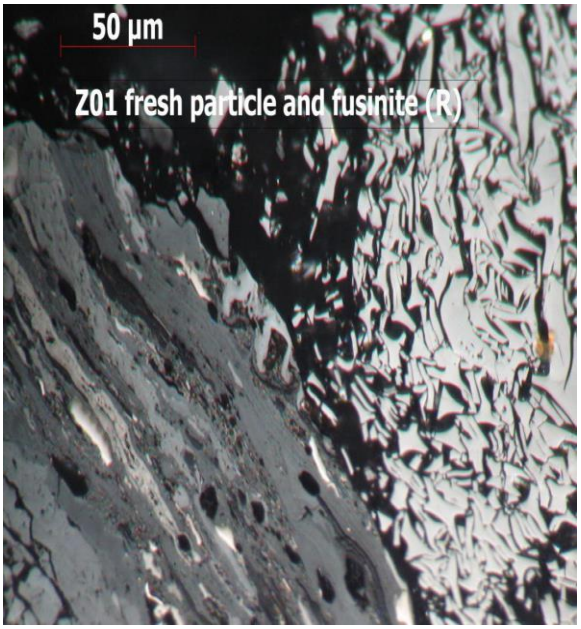
THESE RESULTS RELATE ONLY TO THE SAMPLES ANALYSED

		SAMPLE NUMBER / ID										
		1579	1580	1581	1582	1583	1584	1585	1586	1587	1588	1589
GROUP	**CONDITION**	Z14	Z15	Z16	Z17	Z18	Z19	Z20	Z21	Z22	rom 1	rom 2
FRESH	**total fresh**	**76**	**56.6**	**67.4**	**71.2**	**73.2**	**64.8**	**73.6**	**63.4**	**73.2**	**57.6**	**59**
FISSURES	few	7.6	10.2	6.6	8	7.6	10	8.8	13.6	7.4	12.6	13.6
	extensive	0	0	0	0	0.2	0	0	0.6	0	0.8	0
CRACKS	few	9.4	8.8	6.4	10.2	12.6	**15.8**	6	13	8.6	13.6	10.2
	extensive	1	1.6	1	0.6	4	1.8	0.8	4	2.6	**4.2**	3.4
	desiccated	0.8	0	0	0.2	0	0	0	0.4	0.8	0	0
HOLES	inherent	0	2.6	0.6	0.6	0.2	2	2.8	1.4	0	0.6	0.8
	leaching	0	0	0	0	0	0	0	0	0	0	0
HEAT AFFECTED	organic	0	0	0	0	0	0	0	0	0	0	0
	inorganic / minerals	0	0	0	0	0	0	0	0.4	0	0	0
DISCOLOURATION	whole particle	0	**17.8**	14.2	5.4	0.2	2	6.8	0	0.6	8.6	9.4
	dark zones	0	0	0	0	0	0	0	0	0	0	0
	light zones	0	0	0	0	0	0	0	0	0	0	0
	due to heat	0	0	0	0	0	0	0	0	0	0	0
POROUS FUSINITE	fusinite	2.8	1.2	1.6	1.4	1.6	3.2	0.8	2.8	4.6	1.8	0.4
MINERALS	alteration	0	0	0	0	0	0	0	0	0	0	0
	pyrite	2.4	1.2	2.2	2.4	0.4	0.4	0.4	0.4	2.2	0.2	3.2
	Total abnormal condition	**24**	**43.4**	**32.6**	**28.8**	**26.8**	**35.2**	**26.4**	**36.6**	**26.8**	**42.4**	**41**

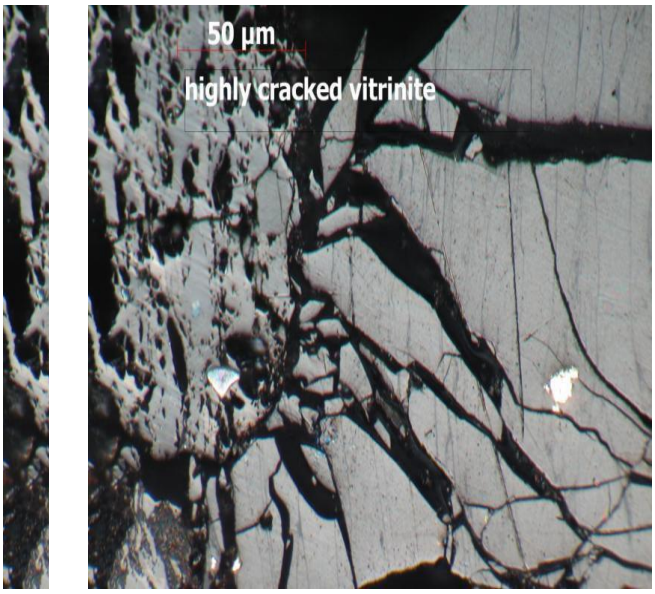
Appendix 182: Micrograph showing highly cracked inertinite



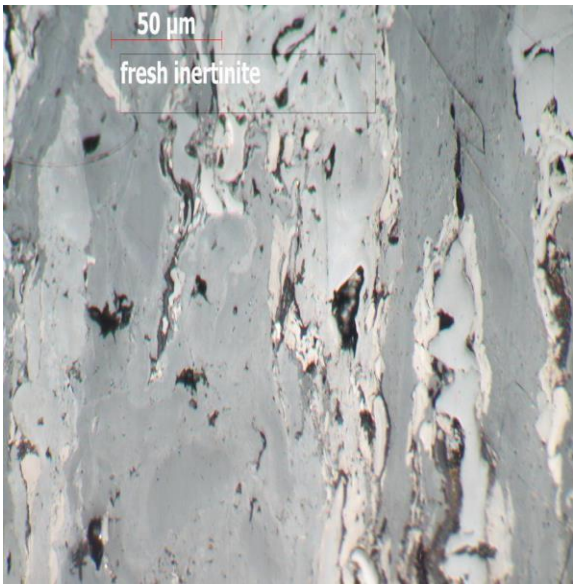
Appendix 183: Micrograph showing fresh particle and fusinite



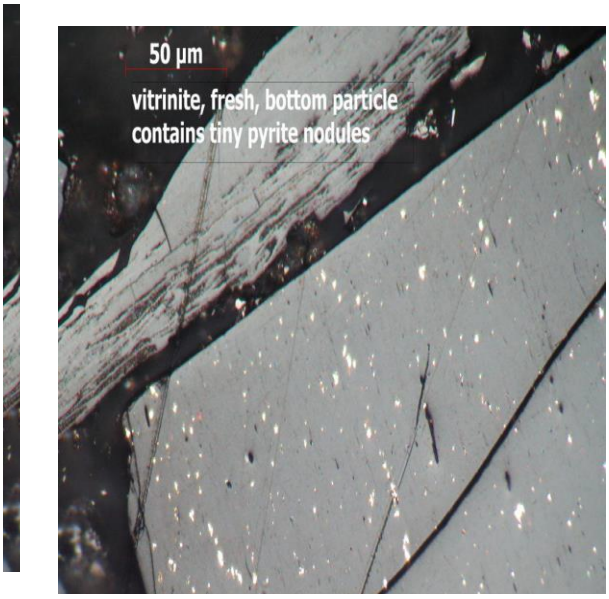
Appendix 184: Micrograph showing highly cracked inertinit



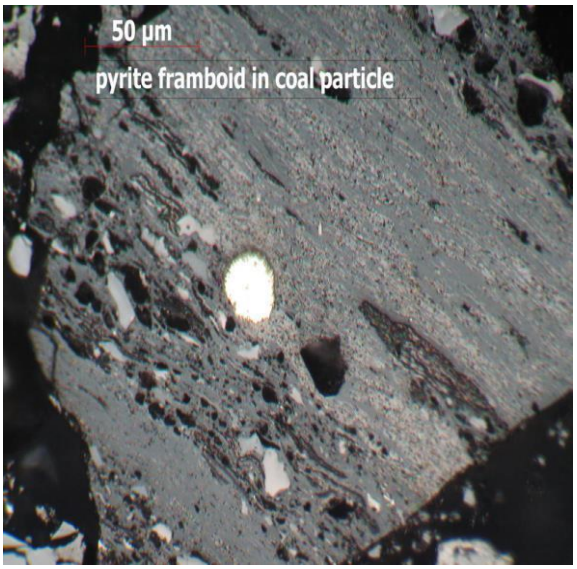
Appendix 185: Micrograph showing fresh inertinite



Appendix 186: Micrograph showing fresh vitrinite and pyrite nodules



Appendix 187: Micrograph showing framboidal pyrite



Appendix 188: Coal maceral analysis

TABLE 1

PETROGRAPHICS SA

COAL AND ORGANIC PETROLOGY

PETROGRAPHICS SA CONTRACT NO. : PSA 2014-416 DATE : 27 DECEMBER 2014

COMPANY NAME : COALTECH RESEARCH ASSOCIATION NPC ATTN:

AUTHORIZATION: MR. JOHANN BEUKES SAMPLES RECEIVED : 21 NOVEMBER 2014

SAMPLE CODES SET ONE						MACERAL ANALYSIS (PERCENT BY VOLUME, MINERAL MATTER BASIS), BASED ON ISO 7404 - 3, 1994																RANK RANDOM/MAXIMUM REFLECTANCE	
						VITRINITE			LIPTINITE			INERTINITE									TOTAL REACTIVES		
		KHUTALA COLLIERY				VIT	PV	TV	S/R/C	ALG	TOT L	RSF	ISF	F/ SEC	MIC	R INT	I INT	TOT I	HEAT ALTERED	VISIBLE MINERALS	(mmb)	Rr determined	Rmax calculated
SGS NO.	SABS 2014/C		COMPANY ID		PSA NO.																		
NO.		BH SP32814	THICKNESS (m)	2014		%	%	%	%	%	%	%	%	%	%	%	%	%	%	%	%	%	%
216943	287	1 Z01	1.85	1079		55	5	**60**	7	0	**7**	6	9	6	1	1	4	**27**	**0**	**6**	**74**	**0.68**	**0.73**
216944	288	2 Z02	1.30	1080		31	2	**33**	4	0	**4**	4	11	6	1	3	10	**35**	**0**	**28**	**44**	**0.70**	**0.75**
216945	289	3 Z03	0.50	1081		9	<1	**9**	2	0	**2**	2	7	3	1	2	10	**25**	**0**	**64**	**15**	**0.78**	**0.83**
216946	290	4 Z04	0.80	1082		13	1	**14**	4	0	**4**	6	14	3	2	7	20	**52**	**0**	**30**	**31**	**0.85**	**0.89**
216947	291	5 Z05	1.04	1083		12	1	**13**	3	0	**3**	4	13	3	1	4	17	**42**	**0**	**42**	**24**	**0.75**	**0.80**
216948	292	6 Z06	2.20	1084		39	2	**41**	7	0	**7**	6	9	7	1	3	14	**40**	**0**	**12**	**57**	**0.67**	**0.72**
216942	293	7 Z07	0.96	1085		20	1	**21**	2	0	**2**	8	11	4	1	3	7	**34**	**0**	**43**	**34**	**0.72**	**0.77**
216949	294	8 Z08	1.00	1086		13	<1	**13**	2	0	**2**	14	20	5	3	6	15	**63**	**0**	**22**	**35**	**0.76**	**0.81**
216950	295	9 Z09	0.90	1087		13	1	**14**	2	0	**2**	8	16	3	2	4	13	**46**	**0**	**38**	**28**	**0.79**	**0.84**
216951	296	10 Z10	1.10	1088		19	1	**20**	4	0	**4**	8	12	6	1	2	8	**37**	**0**	**39**	**34**	**0.75**	**0.80**
216952	297	11 Z11	1.00	1089		11	0	**11**	2	0	**2**	2	4	2	<1	1	2	**11**	**0**	**76**	**16**	**0.63**	**0.69**
216953	298	12 Z12	2.00	1090		38	2	**40**	4	0	**4**	5	16	5	2	4	13	**45**	**0**	**11**	**53**	**0.68**	**0.73**
216954	299	13 Z13	1.10	1091		34	2	**36**	3	0	**3**	3	8	5	1	2	11	**30**	**0**	**31**	**44**	**0.67**	**0.72**

THESE RESULTS RELATE ONLY TO THE SAMPLES ANALYSED

Total Reactives = Vitrinite + Liptinite + Reactive Semifusinite + Reactive Inertodetrinite

Organic composition analysis carried out by Petrographics SA

VM du Cann

Accredited Full Member of the International Committee for Coal and Organic Petrology

ICCP Accreditation Certificate Number: ICCP/SCAP-001/AB (Expiry date: 31/12/2014)

TABLE 1

PETROGRAPHICS SA

COAL AND ORGANIC PETROLOGY

PETROGRAPHICS SA CONTRACT NO.: PSA 2015-439 — DATE: 27 MAY 2015

COMPANY NAME: SGS SOUTH AFRICA (PTY) LTD, PO BOX 82582, SOUTH DALE 2135, SOUTH AFRICA — ATTN: Mr. G. GEMMELL

SGS ORDER NO: PO 10000767 — BLOCKS RECEIVED: 09 APRIL 2015

					MACERAL ANALYSIS (PERCENT BY VOLUME, MINERAL MATTER BASIS), BASED ON ISO 7404 - 3, 1994																RANK	
SAMPLE CODES					VITRINITE			LIPTINITE			INERTINITE									TOTAL	RANDOM/MAXIMUM REFLECTANCE	
SET TWO																				REACTIVES		
		KHUTALA COLLIERY			VIT	PV	TV	S/R/C	ALG	TOT L	RSF	ISF	F/	MIC	R	I	TOT I	HEAT	VISIBLE	(mmb)	Rr	Rmax
SGS NO.	SABS NO. 2015/C	COMPANY ID BH S10014	THICKNESS (m)	PSA NO. 2015									SEC		INT	INT		ALTERED	MINERALS		determined	calculated
					%	%	%	%	%	%	%	%	%	%	%	%	%	%	%	%	%	%
197738	4 1	Z14		1165	52	2	**54**	5	0	**5**	5	13	4	1	2	10	**35**	**0**	**6**	**66**	**0.74**	**0.79**
197739	5 2	Z15		1166	8	0	**8**	6	0	**6**	5	17	5	1	3	17	**48**	**0**	**38**	**22**	**0.78**	**0.83**
197740	6 3	Z16		1167	28	1	**29**	6	0	**6**	3	15	7	1	2	11	**39**	**0**	**26**	**40**	**0.69**	**0.74**
197741	7 4	Z17		1168	24	1	**25**	6	0	**6**	7	16	4	1	6	14	**48**	**0**	**21**	**44**	**0.67**	**0.72**
197742	8 5	Z18		1169	38	2	**40**	6	0	**6**	9	18	6	1	4	9	**47**	**0**	**7**	**59**	**0.66**	**0.71**
197743	9 6	Z19		1170	18	1	**19**	4	0	**4**	7	16	8	2	10	17	**60**	**0**	**17**	**40**	**0.70**	**0.75**
197744	10 7	Z20		1171	15	1	**16**	3	0	**3**	6	13	8	2	8	14	**51**	**0**	**30**	**33**	**0.72**	**0.77**
197745	11 8	Z21		1172	27	0	**27**	4	0	**4**	10	22	8	1	6	13	**60**	**0**	**9**	**47**	**0.74**	**0.79**
197746	12 9	Z22		1173	46	2	**48**	8	0	**8**	4	7	5	1	2	5	**24**	**0**	**20**	**62**	**0.69**	**0.74**
198116	13 10	ROM 1		1174	22	1	**23**	4	0	**4**	6	13	4	1	4	17	**45**	**0**	**28**	**37**	**0.73**	**0.78**
198117	14 11	ROM 2		1175	11	1	**12**	3	0	**3**	8	16	5	2	4	18	**53**	**0**	**32**	**27**	**0.69**	**0.74**

THESE RESULTS RELATE ONLY TO THE SAMPLES ANALYSED

Total Reactives = Vitrinite + Liptinite + Reactive Semifusinite + Reactive Inertodetrinite

Organic composition analysis carried out by Petrographics SA

VM du Cann

Accredited Full Member of the International Committee for Coal and Organic Petrology

ICCP Accreditation Certificate Number: ICCP/SCAP-001/AB (Expiry date: 31/12/2016)

Appendix 189: Vitrinite random reflectance

TABLE2

SOUTH AFRICAN BUREAU OF STANDARDS | CSIR CAMPUS, PRETORIA

VITRINITE RANDOM REFLECTANCE DATA

SAMPLE CODES						REFLECTANCE CLASSES (%)																				STANDARD DEVIATION	MEAN RANDOM REFLECTANCE
			KHUTALA COLLIERY																								
SGS	SABS NO.		COMPANY ID		PSA NO.	V 2	V 3	V 4	V 5	V 6	V 7	V 8	V 9	V 10	V 11	V 12	V 13	V 14	V 15	V 16	V 17	V 18	V 19	V 20	σ	Rr%
NO.	2014/C		BH SP32814	THICKNESS (m)	2014																			and>		
216943	287	1	Z01	1.85	1079				13	39	47	1													0.062	0.68
216944	288	2	Z02	1.30	1080				5	39	53	3													0.056	0.70
216945	289	3	Z03	0.50	1081				1	22	28	40	9												0.088	0.78
216946	290	4	Z04	0.80	1082				1	6	17	46	27	2	1										0.095	0.85
216947	291	5	Z05	1.04	1083				2	26	43	26	3												0.075	0.75
216948	292	6	Z06	2.20	1084				14	45	39	2													0.063	0.67
216942	293	7	Z07	0.96	1085				3	36	46	15													0.071	0.72
216949	294	8	Z08	1.00	1086				1	17	49	31	2												0.072	0.76
216950	295	9	Z09	0.90	1087					6	46	46	2												0.061	0.79
216951	296	10	Z10	1.10	1088					19	56	25													0.061	0.75
216952	297	11	Z11	1.00	1089				28	56	15	1													0.060	0.63
216953	298	12	Z12	2.00	1090				8	50	42														0.055	0.68
216954	299	13	Z13	1.10	1091				10	59	29	2													0.054	0.67

THESE RESULTS RELATE ONLY TO THE SAMPLES ANALYSED

ACTIVITY/TEST	METHOD USED
SAMPLE PREPARATION	ISO 7404-2, 1985
RANDOM REFLECTANCE OF VITRINITE	ISO 7404 - 5, 1994

Vongani Chabalala Pr.Sci.Nat.

Senior Test Officer | Mining and Minerals

SOUTH AFRICAN BUREAU OF STANDARDS | CSIR CAMPUS, PRETORIA

ICCP Accreditation Certificate Number: ICCP/SCAP-131/AB (Expiry date: 31/12/2014)

Signature

Date

PAGE 1 OF 14

TABLE2

SABS

SOUTH AFRICAN BUREAU OF STANDARDS | CSIR CAMPUS, PRETORIA

VITRINITE RANDOM REFLECTANCE DATA

SAMPLE CODES						REFLECTANCE CLASSES (%)																				STANDARD DEVIATION	MEAN RANDOM REFLECTANCE
			KHUTALA COLLIERY																								
SGS	SABS NO.		COMPANY ID		PSA NO.	V2	V3	V4	V5	V6	V7	V8	V9	V10	V11	V12	V13	V14	V15	V16	V17	V18	V19	V20		σ	Rr%
NO.	2015/C		BH S10014	THICKNESS (m)	2015																			and >		
197738	4	1	Z14		1165				3	26	41	30													0.080	0.74
197739	5	2	Z15		1166				2	19	34	30	15												0.098	0.78
197740	6	3	Z16		1167				8	49	35	8													0.073	0.69
197741	7	4	Z17		1168				13	55	29	3													0.609	0.67
197742	8	5	Z18		1169				14	62	22	2													0.060	0.66
197743	9	6	Z19		1170				10	41	37	12													0.078	0.70
197744	10	7	Z20		1171				1	36	49	14													0.063	0.72
197745	11	8	Z21		1172				1	22	57	20													0.064	0.74
197746	12	9	Z22		1173				7	47	43	3													0.063	0.69
198116	13	10	ROM 1		1174				2	33	46	18	1												0.074	0.73
198117	14	11	ROM 2		1175				11	46	33	9	1												0.078	0.69

THESE RESULTS RELATE ONLY TO THE SAMPLES ANALYSED

Vongani Chabalala Pr.Sci.Nat.

Senior Test Officer | Mining and Minerals

SOUTH AFRICAN BUREAU OF STANDARDS | CSIR CAMPUS, PRETORIA

ACTIVITY/TEST	METHOD USED
SAMPLE PREPARATION	ISO 7404-2, 1985
RANDOM REFLECTANCE OF VITRINITE	ISO 7404 - 5, 1994

ICCP Accreditation Certificate Number: ICCP/SCAP-131/AB (Expiry date: 31/12/2016)

Signature

Date

Appendix 190: Abbreviations and terms

TABLE 3: AN EXPLANATION OF ABBREVIATIONS AND TERMS		
SAMPLE PREPARATION - CARRIED OUT BY SABS, PRETORIA		
Petrographic sample preparation was carried out in accordance with the ISO 7404 - 2, 1985.		
REFLECTANCE MEASUREMENTS - CARRIED OUT BY SABS, PRETORIA - see Tables 1and 2		
Readings were taken in accordance with the ISO Standard 7404 - 5, 1994.		
Rr %	:	Random reflectance of vitrinite, oil immersion (determined)
σ	:	Standard deviation
Rmax %	:	Maximum reflectance of vitrinite (calculated)
MACERAL ANALYSIS - CARRIED OUT BY PETROGRAPHICS SA *(% by volume, mineral matter basis)* - see Table 1		
The group maceral analyses were carried out in accordance with ISO 7404 - 3, 1994.		
The reactive inertinite macerals were identified according to Steyn & Smith for South African coals.		
VIT	:	Vitrinite
PV	:	Pseudovitrinite
TV	:	Total vitrinite
S/R/C	:	Sporinite/resinite/cutinite
ALG	:	Alginite
TOT L	:	Total liptinite (formerly referred to as exinite)
RSF	:	Reactive semifusinite
ISF	:	Inert semifusinite
F/SEC	:	Fusinite/secretinite
MIC	:	Micrinite
R INT	:	Reactive inertodetrinite
I INT	:	Inert inertodetrinite
TOT I	:	Total inertinite
Total reactive macerals = Vitrinite + liptinite + RSF + reactive inertodetrinite		

Appendix 191: Major coal characteristics

TABLE 5: SUMMARY OF MAJOR COAL CHARACTERISTICS (1)

	1	2	3	4	5	6
BH SP32814	Z01	Z02	Z03	Z04	Z05	Z06
SABS NO.	287	288	289	290	291	292
PSA 2014-416	1079	1080	1081	1082	1083	1084
RANK (degree of maturity)	**Bituminous**	**Bituminous**	**Bituminous**	**Bituminous**	**Bituminous**	**Bituminous**
ISO 11760-2005 Classification of Coals	**Medium Rank C**	**Medium Rank C**	**Medium Rank C**	**Medium Rank C**	**Medium Rank C**	**Medium Rank C**
Mean random reflectance of vitrinite % (determined)	**0.68**	**0.70**	**0.78**	**0.85**	**0.75**	**0.67**
Vitrinite-class distribution	V 5 to V 8	V 5 to V 8	V 5 to V 9	V 5 to V 11	V 5 to V 9	V 5 to V 8
Standard deviation σ	0.062	0.056	0.088	0.095	0.075	0.063
Mean maximum reflectance of vitrinite % (calculated)	**0.73**	**0.75**	**0.83**	**0.89**	**0.80**	**0.72**
Abnormalities	None observed	None observed	None observed	None observed	None observed	None observed
PETROGRAPHIC COMPOSITION (% by volume)						
Maceral analysis (mineral matter basis)						
Total reactive macerals %	**74**	**44**	**15**	**31**	**24**	**57**
Vitrinite content %	60	33	9	14	13	**41**
Liptinite content %	7	4	2	4	3	**7**
Total inertinite %	27	35	25	52	42	**40**
Heat altered (coke, char etc.) %	0	0	0	0	0	**0**
Visible minerals %	6	28	64	30	42	**12**
Maceral analysis - Total %	**100**	**100**	**100**	**100**	**100**	**100**
Condition analysis						
Condition analysis - Total %	**0**	**0**	**0**	**0**	**0**	**0**

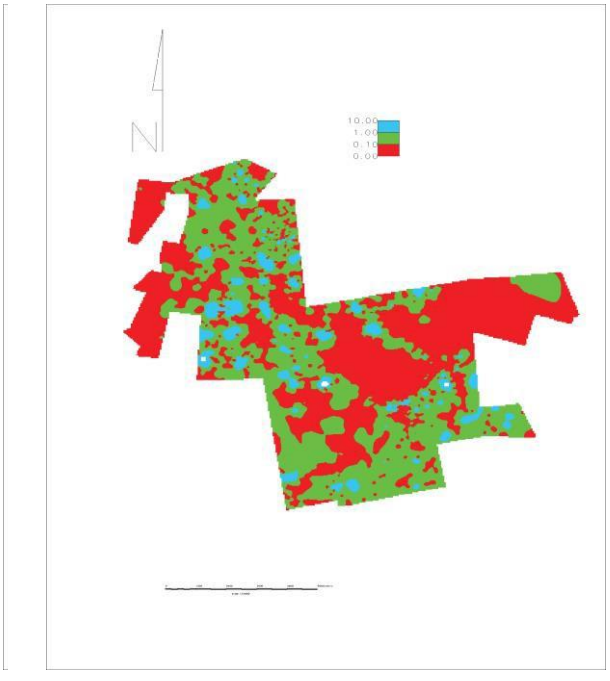
TABLE 5 : SUMMARY OF MAJOR COAL CHARACTERISTICS (2)

	7	8	9	10	11	12	13
BH SP32814	Z07	Z08	Z09	Z10	Z11	Z12	Z13
SABS NO.	293	294	295	296	297	298	299
PSA 2014-416	1085	1086	1087	1088	1089	1090	1091
RANK (degree of maturity)	Bituminous	Bituminous	Bituminous	Bituminous	Bituminous	Bituminous	Bituminous
ISO 11760-2005 Classification of Coals	Medium Rank C	Medium Rank C	Medium Rank C	Medium Rank C	Medium Rank C	Medium Rank C	Medium Rank C
Mean random reflectance of vitrinite % (determined)	0.72	0.76	0.79	0.75	0.63	0.68	0.67
Vitrinite-class distribution	V 5 to V 8	V 5 to V 9	V 6 to V 9	V 6 to V 8	V 5 to V 8	V 5 to V 7	V 5 to V 8
Standard deviation σ	0.071	0.072	0.061	0.061	0.060	0.055	0.054
Mean maximum reflectance of vitrinite % (calculated)	0.77	0.81	0.84	0.80	0.69	0.73	0.72
Abnormalities	None observed	None observed	None observed	None observed	None observed	None observed	None observed
PETROGRAPHIC COMPOSITION (% by volume)							
Maceral analysis (mineral matter basis)							
Total reactive macerals %	34	35	28	34	16	53	44
Vitrinite content %	21	13	14	20	11	40	36
Liptinite content %	2	2	2	4	2	4	3
Total inertinite %	34	63	46	37	11	45	30
Heat altered (coke, char etc.) %	0	0	0	0	0	0	0
Visible minerals %	43	22	38	39	76	11	31
Maceral analysis - Total %	100	100	100	100	100	100	100
Condition analysis							
Condition analysis - Total %	0	0	0	0	0	0	0

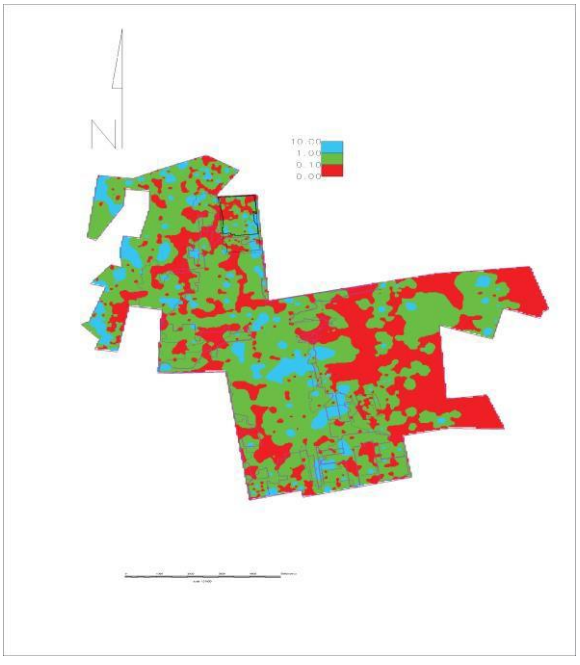
SET 2	1	2	3	4	5	6
BH S10014	Z14	Z15	Z16	Z17	Z18	Z19
SABS NO. 2015	4	5	6	7	8	9
PSA 2015-439	1165	1166	1167	1168	1169	1170
RANK (degree of maturity)	Bituminous	Bituminous	Bituminous	Bituminous	Bituminous	Bituminous
ISO 11760-2005 Classification of Coals	Medium Rank C	Medium Rank C	Medium Rank C	Medium Rank C	Medium Rank C	Medium Rank C
Mean random reflectance of vitrinite % (determined)	0.74	0.78	0.69	0.67	0.66	0.70
Vitrinite-class distribution	V 5 to V 8	V 5 to V 9	V 5 to V 8	V 5 to V 8	V 5 to V 8	V 5 to V 8
Standard deviation σ	0.080	0.098	0.073	0.609	0.060	0.078
Mean maximum reflectance of vitrinite % (calculated)	0.79	0.83	0.74	0.72	0.71	0.75
Abnormalities	None observed	None observed	None observed	None observed	None observed	None observed
PETROGRAPHIC COMPOSITION (% by volume)						
Maceral analysis (mineral matter basis)						
Total reactive macerals %	66	22	40	44	59	40
Vitrinite content %	54	8	29	25	40	19
Liptinite content %	5	6	6	6	6	4
Total inertinite %	35	48	39	48	47	60
Heat altered (coke, char etc.) %	0	0	0	0	0	0
Visible minerals %	6	38	26	21	7	17
Maceral analysis - Total %	100	100	100	100	100	100
Condition analysis						
Condition analysis - Total %	0	0	0	0	0	0

SET 2	7	8	9	10	11
BH S10014	Z20	Z21	Z22	ROM 1	ROM 2
SABS NO. 2015	10	11	12	13	14
PSA 2015-439	1171	1172	1173	1174	1175
RANK (degree of maturity)	Bituminous	Bituminous	Bituminous	Bituminous	Bituminous
ISO 11760-2005 Classification of Coals	Medium Rank C	Medium Rank C	Medium Rank C	Medium Rank C	Medium Rank C
Mean random reflectance of vitrinite % (determined)	0.72	0.74	0.69	0.73	0.69
Vitrinite-class distribution	V 5 to V 8	V 5 to V 8	V 5 to V 8	V 5 to V 9	V 5 to V 9
Standard deviation σ	0.063	0.064	0.063	0.074	0.078
Mean maximum reflectance of vitrinite % (calculated)	0.77	0.79	0.74	0.78	0.74
Abnormalities	None observed	None observed	None observed	None observed	None observed
PETROGRAPHIC COMPOSITION (% by volume)					
Maceral analysis (mineral matter basis)					
Total reactive macerals %	33	47	62	37	27
Vitrinite content %	16	27	48	23	12
Liptinite content %	3	4	8	4	3
Total inertinite %	51	60	24	45	53
Heat altered (coke, char etc.) %	0	0	0	0	0
Visible minerals %	30	9	20	28	32
Maceral analysis - Total %	100	100	100	100	100
Condition analysis					
Condition analysis - Total %	0	0	0	0	0

Appendix 192: No.S5 seam mudstone floor thickness



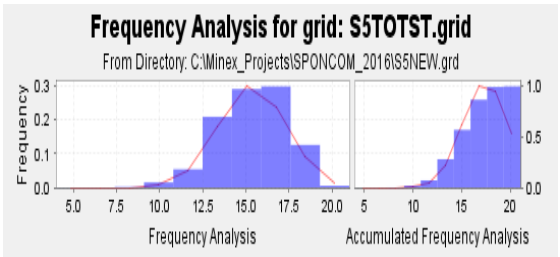
Appendix 193: No. S4U seam mudstone floor thickness



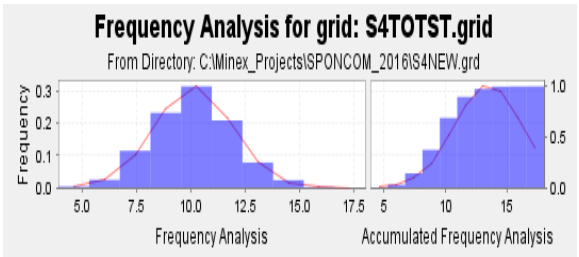
Appendix 194: No.S2U seam mudstone floor thickness



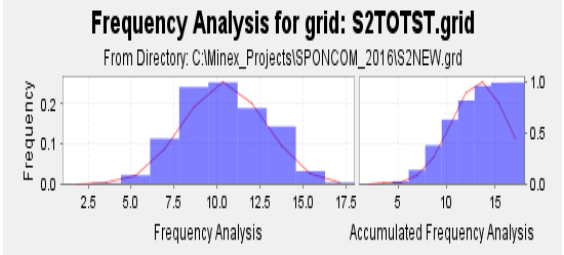
Appendix 195 :Frequency analysis for risk matrix grids



Number of Values: 38201.00
Minimum Value: 4.00
Maximum Value: 21.00
Mean: 15.37
Standard Deviation: 1.9687
Skewness: 0.2012



Number of Values: 38201.00
Minimum Value: 3.88
Maximum Value: 18.00
Mean: 10.09
Standard Deviation: 1.8021
Skewness: 0.0054



Number of Values: 38201.00
Minimum Value: 1.00
Maximum Value: 18.00
Mean: 10.42
Standard Deviation: 2.3539
Skewness: 0.0085

Appendix 198: sponcom image



Appendix 199: sponcom image



Appendix 200: sponcom image



Appendix 201: sponcom image



Appendix 202: Difference between sample database correlations and modelling dataset correlations

		1	2	3	4	5	6	7	8	9	10	11	12	13	14	15	16	17	18	19	20	21	22	23	24	25	26	27	28	29	30	31	32	33	34	35		
		AB	Al2O3	Ash	Carbon	CaO	CPT	CV	DerWt	FC	Fe2O3	GLI	H	IM	K2O	MGO	MNO	MS	N	Na2O	O	OS	P2O5	PS	RD	SiO2	S03	SS	Tstart	Tpeak	Ti02	TR	TS	VM	VR	WT		
1	AB	0.00																																			1	AB
2	Al2O3	0.19	0.00																																		2	Al2O3
3	Ash	0.15	0.22	0.00																																	3	Ash
4	Carbon	-0.16	-0.22	0.02	0.00																																4	Carbon
5	CaO	-0.02	0.05	0.27	-0.26	0.00																															5	CaO
6	CPT	-0.05	0.00	-0.01	0.00	0.35	0.00																														6	CPT
7	CV	-0.12	0.76	0.01	0.00	-0.27	0.02	0.00																													7	CV
8	DerWt	0.00	0.30	0.24	-0.26	-0.33	0.01	-0.24	0.00																												8	DerWt
9	FC	-0.15	-0.15	-1.86	-0.11	-0.22	0.04	-0.09	-0.27	0.00																											9	FC
10	Fe2O3	-0.20	-0.10	-0.08	0.10	-0.27	0.06	0.07	-0.15	0.00	0.00																										10	Fe2O3
11	GLI	-0.25	-0.12	0.17	-0.15	-0.04	0.00	-0.13	-0.25	-0.16	0.03	0.00																									11	GLI
12	H	-0.07	-0.15	0.04	-0.03	-0.18	-0.03	-0.02	-0.37	-0.10	0.00	-0.16	0.00																								12	H
13	IM	-0.16	-0.13	0.41	-0.46	-0.32	0.39	-0.44	-0.02	-0.55	-0.16	-0.55	-0.37	0.00																							13	IM
14	K2O	-0.03	-0.01	-0.22	0.23	0.00	-0.25	0.27	-0.01	0.25	0.22	0.33	0.22	-0.11	0.00																						14	K2O
15	MGO	0.11	0.24	0.31	-0.31	-0.09	-0.01	-0.26	-0.08	-0.29	0.85	-0.36	-0.22	-0.32	-0.29	0.00																					15	MGO
16	MNO	0.03	0.06	0.21	-0.19	0.00	0.25	-0.23	-0.28	-0.20	0.04	-0.13	-0.06	-0.10	-0.08	0.28	0.00																				16	MNO
17	MS	-0.34	0.06	-0.10	0.10	-0.32	-0.13	0.09	-0.02	0.02	0.12	-0.02	-0.05	-0.11	0.20	-0.13	-0.25	0.00																			17	MS
18	N	-0.18	-0.20	1.85	0.04	-0.26	-0.11	0.05	-0.30	-0.06	0.13	-0.14	-0.01	-0.35	0.26	-0.37	-0.16	0.13	0.00																		18	N
19	Na2O	0.16	0.09	0.15	-0.16	-0.08	-0.04	-0.12	0.14	-0.11	-0.01	0.01	-0.17	-0.29	0.02	-0.06	-0.03	0.18	-0.15	0.00																	19	Na2O
20	O	0.29	-0.03	0.23	-0.22	0.29	0.25	-0.26	-0.01	-0.12	-0.28	0.04	0.01	-0.14	0.04	0.21	0.21	-0.18	-0.21	0.00	0.00																20	O
21	OS	-0.10	0.11	-0.06	0.06	-0.06	-0.12	0.06	0.06	0.11	-0.02	0.25	0.52	-0.31	0.03	0.00	-0.01	0.07	0.14	0.00	-0.04	0.00															21	OS
22	P2O5	0.20	0.04	0.36	-0.26	0.04	0.16	-0.26	0.08	-0.24	-0.12	-0.18	-0.19	-0.25	-0.16	0.08	0.05	-0.18	-0.23	0.00	0.00	-0.10	0.00														22	P2O5
23	PS	-0.34	0.06	-0.10	0.10	-0.32	-0.14	0.10	-0.03	0.02	0.13	-0.03	-0.05	-0.11	0.19	-0.13	-0.25	0.00	0.13	0.00	-0.18	0.07	-0.10	0.00													23	PS
24	RD	0.18	0.23	-0.02	0.04	0.28	-0.02	0.02	0.25	-1.82	-0.11	0.20	-1.83	0.44	-0.23	0.33	0.22	-0.10	-0.01	0.00	0.24	-0.04	0.31	-0.10	0.00												24	RD
25	SiO2	0.02	0.07	-0.21	0.17	0.11	-0.10	0.19	-0.07	0.19	0.06	1.15	0.19	0.49	-0.13	0.05	0.16	-0.12	0.14	0.00	0.17	-0.15	0.00	-0.11	-0.22	0.00											25	SiO2
26	S03	-0.22	-0.21	-0.13	0.15	-0.08	-0.16	0.15	-0.35	0.03	0.24	-0.09	0.09	-0.05	0.08	-0.18	0.00	0.18	0.18	0.00	-0.17	0.01	-0.38	0.18	-0.13	0.19	0.00										26	S03
27	SS	0.35	0.19	0.05	-0.10	0.03	0.13	-0.11	-0.04	0.04	-0.37	0.10	0.10	-0.02	0.11	0.42	0.18	-0.34	-0.03	0.00	0.23	0.03	0.20	-0.34	0.05	0.00	0.01	0.00									27	SS
28	Tstart	0.21	0.23	-0.02	0.01	0.00	-0.08	0.00	0.26	0.07	-0.12	0.23	-0.03	0.45	-0.01	0.12	-0.03	0.12	0.00	0.00	0.04	0.16	0.15	0.16	-0.08	-0.12	-0.01	0.00	0.00								28	Tstart
29	Tpeak	-0.43	0.02	0.07	-0.04	-0.07	-0.01	-0.02	0.16	-0.14	0.20	-0.14	-0.20	-0.29	-0.10	-0.30	-0.21	0.13	-0.10	0.00	-0.10	-0.07	0.05	0.12	0.09	-0.21	-0.19	0.00	0.24	0.00							29	Tpeak
30	Ti02	0.11	0.04	0.28	-0.04	0.00	0.14	-0.06	0.04	-0.06	-0.12	-0.13	-0.03	0.22	-0.06	-0.34	-0.02	-0.13	-0.06	0.00	-0.05	-0.13	0.23	-0.13	0.02	0.02	-0.08	0.00	-0.11	0.11	0.00						30	Ti02
31	TR	0.04	-0.21	0.00	0.01	0.02	-0.02	0.00	-0.19	-0.03	0.04	-0.02	0.02	-0.36	0.34	-0.20	-0.24	0.19	0.11	0.00	-0.27	0.16	-0.31	0.19	0.00	0.25	0.17	0.00	0.00	0.03	-0.16	0.00					31	TR
32	TS	-0.09	-0.17	-0.50	0.79	-0.16	0.06	0.48	-0.42	0.37	0.19	0.37	0.50	0.33	0.20	0.28	-0.64	-0.11	0.52	0.00	-0.12	-0.05	0.23	-0.10	-0.50	0.02	0.36	0.00	-0.53	0.01	0.20	0.38	0.00				32	TS
33	VM	-0.10	-0.12	0.07	-0.09	-0.25	0.13	-0.10	-0.15	-0.32	-0.03	-0.27	-0.14	-0.30	0.04	-0.20	-0.20	0.06	-0.05	0.00	-0.25	-0.13	-0.20	0.07	0.07	0.18	0.13	0.00	-0.03	0.14	0.00	-0.18	0.49	0.00			33	VM
34	VR	-0.32	0.01	-0.02	0.07	-0.11	0.07	0.06	0.42	-0.04	0.21	-0.17	-0.07	-0.15	-0.18	-0.12	-0.27	0.15	0.06	0.00	-0.21	-0.28	0.22	0.16	-0.01	-0.14	0.40	0.00	0.09	0.10	0.25	0.74	-0.09	0.18	0.00		34	VR
35	WT	0.00	-0.03	0.16	-0.16	-0.15	0.12	-0.16	-0.30	-0.20	-0.15	-0.38	-0.05	-0.29	0.03	0.08	0.04	-0.32	-0.10	0.00	0.04	-0.08	-0.04	-0.31	0.19	0.21	-0.04	0.00	0.04	-0.30	0.14	-0.14	0.38	-0.17	-0.10	0.00	35	WT
		1	2	3	4	5	6	7	8	9	10	11	12	13	14	15	16	17	18	19	20	21	22	23	24	25	26	27	28	29	30	31	32	33	34	35		
		AB	Al2O3	Ash	Carbon	CaO	CPT	CV	DerWt	FC	Fe2O3	GLI	H	IM	K2O	MGO	MNO	MS	N	Na2O	O	OS	P2O5	PS	RD	SiO2	S03	SS	Tstart	Tpeak	Ti02	TR	TS	VM	VR	WT		